

Aus der Klinik für Endokrinologie und Diabetologie  
des Universitätsklinikums Düsseldorf  
an der Heinrich-Heine-Universität Düsseldorf  
und  
dem Deutschen Diabetes-Zentrum  
Leibniz-Zentrum für Diabetesforschung  
Direktor: Univ.-Prof. Dr. Michael Roden

**Hepatic and Skeletal Muscle Energy Metabolism in Metabolic Diseases and Changes after  
Metabolic Surgery**

Habilitationsschrift  
zur Erlangung der Venia Legendi für das Fach: Innere Medizin der  
Medizinischen Fakultät der Heinrich-Heine-Universität  
Düsseldorf

vorgelegt von  
Dr. med. Sofiya Gancheva  
2023

## Table of contents

Original publications underlying this thesis .....	3
Frequently used abbreviations.....	5
Deutsche Zusammenfassung.....	7
<b>1. Introduction .....</b>	<b>9</b>
<b>1.1. Type 2 diabetes and insulin resistance .....</b>	<b>9</b>
<b>1.1 Liver lipid accumulation and insulin resistance .....</b>	<b>11</b>
<b>1.1.1 Approaches to reduce liver lipid content.....</b>	<b>13</b>
<b>1.2 Role of mitochondrial function for insulin resistance .....</b>	<b>15</b>
<b>1.2.1 Hepatic mitochondrial function in type 1 diabetes .....</b>	<b>16</b>
<b>1.2.2 Hepatic mitochondrial function in NAFLD .....</b>	<b>18</b>
<b>1.2.3 Hepatic mitochondrial function in organic acidemias.....</b>	<b>20</b>
<b>1.2.4 Bariatric surgery effects on skeletal muscle mitochondrial function and insulin resistance .....</b>	<b>21</b>
<b>2. Hypotheses.....</b>	<b>22</b>
<b>3. Results .....</b>	<b>23</b>
<b>3.1 Empagliflozin reduces hepatic lipid content in well-controlled people with type 2 diabetes. 24</b>	
<b>3.2 Non-invasive vagus nerve stimulation does not affect hepatic lipid content and energy metabolism in healthy humans.....</b>	<b>27</b>
<b>3.3 Lower hepatic ATP concentrations in humans with type 1 diabetes relate to variants in genes controlling oxidative metabolism .....</b>	<b>30</b>
<b>3.4 Loss of adaptation of hepatic oxidative capacity in people with type 2 diabetes and non- alcoholic steatohepatitis .....</b>	<b>33</b>
<b>3.5 Genetic alteration of mitochondrial function in organic acidemias does not relate to changes in hepatic ATP concentrations .....</b>	<b>35</b>
<b>3.6 Epigenetic and metabolic changes in skeletal muscle underlying the improvement of insulin sensitivity after bariatric surgery .....</b>	<b>37</b>
<b>3.7 Bariatric surgery-induced restoration of the growth hormone system relates to improved adipose tissue insulin sensitivity.....</b>	<b>39</b>
<b>4. Conclusions .....</b>	<b>41</b>
<b>4.1. Effects of empagliflozin, prolonged fasting and transcutaneous vagus nerve stimulation on liver lipid content.....</b>	<b>41</b>
<b>4.2. Alterations of hepatic energy metabolism in metabolic disease.....</b>	<b>44</b>
<b>4.3. Dynamic metabolic and mitochondrial changes after bariatric surgery .....</b>	<b>48</b>
<b>5. Outlook.....</b>	<b>52</b>
<b>6. References.....</b>	<b>54</b>
<b>7. Acknowledgements .....</b>	<b>61</b>
<b>8. Attached articles (Study 1-7) .....</b>	<b>62</b>

## Original publications underlying this thesis

1. Kahl S\*, **Gancheva S\***, Straßburger K, Herder C, Machann J, Katsuyama H, Kabisch S, Henkel E, Kopf S, Lagerpusch M, Kantartzis K, Kupriyanova Y, Markgraf D, van Gemert T, Knebel B, Wolkersdorfer MF, Kuss O, Hwang JH, Bornstein SR, Kasperk C, Stefan N, Pfeiffer A, Birkenfeld AL, Roden M. Empagliflozin Effectively Lowers Liver Fat Content in Well-Controlled Type 2 Diabetes: A Randomized, Double-Blind, Phase 4, Placebo-Controlled Trial. *Diabetes Care*. 2020 43(2):298-305 Impact factor 2020: 19,11
2. **Gancheva S**, Bierwagen A, Markgraf D, Boenhof G, Murphy K, Hatziagelaki E, Lundbom J, Ziegler D, Roden M. Constant hepatic ATP concentrations during prolonged fasting and absence of effects of Cerbomed Nemos® on parasympathetic tone and hepatic energy metabolism. *Molecular Metabolism* 2018 7:71-79 Impact factor 2018: 5,81
3. **Gancheva S\***, Bierwagen A\*, Kaul K, Herder C, Nowotn P, Kahl S, Giani G, Klueppelholz B, Knebel B, Begovatz P, Strassburger K, Al-Hasani H, Lundbom J, Szendroedi J, Roden M. Variants in Genes Controlling Oxidative Metabolism Contribute to Lower Hepatic ATP Independent of Liver Fat Content in Type 1 Diabetes. *Diabetes* 2016 65(7):1849-57 Impact factor 2016: 8,68
4. **Gancheva S**, Kahl S, Pesta D, Mastrototaro L, Dewidar B, Strassburger K, Sabah E, Esposito I, Weiß J, Sarabhai T, Wolkersdorfer M, Fleming T, Nawroth P, Zimmermann M, Reichert AS, Schlensak M, Roden M. Impaired Hepatic Mitochondrial Capacity in Nonalcoholic Steatohepatitis Associated With Type 2 Diabetes. *Diabetes Care* 2022 Apr 1;45(4):928-937. Impact factor 2022: 17,15
5. **Gancheva S\***, Caspari D\*, Bierwagen A, Jelenik T, Caprio S, Santoro N, Rothe M, Markgraf DF, Herebian D, Hwang JH, Meissner T, Vom Dahl T, Klee D, Mayatepek E, Roden M, Ensenauer R. Cardiometabolic Risk Factor Clustering in Patients With Deficient Branched-Chain Amino Acid Catabolism: A Case-Control Study. *J Inherit Metab Dis*. 2020 43(5):981-993 Impact factor 2020: 4,98
6. **Gancheva S\***, Ouni M\*, Jelenik T, Koliaki C, Szendroedi J, Toledo FGS, Markgraf DF, Pesta DH, Mastrototaro L, De Filippo E, Herder C, Jähnert M, Weiss J, Strassburger K, Schlensak M, Schürmann

A, Roden M. Dynamic changes of muscle insulin sensitivity after metabolic surgery. Nat Commun. 2019 Sep 13;10(1):4179 Impact factor 2019: 12,12

**Gancheva S\***, Ouni M\*, Jelenik T, Koliaki C, Szendroedi J, Toledo FGS, Markgraf DF, Pesta DH, Mastrototaro L, De Filippo E, Herder C, Jähnert M, Weiss J, Strassburger K, Schlensak M, Schürmann A, Roden M. Author Correction: Dynamic changes of muscle insulin sensitivity after metabolic surgery. Nat Commun 2022 Jun 10;13(1):3353 Impact factor 2022: 16,6

7. **Gancheva S**, Kahl S, Herder C, Strassburger K, Sarabhai T, Pafili K, Szendroedi J, Schlensak M, Roden M. Metabolic Surgery-induced Changes of the Growth Hormone System Relate to Improved Adipose Tissue Function. Int J Obesity 2023 Jun;47(6):505-511 Impact factor 2022-2023: 5,09

\*Authors contributed equally

### Frequently used abbreviations

<sup>1</sup> H MRS	Proton magnetic resonance spectroscopy
<sup>31</sup> P MRS	Phosphorus magnetic resonance spectroscopy
β ox	β oxidation
AMPK	AMP-activated protein kinase
ATP	Adenosine triphosphate, Adenosintriphosphat
BMI	Body mass index
BCAA	Branched-chain amino acids
CI, II, III	Complex I, II, III of the respiratory chain
CoA	Conezyme A
CSA	Citrate synthase activity
DAG	Diacylglycerols
DNL	<i>de-novo</i> lipogenesis
EGP	Endogenous glucose production
EMPA	Empagliflozin
FCCP	Carbonyl cyanide-4-(trifluoromethoxy)phenylhydrazone
FFA	Free fatty acids
G6P	Glucose-6-phosphate
GH	Growth hormone
GLUT 2	Glucose transporter 2
GNG	Gluconeogenesis
GPX1	Glutathione
HbA1c	Hemoglobin A1c
HCL	Hepatocellular lipids
IGF-1	Insulin-like growth factor 1
IGFBP1	Insulin-like growth factor binding protein 1
IR	Insulin resistance

IVA	Isovaleric acidemia
MMA	Methylmalonic acidemia
MRS	Magnetic resonance spectroscopy
mtDNA	Mitochondrial DNA
NAFL	Non-alcoholic fatty liver
NAFLD	Non-alcoholic fatty liver disease
NASH	Non-alcoholic steatohepatitis
NFκB	Nuclear factor κ-light-chain-enhancer of activated B cells
OA	Organic acidemia
OGTT	Oral glucose tolerance test
OXPHOS	Oxidative phosphorylation
PA	Propionic acidemia
PGC-1α	Peroxisome proliferator-activated receptor γ coactivator-1α
Pi	Inorganic phosphate
PKCθ, ε	Protein kinase Cθ, ε
PPARγ	Peroxisome proliferator-activated receptor γ
ROS	Reactive oxygen species
SGLT2i	Sodium glucose transporter 2 inhibitor
T1D	Type 1 diabetes mellitus
T2D	Type 2 diabetes mellitus
taVNS	Transcutaneous auricular vagus nerve stimulation
TBARS	Thiobarbituric acid reactive substances
TCA	Tricarboxylic acid cycle
TG	Triglycerides
VLDL	Very low density lipoproteins

## Deutsche Zusammenfassung

**Hintergrund:** Typ 2 Diabetes, Adipositas und Nicht-alkoholische Fettlebererkrankung sind mit Insulinresistenz und Störungen des Energiestoffwechsels von Skelettmuskel und Leber assoziiert. Störungen des Energiestoffwechsels betreffen im besonderen Veränderungen der mitochondrialen Funktionalität, das heißt: der oxidativen Phosphorylierung, des Gehalts und/oder der Umsatzrate der Mitochondrien. Diese Veränderungen sind jedoch nicht immer angeboren, sondern können auch eine Anpassung an vermehrte Verfügbarkeit von Glukose, Lipiden oder speziellen Aminosäuren widerspiegeln. Die Rolle von Hyperglykämie und Dyslipidämie bei Typ 1 und Typ 2 Diabetes sowie von Störungen des Stoffwechsels verzweigtkettiger Aminosäuren für den Energiestoffwechsel war bis vor kurzem unklar. Ebenso waren die Effekte von Verbesserung der Hyperglykämie mittels antihyperglykämischer Medikamente und Modulation des parasymphatischen Nervensystems oder von Gewichtsreduktion mittels bariatrischer Chirurgie auf die Mitochondrienfunktion weitgehend unbekannt. Die vorliegenden Untersuchungen prüften daher folgende Hypothesen: (i) Verbesserung der Glykämie mittels nicht-invasiver elektrischer Vagusstimulation oder Hemmung des Natrium-abhängigen Glukosetransporters-2 (SGLT2) senken die Speicherung von Triglyzeriden in der Leber, (ii) erhöhte Verfügbarkeit von Glukose aber auch von Metaboliten des Aminosäurenstoffwechsels reduziert die mitochondriale Aktivität in der Leber, (iii) bariatrische Chirurgie verbessert die Insulinsensitivität durch Abnahme der Lipidverfügbarkeit, Zunahme der mitochondrialen Kapazität des Skelettmuskels und Modulation des Wachstumshormon-Systems.

**Methoden:** Die Hypothesen wurden in klinisch-experimentellen Studien an Menschen geprüft. Mittels hyperinsulinämisch-euglykämischer Clamps und stabil-markierter Glukose wurde die Insulinsensitivität von Muskel und Leber bestimmt. In Muskelbiopsien wurden Substratkonzentrationen, Lipidom, Transkriptom und Methylom analysiert. In Muskel- und Leberbiopsien wurde die oxidative Phosphorylierung mittels hochauflösender Respirometrie sowie die Freisetzung von freien Sauerstoffradikalen und die Lipidperoxidation *ex vivo* gemessen. Mittels Magnetresonanzbildgebung und -spektroskopie wurden Triglyzeridgehalt sowie ATP-Gehalt der Leber nicht-invasiv *in vivo* quantifiziert.

**Ergebnisse:** Eine antihyperglykämische Therapie mit dem SGLT2-Hemmer Empagliflozin reduziert effektiv die Triglyzeridspeicherung in der Leber, was mit Verbesserung des Harnsäurespiegels und des Adiponektins in Zusammenhang steht. Die elektrische Stimulation mittels Cerbomed Nemos® moduliert nicht den viszeralen parasymphatischen Tonus und ist daher nicht in der Lage metabolische Effekte hervorzurufen. Entsprechend bleiben die hepatischen Konzentrationen an ATP und Triglyzeriden über eine verlängerte Fastenperiode konstant. Die Hyperglykämie und der oxidative Stress tragen zur Verminderung des ATP-Gehalts der Leber bei Typ 1 Diabetes sowie zur Reduktion der

oxidativen Kapazität bei nicht-alkoholischer Fettleberentzündung (NASH) und Typ 2 Diabetes bei. Es finden sich keine Unterschiede der hepatischen ATP-Konzentration bei genetischen Störungen der Mitochondrienfunktion im Rahmen von Organazidämien, trotz Häufung von Merkmalen des metabolischen Syndroms bei diesen Kindern und Jugendlichen. Nach bariatrischer Operation verhindert eine vorübergehend erhöhte Lipidverfügbarkeit trotz rascher Gewichtsreduktion durch Mechanismen der Lipotoxizität die rasche Steigerung der Insulinsensitivität. Später zeigt sich jedoch eine deutliche Verbesserung der peripheren Insulinsensitivität, die mit spezifischen Expressions- und Methylierungs-Veränderungen im Skelettmuskel, aber nicht mit der Wiederherstellung der Wachstumshormons-Achse einhergeht.

**Zusammenfassung:** Störungen der hepatischen mitochondrialen Funktion sind relevante Kennzeichen von NASH, aber auch von Typ 2 und Typ 1 Diabetes und sind als Frühzeichen einer Leberschädigung anzusehen. Außerdem sind die metabolischen Effekte von SGLT2-Hemmern und bariatrischer Chirurgie nicht nur durch die Gewichtsabnahme erklärbar, sondern auch durch dynamische Veränderungen der Lipidverfügbarkeit und der Funktion des Fettgewebes bedingt. Die Modifikation des hepatischen Energiestoffwechsels und der Fettgewebefunktion stellt somit auch einen neuen Ansatz zur Therapie von metabolischen Erkrankungen dar.

Diese kumulative Habilitationsschrift beruht auf 7 begutachteten Originalarbeiten, die als Erstautorin oder Ko-Erstautorin publiziert wurden (Anlagen 1-7).

## **1. Introduction**

### **1.1. Type 2 diabetes and insulin resistance**

Hyperglycemia resulting from impaired insulin action and/or abnormal insulin secretion is a common feature of diabetes mellitus, which together with obesity represent the most frequent metabolic disorders [1]. Diabetes mellitus relates to increased risk of dysfunction and failure of multiple systems and organs, most important of which are the eyes, the kidneys, the cardiovascular and the nervous system.

Type 2 diabetes is the most common form of diabetes that affects the majority of people with diabetes [2]. It is characterized by insulin resistance (IR), which is marked by sustained hyperinsulinemia both in pre-and postprandial conditions. As insulin secretion decreases, blood glucose levels rise until they reach the threshold for type 2 diabetes diagnosis [3]. While some individuals may have impaired  $\beta$ -cell function as the primary defect, most affected humans exhibit IR before any alterations in insulin secretion occur. It has been shown that certain genetic variants may contribute to the risk of type 2 diabetes especially through promoting  $\beta$ -cell failure [4], but their impact is small and not practical for widespread genetic screening [5]. Therefore, identifying and addressing modifiable factors that contribute to IR is crucial in preventing type 2 diabetes and developing new treatments. Furthermore, multiple circulating metabolites serve as mediators of interorgan crosstalk regulating insulin sensitivity and energy metabolism and might represent future therapeutic targets (Figure 1) [6].

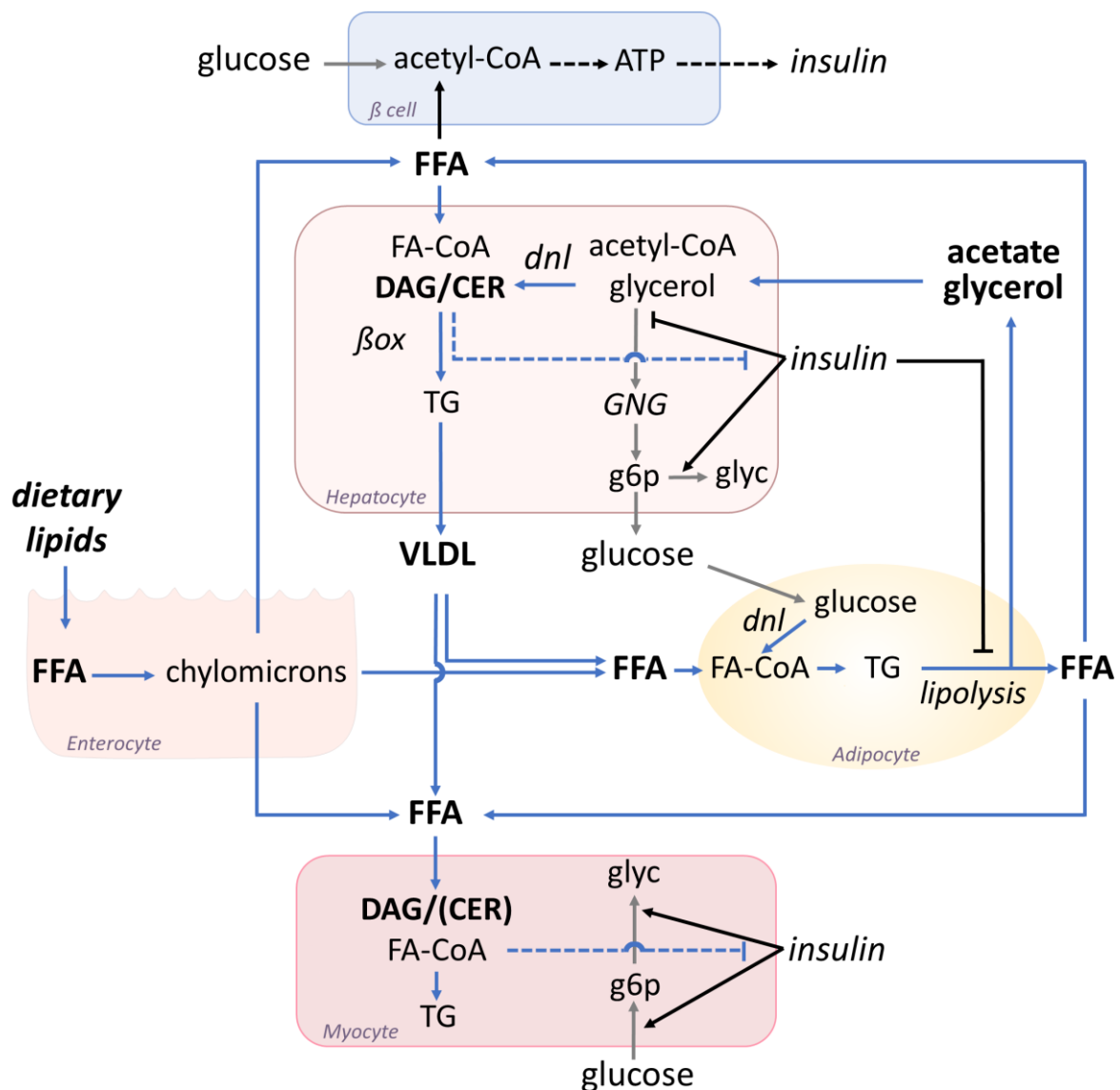


**Figure 1.** Lipid-mediated interorgan crosstalk in the development of insulin resistance. Illustration by S. Gancheva adapted from Gancheva et al. [6]

Excess caloric intake and unrestrained adipose tissue lipolysis raise systemic availability of free fatty acids (FFA), acetate and glycerol. These metabolites can cause hyperglycemia as substrates of hepatic gluconeogenesis and steatosis via lipogenesis with triglyceride (TG) storage and very low density lipoproteins (VLDL) production. In addition, intracellular lipid mediators such as diacylglycerols (DAG) and ceramides (CER) can further impair insulin-mediated inhibition of hepatic gluconeogenesis and glycogenolysis thereby also contributing to elevated endogenous glucose production (EGP) [7]. In skeletal muscle, increased FFA availability gives rise to intracellular lipid mediators (in humans mainly DAG), which cause diminished insulin-stimulated glucose transport/ phosphorylation with subsequently lower glycogen synthesis.

Prediabetes and type 2 diabetes are closely linked to cardiovascular diseases and an increased risk of certain cancers as well as to microvascular complications such as retinopathy, nephropathy and neuropathy [8, 9]. Even newly diagnosed people with type 2 diabetes may present with comorbidities due to long-term undetected insulin resistance and hyperglycemia prior to diabetes diagnose [10, 11]. While the metabolic syndrome has been thought to be a better predictor of diabetes complications prognosis than insulin resistance [12], recent evidence has shown that insulin resistance alone can increase cardiac mortality independently of type 2 diabetes [13, 14]. However, whether insulin resistance can predict the development of diabetes complications and how it affects individualized treatment approaches remains unclear. Recent studies reveal that humans with diabetes and insulin resistance are particularly susceptible for complications such as nephropathy, cardiovascular disease, erectile dysfunction and non-alcoholic fatty liver disease (NAFLD) [15, 16]. The relationship between hyperglycemia and comorbidities is complex, but intensive glycemic control early on in type 2 diabetes can have long-term protective effects [17, 18]. Further evidence suggests that mitochondrial impairment together with increased reactive oxygen species may lead to irreversible cell damage and apoptosis in diabetes [19, 20]. Therefore, novel therapies targeting mitochondrial function or insulin sensitivity may prove as valuable treatment options.

### **1.1 Liver lipid accumulation and insulin resistance**

Non-alcoholic fatty liver disease is strongly associated with insulin resistance and is considered as the hepatic complication of type 2 diabetes and obesity. An individual is diagnosed with NAFLD if they have at least 5 % infiltration of hepatocytes with lipids, or a magnetic resonance imaging proton density fat fraction (MRI-PDFF) of 5 % or higher, or magnetic resonance spectroscopy liver lipid content of more than 5.56 %, as evaluated through either imaging or liver biopsy [21, 22]. However, this diagnosis only applies to individuals who consume minimal or no alcohol and do not have any secondary causes of hepatic steatosis (such as metabolic liver diseases or drug use). NAFLD encompasses a spectrum of conditions ranging from simple steatosis or nonalcoholic fatty liver (NAFL) to the inflammatory form non-alcoholic steatohepatitis (NASH), which can further progress to hepatic fibrosis, cirrhosis and hepatocellular carcinoma [23, 24]. To diagnose NASH, a histological assessment is necessary in the presence of suspected NAFLD. Typically, NASH is characterized by the presence of steatosis, lobular inflammation, and ballooning with or without perisinusoidal fibrosis [25]. Recently, a new fatty liver disease nomenclature has been proposed from the leading international expert organizations in order to better reflect the etiology and pathophysiology of the underlying conditions and to reduce stigmatization [26]. According to this new nomenclature NAFLD should be replaced by metabolic dysfunction-associated steatotic liver disease (MASLD) and NASH - with metabolic dysfunction-associated steatohepatitis (MASH). However, as of today, this is not uniformly accepted by all experts

in the field. The articles underlying this work have been published before this new nomenclature has been suggested, so that NAFLD and NASH will be used throughout the text.

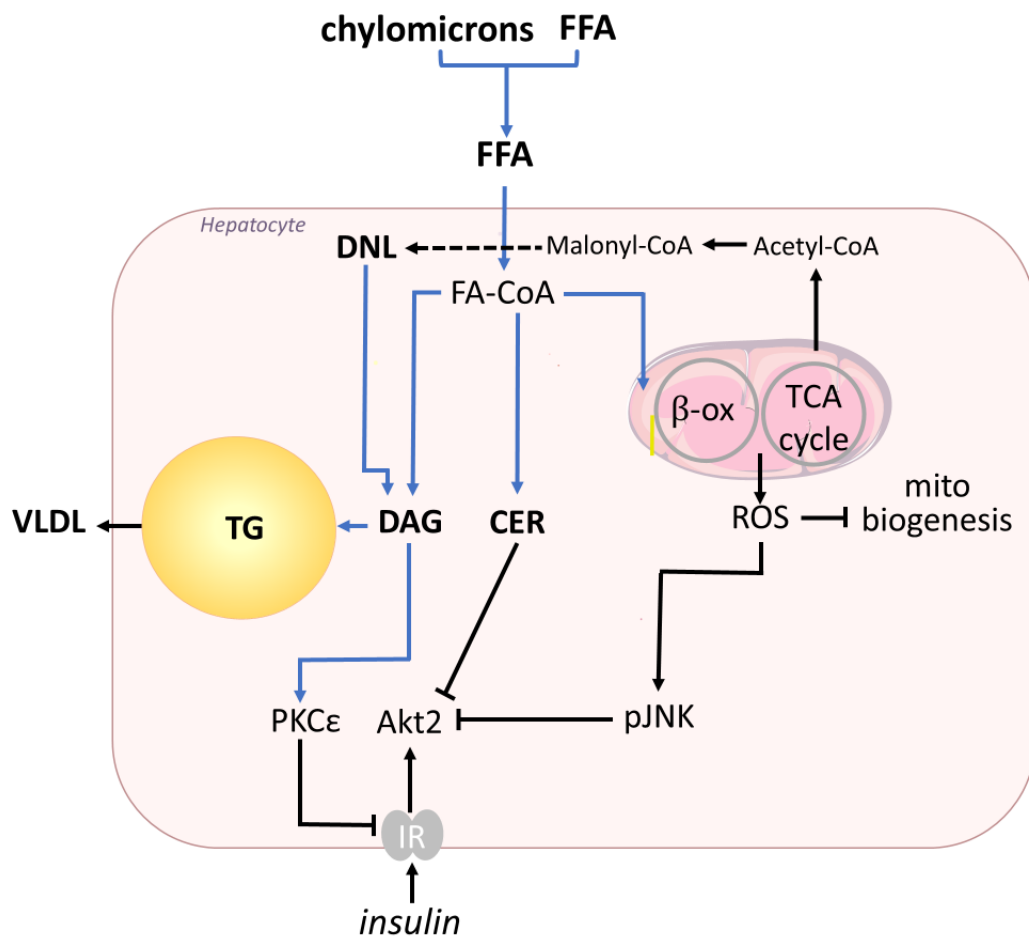


**Figure 2.** Hepatic insulin resistance and lipid accumulation. Illustration by S. Gancheva adapted from Gancheva et al. [6]

The metabolic mechanisms that contribute to the development of NAFLD reflect an imbalance in energy metabolism in the liver [27]. This occurs due to excessive energy intake (primarily in the form of carbohydrates and fat) relative to the liver's ability to oxidize this energy to CO<sub>2</sub> or export it as VLDL (Figure 2). Increased lipid availability not only increases the hepatocellular TG storage and VLDL production, but also the levels of activated FFA (FA-CoA) and in turn raises concentrations of DAG as well as CER, which may also derive from other sources. DAG activates PKCε, which results in inhibitory insulin receptor Thr<sup>1160</sup>-phosphorylation, leading to diminished insulin-mediated stimulation of net glycogen synthesis and inhibition of gluconeogenesis [28]. Specific ceramides and other sphingolipids have been shown to be elevated only in obese individuals with NASH, but not in those with or without steatosis [29, 30]. Interestingly, some sphingolipids correlate with markers of hepatic oxidative stress and inflammatory pathways, suggesting an important role of these lipid metabolites for NAFLD progression [30]. In addition, elevated lipid availability may induce transient mitochondrial adaptation

to increased ROS generation, which over time exhausts the antioxidant capacity and aggravates inflammation and insulin resistance in NAFLD [31].

In addition to insulin resistance, other factors that contribute to the development of NAFLD include a high-fat, high-sugar diet, sedentary lifestyle, and obesity. These factors can increase circulating levels of free fatty acids and promote hepatic triglyceride accumulation. Chronic inflammation also plays a role in the pathogenesis of NAFLD, as it can promote insulin resistance and further contribute to lipid accumulation in the liver [32, 33]. Overall, the development of NAFLD is multifactorial and involves complex interactions between genetic, metabolic, and environmental factors. The early onset of metabolic syndrome and prediabetes is often associated with skeletal muscle insulin resistance, which can contribute to the development of NAFLD by promoting increased hepatic *de novo* lipogenesis (DNL) and hypertriglyceridemia [34, 35]. When glucose is diverted away from skeletal muscle glycogen synthesis and towards the liver for DNL, it can lead to the accumulation of triglycerides in the liver [36]. The development of hepatic insulin resistance with impaired insulin activation of glycogen synthase, can also redirect glucose towards lipogenic pathways, thereby exacerbating the development of NAFLD [37]. Whether hyperglycemia in diabetes mellitus contributes to NAFLD progression via mechanisms of oxidative stress and/or advanced glycation end products accumulation remains unclear.

### **1.1.1 Approaches to reduce liver lipid content**

Weight loss has been shown to be effective in treating NAFLD, although it is difficult to achieve [38]. While certain medications, including glucagon-like peptide 1 receptor agonists and thiazolidinediones, have demonstrated beneficial effects for people with T2D and NAFLD, there is currently no widely accepted pharmacological treatment option [38, 39]. Sodium-glucose cotransporter 2 inhibitors (SGLT2is) not only improve glycemia, but also have beneficial effects on body weight and blood pressure, as well as cardiovascular and renal outcomes [40, 41]. Studies have suggested that SGLT2is may also alleviate NAFLD, with canagliflozin and dapagliflozin showing a trend towards decreased liver lipid content compared to placebo [42-44]. Canagliflozin's reduction in body weight and HbA1c levels may underlie the observed decrease in hepatocellular lipid content (HCL) [44, 45]. On the other hand, empagliflozin (EMPA) may improve NAFLD independently of body weight and glycemia [46, 47]. It is important to note that SGLT2is have demonstrated a positive effect on inflammation, oxidative stress, and dysregulated hormone secretion in preclinical studies [40]. The effect of SGLT2is alone or in combination with other antihyperglycemic treatments on NAFLD and its progression remain of high relevance for the clinical practice and need to be tested in randomized controlled clinical trials as they hold promise as future NAFLD treatment options.

Studies have shown that insulin signaling in the central nervous system plays a crucial role in regulating peripheral energy and glucose homeostasis in rodents and dogs (Figure 3) [48, 49]. Furthermore, the

vagus nerve mediates brain-liver crosstalk, as brain insulin effects are eliminated when hepatic vagotomy is performed [50]. Additionally, it has been suggested that brain insulin's ability to suppress hepatic gluconeogenesis via hepatic IL-6/STAT3 activation depends on the hepatic vagal branches [51]. Although research suggests that the vagus nerve could play a significant role in regulating glucose homeostasis, its relevance in humans remains unclear.

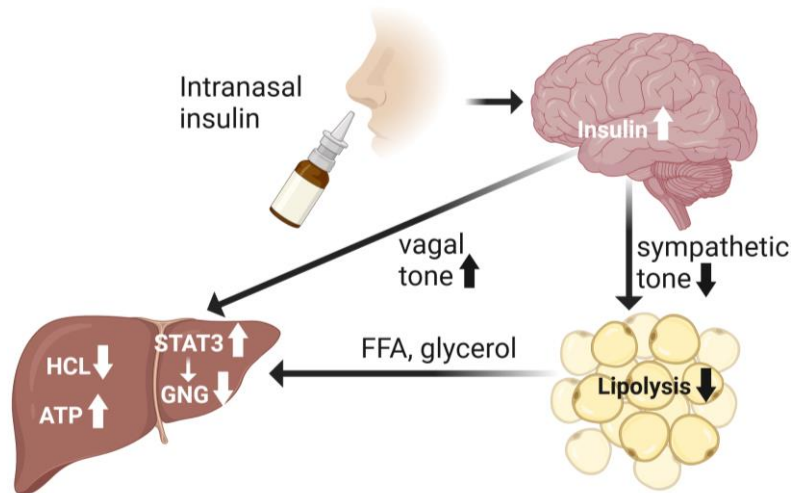


**Figure 3.** Central insulin effects on hepatic glucose and energy metabolism. Illustration by S. Gancheva created with BioRender.com

Studies using the intranasal delivery of insulin to the brain have provided evidence supporting the idea of central regulation of whole-body glucose uptake and adipose tissue lipolysis [52, 53]. We have previously shown that intranasal insulin improves hepatic energy metabolism and reduces liver lipid content in lean, healthy individuals but not in those with type 2 diabetes (Figure 3) [54]. However, the mechanism underlying this brain-liver crosstalk remains unclear. Studies have demonstrated that parasympathetic tone, as measured by heart rate variability, is correlated with changes in whole-body insulin sensitivity following intranasal insulin administration in humans [55], indicating that vagal outputs may also mediate peripheral insulin sensitization. Transcutaneous auricular vagus nerve stimulation (taVNS) applied to the external ear of humans can activate the central projections of the auricular branch of the vagus nerve without invasive procedures [56]. This technique induces an increase in the activity of the nucleus tractus solitarii (NTS), as observed through functional magnetic resonance imaging [56]. Another taVNS study found reduced sympathetic outflow, as assessed through microneurography and increased heart rate variability which point towards reduced sympathetic tone after taVNS stimulation [57]. Moreover, taVNS appears to lower sympathetic tone through the induction of caudal ventrolateral medulla activity, which inhibits rostral ventrolateral medulla and thus reduces sympathetic output. This suggests that taVNS may act on the sympathetic nervous system independent of vagal activation. Of note, brain insulin action on adipose tissue lipolysis has been

suggested to be mediated by sympathetic outputs in rodent models (Figure 3) [58]. Thereby the peripheral effects of central insulin might be mimicked by modulation of the sympathetic/parasympathetic tone. VNS is currently used as an adjunctive therapy for medically refractory epilepsy [59], but it has also shown potential as a treatment option for major depressive disorder [60] and Alzheimer's disease [61]. Although the metabolic effects of vagal stimulation are not fully understood, some studies have shown increased energy expenditure [62] and reduced postprandial insulin secretion [63] in humans. Studies on Zucker diabetic fatty rats suggest that taVNS has the potential to prevent hyperglycemia [64]. Nevertheless, it is currently unclear whether hepatic glucose and lipid metabolism can be modulated by non-invasive taVNS in humans.

### 1.2 Role of mitochondrial function for insulin resistance

Mitochondria are intracellular organelles that are actively involved in a variety of critical metabolic processes, including the oxidative catabolism of substrates through the tricarboxylic acid cycle and fatty acid  $\beta$ -oxidation, the production of energy in the form of ATP through oxidative phosphorylation, and the generation of reactive oxygen species (Figure 4) [65]. These organelles are also vital for maintaining processes such as cellular growth, programmed cell death, and intracellular signaling while playing a key role in the regulation of nitric oxide and calcium homeostasis. Because of the diverse range of functions carried out by mitochondria, assessing the extent of potential impairments to their function can be challenging and depends on the specific criteria used for evaluation.

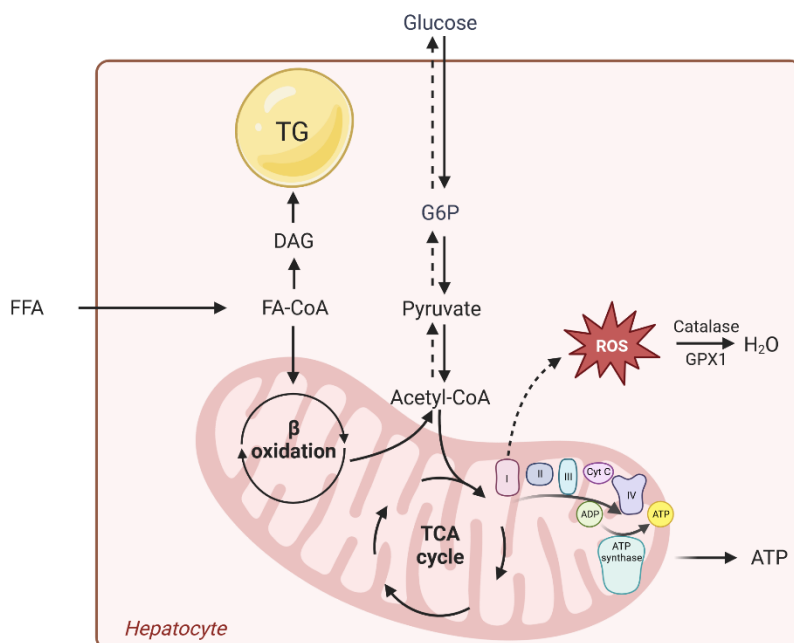


**Figure 4.** Hepatic mitochondrial function and lipid metabolism. Illustration by S. Gancheva created with BioRender.com

Insulin resistance is a crucial characteristic of T2D that is associated with various alterations in mitochondrial function and content in insulin-responsive tissues [7]. Besides obesity, genetic predisposition and aging play important roles in insulin resistance and mitochondrial function [66, 67]. Impaired mitochondrial functionality is present in first-degree relatives of individuals with T2D who are also insulin resistant [68]. Notably, healthy elderly individuals with normal weight exhibit lower insulin sensitivity, higher triglyceride content in the skeletal muscles and liver, along with reduced mitochondrial TCA cycle flux and ATP synthesis, which were measured by combined  $^{13}\text{C}/^{31}\text{P}$  MRS [69]. This points to the key role of insulin resistance and aging for mitochondrial alterations.

There is a correlation between insulin resistance in skeletal muscle and changes in mitochondrial dynamics, flexibility, content, and decreased responsiveness of mitochondrial ATP production in response to high-dose insulin infusion [70, 71]. As insulin resistance worsens, there is a reduction in electron transport chain (ETC) activity, as evidenced by a significant decrease in skeletal muscle complex I activity and protein content [72]. A study of respiratory capacity in insulin-resistant human skeletal muscle revealed a 25% reduction *in vivo* (PCr recovery post-exercise) and *ex vivo* (basal and maximal ADP-stimulated respiration) compared to controls, independent of differences in mitochondrial content [73]. In addition, individuals with overweight and T2D exhibit up to a 40% reduction in mitochondrial content in skeletal muscle when compared to lean healthy participants, which is due to decrease in intermyofibrillar mitochondrial population [72]. Mitochondrial content and function have been shown to improve after bariatric surgery [74, 75]. Of note, dissociation between muscle mitochondrial function and insulin sensitivity with aging [76] as well as between mitochondrial substrate preference and insulin sensitivity [77] have been described previously. Whether muscle mitochondrial function and content are changed in parallel to improved insulin sensitivity following bariatric surgery as well as the time course of the respective changes remain unclear.

### **1.2.1 Hepatic mitochondrial function in type 1 diabetes**

NAFLD is closely related to insulin resistance, which is the key characteristic of type 2 diabetes. However, recent research has also revealed a link between NAFLD and type 1 diabetes, as this association results in similar negative outcomes as those observed in people with type 2 diabetes [78, 79]. Furthermore, the role of insulin resistance in the development of type 1 diabetes has become increasingly important [80, 81]. Insulin resistance was initially attributed to long-term glucose toxicity, but it is now believed that mitochondrial function may also be impaired, as evidenced by lower muscle ATP synthase flux in type 1 diabetes individuals [82]. Notably, there is an inverse correlation between muscle ATP synthesis and HCL [83], suggesting a close connection between liver and muscle energy metabolism.

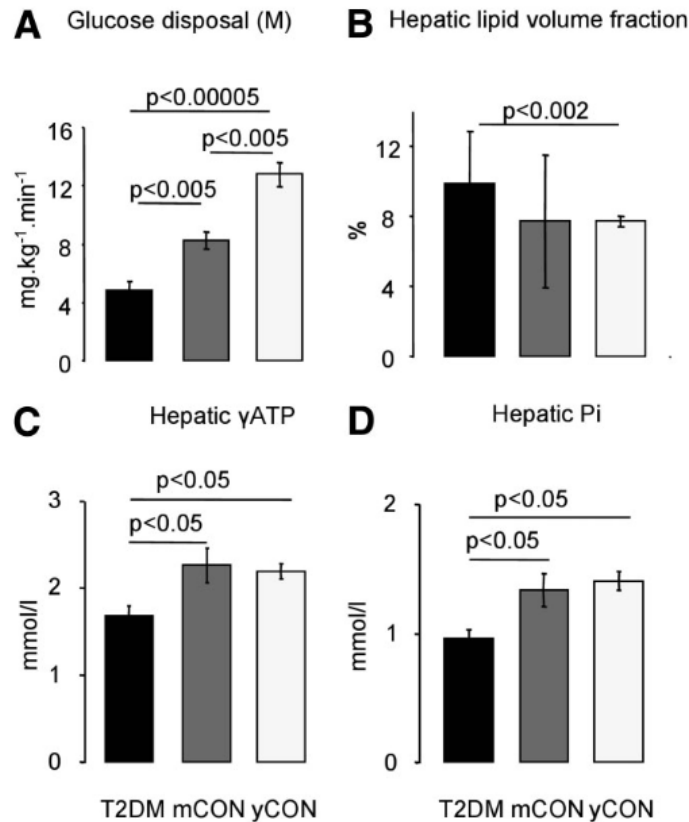


**Figure 5.** Insulin sensitivity (A), hepatic lipid content (B), ATP (C) and inorganic phosphate (D) concentrations in people with type 2 diabetes (T2DM), age-matched healthy controls (mCON) and young healthy controls (yCON). Illustration from Szendroedi et al [84] with the permission of Wolters Kluwer Health.

In overt type 2 diabetes, hepatic concentrations of energy-rich substrates such as inorganic phosphate (Pi) and ATP are decreased and are associated with increased lipid accumulation and insulin resistance in the liver (Figure 5) [84]. Furthermore, hepatic flux through ATP synthase has also been shown to be reduced in T2D [85]. However, in the NOD mouse, which is a model of human type 1 diabetes, hepatic respiratory capacity was transiently elevated paralleled by an increase in lipid peroxide production [86]. Human studies have shown evidence of enhanced hepatic energy metabolism in people with obesity and hepatic steatosis [31, 87]. Therefore, it remains unclear whether hepatic energy homeostasis is altered in the context of type 1 diabetes-related NAFLD and which factors contribute to the abnormalities.

Insulin resistance and obesity have been found to increase over time in individuals with T1D [88], and the mechanisms described in T2D-related NAFLD development may also be relevant to T1D [81, 89]. As humans with T1D rely on external subcutaneous insulin administration, one factor that can affect the pathophysiology of NAFLD in these individuals is the altered dynamic of insulin delivery and

clearance. In people with NAFLD, hyperinsulinemia appears to be more closely linked to impaired insulin clearance than increased insulin secretion [90]. A recent study explored the metabolic factors associated with NAFLD in T1D and found that poor glycemic control (HbA1c >7%) doubled the risk of developing NAFLD [91]. In addition, NAFLD prevalence was higher in people who were overweight compared to overall NAFLD prevalence. In normal-weight individuals with type 1 diabetes NAFLD prevalence relates directly with the insulin dose, pointing at the critical role of exogenous insulin and obesity for NAFLD development.

Elevated blood glucose levels resulting from poor glycemic control can increase the expression of GLUT-2, a glucose transporter present in hepatocytes. This leads to insulin resistance and hyperinsulinemia with hyperglycemia, which prompts an increase in hepatic lipogenesis [92]. The availability of lipogenic substrates (such as glucose) is increased through the rise in GLUT-2, and the lipogenic effect of insulin on *de novo* lipogenesis also contributes to this upregulation. While glycogen synthesis is augmented due to the high blood glucose levels and insulin activity, prolonged exposure to hyperglycemia can saturate glycogen synthesis pathways, causing glucose to be redirected towards lipogenic pathways [93], which favors the development of NAFLD. Whether this also contributes to alterations in hepatic energy metabolism and changes in hepatic ATP content in type 1 diabetes remains unclear.

### **1.2.2 Hepatic mitochondrial function in NAFLD**

Hepatic mitochondria play a key role in energy production through the oxidation of various substrates including amino acids, pyruvate, and fatty acids. The tight coupling between substrate oxidation and ATP synthesis through oxidative phosphorylation (OXPHOS) is precisely regulated by different factors present within and outside hepatocytes (Figure 4). Hepatic mitochondria exhibit alterations in obesity and T2D, which reflect their essential role for liver function, substrate metabolism and cellular signaling [94]. Studies examining hepatic mitochondrial function in individuals with T2D have yielded varying results partly due to the use of different methods and experimental conditions as well as the inclusion of different T2D groups. Hepatic ATP content and synthesis measured *in vivo* with MRS were found to be lower in elderly individuals with long-standing T2D [84, 85]. At 5 years after T2D diagnosis, hepatic inorganic phosphate, but not ATP, appears to decrease alongside an increase in visceral adipose tissue (VAT) and liver lipid content [88]. Another study using <sup>13</sup>C-ketoisocaproate revealed that reduced mitochondrial function in individuals with non-alcoholic fatty liver disease was inversely associated with age, obesity and diabetes status [95]. On the contrary, a high-resolution respirometry study showed no changes in OXPHOS capacity and citrate synthase activity among individuals with normal weight, obesity and T2D [96]. However, the similarity in liver lipid droplet area and density among all groups indicates that this cohort represents specific phenotypes since the vast majority of individuals

with overt T2D has elevated liver lipid content. Recent cluster analyses have identified endotypes of diabetes mellitus, distinguishing between those with severe insulin-deficiency and severe insulin-resistance from more moderate obesity-related or age-related diabetes [15]. In this analysis, the severe insulin-resistant diabetes endotype was not only associated with the highest liver lipid content at diagnosis, but also with greater risk of liver fibrosis and higher frequency of the rs738409(G) single nucleotide polymorphism in the PNPLA3 (patatin-like phospholipase domain containing 3) gene [97]. In overall, the specific alterations of hepatic mitochondrial functionality in diabetes appear complex and further investigation of the role of insulin resistance, hyperglycemia and oxidative stress for these changes is warranted.

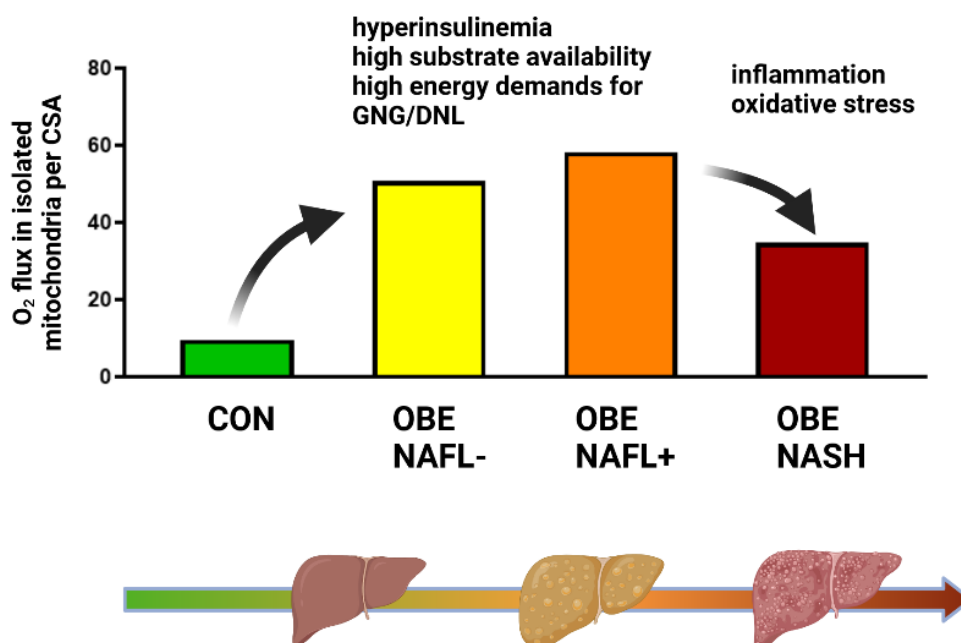


**Figure 6.** Hepatic oxidative capacity in different stages of NAFLD. Illustration by S. Gancheva created with BioRender.com

Hepatic energy metabolism alterations have been described in obesity and NAFLD from direct and indirect assessments of hepatic mitochondrial function in humans. *In vivo* <sup>31</sup>P MRS studies have shown that hepatic ATP content in individuals with obesity and NAFLD are similar to those of lean individuals in the fasting state, but a 6-fold higher postprandial ATP increase is observed in the obese individuals compared to lean controls [84, 87]. Oxygen fluxes in whole-liver tissue and mitochondria isolated from intraoperative liver samples of individuals with obesity and various stages of biopsy-proven nonalcoholic fatty liver disease, including nonalcoholic steatohepatitis revealed substantially greater OXPHOS capacity and respiratory control in obesity with and without simple steatosis but not in NASH when compared to lean individuals without NAFLD (Figure 6) [31]. The elevated OXPHOS capacity paralleled by low intrahepatic triglyceride levels supports the concept of an adaptation of hepatic

mitochondria to rising lipid availability, which helps to protect the liver from lipotoxicity and steatosis in the settings of obesity. A further study in lean people without steatosis revealed an increase in hepatic ATP content by 16 % measured *in vivo* by <sup>31</sup>P magnetic resonance spectroscopy after an oral fat load, which additionally supports the concept of hepatic mitochondrial adaptation to higher lipid influx [98]. Of note, hepatic OXPHOS capacity was ~40–51% lower in NASH than in obese individuals with/without steatosis and ~10% lower than in lean non-steatotic humans, while proton leak across inner mitochondrial membrane, H<sub>2</sub>O<sub>2</sub> production and oxidative DNA damage were increased [31]. The elevation of ROS levels could promote mitochondrial fission and hinder mitophagy, resulting in a buildup of damaged mitochondria within hepatocytes, which cannot be recycled properly. This scenario may lead to the release of mitokines and cytochrome c-related apoptosis, as indicated by previous studies [99]. To what extent hyperglycemia and hepatic fibrosis contribute to the reduction of hepatic OXPHOS capacity in NASH remains unclear. Additional studies are required to assess the potential role of lipotoxins in mediating mitochondrial damage and the progression of NAFLD as well as their potential utility as biomarkers in NASH. Considering that T2D is not only linked to increased insulin resistance and lipotoxicity but also to an accelerated progression of NAFLD, it is reasonable to propose that T2D is associated with more pronounced hepatic mitochondrial abnormalities. However, further studies are needed to confirm this hypothesis and elucidate the specific mechanisms involved.

### **1.2.3 Hepatic mitochondrial function in organic acidemias**

Metabolic disease-related liver conditions occur mainly in individuals with obesity and T2D but are also present in those with rare diseases such as lipodystrophies and inborn errors of metabolism, such as organic acidemias. Organic acidemias (OAs) are metabolic disorders resulting from deficiencies in mitochondrial enzymes or co-factors participating in branched-chain amino acid (BCAA) catabolism [100]. Accumulation of specific metabolites such as propionic acid, isovaleric acid, and methylmalonic acid in OAs have been shown to induce toxic effects [101, 102]. Isolated methylmalonic acidemia (MMA) arises from a deficiency of the enzyme methylmalonyl-CoA mutase, defects in the transport or synthesis of its cofactor adenosylcobalamin or a deficiency of the enzyme methylmalonyl-CoA epimerase. In cases of MMA and propionic acidemia (PA), excess propionyl-CoA production blocks the activity of TCA cycle and urea cycle [103]. In addition, isovaleric and methylmalonic acid accumulation also can impair mitochondrial function and structure. As a result of defect branched-chain amino acid catabolism, lack of substrates for TCA cycle may further damage mitochondrial functionality [104]. Many of the insights into mitochondrial abnormalities in organic acidemias stem from preclinical and postmortem studies, while *in vivo* assessments of mitochondrial function are scarce. As anaplerotic and/or antioxidant therapy targeting normalization of mitochondrial function and oxidative stress hold promise as treatment strategies for these humans [105], further investigation of the specific alterations of mitochondrial functionality is necessary.

#### **1.2.4 Bariatric surgery effects on skeletal muscle mitochondrial function and insulin resistance**

Bariatric or metabolic surgery leads to pronounced weight loss and has emerged as promising treatment option for people with type 2 diabetes as it appears superior to current best medical treatment [106]. While bariatric surgery has been shown to improve whole-body insulin sensitivity in the long term, the early metabolic effects and underlying mechanisms remain unclear [107, 108]. Skeletal muscle plays a key role in whole-body insulin sensitivity, and insulin-resistant individuals present with reduced muscle mitochondrial capacity [109]. Recent research has demonstrated that diet-induced weight loss swiftly enhances hepatic, but not muscle insulin resistance in humans [110]. The impact of metabolic surgery on mitochondria is variable and may also affect lipolysis and intracellular lipid intermediates [74], but the precise time course of changes remains unclear. Furthermore, current data on DNA methylation changes in skeletal muscle following gastric bypass surgery is conflicting [111, 112] and it remains uncertain whether epigenetic changes happen early on or later after metabolic surgery, and how this might relate to gene expression.

Weight loss can not only improve insulin sensitivity but also normalize growth hormone (GH) secretion [113]. Bariatric surgery has been shown effective in altering gastrointestinal hormones controlling energy homeostasis and increasing circulating GH concentrations [114]. However, cross-sectional studies on its impact on insulin-like growth factor 1 (IGF-1) have yielded conflicting results [115-118]. IGF-1 plays a role in regulating both GH and insulin secretion to promote physiological carbohydrate and lipid metabolism. However, the contribution of IGF-1 in improving tissue-specific insulin sensitivity after bariatric surgery remains uncertain. The GH-IGF-1 axis involves complex regulation that includes hypothalamic neuropeptides, ghrelin, insulin, free fatty acids, nutritional factors, and IGF-1 binding proteins (IGFBPs) [119]. Leptin, an indicator of fat mass and a key signal of long-term energy availability, inhibits GH secretion and can regulate IGF-1 secretion. Recent studies have shown that leptin substitution in children with leptin deficiency increases IGF-1 levels [120]. The enhancement of insulin sensitivity following metabolic surgery has been shown to reinstate leptin sensitivity, through a molecular process facilitated by fatty acid modulation of muscle malonyl-Co-A synthesis [121]. This highlights a direct correlation between the availability of lipids after bariatric surgery and leptin levels. Nonetheless, a conclusive relation between the growth hormone system and insulin sensitivity after bariatric surgery as well as the underlying mediators have yet to be determined.

## **2. Hypotheses**

### **2.1. Interventions to reduce liver lipid content**

**2.1.1. Liver lipid content is lowered by antihyperglycemic treatment with SGLT2 inhibitor empagliflozin in people with T2D**

**2.1.2. Liver lipid content is lowered by non-invasive vagus nerve stimulation in healthy humans**

### **2.2. Increased substrate availability and hepatic energy metabolism**

**2.2.1. Hepatic ATP concentrations are reduced in T1D and relate to hyperglycemia**

**2.2.2. Hepatic mitochondrial oxidative capacity is reduced in NASH with T2D and relates to hyperglycemia and oxidative stress**

**2.2.3. Hepatic ATP content is reduced in branched-chain amino acid metabolism disorders and relates to insulin resistance**

### **2.3. Muscle insulin sensitivity improvement after bariatric surgery-induced weight loss in people with obesity:**

**2.3.1. is paralleled by reduction in lipid availability and increase in muscle mitochondrial function**

**2.3.2. relates to the restoration of the growth hormone-IGF1-axis**

### **3. Results**

We addressed the above-mentioned hypotheses in clinical-experimental studies in humans. The main findings are briefly summarized in the following sections. The full texts are attached to this document.

#### **Effects of antihyperglycemic treatment with empagliflozin and vagus stimulation on hepatic lipid content and energy metabolism**

- 3.1.** Empagliflozin reduces hepatic lipid content in people with well-controlled type 2 diabetes (study 1)
- 3.2.** Non-invasive vagus nerve stimulation does not affect hepatic lipid content and energy metabolism in healthy humans (study 2)

#### **Alterations of hepatic mitochondrial function in diabetes, NAFLD and organic acidemias**

- 3.3.** Lower hepatic ATP concentrations in humans with type 1 diabetes relate to variants in genes controlling oxidative metabolism, but not with insulin sensitivity (study 3)
- 3.4.** Loss of adaptation of hepatic oxidative capacity in humans with type 2 diabetes and non-alcoholic steatohepatitis (study 4)
- 3.5.** Genetic alteration in mitochondrial function in organic acidemias does not relate to changes in hepatic ATP concentrations (study 5)

#### **Mitochondrial function and insulin sensitivity after bariatric surgery**

- 3.6.** Epigenetic and mitochondrial changes in skeletal muscle underlie the improvement of insulin sensitivity after bariatric surgery (study 6)
- 3.7.** Bariatric surgery-induced restoration of the growth hormone system relates to improved adipose tissue insulin sensitivity (study 7)

### 3.1 Empagliflozin reduces hepatic lipid content in well-controlled people with type 2 diabetes

**Background:** Humans with T2D are at increased risk of developing NAFLD with faster progression from steatosis to non-alcoholic steatohepatitis, fibrosis and cirrhosis [39]. Currently, no approved pharmacological treatment for NAFLD is available, but substantial weight loss has been shown to improve NAFLD. The sodium-glucose cotransporter 2 inhibitor empagliflozin not only improves glycemia, but also leads to weight loss and improves cardiovascular [40] and renal [41] outcomes. Whether empagliflozin reduces liver lipid content in recent-onset and metabolically well-controlled humans with T2D remains unknown.

**Methods:** Humans with known T2D duration of  $39 \pm 27$  months ( $n = 84$ , HbA1c  $6.6 \pm 0.5\%$  [ $49 \pm 10$  mmol/mol]) were randomly assigned to 24 weeks of treatment with 25 mg daily empagliflozin or placebo. The change in liver lipid content from 0 (baseline) to 24 weeks between groups was measured with magnetic resonance methods. Tissue-specific insulin sensitivity was assessed by hyperinsulinemic euglycemic clamps using isotope dilution technique. In addition, hepatokines FGF21, CK18 M30 and CK18 M65 as well as the adipokine adiponectin were assessed using ELISAs. Statistical comparison was done by ANCOVA with adjustment for baseline values, age, sex, and BMI.

**Results:** At 24 week a placebo-corrected absolute change of  $-1.8\%$  (95% CI  $-3.4, -0.2$ ;  $P = 0.02$ ) and relative change in liver lipid content of  $-22\%$  ( $-36, -7$ ;  $P = 0.009$ ) was found with empagliflozin treatment, corresponding to a 2.3-fold higher reduction in liver lipids (Figure 7). Empagliflozin treatment resulted in placebo-corrected weight loss of  $-2.5$  kg (95% CI  $-3.7, -1.4$ ;  $P < 0.001$ ) from baseline to 24 weeks, while no placebo-corrected change in tissue-specific insulin sensitivity was found. Serum uric acid decreased and high-molecular-weight adiponectin increased with empagliflozin treatment from 0 to 24 weeks, while FGF21 did not differ between groups.

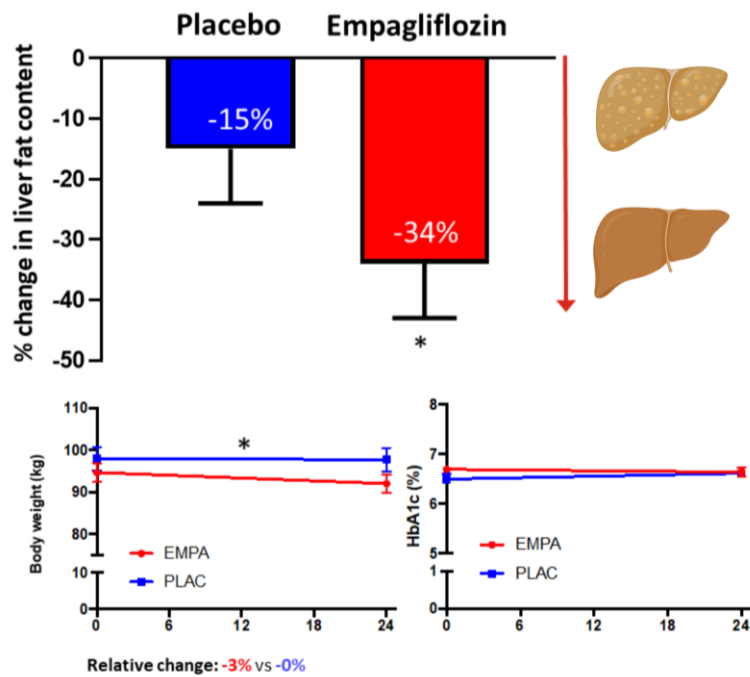


**Figure 7.** Changes in liver lipid content, body weight and HbA1c after empagliflozin treatment. Adapted from Kahl et al. [122] American Diabetes Association. Copyright and all rights reserved. Material from this publication has been used with the permission of American Diabetes Association.

**Conclusions:** Effective reduction of hepatic lipid accumulation can be achieved with empagliflozin treatment in humans with well-controlled T2D and short known disease duration. However, no major effect on muscle, hepatic and adipose tissue insulin sensitivity is found in the settings of moderate weight loss and minor changes in glycemia. Of note, empagliflozin also decreases circulating uric acid and raises adiponectin levels, which are known to associate with body weight, metabolic syndrome features and NAFLD. Empagliflozin could therefore contribute to the early treatment of nonalcoholic fatty liver disease in T2D.

**Limitations:** The good metabolic control and short disease duration of the participants possibly lead to an underestimation of the efficacy of empagliflozin on liver lipid content, as high HbA1c and longer diabetes duration relate to increased NAFLD incidence. Thereby the results are not applicable to humans with uncontrolled hyperglycemia, long standing T2D or advanced forms of metabolic liver disease. No liver biopsies were obtained in this study due to ethical considerations, which did not allow a pathomechanistic investigation of possible underlying liver glucose and lipid metabolism changes. Furthermore, predominantly male participants were included in the study and reductions in liver lipid were found in males, but not in females without significant interaction of sex and treatment, so that sex-dependent differences in the metabolic effects on hepatic steatosis cannot be excluded and need further examination.

**Advantages:** The study provides proof-of-concept that empagliflozin effectively decreases liver lipid content, while reducing body weight and increasing adiponectin. Thereby empagliflozin might serve as a partner for future combined NAFLD treatment strategies in T2D, which simultaneously address the different mechanisms underlying metabolic liver disease.

### 3.2 Non-invasive vagus nerve stimulation does not affect hepatic lipid content and energy metabolism in healthy humans

**Background:** Insulin signaling in the brain is a key regulator of peripheral metabolism and brain insulin-induced suppression of endogenous glucose production has been suggested to be mediated by the vagus nerve. Transcutaneous auricular vagus nerve stimulation (taVNS) reduces sympathetic outflow and might increase the nucleus tractus solitarii activity, which is an important central vagus nerve projection. Intranasal insulin application, which mimics brain insulin delivery in humans, has been shown to improve hepatic energy metabolism and reduce liver lipid content in healthy humans [54]. Whether these effects could be mediated by the parasympathetic nervous system remains unclear. While rodent data demonstrated amelioration of hyperglycemia in diabetes models via vagus stimulation, these findings have not been translated to humans yet.

**Methods:** The effects of 14-min taVNS via Cerbomed Nemos® on glucose metabolism, lipids, and hepatic energy homeostasis were studied in fasted healthy humans ( $n = 10$ , age  $51 \pm 6$  yrs, BMI  $25.5 \pm 2.7$  kg/m<sup>2</sup>). Sham stimulation was performed as a control condition. As a readout of sympathetic and parasympathetic nerve activity, heart rate variability (HRV) and serum pancreatic polypeptide were measured before, during and after taVNS or sham stimulation. Isotopic dilution with [6,6-<sup>2</sup>H<sub>2</sub>]glucose was used to assess endogenous glucose production while hepatic concentrations of triglycerides (HCL), adenosine triphosphate (ATP), and inorganic phosphate (Pi) were quantified from <sup>1</sup>H/<sup>31</sup>P magnetic resonance spectroscopy at baseline and at 180 min after the stimulation.

**Results:** No differences were found in circulating glucose, free fatty acids, insulin, glucagon, or pancreatic polypeptide after taVNS compared to sham stimulation. Rates of endogenous glucose production, hepatic HCL, ATP, and Pi were also comparable (Figure 8). Prolonged fasting over 13 h did not cause changes in hepatic HCL, ATP, and Pi. HRV was not altered towards sympathetic or parasympathetic predominance after taVNS.

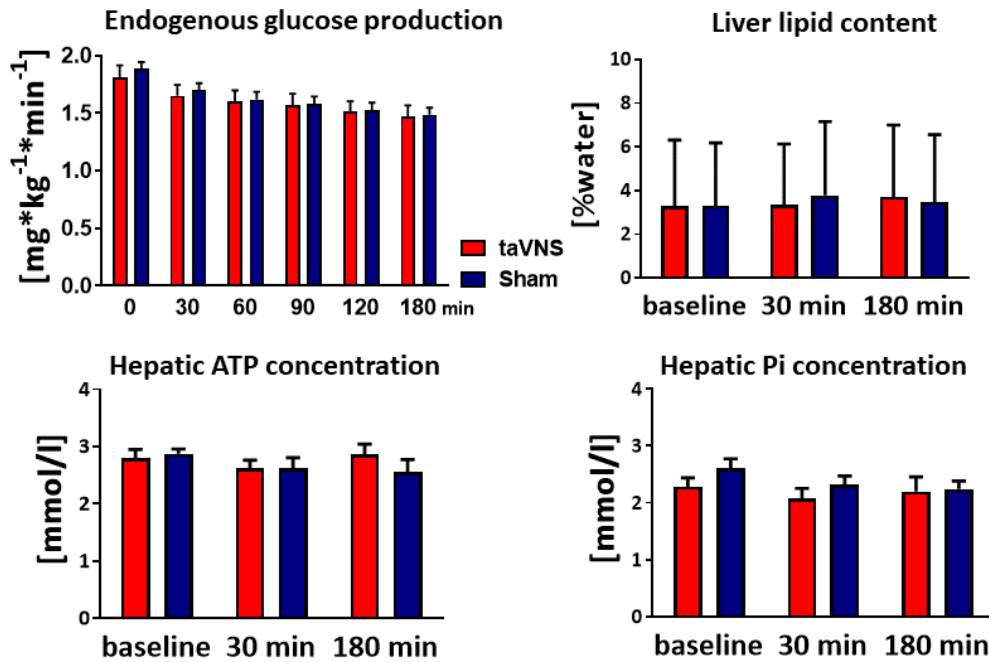


**Figure 8.** Time course of endogenous glucose production, liver lipid content and energy metabolism after taVNS and sham stimulation. Adapted from Gancheva et al. [123] by adding color to original graphs under the [CC BY-NC-ND license](https://creativecommons.org/licenses/by-nc-nd/4.0/)

**Conclusion:** No change in parasympathetic tone to the pancreas and the heart was found after non-invasive vagus stimulation using Cerbomed Nemos<sup>®</sup> compared to sham procedure. Thereby no changes were observed in hepatic glucose and energy metabolism, suggesting that this technique is unable to mimic intranasal insulin- effects and modulate hepatic energy homeostasis in humans. Hepatic energy rich substrates as well as lipid content remain stable over prolonged fasting in the face of fasting-related alterations of circulating metabolites such as increase in free fatty acids and decrease in endogenous glucose production over time. Promising findings from rodent studies using taVNS to improve glucose metabolism could not be translated to humans and cutaneous electrical stimulation with Cerbomed Nemos<sup>®</sup> does not seem to have potential as a future treatment in type 2 diabetes.

**Limitations:** The non-invasively applied taVNS did not alter parasympathetic output and thereby metabolic effects could not be analyzed. While the study shows that the Cerbomed Nemos® stimulation with the described parameters and duration does not affect human metabolism, it could not be excluded that other vagal stimulation techniques, such as cervical vagus branch stimulation, might be effective. Thereby an important limitation of the paper is the use of a single specific non-invasive technique to modulate parasympathetic tone, while other more invasive approaches might be able to affect peripheral metabolism.

**Advantages:** The study benefits from the simultaneous close monitoring of peripheral nervous system activity together with metabolic changes using *in vivo* non-invasive techniques. Despite revealing negative results, the study provides important insights into the possibilities for metabolic control based on modulation of the nervous system.

### 3.3 Lower hepatic ATP concentrations in humans with type 1 diabetes relate to variants in genes controlling oxidative metabolism

**Background:** Nonalcoholic fatty liver disease closely relates to insulin resistance, obesity, and type 2 diabetes. Type 1 diabetes has also been linked to insulin resistance and fatty liver disease [81, 124]. In addition, muscle mitochondrial function as measured from muscle ATP synthase flux is impaired in type 1 diabetes [82]. In a mouse model of human type 1 diabetes hepatic respiratory capacity is increased and relates to oxidative stress [86]. Still, the role of insulin resistance, liver lipid content and hyperglycemia for hepatic energy metabolism in type 1 diabetes remains unclear.

**Methods:** To assess early abnormalities in hepatic energy metabolism 55 humans were included in this study. They were recently diagnosed with type 1 diabetes and underwent hyperinsulinemic-normoglycemic clamps with [6,6-<sup>2</sup>H<sub>2</sub>]glucose to measure whole-body and hepatic insulin sensitivity. Multinuclei magnetic resonance spectroscopy (<sup>31</sup>P/<sup>1</sup>H-MRS) was used to quantify absolute concentrations of hepatic ATP, inorganic phosphate (Pi) as well as hepatocellular lipid content. The control group consisted of humans with normal glucose tolerance (n = 57).

**Results:** Humans with type 1 diabetes exhibited 44 % lower whole-body insulin sensitivity than the age- and BMI-matched control group. While hepatic Pi and HCL were comparable in humans with type 1 diabetes and healthy humans, hepatic ATP was 15% lower in humans with type 1 diabetes ( $2.3 \pm 0.6$  vs.  $2.7 \pm 0.6$  mmol/L,  $P < 0.001$ ) (Figure 9). A negative association was found between hepatic ATP and glycemia as well as oxidized LDL across all participants. Hepatic ATP concentrations were 21 and 13 % lower in carriers of the PPARG G allele (rs1801282) and noncarriers of PPARGC1A A allele (rs8192678), respectively.

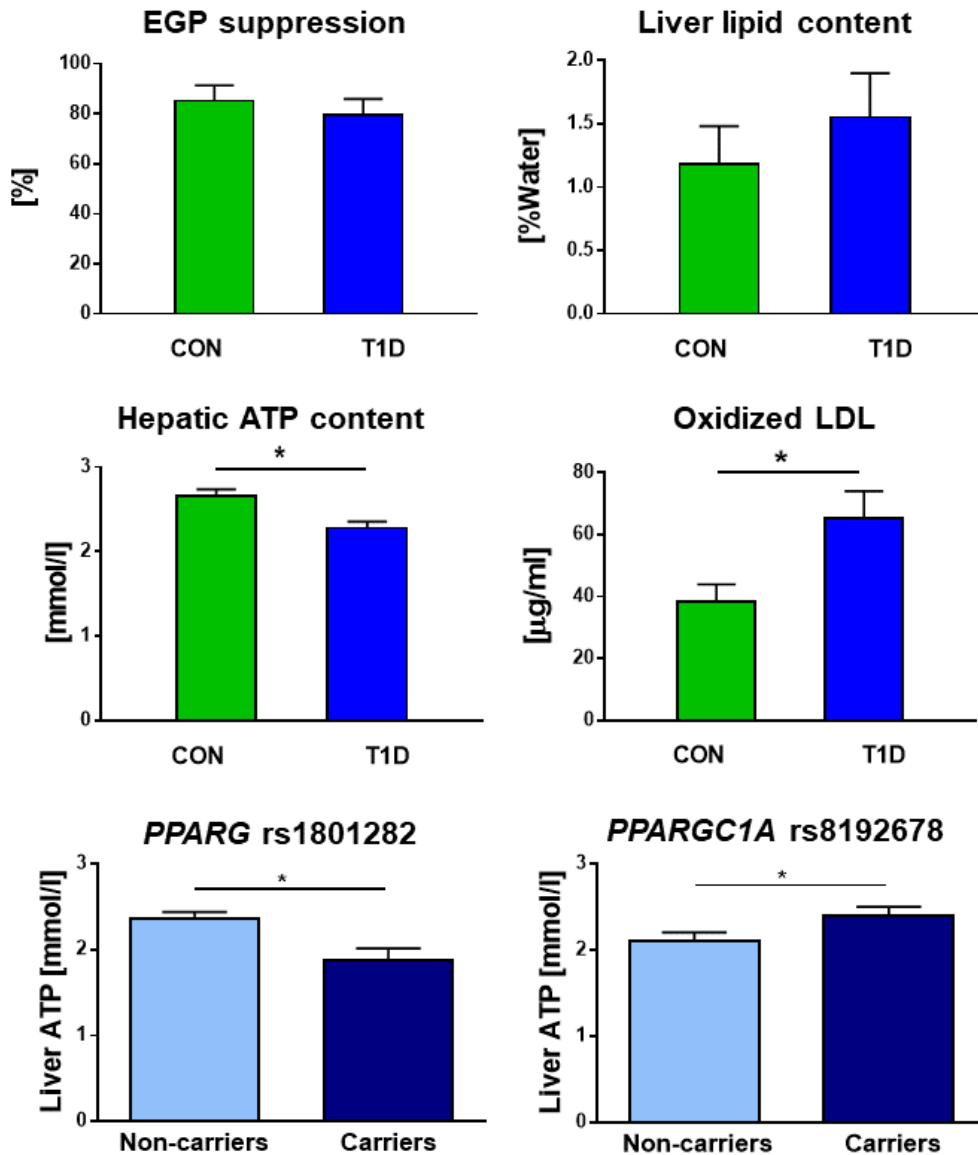


**Figure 9.** Hepatic glucose, lipid and energy metabolism in type 1 diabetes. Adapted from Gancheva et al. [125] American Diabetes Association. Copyright and all rights reserved. Material from this publication has been used with the permission of American Diabetes Association.

**Conclusions:** Hepatic energy metabolism is already impaired in recent onset well-controlled type 1 diabetes independent of hepatic steatosis and insulin sensitivity. Variants in genes controlling oxidative metabolism contribute to lower hepatic ATP in the absence of NAFLD, suggesting that alterations in hepatic mitochondrial function manifest early in the course of the disease and may precede diabetes-related liver diseases. While previous studies demonstrated reduced hepatic ATP and Pi concentrations as well as lower flux through ATP synthase in T2D, this work suggests abnormal liver energy homeostasis could be associated with common hallmarks of type 1 and 2 diabetes such as

hyperglycemia or muscle and hepatic insulin resistance. The data underlines the relevance of liver mitochondrial function as an early metabolic marker of liver disease in diabetes.

**Limitations:** The cross-sectional design of the study does not allow to draw conclusions on the role of type 1 diabetes for NAFLD pathogenesis. Of note, no liver biopsies were available here for assessment of hepatic mitochondrial capacity in order to relate the findings to previously described alterations in hepatic mitochondrial function in humans with obesity with or without NAFLD. In addition, whether diminished production or increased consumption of ATP was responsible for the observed alterations could not be differentiated by this study, but increased rates of energy consuming processes like unrestrained hepatic gluconeogenesis in the settings of portal hypoinsulinemia might contribute to the reduction of hepatic energy status.

**Advantages:** The study benefits from the combination of in-depth metabolic characterization using *in vivo* techniques such as multinuclei MRS and hyperinsulinemic-euglycemic clamps with genotyping in a unique cohort of humans with newly-diagnosed type 1 diabetes.

### 3.4 Loss of adaptation of hepatic oxidative capacity in people with type 2 diabetes and non-alcoholic steatohepatitis

**Background:** Non-alcoholic fatty liver disease tightly relates to type 2 diabetes as the majority of humans with T2D exhibit NAFLD and prevalence of NASH in T2D, in particular, is very high. People with type 2 diabetes are at higher risk of progression of simple steatosis to steatohepatitis, fibrosis, and cirrhosis. Altered mitochondrial function might be involved in NAFLD progression as hepatic energy metabolism in T2D exhibits perturbations, including reduced hepatic ATP concentrations, and lower flux through ATP synthase [84, 85]. Hepatic mitochondrial function of individuals with obesity adapts by upregulation of mitochondrial capacity, which may be lost during the progression of NAFLD [31]. Whether T2D plays a role for the loss of adaptation of hepatic mitochondrial function in states of severe obesity and insulin resistance as well as the possible contribution of oxidative stress and advanced glycation endproducts in this process remain unclear.

**Methods:** Humans with obesity with histologically proven NASH without ( $n = 30$ ; BMI  $52 \pm 9$  kg/m<sup>2</sup>) or with type 2 diabetes ( $n = 15$ ;  $51 \pm 7$  kg/m<sup>2</sup>) were studied. Healthy participants without liver disease ( $n = 14$ ;  $25 \pm 2$  kg/m<sup>2</sup>) served as controls. Hyperinsulinemic-euglycemic clamps with [6,6-<sup>2</sup>H<sub>2</sub>]glucose were performed to assess insulin sensitivity. Hepatic mitochondrial capacity was measured by high-resolution respirometry in intraoperative liver biopsies. Hepatic protein expression of markers of mitochondrial content and dynamics as well as mitophagy were quantified.

**Results:** Participants with NASH and T2D had similar liver lipid content, lobular inflammation, and fibrosis as humans without T2D, while hepatic insulin sensitivity was lower than in CON. Age-adjusted hepatic oxidative capacity in liver tissue was 59 % higher in people with NASH without T2D than in controls, whereas humans with T2D presented with 33 % lower complex II-linked oxidative capacity than humans without T2D and higher H<sub>2</sub>O<sub>2</sub> production than healthy humans (Figure 10). Humans with T2D also exhibited evidence of lower hepatic mitochondrial fusion (MFN2), while mitophagy (PINK1, PARKIN) was not altered. Among the NASH groups oxidative capacity correlated negatively with hepatic insulin resistance, glycemia and systemic lipid peroxidation. Humans with NASH with hepatic fibrosis score  $\geq 1$  had reduced oxidative capacity and antioxidant defense than those without fibrosis.

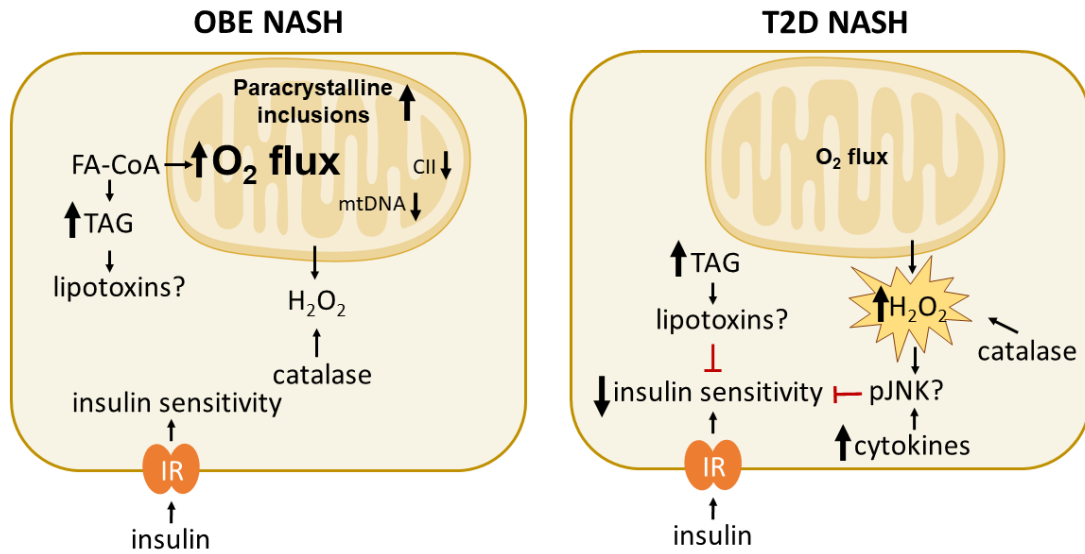


**Figure 10.** Hepatic mitochondrial function in NASH with and without T2D. Illustration created by S. Gancheva.

**Conclusions:** Hepatic mitochondrial oxidative capacity is increased in non-diabetic humans with NASH independent of hepatic mitochondrial content in agreement with previous findings of upregulated oxidative capacity in obesity and hepatic steatosis [31]. The negative relation between fasting blood glucose and hepatic oxidative capacity supports a role of glucotoxicity and hyperglycemia for impairment of hepatic energy metabolism in NAFLD as seen previously in type 1 diabetes [125]. Hepatic fibrosis is key to liver disease progression and the present findings further corroborate the relevance of hepatic mitochondria in the development of NAFLD as well as in metabolic liver injury. Thereby loss of hepatic mitochondrial adaptation may favor metabolic liver disease and is possibly linked to its progression [126].

**Limitations:** An important limitation of the study is the limited number of control participants from which intraoperative samples could be obtained due to ethical considerations. Furthermore, there is currently a lack of uniformly accepted gold standards for measuring hepatic mitochondrial mass in human studies. Thereby we used surrogates such as citrate synthase activity and mitochondrial DNA, which revealed similar results in the participants with and without type 2 diabetes.

**Advantages:** Main strength of the study is the direct assessment of hepatic mitochondrial function in intraoperative liver biopsy samples from individuals with NASH with or without diabetes as well as the inclusion of lean healthy humans in this analysis, which enabled us to reveal differences in mitochondrial function, that might have otherwise remained unrecognized in the case of control group of humans with overweight/obesity.

### **3.5 Genetic alteration of mitochondrial function in organic acidemias does not relate to changes in hepatic ATP concentrations**

**Background:** Deficiencies of mitochondrial enzymes or co-factors involved in branched-chain amino acid catabolism lead to development of organic acidemias, in which metabolite accumulation alters mitochondrial morphology and functionality. States of insulin resistance such as obesity and type 2 diabetes have also been linked to abnormal mitochondrial function along with oxidative stress and ectopic lipid storage [7]. In addition, substrates such as free fatty acids and branched chain amino acids can reduce insulin sensitivity by interfering with signaling pathways in liver and skeletal muscle [6]. Thereby we studied whether genetically impaired mitochondrial function caused by altered branched-chain amino acid catabolism relates to abnormal tissue specific energy metabolism, insulin resistance and ectopic lipid storage.

**Methods:** This case-control study included 31 children and young adults with propionic acidemia, methylmalonic acidemia or isovaleric acidemia. They were compared with 30 healthy young humans. In-depth phenotyping with frequent sampling oral glucose tolerance tests, *in vivo*  $^{31}\text{P}/^1\text{H}$  magnetic resonance spectroscopy of liver and skeletal muscle were employed.

**Results:** Abdominal adiposity, IR, fasting hyperglycaemia and hypertriglyceridemia as well as increased liver lipid accumulation were found in the participants with propionic acidemia, despite dietary energy intake within recommendations for age and sex. Humans with methylmalonic acidemia were characterized by hepatomegaly and mildly lower skeletal muscle ATP content. In skeletal muscle of children and adolescents with propionic acidemia, slightly decreased inorganic phosphate levels were detected. Of note, hepatic ATP and inorganic phosphate concentrations were comparable between all humans with organic acidemias and controls. No abnormalities were detected in the isovaleric acidemia group.

**Conclusions:** Genetic defects in branched-chain amino acid catabolism in propionic acidemia, but not in methylmalonic or isovaleric acidemia, relate to a metabolic syndrome-like phenotype with abdominal adiposity potentially resulting from ectopic lipid storage [127]. These findings suggest additional disease burden in propionic acidemia, which points to the need for further screening for cardiometabolic risk factor clustering in these humans. Similar hepatic ATP content between organic acidemia groups and controls suggests that impairment of electron transport chain activity may only be evident in tissues depending primarily on oxidative phosphorylation such as the brain, the heart and skeletal muscle, but not the liver. Thereby hepatic energy metabolism might remain unaltered, but toxicity of specific metabolites might be responsible for hepatomegaly and other hepatic abnormalities in humans with organic acidemias.

**Limitations:** A major limitation of the study is the lack of some variables in the control group due to ethical considerations related to blood drawing in minors. For that reason data from healthy children was used from a different cohort at a different site and time. In addition, important markers of oxidative stress and leucocyte mitochondrial oxidative capacity were not available in the control participants, which limits our insights into energy metabolism alteration and its relation to reactive oxygen species production in the cohort. Differences in physical activity and in energy intake as well as puberty onset also introduce some variation and limit the generalizability of the results.

**Advantages:** The study benefits from the inclusion of a unique cohort of children and adolescents with rare metabolic diseases as well as a control group of healthy children, who are deeply metabolically characterized using non-invasive *in vivo* techniques such as multinuclei MRS. This is the first report of hepatic and skeletal muscle absolute ATP concentrations in humans with organic acidemias.

### 3.6 Epigenetic and metabolic changes in skeletal muscle underlying the improvement of insulin sensitivity after bariatric surgery

**Background:** Insulin sensitivity improves on the long term after surgically-induced weight loss, but the underlying mechanisms remain unclear. Individuals with obesity are characterized by insulin resistance, which relates to altered mitochondrial function in skeletal muscle [109] and liver [72]. Whether epigenetic mechanisms play a role remains also unclear. Metabolic surgery might affect mitochondrial function and result in epigenetic alterations, but the specific time course of changes and their relation to improvement in insulin sensitivity remain unknown.

**Methods:** We monitored skeletal muscle glucose and energy metabolism in individuals with obesity before and over 52 weeks after metabolic surgery as compared to lean healthy humans at baseline. Comprehensive phenotyping included clamp tests and skeletal muscle biopsies to assess mitochondrial function, transcriptome, epigenome and ultrastructure analysis.

**Results:** Initial weight loss in the settings of adipose tissue insulin resistance with unrestrained lipolysis causes transient elevation of circulating free fatty acids and muscle lipid intermediates, which is paralleled by diacylglycerol activation of muscle protein kinase  $\theta$ . These changes along with a reduction in muscle mitochondrial mass and oxidative capacity prevent from a rapid increase in muscle insulin sensitivity. On the long term, changes in skeletal muscle expression of genes involved in calcium/lipid metabolism and mitochondrial function associate with specific epigenetic modifications, which continuously lead to the restoration of muscle metabolism at 1 year after surgery.

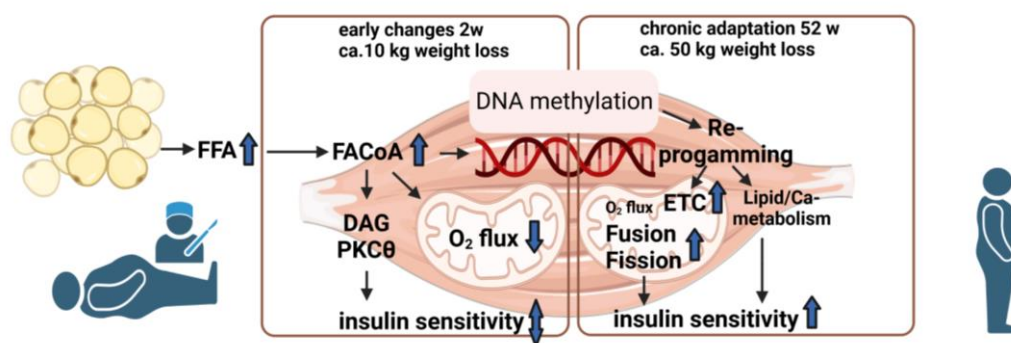


**Figure 11.** Dynamic adaptation of muscle metabolism after bariatric surgery. Illustration by S. Gancheva created with BioRender.com

**Conclusion:** Transient unfavorable metabolic changes shortly after surgery include rise in endogenous free fatty acids inducing insulin resistance via intramyocellular accumulation of specific DAG species and PKC $\theta$  activation [128], which has previously been demonstrated only in lipid infusion studies. This suggests a key role for the DAG-PKC pathway in the early metabolic changes after surgery, while 1 year after operation restored muscle mitochondrial function, reduced lipid availability and inflammatory

activity contribute to improved insulin sensitivity. Time-dependent alterations in muscle transcriptome and methylome provide evidence for specific epigenetic changes related to modified expression of important metabolic genes, additionally contributing to higher insulin sensitivity and improved lipid metabolism on the long term. Thereby dynamic changes in insulin sensitivity after bariatric surgery are possibly mediated by distinct mechanisms including lipotoxic insulin resistance and metabolic reprogramming of gene expression by epigenetic mechanisms.

**Limitations:** An important limitation of the study is the cross sectional design, which does not allow to draw conclusions on causality. Diet and eating behavior were not assessed in this study and their possible contribution to the metabolic changes and confounding effects could not be accounted for. In addition, body composition was not assessed, so the changes in lean and fat mass, which are key for the improvement in insulin sensitivity, could not be taken into account.

**Advantages:** The study provides detailed description of time-dependent changes in muscle metabolism, lipidome, transcriptome and methylome, thereby allowing assessment of complex interrelated biological processes linked to the profound weight loss after bariatric surgery. The combination of different techniques for direct evaluation of mitochondrial function and content deliver consistent results and provide detailed insights into the essential role of muscle mitochondria after metabolic surgery.

### **3.7 Bariatric surgery-induced restoration of the growth hormone system relates to improved adipose tissue insulin sensitivity**

**Background:** Metabolic surgery induced weight loss improves insulin sensitivity and even leads to remission of type 2 diabetes, while also increasing growth hormone concentrations [129] by yet unknown mechanisms. Insulin-like growth factor 1 regulates insulin and growth hormone secretion, but its role for tissue-specific improvement in insulin sensitivity after bariatric surgery remains unclear. Leptin, which reflects fat mass, has also been implicated in the complex regulation of the growth hormone system and might be directly linked to lipid availability decrease after bariatric surgery [121]. Here we investigated how metabolic surgery-induced changes in leptin, lipids and insulin sensitivity relate to the postoperative changes in the human growth hormone system.

**Methods:** People with obesity (n=79, BMI  $50.8 \pm 6.3$  kg/m<sup>2</sup>) were examined before, 2, 12, 24 and 52 weeks after metabolic surgery. Lean healthy humans (n=24, BMI  $24.3 \pm 3.1$  kg/m<sup>2</sup>) served as controls. Hyperinsulinemic-euglycemic clamps with [6,6-<sup>2</sup>H<sub>2</sub>]glucose were used to assess tissue-specific insulin sensitivity. For the quantification of fasting leptin, growth hormone, insulin-like growth factor 1 (IGF-1) and IGF-binding proteins (IGFBP1, IGFBP3) ELISA kits were used.

**Results:** Glycemia and leptinemia were higher in individuals with obesity at baseline compared with controls. Participants with obesity also exhibited pronounced peripheral, adipose tissue and hepatic insulin resistance. Fasting growth hormone and IGFBP1 were lower, while IGF1 was comparable between groups. Weight loss of 33 % was found in people with obesity at 52 weeks which was paralleled by doubled peripheral insulin sensitivity and continuous increases in growth hormone, IGF-1 and IGFBP1 (Figure 12) as well as decreases in leptin. Regression analysis revealed negative link between rise in growth hormone and reductions in free fatty acids, adipose tissue insulin resistance and insulinemia, while no association with changes in body weight, peripheral insulin sensitivity, glycemia or leptinemia was found. The increase in IGF-1 related with lower high-sensitive C-reactive protein.

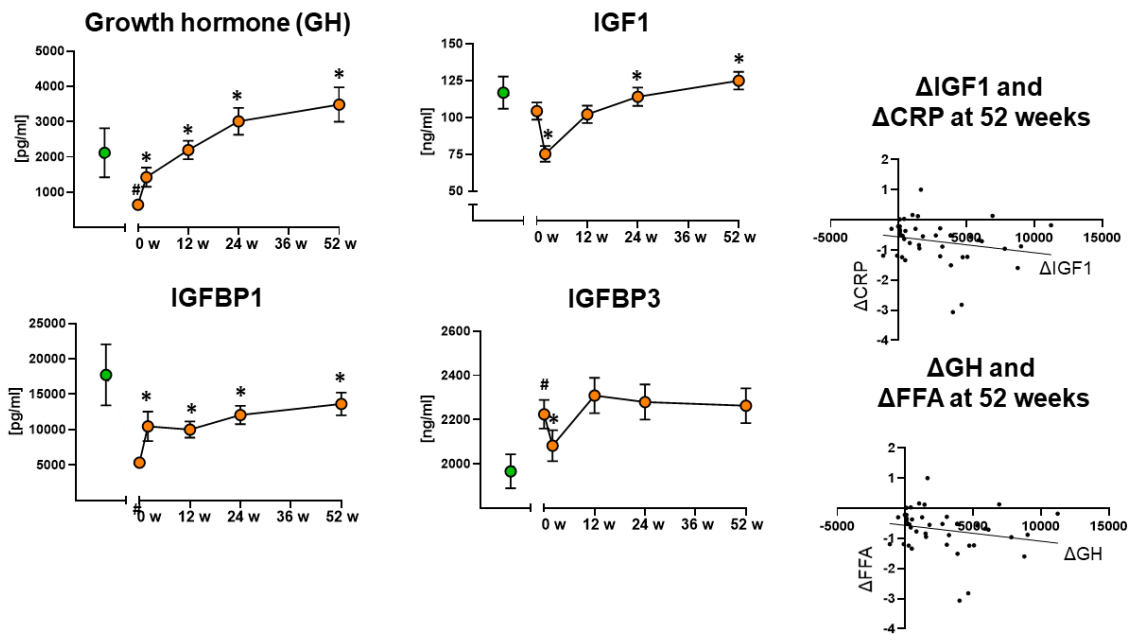


**Figure 12.** Changes in growth hormone, IGF1, IGFBP1 and IGFBP3 as well as relation to changes in CRP and FFA after bariatric surgery. Adapted from Gancheva et al. [130] under a [Creative Commons Attribution 4.0 International License](https://creativecommons.org/licenses/by/4.0/)

**Conclusion:** Restoration of the growth hormone system after bariatric surgery relates to improved adipose tissue insulin resistance, suggesting an important role for adipose tissue function for the regulation of the growth hormone-IGF1-axis in metabolic disorders. Improved growth hormone levels independent of type 2 diabetes status or glycemia point to early metabolic alterations in insulin sensitivity and adipose tissue rather than overt diabetes and hyperglycemia as important determinants of somatotrophic function. Persisting increased leptin levels at 1 year after surgery might explain the dissociation from improvement in the growth hormone system.

**Limitations:** The design of the study does not allow to draw conclusions on causal relationships so that insights into pathophysiological mechanisms could not be obtained here. As growth hormone release is pulsatile, a single fasting measurement does not fully reflect growth hormone secretion. Unfortunately, growth hormone profiles of growth hormone releasing hormone tests were not performed in this study. Also, important aspects of adipose tissue function such as adipose tissue inflammation, oxidative capacity or glucose uptake were not available in this study.

**Advantages:** Time-dependent hormonal and adipokine changes are described here in relation to specific metabolic alterations in order to provide detailed insights into a complex regulatory system, in which adipose tissue function plays a previously under-recognized role.

## 4. Conclusions

### 4.1. Effects of empagliflozin, prolonged fasting and transcutaneous vagus nerve stimulation on liver lipid content

As no accepted pharmacological treatment for NAFLD is currently available, the study of the effects of new antihyperglycemic treatments or novel nervous system based approaches on liver lipid content is of high relevance. Study 1 [122] and study 2 [123] contribute to our understanding on the effects of such novel treatment strategies.

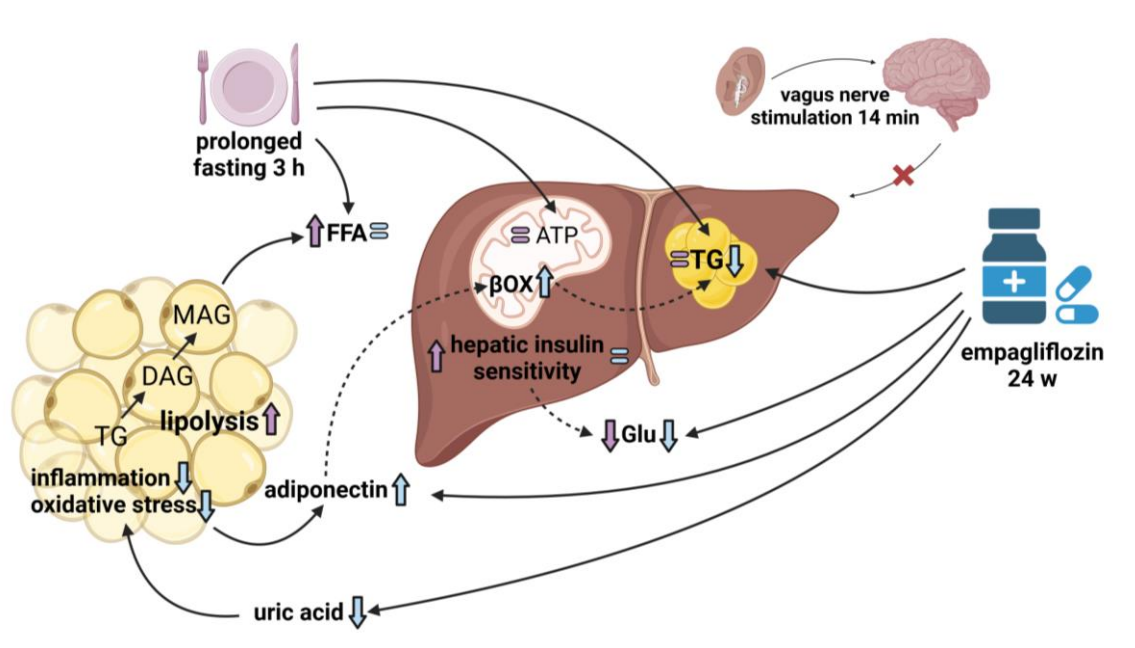


**Figure 13.** Effects of empagliflozin, prolonged fasting and transcutaneous auricular vagus nerve stimulation of hepatic lipid and energy metabolism. Illustration by S. Gancheva created with BioRender.com

Empagliflozin has been found to substantially decrease liver lipid content in comparison to placebo in study 1 [122] (Figure 13), but has no impact on tissue-specific insulin sensitivity. Additional analyses have shown an increase in high molecular weight adiponectin levels. The increase in adiponectin might reduce liver lipid content by activating hepatic  $\beta$ -oxidation as shown previously [131]. Empagliflozin treatment also resulted in a decrease in serum uric acid levels which might underlie the observed liver lipid content reduction via improvement in adipose tissue function. Indeed, high levels of uric acid are known to trigger inflammation in adipose tissue, insulin resistance, and reduced levels of adiponectin [132]. It is noteworthy that elevated uric acid levels and decreased adiponectin levels have been linked to body weight and metabolic syndrome features that include type 2 diabetes and non-alcoholic fatty liver disease [133].

Empagliflozin effects were observed in metabolically well-controlled people with type 2 diabetes who experienced moderate weight loss and minor changes in glycemia despite their short disease duration. SGLT2 inhibitors represent a promising treatment option for type 2 diabetes with additional clinical efficacy on cardiovascular and renal outcomes, which are gaining importance in the medical practice [41]. Thereby the described empagliflozin effects on liver lipid content point at its further potential to induce beneficial metabolic effects. Of note, other substances of the SGLT2 inhibitors class have also been demonstrated to potentially lower liver lipid content [42-44]. Study 1 [122] reveals that empagliflozin results in a nominal decrease in liver lipid content that is greater than dapagliflozin, but slightly less than canagliflozin in terms of change from baseline. However, the current lack of dosage and head-to-head comparative studies precludes drawing definitive conclusions on drug-specific effects. The dietary counseling provided to all groups, based on guidelines, may have contributed to higher rates of liver lipid content improvement observed in the placebo groups of study 1 [122] and one previous study [44], but not in other non-alcoholic fatty liver disease trials [42, 43].

The underlying mechanisms of empagliflozin induced liver lipid content reduction are not completely understood [46, 47], but body weight loss as well as improvement in insulin sensitivity and glucotoxicity have been suggested to play a role. However, it is known that glucosuria elicits an adaptive increase in energy intake that causes less body weight loss than expected [134]. Indeed, reduction in HCL was paralleled by a decrease in body weight (Figure 7). Notably, previous studies have suggested that a substantial reduction in HCL would only be possible with a 5 % weight loss or more, but it has been demonstrated that even minor weight loss of up to 5 % can result in a 33 % decline in liver lipid content [135]. Although only 27 % of the empagliflozin group achieved a body weight reduction of at least 5 %, the 34 % decrease in HCL emphasizes the significance of minor weight loss in the effects of SGLT2 inhibitors on HCL.

Of note, measures of adipose tissue (insulin-stimulated FFA suppression) or hepatic (insulin-stimulated EGP suppression) insulin sensitivity were not different between empagliflozin and placebo and no placebo-corrected effect of empagliflozin on skeletal muscle insulin sensitivity was found. In line, the decrease in HCL did not relate to an improvement in hepatic insulin sensitivity, so that changes in insulin sensitivity likely cannot explain the observed effects. Improvement in hepatic insulin sensitivity has previously been related to lower HbA1c and glycemia [44]. Accordingly, the current study found no changes in HbA1c levels, further supporting the hypothesis of dissociation between HCL and hepatic insulin sensitivity under SGLT2 inhibitor treatment.

Non-pharmacological treatment strategies targeting NAFLD have been studied intensively [27, 135]. Brain insulin action has been shown to acutely modulate hepatic lipid content and energy metabolism in healthy humans (Figure 3) [54]. The effects of central insulin signaling might be mediated via the

parasympathetic nervous system and the vagal nerve has been suggested to play a role [51]. Transcutaneous auricular vagus nerve stimulation represents a non-invasive tool for activation of the parasympathetic nervous system to potentially study its effects on peripheral metabolism [56]. However, study 2 [123] did not demonstrate any effect of non-invasive vagus nerve stimulation on liver lipid content and hepatic energy rich substrates (Figure 13). The absence of any impact of taVNS on pancreatic polypeptide secretion implies that there were no alterations in parasympathetic outflow to the visceral organs, which could potentially account for the lack of metabolic effects.

Study 2 [123] found that taVNS did not result in any substantial changes in systemic glucose, insulin, c-peptide, glucagon, free fatty acids, or triglyceride concentrations. This is consistent with the effects observed after intranasal insulin administration under fasting conditions, where any changes were attributed to spillover into the circulation rather than central insulin effects [54]. The lack of effects on substrate and hormone levels following taVNS suggests a similarity between the effects of taVNS and intranasal insulin. Moreover, the study found no difference in endogenous glucose production after taVNS, further supporting this notion (Figure 13). In overall, study 2 found no effect of taVNS on the parasympathetic tone to the abdominal viscera, so that even if brain insulin effects would be mediated by the vagus nerve, this non-invasive stimulation technique would not allow to study them. However, invasive vagus stimulation using cervical implanted devices has been shown to modulate postprandial glucose metabolism in people with rheumatoid arthritis [63], so that it could not be excluded that direct electric pulses to the vagal nerve might be able to alter glucose metabolism. In overall, whether other stimulation parameters or vagus stimulation techniques such as neck vagus stimulation with gammaCore or VNS Therapy System implantation will be able to modulate the parasympathetic tone to the viscera and thereby affect glucose and energy metabolism remains to be studied.

Notably, study 2 [123] demonstrated constant hepatic ATP concentrations with prolonged fasting without any changes in hepatic glucose metabolism (Figure 13). This finding suggests that a switch towards lipid oxidation in the preprandial state with gradual reduction in endogenous glucose production does not relate to changes in hepatic energy status which remains unaltered and possibly reflects its independence on mild short term changes in substrate availability in healthy humans. Reduction in energy consuming gluconeogenesis resulting in lower EGP rates might be balanced out here by an increase in energy producing  $\beta$ -oxidation from increased lipid availability in the settings of higher free fatty acids, which would eventually lead to constant hepatic energy status. In contrast, substantial change in lipid availability after oral fat load affects hepatic energy metabolism by acutely increasing hepatic lipid content and ATP concentrations. Thereby hepatic energy status adapts dynamically in accordance with the physiological conditions and changes in substrate availability in

healthy humans, while in type 2 diabetes this regulation might be impaired and pharmacological interventions prove to be effective in reducing liver lipid content.

### Key messages

- Empagliflozin effectively lowers liver lipid accumulation in well-controlled individuals with type 2 diabetes, which might be linked to improved adipose tissue function
- Empagliflozin might belong to future combined treatments strategies for NAFLD in T2D
- taVNS does not change endogenous glucose production, liver lipid and energy metabolism and is thereby unable to mimic bran insulin effects on liver homeostasis.
- taVNS does not exert metabolic effects possibly due to absent modulation of the autonomic tone to the visceral organs after stimulation.
- These findings add on to the ongoing discussion on the mechanism of central regulation of liver carbohydrate and fat metabolism, which is derived from rodent studies.

#### 4.2. Alterations of hepatic energy metabolism in metabolic disease

Findings of reduced hepatic energy metabolism in well-controlled newly diagnosed people with type 1 diabetes (study 3, [125]) (Figure 14) as well as in humans with NASH and type 2 diabetes (study 4, [126]) (Figure 15) complement our understanding of liver alterations in metabolic disease and its relation to hepatic steatosis and insulin resistance. Unaltered hepatic energy status in children and adolescents with organic acidemias (study 5, [127]) (Figure 14) points toward a previously unrecognized specific hepatic adaptation in states of increased availability of branched-chain amino acid metabolism intermediates, independent of hepatic lipid accumulation and insulin resistance.

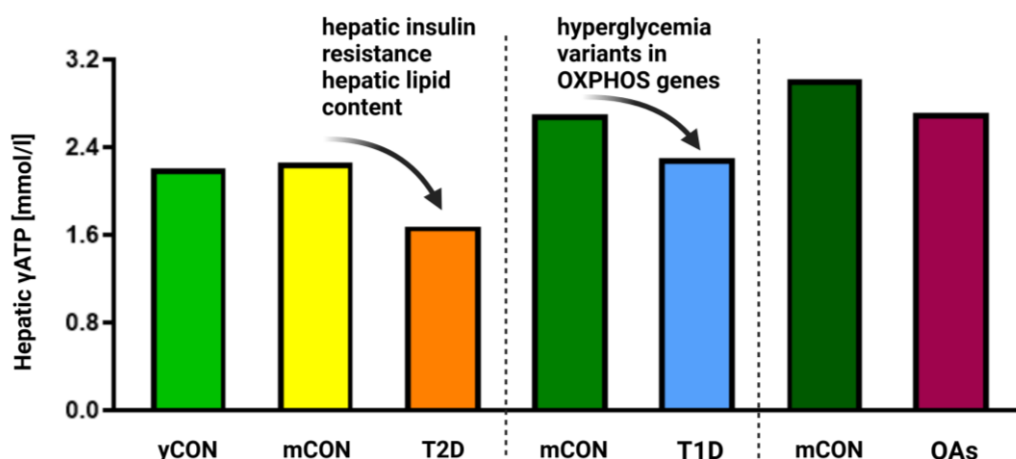


**Figure 14.** Alterations in hepatic energy metabolism in type 1 and type 2 diabetes as well as in organic acidemias. Illustration by S. Gancheva created with BioRender.com

Of note, study 3 [125] demonstrated lower hepatic ATP in type 1 diabetes in the early course of the disease, when hepatic insulin resistance and hepatic steatosis are absent. These findings are of high relevance in the light of evidence of higher risk for liver-related adverse outcomes in type 1 diabetes as seen in type 2 diabetes [79, 80]. Previously, decreased hepatic ATP levels has been described in obesity [136] and alcoholic hepatitis [137] as well as during post-surgical recovery in liver cirrhosis [138]. An early metabolic shift from oxidative phosphorylation to glycolysis in liver injury points at the critical role of hepatic mitochondria in liver adaptation to disease state [139]. In both human and mouse models, glycemia, lipid availability, and oxidative stress have been identified as primary factors affecting hepatic mitochondrial function [72, 140]. Alterations in hepatic energy metabolism have also been associated with changes in oxidative stress, which can be both a cause and a consequence of these alterations. Previous studies, which used  $^{31}\text{P}/^1\text{H}$  MRS to investigate hepatic energy metabolism, found reduced concentrations of hepatic ATP and Pi, as well as decreased flux through ATP synthase in individuals with type 2 diabetes [84, 85]. Study 3 [125] found that hepatic ATP content is reduced in individuals with type 1 diabetes, suggesting that abnormal liver energy homeostasis is also a characteristic of early-stage type 1 diabetes and could therefore be associated with common hallmarks like hyperglycemia or muscle and hepatic insulin resistance. Major determinants of hepatic absolute ATP concentrations and hepatic ATP synthase flux in people with type 2 diabetes are insulin resistance and liver lipid content [84, 85]. Thereby, hepatic absolute ATP content likely indicates ATP synthase flux, so that reduced hepatic ATP synthesis in individuals with type 1 diabetes could be inferred here. In non-obese people with type 1 diabetes, insulin-stimulated flux through muscle ATP synthase is also reduced and correlates with long-term glycemic control measured by HbA1c [82]. Study 3 [125] found that hepatic ATP is negatively associated with fasting glycemia but only before adjusting for diabetes status, age, sex, and BMI, indicating that other factors might influence hepatic energy status.

Compelling evidence supports the concept of hepatic mitochondrial adaptation and flexibility at early stages of NAFLD [87, 94, 141]. However, previous studies also reported declining hepatic respiratory capacity alongside increased oxidative stress in nonalcoholic steatohepatitis [31]. People with type 1 diabetes have higher systemic levels of oxidative stress and lipid peroxidation, along with reduced antioxidant capacity [142]. Such conditions could contribute to impaired mitochondrial function and reduced hepatic ATP content. However, Study 3 [125] found no significant differences between individuals with and without type 1 diabetes in terms of lipid peroxidation assessed from TBARS, DNA oxidative damage as measured by 8-hydroxydeoxyguanosine, protein carbonyl products, or antioxidant defense assessed by glutathione. Possible explanation of this dissociation could be the excellent glucometabolic control and short disease duration of the participants.

Specific variants in genes that control metabolism have also been related to abnormalities in glucose and energy homeostasis. One such common polymorphism, Pro12Ala (rs1801282), in the PPARG gene, has been linked to a decreased risk of type 2 diabetes and links genetically type 2 and type 1 diabetes [143]. Another gene involved in energy metabolism, PPARGC1A, encodes for the PPAR $\gamma$  coactivator-1 $\alpha$ , which regulates oxidative phosphorylation. The variant allele Gly482Ser in the PPARGC1A gene has been associated with an increased risk of obesity and oxidative stress [144]. Surprisingly, study 3 [125] found that individuals carrying the Ala allele (PPARG rs1801282) and those without the Ser allele (PPARGC1A rs8192678) had reduced hepatic ATP concentrations (Figure 9). This finding is unexpected, as hepatic energy metabolism is typically increased in obesity and insulin resistance [31, 87]. As participants with type 1 diabetes were non-obese and had normal hepatic insulin sensitivity, the presence of these protective gene variants may explain the absence of any increase in hepatic ATP concentrations.

Accumulation of intermediate metabolites of branched-chain amino acids metabolism might interfere with hepatic energy metabolism and lead to profound alterations in liver lipid and glucose metabolism, resulting in adverse outcomes in people with organic acidemias. As an example, a deficient mitochondrial catabolism process in propionic acidemia causes an accumulation of metabolites related to propionyl-CoA, leading to potential hyperammonemia by inhibiting N-acetylglutamate synthetase and energy metabolism [145]. This results in mitochondrial abnormalities such as reduced mitochondrial content and oxidative phosphorylation, as previously demonstrated in skeletal muscle of humans with PA [146]. However in study 5 [127], children and adolescents with PA exhibited no changes in hepatic energy metabolism suggesting no evidence of altered mitochondrial function through non-invasive *in vivo* MRS measurements (Figure 14). Of note, unaltered hepatic ATP concentrations were found in the settings of increased liver lipid content and insulin resistance in PA participants compared to matched controls, which is in contrast with findings of reduced hepatic ATP content and higher liver lipid content in people with type 2 diabetes [84]. These findings point towards an adaptation in hepatic energy metabolism with dissociation of hepatic energy status from hepatic insulin resistance and lipid accumulation in young humans with PA, which remains to be further investigated.

Participants with MMA presented with hepatomegaly, consistent with previous findings. However, the hepatomegaly was not accompanied by hepatic steatosis and could be attributed to abnormal liver cell regeneration, as indicated by elevated levels of alpha-fetoprotein in humans with MMA and PA [147]. While previous studies in rodents have reported abnormal mitochondrial morphology and reduced hepatocellular activity of complex IV from *ex vivo* measurements [148], no changes in ATP concentrations were observed in study 5 [127]. This difference could be due to differences in

measurement techniques and the specific features of mitochondrial function being evaluated. In overall, study 5 [127] found no evidence of alterations in hepatic energy metabolism in humans with defects in branched-chain amino acid catabolism, suggesting that concentrations of hepatic energy rich substrates are closely related to changes in lipid and glucose metabolism as seen in study 3 [125] and 4 [126], but not to amino acid catabolism intermediates.

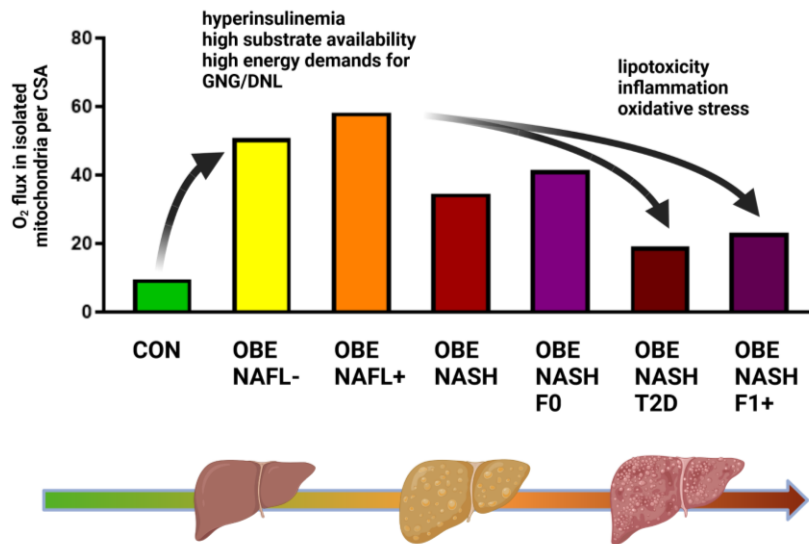


**Figure 15.** Alterations in hepatic oxidative capacity in humans with different stages of NAFLD, with and without type 2 diabetes and hepatic fibrosis. Illustration by S. Gancheva created with BioRender.com

Increased oxidative stress levels were found in the liver of individuals with obesity and advanced NAFLD in the presence of type 2 diabetes but not in humans without diabetes (Figure 15). Study 4 [126] suggests that loss of adaptation of hepatic mitochondrial function can possibly be explained by the presence of type 2 diabetes in individuals with NASH. Of note, the decrease in hepatic oxidative capacity was linked to higher lipid peroxidation and hyperglycemia, regardless of age, sex, and BMI, in individuals with NASH and type 2 diabetes. Moreover, there was an increase in hepatic mitochondrial H<sub>2</sub>O<sub>2</sub> release in these participants, which may indicate increased mitochondrial respiration, but not necessarily elevated ROS production. Nonetheless, the levels of TBARS and 3-nitro-tyrosine did not show any increase, suggesting that hepatic oxidative stress does not substantially contribute to altered mitochondrial function in these conditions.

Reduced mitochondrial functionality demonstrated exclusively in individuals with combined NASH and type 2 diabetes is consistent with previous *in vivo* studies indicating lower hepatic ATP concentrations in individuals with type 2 diabetes (Figure 4) [84]. In the early time course of the disease hepatocellular lipids increase substantially, while hepatic ATP content remains constant, as demonstrated recently [88]. Thereby hepatic mitochondria might fail to adapt to increased lipid availability in the settings of

hyperglycemia, which further corroborates the findings of study 4 [126] and demonstrates the crucial role of type 2 diabetes for the progression of metabolic liver disease.

Hyperglycemia in type 2 diabetes might give rise to reactive dicarbonyls such as glyoxal and methylglyoxal which might enhance oxidative stress in hepatocytes [149]. The negative association between fasting blood glucose and hepatic oxidative capacity in study 4 [126], even after adjusting for age, sex, and BMI, further confirms the detrimental role of hyperglycemia and glucotoxicity for hepatic energy metabolism in NAFLD, as previously suggested in type 1 diabetes (study 3, [125]).

#### **Key messages**

- **Hepatic energy metabolism in nonobese near-normoglycemic humans with type 1 diabetes is lower compared to healthy individuals as measured by high-sensitive non-invasive methods of multinuclei magnetic resonance spectroscopy.**
- **Early changes in liver energy metabolism in the absence of NAFLD are driven by previously unidentified factors such as variations in genes controlling oxidative metabolism suggesting that alterations in hepatic mitochondrial function may precede diabetes-related liver diseases.**
- **Genetic defects of mitochondrial function as seen in organic acidemias are not related to altered hepatic energy metabolism as measured by multinuclei magnetic resonance spectroscopy, suggesting adaptation of hepatic energy status to the accumulation of BCAA intermediates.**
- **Direct evidence from intraoperative liver samples from comprehensively phenotyped humans demonstrates loss of adaptation of hepatic mitochondrial capacity in NASH with compared to NASH without T2D, which likely contributes to accelerated NAFLD progression.**

#### **4.3. Dynamic metabolic and mitochondrial changes after bariatric surgery**

Study 6 [128] provides detailed insights into the time course of changes in metabolism, the lipidome, the transcriptome and the methylome of skeletal muscle in humans with obesity. Although metabolic surgery is known to result in remarkable weight loss and to improve whole-body insulin sensitivity, study 6 [128] revealed that the rapid loss of approximately 7 % of body weight within two weeks does not immediately lead to improved muscle insulin resistance (Figure 16). This is likely due to a transient increase in adipose tissue insulin resistance as well as higher levels of circulating cytokines shortly after operation. Increased growth hormone levels were found as early as 2 weeks after surgery in study 7 [130], so that a contribution of growth hormone-mediated stimulation of lipolysis could not be excluded.

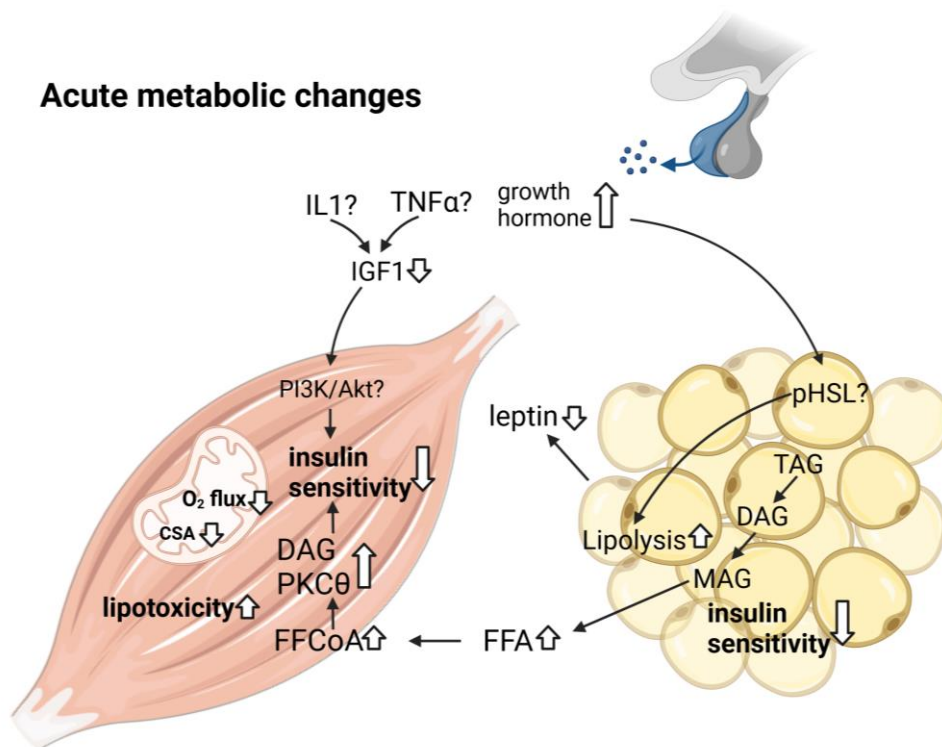


**Figure 16.** Metabolic changes in skeletal muscle and adipose tissue 2 weeks after bariatric surgery. Illustration by S. Gancheva created with BioRender.com

Study 6 [128] has identified a sustained increase in adipose tissue lipolysis leading to a doubling the amount of fasting free fatty acids (Figure 16). This elevated level of FFA persists for up to six months post-surgery, despite an improvement of insulin resistance in adipose tissue. The accumulation of 18:1 DAG species early after surgery and the resulting stimulation of PKC $\theta$  is noteworthy as it demonstrates, for the first time in humans, how changes in endogenous FFA levels can result in activation of the DAG/PKC pathway, a phenomenon that had previously only been described under experimental lipid infusion conditions. Collectively, these findings suggest that the DAG-PKC pathway is the primary cause of the initial failure of metabolic surgery to improve insulin resistance in skeletal muscle. On the long term, DAG species as well as ceramide species are decreased, while insulin sensitivity improves substantially. Therefore, the DAG/PKC pathway, along with decreased inflammatory activity, likely lead to the subsequent increase in insulin sensitivity after surgery.

Impaired mitochondrial function is often associated with insulin resistance, but this relationship is not universal. Study 6 [128] not only validated the previously established observation of lower muscle mitochondrial oxidative capacity, coupling efficiency, and fusion activity in individuals with obesity before surgery, but it also provided evidence of the dynamic regulation of mitochondria in humans during weight loss. Two weeks after surgery, there was a reduction in mitochondrial mass as measured by both biochemical and ultrastructural analyses. Additionally, there were no differences observed in

the ETC complexes I-III at this early time point, indicating that there may be a temporary delay in the improvement of mitochondrial abundance. A possible reason for the decline in mitochondrial mass, oxidative capacity, and coupling efficiency observed in the initial postoperative period is the accumulation of intramyocellular lipids inducing lipotoxicity (Figure 16). Elevated lipid peroxidation and a higher influx of lipids may lead to increased ROS quenching, resulting in the observed decreased antioxidant capacity. Unlike study 6 [128], short-term caloric restriction for 60 hours or 53 days did not have an impact on muscle mitochondrial density, indicating that the effects of weight loss on mitochondria in humans may be specific to the intervention and short-term in nature. The sustained impairment of mitochondrial fusion activity at the two-week mark suggests that changes in mitochondrial functionality persist during periods of elevated lipid availability, only reversing with improved insulin action at 52 weeks.

Two weeks after surgery a number of genes related to lipid metabolism exhibit altered expression levels, but are not related to changes in DNA methylation, so that different regulatory mechanisms are likely responsible for these alterations, such as activation of transcription factors.

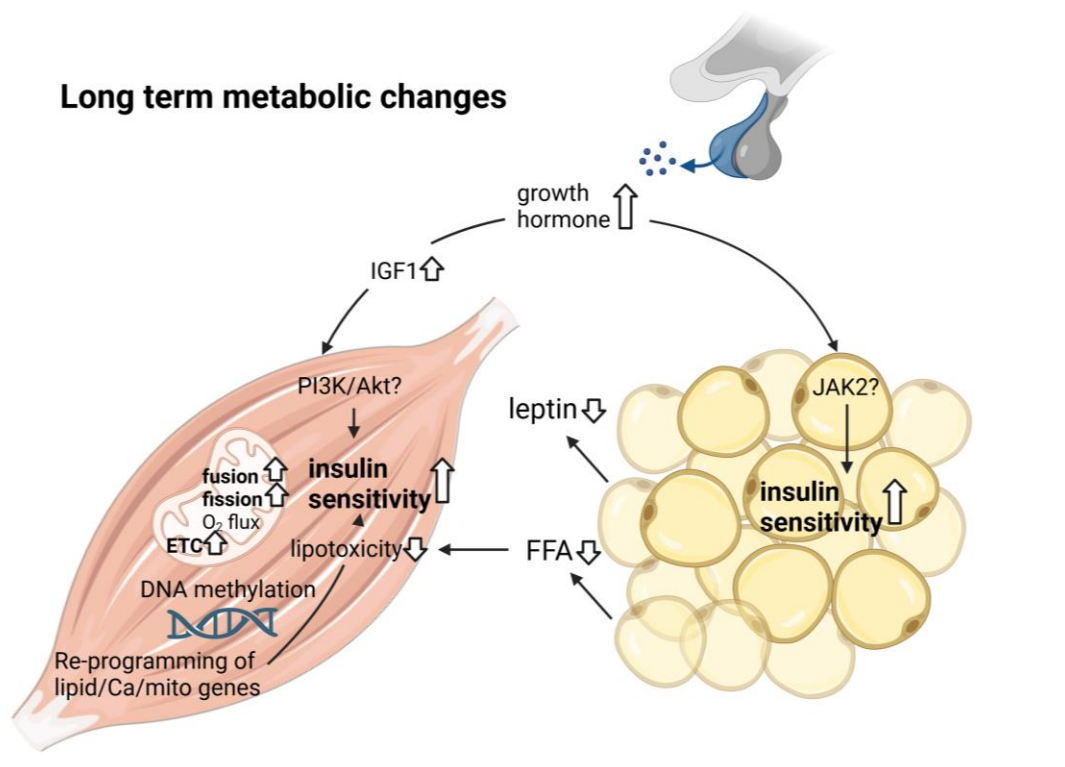


**Figure 17.** Metabolic changes in muscle and adipose tissue one year after bariatric surgery. Illustration by S. Gancheva created with BioRender.com

Lower muscle mitochondrial function is reverted to baseline values within 12 weeks, which is paralleled by a decrease in plasma FFA and these values remain unchanged until the 52-week mark, despite continuous improvement in insulin sensitivity (Figure 17). These findings suggest that insulin sensitivity dissociates from mitochondrial function after surgical weight loss, in similarity to studies using caloric restriction or inhibition of lipolysis [150, 151]. The improvement of peripheral insulin sensitivity after bariatric surgery is tightly related to the dynamic changes in adipose tissue function and thereby needs interpretation beyond weight loss.

At 52 weeks various alterations in the entire skeletal muscle methylome are seen, which are associated with reprogramming of 75 % of the transiently altered genes, so that this mechanism might be responsible for the normalization of the gene expression levels.

Interestingly, study 7 [130] found no association between the improvement in peripheral and hepatic insulin sensitivity and the reversal of the GH-IGF1-axis on the long term. However, there was a direct correlation between the increase of GH levels and an improvement in adipose tissue insulin sensitivity and lipid availability one year after surgery (Figure 17). The dysfunction of adipose tissue is known to be a key factor in causing whole-body insulin resistance through lipotoxicity and low-grade inflammation and GH action is known to affect various aspects of adipocyte function such as lipolysis, lipogenesis, adipocyte proliferation and differentiation, adipose tissue inflammation, and secretion of adipokines. The relation between higher GH levels and improvement in adipose tissue but also skeletal muscle insulin sensitivity could be mediated by adipocyte JAK2 as described previously [152]. A direct IGF1 effect on muscle insulin signaling one year after surgery via PI3K/Akt activation could not be excluded and might additionally contribute to higher insulin sensitivity. It is worth noting that the presence of type 2 diabetes does not seem to have a significant impact on the reversal of GH-IGF-1 axis alterations (study 7, [130]). Most of the observed changes were independent of T2D status, and there was no correlation between blood glucose levels and GH-IGF-1 changes. This indicates that early metabolic changes in adipose tissue function and insulin sensitivity, rather than overt hyperglycemia and diabetes, are linked to changes in the GH system.

### **Key messages**

- **Study on the sequence of effects of metabolic surgery on systemic and tissue specific metabolism revealed early post-surgery metabolic perturbations which associate with delayed improvements in muscle insulin sensitivity due to transiently higher lipolysis with accumulation of specific lipids, inadequate mitochondrial function and most importantly altered gene expression profiles.**

- **One year after metabolic surgery muscle metabolism is restored in parallel to substantial epigenetic modifications, which reprogram muscle gene expression and thereby likely contribute to improved whole-body insulin sensitivity.**
- **The increases in hormones of the GH-IGF-1-axis after metabolic surgery relate to improvement of adipose tissue function and normalization of low-grade inflammation, but neither to whole-body insulin sensitivity nor leptin levels.**
- **These results point to a key role of adipose tissue for the GH-IGF-1 regulation during surgical weight loss.**

## **5. Outlook**

Accumulating evidence points at hepatic mitochondria as key factors for alterations in hepatic metabolism and energy production in metabolic diseases. Because of their involvement in fatty acid oxidation, lipogenesis and gluconeogenesis hepatic mitochondria represent a major player in the pathogenesis of non-alcoholic fatty liver disease and thereby could serve as future therapeutic target. In the settings of greater lipid availability hepatic mitochondrial oxidative capacity adapts accordingly thereby mitigating accumulation of excessive hepatocellular lipids. Whether this adaptation to higher substrate influx by upregulation of oxidative capacity is reversible (e.g. by weight loss) as well as its relation to oxidative stress remain to be elucidated.

Furthermore, the assessment of various features of mitochondrial functionality and mitochondrial content remains challenging, as no gold standard technique has been universally accepted and multiple methods, which are time-consuming, expensive and invasive, are available. Comparative studies of the different techniques could shed light on their utility in various populations and help establish consensus among the experts. Additionally, non-invasive methods such as the measurement of biomarkers of mitochondrial function (e.g. extracellular vesicles or circulating cell-free mitochondria) could enable continuous monitoring of hepatic energy metabolism in clinical trials investigating the progression of metabolic liver disease and replace the currently used invasive techniques.

NAFLD and its metabolic and hepatic complications represent a substantial global challenge for the medical community, but mechanistic studies are setting the stage for the development of promising therapeutic strategies. The excessive accumulation of hepatocellular lipids is a key step in the initiation and progression of NAFLD and its reversal by metabolic interventions could resolve and/or prevent hepatic inflammation, fibrosis and diabetes thereby addressing early on the metabolic dysregulation in NAFLD. Empagliflozin reduces effectively liver lipid content independent of weight loss and in this way it positions itself as an important partner for future combined treatment strategies for NAFLD.

Whether the combination of empagliflozin with the GLP-1 agonist semaglutide, which has multiple beneficial metabolic effects including substantial weight loss, leads to NASH resolution in type 2 diabetes and could serve as future first line therapy in this high-risk population remains to be clarified. In overall, the strategic combination of multiple agents targeting distinct metabolic pathways is essential in order not only to achieve resolution of NASH and improvement of fibrosis but also to enable reduction in cardiovascular and renal outcomes.

## 6. References

1. Sun, H., et al., *IDF Diabetes Atlas: Global, regional and country-level diabetes prevalence estimates for 2021 and projections for 2045*. *Diabetes Res Clin Pract*, 2022. **183**: p. 109119.
2. ElSayed, N.A., et al., *2. Classification and Diagnosis of Diabetes: Standards of Care in Diabetes-2023*. *Diabetes Care*, 2023. **46**(Suppl 1): p. S19-s40.
3. Martin, B.C., et al., *Role of glucose and insulin resistance in development of type 2 diabetes mellitus: results of a 25-year follow-up study*. *Lancet*, 1992. **340**(8825): p. 925-9.
4. Dimas, A.S., et al., *Impact of type 2 diabetes susceptibility variants on quantitative glycemic traits reveals mechanistic heterogeneity*. *Diabetes*, 2014. **63**(6): p. 2158-71.
5. Herder, C. and M. Roden, *Genetics of type 2 diabetes: pathophysiologic and clinical relevance*. *Eur J Clin Invest*, 2011. **41**(6): p. 679-92.
6. Gancheva, S., et al., *Interorgan Metabolic Crosstalk in Human Insulin Resistance*. *Physiol Rev*, 2018. **98**(3): p. 1371-1415.
7. Roden, M. and G.I. Shulman, *The integrative biology of type 2 diabetes*. *Nature*, 2019. **576**(7785): p. 51-60.
8. Schlesinger, S., et al., *Prediabetes and risk of mortality, diabetes-related complications and comorbidities: umbrella review of meta-analyses of prospective studies*. *Diabetologia*, 2022. **65**(2): p. 275-285.
9. Lega, I.C. and L.L. Lipscombe, *Review: Diabetes, Obesity, and Cancer-Pathophysiology and Clinical Implications*. *Endocr Rev*, 2020. **41**(1).
10. Schröder, K., et al., *German Diabetes Study - Baseline data of retinal layer thickness measured by SD-OCT in early diabetes mellitus*. *Acta Ophthalmol*, 2019. **97**(2): p. e303-e307.
11. Herder, C., M. Roden, and D. Ziegler, *Novel Insights into Sensorimotor and Cardiovascular Autonomic Neuropathy from Recent-Onset Diabetes and Population-Based Cohorts*. *Trends Endocrinol Metab*, 2019. **30**(5): p. 286-298.
12. Kahn, R., et al., *The metabolic syndrome: time for a critical appraisal: joint statement from the American Diabetes Association and the European Association for the Study of Diabetes*. *Diabetes Care*, 2005. **28**(9): p. 2289-304.
13. Jia, G., V.G. DeMarco, and J.R. Sowers, *Insulin resistance and hyperinsulinaemia in diabetic cardiomyopathy*. *Nat Rev Endocrinol*, 2016. **12**(3): p. 144-53.
14. Adeva-Andany, M.M., et al., *Insulin resistance is a cardiovascular risk factor in humans*. *Diabetes Metab Syndr*, 2019. **13**(2): p. 1449-1455.
15. Zaharia, O.P., et al., *Risk of diabetes-associated diseases in subgroups of patients with recent-onset diabetes: a 5-year follow-up study*. *Lancet Diabetes Endocrinol*, 2019. **7**(9): p. 684-694.
16. Saatmann, N., et al., *Physical Fitness and Cardiovascular Risk Factors in Novel Diabetes Subgroups*. *J Clin Endocrinol Metab*, 2022. **107**(4): p. 1127-1139.
17. *The relationship of glycemic exposure (HbA1c) to the risk of development and progression of retinopathy in the diabetes control and complications trial*. *Diabetes*, 1995. **44**(8): p. 968-83.
18. Ray, K.K., et al., *Effect of intensive control of glucose on cardiovascular outcomes and death in patients with diabetes mellitus: a meta-analysis of randomised controlled trials*. *Lancet*, 2009. **373**(9677): p. 1765-72.
19. Nishikawa, T., et al., *Normalizing mitochondrial superoxide production blocks three pathways of hyperglycaemic damage*. *Nature*, 2000. **404**(6779): p. 787-90.
20. Pesta, D. and M. Roden, *The Janus Head of Oxidative Stress in Metabolic Diseases and During Physical Exercise*. *Curr Diab Rep*, 2017. **17**(6): p. 41.
21. Szczepaniak, L.S., et al., *Magnetic resonance spectroscopy to measure hepatic triglyceride content: prevalence of hepatic steatosis in the general population*. *Am J Physiol Endocrinol Metab*, 2005. **288**(2): p. E462-8.
22. Chalasani, N., et al., *The diagnosis and management of nonalcoholic fatty liver disease: Practice guidance from the American Association for the Study of Liver Diseases*. *Hepatology*, 2018. **67**(1): p. 328-357.

23. Singh, S., et al., *Fibrosis progression in nonalcoholic fatty liver vs nonalcoholic steatohepatitis: a systematic review and meta-analysis of paired-biopsy studies*. Clin Gastroenterol Hepatol, 2015. **13**(4): p. 643-54.e1-9; quiz e39-40.
24. Dulai, P.S., et al., *Increased risk of mortality by fibrosis stage in nonalcoholic fatty liver disease: Systematic review and meta-analysis*. Hepatology, 2017. **65**(5): p. 1557-1565.
25. Kleiner, D.E., et al., *Design and validation of a histological scoring system for nonalcoholic fatty liver disease*. Hepatology, 2005. **41**(6): p. 1313-21.
26. Rinella, M.E., et al., *A multi-society Delphi consensus statement on new fatty liver disease nomenclature*. J Hepatol, 2023.
27. Pafili, K. and M. Roden, *Nonalcoholic fatty liver disease (NAFLD) from pathogenesis to treatment concepts in humans*. Mol Metab, 2021. **50**: p. 101122.
28. Ter Horst, K.W., et al., *Hepatic Diacylglycerol-Associated Protein Kinase Cε Translocation Links Hepatic Steatosis to Hepatic Insulin Resistance in Humans*. Cell Rep, 2017. **19**(10): p. 1997-2004.
29. Yki-Järvinen, H., *Ceramides: A Cause of Insulin Resistance in Nonalcoholic Fatty Liver Disease in Both Murine Models and Humans*. Hepatology, 2020. **71**(4): p. 1499-1501.
30. Apostolopoulou, M., et al., *Specific Hepatic Sphingolipids Relate to Insulin Resistance, Oxidative Stress, and Inflammation in Nonalcoholic Steatohepatitis*. Diabetes Care, 2018. **41**(6): p. 1235-1243.
31. Koliaki, C., et al., *Adaptation of hepatic mitochondrial function in humans with non-alcoholic fatty liver is lost in steatohepatitis*. Cell Metab, 2015. **21**(5): p. 739-46.
32. Thibaut, R., et al., *Liver macrophages and inflammation in physiology and physiopathology of non-alcoholic fatty liver disease*. Febs j, 2022. **289**(11): p. 3024-3057.
33. Tilg, H. and A.R. Moschen, *Relevance of TNF-α gene polymorphisms in nonalcoholic fatty liver disease*. Expert Rev Gastroenterol Hepatol, 2011. **5**(2): p. 155-8.
34. Perseghin, G., et al., *Increased glucose transport-phosphorylation and muscle glycogen synthesis after exercise training in insulin-resistant subjects*. N Engl J Med, 1996. **335**(18): p. 1357-62.
35. Rothman, D.L., et al., *Decreased muscle glucose transport/phosphorylation is an early defect in the pathogenesis of non-insulin-dependent diabetes mellitus*. Proc Natl Acad Sci U S A, 1995. **92**(4): p. 983-7.
36. Flannery, C., et al., *Skeletal muscle insulin resistance promotes increased hepatic de novo lipogenesis, hyperlipidemia, and hepatic steatosis in the elderly*. Diabetes, 2012. **61**(11): p. 2711-7.
37. Petersen, M.C. and G.I. Shulman, *Mechanisms of Insulin Action and Insulin Resistance*. 2018. **98**(4): p. 2133-2223.
38. Younossi, Z.M., et al., *Lifestyle interventions in nonalcoholic fatty liver disease*. Nat Rev Gastroenterol Hepatol, 2023.
39. Targher, G., et al., *The complex link between NAFLD and type 2 diabetes mellitus - mechanisms and treatments*. Nat Rev Gastroenterol Hepatol, 2021. **18**(9): p. 599-612.
40. Ferrannini, E., *Sodium-Glucose Co-transporters and Their Inhibition: Clinical Physiology*. Cell Metab, 2017. **26**(1): p. 27-38.
41. McGuire, D.K., et al., *Association of SGLT2 Inhibitors With Cardiovascular and Kidney Outcomes in Patients With Type 2 Diabetes: A Meta-analysis*. JAMA Cardiol, 2021. **6**(2): p. 148-158.
42. Latva-Rasku, A., et al., *The SGLT2 Inhibitor Dapagliflozin Reduces Liver Fat but Does Not Affect Tissue Insulin Sensitivity: A Randomized, Double-Blind, Placebo-Controlled Study With 8-Week Treatment in Type 2 Diabetes Patients*. Diabetes Care, 2019. **42**(5): p. 931-937.
43. Eriksson, J.W., et al., *Effects of dapagliflozin and n-3 carboxylic acids on non-alcoholic fatty liver disease in people with type 2 diabetes: a double-blind randomised placebo-controlled study*. Diabetologia, 2018. **61**(9): p. 1923-1934.

44. Cusi, K., et al., *Effect of canagliflozin treatment on hepatic triglyceride content and glucose metabolism in patients with type 2 diabetes*. *Diabetes Obes Metab*, 2019. **21**(4): p. 812-821.
45. Leiter, L.A., et al., *Long-term maintenance of efficacy of dapagliflozin in patients with type 2 diabetes mellitus and cardiovascular disease*. *Diabetes Obes Metab*, 2016. **18**(8): p. 766-74.
46. Kuchay, M.S., et al., *Effect of Empagliflozin on Liver Fat in Patients With Type 2 Diabetes and Nonalcoholic Fatty Liver Disease: A Randomized Controlled Trial (E-LIFT Trial)*. *Diabetes Care*, 2018. **41**(8): p. 1801-1808.
47. Sattar, N., et al., *Empagliflozin is associated with improvements in liver enzymes potentially consistent with reductions in liver fat: results from randomised trials including the EMPA-REG OUTCOME® trial*. *Diabetologia*, 2018. **61**(10): p. 2155-2163.
48. Vogt, M.C. and J.C. Brüning, *CNS insulin signaling in the control of energy homeostasis and glucose metabolism - from embryo to old age*. *Trends Endocrinol Metab*, 2013. **24**(2): p. 76-84.
49. Ramnanan, C.J., et al., *Brain insulin action augments hepatic glycogen synthesis without suppressing glucose production or gluconeogenesis in dogs*. *J Clin Invest*, 2011. **121**(9): p. 3713-23.
50. Pocai, A., et al., *Hypothalamic K(ATP) channels control hepatic glucose production*. *Nature*, 2005. **434**(7036): p. 1026-31.
51. Kimura, K., et al., *Central Insulin Action Activates Kupffer Cells by Suppressing Hepatic Vagal Activation via the Nicotinic Alpha 7 Acetylcholine Receptor*. *Cell Rep*, 2016. **14**(10): p. 2362-74.
52. Heni, M., et al., *Hypothalamic and Striatal Insulin Action Suppresses Endogenous Glucose Production and May Stimulate Glucose Uptake During Hyperinsulinemia in Lean but Not in Overweight Men*. *Diabetes*, 2017. **66**(7): p. 1797-1806.
53. Iwen, K.A., et al., *Intranasal insulin suppresses systemic but not subcutaneous lipolysis in healthy humans*. *J Clin Endocrinol Metab*, 2014. **99**(2): p. E246-51.
54. Gancheva, S., et al., *Effects of intranasal insulin on hepatic fat accumulation and energy metabolism in humans*. *Diabetes*, 2015. **64**(6): p. 1966-75.
55. Heni, M., et al., *Central insulin administration improves whole-body insulin sensitivity via hypothalamus and parasympathetic outputs in men*. *Diabetes*, 2014. **63**(12): p. 4083-8.
56. Frangos, E., J. Ellrich, and B.R. Komisaruk, *Non-invasive Access to the Vagus Nerve Central Projections via Electrical Stimulation of the External Ear: fMRI Evidence in Humans*. *Brain Stimul*, 2015. **8**(3): p. 624-36.
57. Clancy, J.A., et al., *Non-invasive vagus nerve stimulation in healthy humans reduces sympathetic nerve activity*. *Brain Stimul*, 2014. **7**(6): p. 871-7.
58. Scherer, T., et al., *Brain insulin controls adipose tissue lipolysis and lipogenesis*. *Cell Metab*, 2011. **13**(2): p. 183-94.
59. Panebianco, M., et al., *Vagus nerve stimulation for partial seizures*. *Cochrane Database Syst Rev*, 2015. **2015**(4): p. Cd002896.
60. Rong, P., et al., *Effect of transcutaneous auricular vagus nerve stimulation on major depressive disorder: A nonrandomized controlled pilot study*. *J Affect Disord*, 2016. **195**: p. 172-9.
61. Merrill, C.A., et al., *Vagus nerve stimulation in patients with Alzheimer's disease: Additional follow-up results of a pilot study through 1 year*. *J Clin Psychiatry*, 2006. **67**(8): p. 1171-8.
62. Vijgen, G.H., et al., *Vagus nerve stimulation increases energy expenditure: relation to brown adipose tissue activity*. *PLoS One*, 2013. **8**(10): p. e77221.
63. Tang, M.W., et al., *Single vagus nerve stimulation reduces early postprandial C-peptide levels but not other hormones or postprandial metabolism*. *Clin Rheumatol*, 2018. **37**(2): p. 505-514.
64. Wang, S., et al., *Transcutaneous vagus nerve stimulation induces tidal melatonin secretion and has an antidiabetic effect in Zucker fatty rats*. *PLoS One*, 2015. **10**(4): p. e0124195.

65. Nunnari, J. and A. Suomalainen, *Mitochondria: in sickness and in health*. Cell, 2012. **148**(6): p. 1145-59.
66. Misu, H., et al., *Genes involved in oxidative phosphorylation are coordinately upregulated with fasting hyperglycaemia in livers of patients with type 2 diabetes*. Diabetologia, 2007. **50**(2): p. 268-77.
67. Phielix, E., J. Szendroedi, and M. Roden, *Mitochondrial function and insulin resistance during aging: a mini-review*. Gerontology, 2011. **57**(5): p. 387-96.
68. Befroy, D.E., et al., *Impaired mitochondrial substrate oxidation in muscle of insulin-resistant offspring of type 2 diabetic patients*. Diabetes, 2007. **56**(5): p. 1376-81.
69. Petersen, K.F., et al., *Mitochondrial dysfunction in the elderly: possible role in insulin resistance*. Science, 2003. **300**(5622): p. 1140-2.
70. Krako Jakovljevic, N., et al., *Targeting Mitochondria in Diabetes*. Int J Mol Sci, 2021. **22**(12).
71. Mootha, V.K., et al., *PGC-1alpha-responsive genes involved in oxidative phosphorylation are coordinately downregulated in human diabetes*. Nat Genet, 2003. **34**(3): p. 267-73.
72. Koliaki, C. and M. Roden, *Alterations of Mitochondrial Function and Insulin Sensitivity in Human Obesity and Diabetes Mellitus*. Annu Rev Nutr, 2016. **36**: p. 337-67.
73. Phielix, E., et al., *Lower intrinsic ADP-stimulated mitochondrial respiration underlies in vivo mitochondrial dysfunction in muscle of male type 2 diabetic patients*. Diabetes, 2008. **57**(11): p. 2943-9.
74. Coen, P.M., et al., *Exercise and Weight Loss Improve Muscle Mitochondrial Respiration, Lipid Partitioning, and Insulin Sensitivity After Gastric Bypass Surgery*. Diabetes, 2015. **64**(11): p. 3737-50.
75. Vijgen, G.H., et al., *Impaired skeletal muscle mitochondrial function in morbidly obese patients is normalized one year after bariatric surgery*. Surg Obes Relat Dis, 2013. **9**(6): p. 936-41.
76. Karakelides, H., et al., *Age, Obesity, and Sex Effects on Insulin Sensitivity and Skeletal Muscle Mitochondrial Function*. Diabetes, 2009. **59**(1): p. 89-97.
77. Song, J.D., et al., *Dissociation of Muscle Insulin Resistance from Alterations in Mitochondrial Substrate Preference*. Cell Metab, 2020. **32**(5): p. 726-735.e5.
78. Targher, G., et al., *Nonalcoholic fatty liver disease is independently associated with an increased incidence of chronic kidney disease in patients with type 1 diabetes*. Diabetes Care, 2014. **37**(6): p. 1729-36.
79. Targher, G., et al., *Prevalence of non-alcoholic fatty liver disease and its association with cardiovascular disease in patients with type 1 diabetes*. J Hepatol, 2010. **53**(4): p. 713-8.
80. Cusi, K., et al., *Non-alcoholic fatty liver disease (NAFLD) prevalence and its metabolic associations in patients with type 1 diabetes and type 2 diabetes*. Diabetes Obes Metab, 2017. **19**(11): p. 1630-1634.
81. Kaul, K., M. Apostolopoulou, and M. Roden, *Insulin resistance in type 1 diabetes mellitus*. Metabolism, 2015. **64**(12): p. 1629-39.
82. Kacerovsky, M., et al., *Impaired insulin stimulation of muscular ATP production in patients with type 1 diabetes*. J Intern Med, 2011. **269**(2): p. 189-99.
83. Szendroedi, J., et al., *Lower fasting muscle mitochondrial activity relates to hepatic steatosis in humans*. Diabetes Care, 2014. **37**(2): p. 468-74.
84. Szendroedi, J., et al., *Abnormal hepatic energy homeostasis in type 2 diabetes*. Hepatology, 2009. **50**(4): p. 1079-86.
85. Schmid, A.I., et al., *Liver ATP synthesis is lower and relates to insulin sensitivity in patients with type 2 diabetes*. Diabetes Care, 2011. **34**(2): p. 448-53.
86. Jelenik, T., et al., *Tissue-specific differences in the development of insulin resistance in a mouse model for type 1 diabetes*. Diabetes, 2014. **63**(11): p. 3856-67.
87. Fritsch, M., et al., *Time course of postprandial hepatic phosphorus metabolites in lean, obese, and type 2 diabetes patients*. Am J Clin Nutr, 2015. **102**(5): p. 1051-8.

88. Kupriyanova, Y., et al., *Early changes in hepatic energy metabolism and lipid content in recent-onset type 1 and 2 diabetes mellitus*. J Hepatol, 2020.
89. Parente, E.B., et al., *The Relationship Between Body Fat Distribution and Nonalcoholic Fatty Liver in Adults With Type 1 Diabetes*. Diabetes Care, 2021. **44**(7): p. 1706-1713.
90. Bril, F., et al., *Relationship between disease severity, hyperinsulinemia, and impaired insulin clearance in patients with nonalcoholic steatohepatitis*. Hepatology, 2014. **59**(6): p. 2178-87.
91. Serdarova, M., et al., *Metabolic determinants of NAFLD in adults with type 1 diabetes*. Diabetes Res Clin Pract, 2022. **186**: p. 109819.
92. Mertens, J., et al., *Hepatopathy Associated With Type 1 Diabetes: Distinguishing Non-alcoholic Fatty Liver Disease From Glycogenic Hepatopathy*. Front Pharmacol, 2021. **12**: p. 768576.
93. Flatt, J.P., *Use and storage of carbohydrate and fat*. Am J Clin Nutr, 1995. **61**(4 Suppl): p. 952s-959s.
94. Fromenty, B. and M. Roden, *Mitochondrial alterations in fatty liver diseases*. J Hepatol, 2023. **78**(2): p. 415-429.
95. Afolabi, P.R., et al., *The characterisation of hepatic mitochondrial function in patients with non-alcoholic fatty liver disease (NAFLD) using the (13)C-ketoisocaproate breath test*. J Breath Res, 2018. **12**(4): p. 046002.
96. Lund, M.T., et al., *Hepatic mitochondrial oxidative phosphorylation is normal in obese patients with and without type 2 diabetes*. J Physiol, 2016. **594**(15): p. 4351-8.
97. Zaharia, O.P., et al., *Role of Patatin-Like Phospholipase Domain-Containing 3 Gene for Hepatic Lipid Content and Insulin Resistance in Diabetes*. Diabetes Care, 2020. **43**(9): p. 2161-2168.
98. Hernández, E., et al., *Acute dietary fat intake initiates alterations in energy metabolism and insulin resistance*. J Clin Invest, 2017. **127**(2): p. 695-708.
99. Longo, M., et al., *Mitochondrial dynamics and nonalcoholic fatty liver disease (NAFLD): new perspectives for a fairy-tale ending?* Metabolism, 2021. **117**: p. 154708.
100. Baumgartner, M.R., et al., *Proposed guidelines for the diagnosis and management of methylmalonic and propionic acidemia*. Orphanet J Rare Dis, 2014. **9**: p. 130.
101. Ando, T., et al., *Propionic acidemia in patients with ketotic hyperglycinemia*. J Pediatr, 1971. **78**(5): p. 827-32.
102. Oberholzer, V.G., et al., *Methylmalonic aciduria. An inborn error of metabolism leading to chronic metabolic acidosis*. Arch Dis Child, 1967. **42**(225): p. 492-504.
103. de Keyzer, Y., et al., *Multiple OXPHOS deficiency in the liver, kidney, heart, and skeletal muscle of patients with methylmalonic aciduria and propionic aciduria*. Pediatr Res, 2009. **66**(1): p. 91-5.
104. Wajner, M. and S.I. Goodman, *Disruption of mitochondrial homeostasis in organic acidurias: insights from human and animal studies*. J Bioenerg Biomembr, 2011. **43**(1): p. 31-8.
105. Longo, N., et al., *Anaplerotic therapy in propionic acidemia*. Mol Genet Metab, 2017. **122**(1-2): p. 51-59.
106. Mingrone, G., et al., *Metabolic surgery versus conventional medical therapy in patients with type 2 diabetes: 10-year follow-up of an open-label, single-centre, randomised controlled trial*. Lancet, 2021. **397**(10271): p. 293-304.
107. Mingrone, G. and D.E. Cummings, *Changes of insulin sensitivity and secretion after bariatric/metabolic surgery*. Surg Obes Relat Dis, 2016. **12**(6): p. 1199-205.
108. Gastaldelli, A., et al., *Short-term Effects of Laparoscopic Adjustable Gastric Banding Versus Roux-en-Y Gastric Bypass*. Diabetes Care, 2016. **39**(11): p. 1925-1931.
109. Toledo, F.G. and B.H. Goodpaster, *The role of weight loss and exercise in correcting skeletal muscle mitochondrial abnormalities in obesity, diabetes and aging*. Mol Cell Endocrinol, 2013. **379**(1-2): p. 30-4.

110. Taylor, R., et al., *Remission of Human Type 2 Diabetes Requires Decrease in Liver and Pancreas Fat Content but Is Dependent upon Capacity for beta Cell Recovery*. *Cell Metab*, 2018. **28**(4): p. 547-556.e3.
111. Barres, R., et al., *Weight loss after gastric bypass surgery in human obesity remodels promoter methylation*. *Cell Rep*, 2013. **3**(4): p. 1020-7.
112. Garcia, L.A., et al., *Weight loss after Roux-En-Y gastric bypass surgery reveals skeletal muscle DNA methylation changes*. *Clin Epigenetics*, 2021. **13**(1): p. 100.
113. Scacchi, M., A.I. Pincelli, and F. Cavagnini, *Growth hormone in obesity*. *Int J Obes Relat Metab Disord*, 1999. **23**(3): p. 260-71.
114. Perakakis, N., et al., *Circulating levels of gastrointestinal hormones in response to the most common types of bariatric surgery and predictive value for weight loss over one year: Evidence from two independent trials*. *Metabolism*, 2019. **101**: p. 153997.
115. Yu, A.P., et al., *Obestatin and growth hormone reveal the interaction of central obesity and other cardiometabolic risk factors of metabolic syndrome*. *Scientific Reports*, 2020. **10**(1): p. 5495.
116. Cordido, F., et al., *Study of insulin-like growth factor I in human obesity*. *Horm Res*, 1991. **36**(5-6): p. 187-91.
117. Utz, A.L., et al., *Androgens May Mediate a Relative Preservation of IGF-I Levels in Overweight and Obese Women Despite Reduced Growth Hormone Secretion*. *The Journal of Clinical Endocrinology & Metabolism*, 2008. **93**(10): p. 4033-4040.
118. Edén Engström, B., et al., *Effects of gastric bypass on the GH/IGF-I axis in severe obesity--and a comparison with GH deficiency*. *Eur J Endocrinol*, 2006. **154**(1): p. 53-9.
119. Haywood, N.J., et al., *The insulin like growth factor and binding protein family: Novel therapeutic targets in obesity & diabetes*. *Mol Metab*, 2019. **19**: p. 86-96.
120. Beghini, M., et al., *Serum IGF1 and linear growth in children with congenital leptin deficiency before and after leptin substitution*. *Int J Obes (Lond)*, 2021. **45**(7): p. 1448-1456.
121. Mingrone, G., et al., *Leptin pulsatility in formerly obese women*. *Faseb j*, 2005. **19**(10): p. 1380-2.
122. Kahl, S., et al., *Empagliflozin Effectively Lowers Liver Fat Content in Well-Controlled Type 2 Diabetes: A Randomized, Double-Blind, Phase 4, Placebo-Controlled Trial*. *Diabetes Care*, 2020. **43**(2): p. 298-305.
123. Gancheva, S., et al., *Constant hepatic ATP concentrations during prolonged fasting and absence of effects of Cerbomed Nemos(®) on parasympathetic tone and hepatic energy metabolism*. *Mol Metab*, 2018. **7**: p. 71-79.
124. Bergman, B.C., et al., *Features of hepatic and skeletal muscle insulin resistance unique to type 1 diabetes*. *J Clin Endocrinol Metab*, 2012. **97**(5): p. 1663-72.
125. Gancheva, S., et al., *Variants in Genes Controlling Oxidative Metabolism Contribute to Lower Hepatic ATP Independent of Liver Fat Content in Type 1 Diabetes*. *Diabetes*, 2016. **65**(7): p. 1849-57.
126. Gancheva, S., et al., *Impaired Hepatic Mitochondrial Capacity in Nonalcoholic Steatohepatitis Associated With Type 2 Diabetes*. *Diabetes Care*, 2022. **45**(4): p. 928-937.
127. Gancheva, S., et al., *Cardiometabolic risk factor clustering in patients with deficient branched-chain amino acid catabolism: A case-control study*. *J Inherit Metab Dis*, 2020. **43**(5): p. 981-993.
128. Gancheva, S., et al., *Dynamic changes of muscle insulin sensitivity after metabolic surgery*. *Nat Commun*, 2019. **10**(1): p. 4179.
129. Rasmussen, M.H., et al., *Massive weight loss restores 24-hour growth hormone release profiles and serum insulin-like growth factor-I levels in obese subjects*. *J Clin Endocrinol Metab*, 1995. **80**(4): p. 1407-15.
130. Gancheva, S., et al., *Metabolic surgery-induced changes of the growth hormone system relate to improved adipose tissue function*. *Int J Obes (Lond)*, 2023. **47**(6): p. 505-511.

131. Goldfine, A.B. and C.R. Kahn, *Adiponectin: linking the fat cell to insulin sensitivity*. The Lancet, 2003. **362**(9394): p. 1431-1432.
132. Johnson, R.J., et al., *Sugar, uric acid, and the etiology of diabetes and obesity*. Diabetes, 2013. **62**(10): p. 3307-15.
133. Bellou, V., et al., *Risk factors for type 2 diabetes mellitus: An exposure-wide umbrella review of meta-analyses*. PLoS One, 2018. **13**(3): p. e0194127.
134. Ferrannini, G., et al., *Energy Balance After Sodium-Glucose Cotransporter 2 Inhibition*. Diabetes Care, 2015. **38**(9): p. 1730-5.
135. Romero-Gómez, M., S. Zelber-Sagi, and M. Trenell, *Treatment of NAFLD with diet, physical activity and exercise*. J Hepatol, 2017. **67**(4): p. 829-846.
136. Nair, S., et al., *Hepatic ATP reserve and efficiency of replenishing: comparison between obese and nonobese normal individuals*. Am J Gastroenterol, 2003. **98**(2): p. 466-70.
137. Meyerhoff, D.J., et al., *Alcoholic liver disease: quantitative image-guided P-31 MR spectroscopy*. Radiology, 1989. **173**(2): p. 393-400.
138. Mann, D.V., et al., *Human liver regeneration: hepatic energy economy is less efficient when the organ is diseased*. Hepatology, 2001. **34**(3): p. 557-65.
139. Nishikawa, T., et al., *A switch in the source of ATP production and a loss in capacity to perform glycolysis are hallmarks of hepatocyte failure in advance liver disease*. J Hepatol, 2014. **60**(6): p. 1203-11.
140. Gastaldelli, A. and K. Cusi, *From NASH to diabetes and from diabetes to NASH: Mechanisms and treatment options*. JHEP Rep, 2019. **1**(4): p. 312-328.
141. Sunny, N.E., et al., *Excessive hepatic mitochondrial TCA cycle and gluconeogenesis in humans with nonalcoholic fatty liver disease*. Cell Metab, 2011. **14**(6): p. 804-10.
142. Vessby, J., et al., *Oxidative stress and antioxidant status in type 1 diabetes mellitus*. J Intern Med, 2002. **251**(1): p. 69-76.
143. Raj, S.M., et al., *No association of multiple type 2 diabetes loci with type 1 diabetes*. Diabetologia, 2009. **52**(10): p. 2109-16.
144. Weng, S.W., et al., *Gly482Ser polymorphism in the peroxisome proliferator-activated receptor gamma coactivator-1alpha gene is associated with oxidative stress and abdominal obesity*. Metabolism, 2010. **59**(4): p. 581-6.
145. Gregersen, N., *The specific inhibition of the pyruvate dehydrogenase complex from pig kidney by propionyl-CoA and isovaleryl-Co-A*. Biochem Med, 1981. **26**(1): p. 20-7.
146. Schwab, M.A., et al., *Secondary mitochondrial dysfunction in propionic aciduria: a pathogenic role for endogenous mitochondrial toxins*. Biochem J, 2006. **398**(1): p. 107-12.
147. Imbard, A., et al., *Long-term liver disease in methylmalonic and propionic acidemias*. Mol Genet Metab, 2018. **123**(4): p. 433-440.
148. Chandler, R.J., et al., *Mitochondrial dysfunction in mut methylmalonic acidemia*. Faseb j, 2009. **23**(4): p. 1252-61.
149. Shangari, N., et al., *Glyoxal markedly compromises hepatocyte resistance to hydrogen peroxide*. Biochem Pharmacol, 2006. **71**(11): p. 1610-8.
150. Toledo, F.G., et al., *Mitochondrial capacity in skeletal muscle is not stimulated by weight loss despite increases in insulin action and decreases in intramyocellular lipid content*. Diabetes, 2008. **57**(4): p. 987-94.
151. Phielix, E., et al., *Reduction of non-esterified fatty acids improves insulin sensitivity and lowers oxidative stress, but fails to restore oxidative capacity in type 2 diabetes: a randomised clinical trial*. Diabetologia, 2014. **57**(3): p. 572-81.
152. Corbit, K.C., et al., *Adipocyte JAK2 mediates growth hormone-induced hepatic insulin resistance*. JCI Insight, 2017. **2**(3): p. e91001.

## **7. Acknowledgements**

I express my deepest gratitude to my supervisor and mentor, Professor Michael Roden, Director of the German Diabetes Center, Leibniz Center for Diabetes Research, and of the Department of Endocrinology and Diabetology at the University Hospital Düsseldorf. I am sincerely thankful to him for sharing his expertise and providing me with all the necessary facilities for our research, his continuous scientific guidance, his enthusiasm, patience and encouragement. I take this opportunity to express gratitude to all coworkers of the included papers for their constructive criticism and friendly advice during the project work. I would also like to show my gratitude to the participants of these studies for their endurance, curiosity and interest in our work.

My friends and colleagues from the German Diabetes Center and the Department of Endocrinology and Diabetology have helped me to stay strong and happy throughout the years. Their support and care helped me overcome setbacks and stay focused on my work: very special thanks to Patricia Zaharia, Julia Szendroedi, Kalman Bodis, Gidon Bönhof and Kalliopi Pafili who were always there for me and kept me grounded.

Most importantly, none of this would have been possible without the endless love and support from my wonderful father and sister - Maxim and Irina Ganchevi - as well as my loving husband Jose Moya Cancino. They have been a constant source of strength all these years and this work is dedicated to them.

## **8. Attached articles (Study 1-7)**

Permission for reuse has been obtained from the respective publishing houses where required.



# Empagliflozin Effectively Lowers Liver Fat Content in Well-Controlled Type 2 Diabetes: A Randomized, Double-Blind, Phase 4, Placebo-Controlled Trial

*Diabetes Care* 2020;43:298–305 | <https://doi.org/10.2337/dc19-0641>

Sabine Kahl,<sup>1,2</sup> Sofiya Gancheva,<sup>1,2,3</sup>  
 Klaus Straßburger,<sup>2,4</sup> Christian Herder,<sup>1,2</sup>  
 Jürgen Machann,<sup>2,5</sup> Hisayuki Katsuyama,<sup>1,2</sup>  
 Stefan Kabisch,<sup>2,6</sup> Elena Henkel,<sup>7</sup>  
 Stefan Kopf,<sup>2,8</sup> Merit Lagerpusch,<sup>2,6</sup>  
 Konstantinos Kantartzis,<sup>2,5</sup>  
 Yuliya Kupriyanova,<sup>1,2</sup> Daniel Markgraf,<sup>1,2</sup>  
 Theresa van Gemert,<sup>1,2,3</sup> Birgit Knebel,<sup>2,9</sup>  
 Martin F. Wolkersdorfer,<sup>10</sup> Oliver Kuss,<sup>2,4</sup>  
 Jong-Hee Hwang,<sup>1,2</sup> Stefan R. Bornstein,<sup>11</sup>  
 Christian Kasperk,<sup>2,8</sup> Norbert Stefan,<sup>2,5</sup>  
 Andreas Pfeiffer,<sup>2,6,12</sup>  
 Andreas L. Birkenfeld,<sup>2,9</sup> and  
 Michael Roden<sup>1,2,3</sup>

## OBJECTIVE

To evaluate whether the sodium–glucose cotransporter 2 inhibitor empagliflozin (EMPA) reduces liver fat content (LFC) in recent-onset and metabolically well-controlled type 2 diabetes (T2D).

## RESEARCH DESIGN AND METHODS

Patients with T2D ( $n = 84$ ) ( $\text{HbA}_{1c}$   $6.6 \pm 0.5\%$  [ $49 \pm 10$  mmol/mol], known disease duration  $39 \pm 27$  months) were randomly assigned to 24 weeks of treatment with 25 mg daily EMPA or placebo. The primary end point was the difference of the change in LFC as measured with magnetic resonance methods from 0 (baseline) to 24 weeks between groups. Tissue-specific insulin sensitivity (secondary outcome) was assessed by two-step clamps using an isotope dilution technique. Exploratory analysis comprised circulating surrogate markers of insulin sensitivity and liver function. Statistical comparison was done by ANCOVA adjusted for respective baseline values, age, sex, and BMI.

## RESULTS

EMPA treatment resulted in a placebo-corrected absolute change of  $-1.8\%$  (95% CI  $-3.4, -0.2$ ;  $P = 0.02$ ) and relative change in LFC of  $-22\%$  ( $-36, -7$ ;  $P = 0.009$ ) from baseline to end of treatment, corresponding to a 2.3-fold greater reduction. Weight loss occurred only with EMPA (placebo-corrected change  $-2.5$  kg [ $-3.7, -1.4$ ];  $P < 0.001$ ), while no placebo-corrected change in tissue-specific insulin sensitivity was observed. EMPA treatment also led to placebo-corrected changes in uric acid ( $-74$  mol/L [ $-108, -42$ ];  $P < 0.001$ ) and high-molecular-weight adiponectin (36% [ $16, 60$ ];  $P < 0.001$ ) levels from 0 to 24 weeks.

## CONCLUSIONS

EMPA effectively reduces hepatic fat in patients with T2D with excellent glycemic control and short known disease duration. Interestingly, EMPA also decreases circulating uric acid and raises adiponectin levels despite unchanged insulin sensitivity. EMPA could therefore contribute to the early treatment of nonalcoholic fatty liver disease in T2D.

<sup>1</sup>Institute for Clinical Diabetology, German Diabetes Center, Leibniz Institute for Diabetes Research at Heinrich-Heine University, Düsseldorf, Germany

<sup>2</sup>German Center for Diabetes Research, München-Neuherberg, Germany

<sup>3</sup>Division of Endocrinology and Diabetology, Medical Faculty, Heinrich-Heine University Düsseldorf, Düsseldorf, Germany

<sup>4</sup>Institute for Biometrics and Epidemiology, German Diabetes Center, Leibniz Institute for Diabetes Research at Heinrich-Heine University, Düsseldorf, Germany

<sup>5</sup>Institute for Diabetes Research and Metabolic Diseases, Helmholtz Center Munich at the University of Tübingen, Tübingen, Germany

<sup>6</sup>Department of Clinical Nutrition, German Institute of Human Nutrition Potsdam-Rehbrücke, Nuthetal, Germany

<sup>7</sup>Clinical Study Center of Metabolic Vascular Medicine, GWT-TUD GmbH, Dresden, Germany

<sup>8</sup>Department of Internal Medicine 1 and Clinical Chemistry, University Hospital of Heidelberg, Heidelberg, Germany

Patients with type 2 diabetes (T2D) are prone to develop nonalcoholic fatty liver disease (NAFLD) (1), and NAFLD itself is associated with a doubled risk of incident T2D (2). NAFLD associates not only with cardiovascular disease but also with diabetes-related chronic kidney disease and retinopathy (1). Moreover, patients with T2D are at a higher risk of progressing from steatosis to nonalcoholic steatohepatitis (NASH), fibrosis, and cirrhosis (1).

Pronounced weight loss is effective for the treatment of NAFLD but difficult to achieve in many cases. Although well-known (glucagon-like peptide 1 receptor agonists, thiazolidinediones) and novel (e.g., pegbelfermin, elafibranor) compounds have demonstrated beneficial effects in patients with T2D and NAFLD, there is no accepted pharmacological treatment for these patients (3).

Sodium–glucose cotransporter 2 inhibitors (SGLT2is) not only improve glycemia by increasing urinary glucose excretion but also reduce body weight and blood pressure (4) and improve cardiovascular and renal outcomes (5). Some open-label and placebo-controlled studies have reported that SGLT2is may also alleviate NAFLD (6,7), while canagliflozin and dapagliflozin trended toward decreased liver fat content (LFC) compared with placebo (8,9). Body weight loss and glycated hemoglobin (HbA<sub>1c</sub>) reduction may be mainly responsible for LFC reduction with canagliflozin (8,10), but empagliflozin (EMPA) could improve NAFLD independently of body weight and glycemia (7,11). Of note, SGLT2is ameliorated inflammation, oxidative stress, and dysregulated hormone secretion in preclinical studies (4). The current randomized, placebo-controlled clinical trial examined the effectiveness of EMPA on LFC reduction in patients with recent-onset, well-controlled T2D and explored its effects on tissue-specific insulin sensitivity.

## RESEARCH DESIGN AND METHODS

### Study Design

This randomized, parallel-group, double-blind, phase 4 trial was performed at five centers in Germany (Düsseldorf, Potsdam-Rehbrücke, Dresden, Tübingen, and Heidelberg) with a 1:1 allocation to treatment arms. The lead ethics committee of Heinrich-Heine University Düsseldorf approved all trial procedures.

### Patients

The study population consisted of well-controlled patients with T2D with short known disease duration to exclude that the observed effects of EMPA were mainly driven by improvement of glycaemic control. The rationale for this selection was the research question of whether SGLT2is would also be effective in early T2D, where effects on glycemia and changes in additional antihyperglycemic treatment during the intervention would be minimized. Participants were recruited by newspaper and Internet advertisements. Before inclusion, all patients gave written informed consent. Principal inclusion criteria were age 18–75 years, BMI <45 kg/m<sup>2</sup>, known diabetes duration ≤7 years, HbA<sub>1c</sub> of 6–8%, and no previous antihyperglycemic treatment or a 1-month washout period. Principal exclusion criteria included uncontrolled hyperglycemia at screening (fasting blood glucose [FBG] ≥240 mg/dL), liver disease other than NAFLD, previous thiazolidinedione treatment, and use of immunomodulatory, antiobesity, anti-NASH drugs. Full inclusion and exclusion criteria are listed in the Supplementary Data.

### Randomization and Masking

All participants were randomized by a stratified computed randomization procedure to account for age, sex, and BMI to EMPA or placebo and were masked to the treatment assignment. The electronic

master randomization list was only accessible to the assigned randomization list managers, and study sites received sealed opaque envelopes for unblinding in cases of emergency. Enrollment was performed at the respective site. Randomization and assignment to the double-blind study drug was done by central pharmacy personnel, who had access to the computer-generated randomization scheme. No open access to the code was available at study centers to monitors, statisticians, or sponsors' teams. Blinding of investigators and patients was achieved by providing EMPA and placebo tablets with identical appearance and packaging. Unblinding was performed after the final database lock.

### Procedures

All procedures are summarized in the Supplementary Data. Eligibility of patients was assessed at screening and at the end of the 1-month washout period (for patients with previous antihyperglycemic treatment only). Participants received one individual dietary counseling before the baseline visit according to recommendations of the American Diabetes Association (12).

All baseline measures were performed before the first intake of study medication. From screening on, FBG levels were self-monitored daily with a glucose meter.

Enrolled patients were allocated to one treatment arm (EMPA 25 mg once daily or matching placebo orally; both from Boehringer Ingelheim, Ingelheim/Rhein, Germany) and returned to the study center at baseline; at weeks 1, 4, 8, 12, 16, 20, and 24 for efficacy and safety (including adverse events) assessments; and at 2 weeks after discontinuation of study medication.

Assessments of visceral adipose tissue (VAT) and subcutaneous adipose tissue (SCAT) volume and LFC, respectively, were performed at baseline and 12 and 24 weeks.

<sup>9</sup>Institute for Clinical Biochemistry and Pathobiochemistry, German Diabetes Center, Leibniz Institute for Diabetes Research at Heinrich-Heine University, Düsseldorf, Germany

<sup>10</sup>Landesapotheke Salzburg, Salzburg, Austria

<sup>11</sup>Paul Langerhans Institute Dresden, Helmholtz Center Munich at University Hospital MKIII, and Faculty of Medicine, TU Dresden, Dresden, Germany

<sup>12</sup>Department of Endocrinology, Diabetes and Nutrition, Campus Benjamin Franklin, Charité University Medicine, Berlin, Germany

Corresponding author: Michael Roden, michael.roden@ddz.de

Received 29 March 2019 and accepted 21 August 2019

Clinical trial reg. no. NCT02637973, clinicaltrials.gov

This article contains Supplementary Data online at <http://care.diabetesjournals.org/lookup/suppl/doi:10.2337/dc19-0641/-/DC1>.

S.Kah. and S.G. contributed equally.

This article is part of a special article collection available at <https://care.diabetesjournals.org/collection/naflid-in-diabetes>.

This article is featured in a podcast available at <http://www.diabetesjournals.org/content/diabetes-core-update-podcasts>.

© 2019 by the American Diabetes Association. Readers may use this article as long as the work is properly cited, the use is educational and not for profit, and the work is not altered. More information is available at <http://www.diabetesjournals.org/content/license>.

See accompanying articles, pp. 275, 283, and 290.

LFC was assessed at each center using volume-selective proton MRS ( $^1\text{H}$ -MRS) using a stimulated echo acquisition mode (coefficient of variation [CV] 0.3–1.7%) as reported previously (13) or chemical shift-selective in-phase/opposed-phase imaging technique in one center (14). All measurements were performed in liver segment 7, and LFC was calculated as fat / (water + fat) \* 100% by central reading.

SCAT (CV 1.5% [J.M., personal communication]) and VAT (CV 1.1% [15]) were measured using T1-weighted axial fast spin-echo (16) and quantified using an automated algorithm on the basis of fuzzy clustering and orthonormal snakes (15). Central reading was done at the Institute for Diabetes Research and Metabolic Diseases of the Helmholtz Center Munich at University of Tübingen by a spectroscopist blinded to patients' treatment allocation.

Two-step euglycemic insulin clamps with  $[6,6\text{-}^2\text{H}_2]$ glucose (17) were done to assess whole-body, mainly skeletal muscle, insulin sensitivity (M value,  $R_d$ ) and adipose tissue (% suppression of free fatty acids [FFAs]) insulin sensitivity as well as parameters related to endogenous glucose production (EGP) (absolute EGP rates, % EGP suppression) during low and high insulinemia at baseline and week 24. Briefly, participants fasted overnight for at least 10 h and refrained from any exercise and alcohol for at least 24 h before the test.  $[6,6\text{-}^2\text{H}_2]$ glucose was given as primed-continuous intravenous infusion throughout the clamp. After 120 min, a primed (40 mU/m<sup>2</sup>/min for 8 min) insulin intravenous infusion (Insulin Rapid; Sanofi, Paris, France) was given for the next 120 min at 20 mU/m<sup>2</sup>/min (low insulin) and for the final 120 min at 40 mU/m<sup>2</sup>/min (high insulin). A variable 20% glucose infusion enriched with  $[6,6\text{-}^2\text{H}_2]$ glucose was used to maintain blood glucose at ~90 mg/dL. The M value was calculated from glucose infusion rates during the last 20–30 min of both low- and high-insulin periods. Patients in whom steady-state conditions were not achieved were excluded from analysis. Because the study drug was discontinued at least 3 days before the clamps to account for the half-life of EMPA 25 mg (~10.7 h [8]), urinary glucose excretion was not measured.

Fasting hepatic insulin resistance (HIR) was calculated as fasting plasma insulin \* basal EGP (8). Fasting adipose

tissue insulin resistance was calculated as fasting FFA \* fasting plasma insulin.

Daily energy intake was analyzed from 3-day food diaries, which were filled in by patients before each visit at the site using the Prodi system (Prodi 6.3.0.1 [Nbase 3.60]; Nutri-Science GmbH, Freiburg, Germany). Physical activity was assessed by Baecke index (18).

Glucose, insulin (hemolytic blood samples were excluded from analysis), C-peptide, and FFA concentrations were measured as previously described (19). Serum levels of cytokeratin 18 (CK18)-M30 and -M65, adiponectin, fibroblast growth factor 21 (FGF-21), tumor necrosis factor- $\alpha$  (TNF- $\alpha$ ), interleukin-1 receptor antagonist (IL-1Ra), IL-6, and resistin were measured at baseline and after 12 and 24 weeks. IL-6 and TNF- $\alpha$  were measured with Quantikine High Sensitivity ELISA Kits (R&D Systems, Abington, U.K.), and IL-1Ra, FGF-21, and resistin were measured with Quantikine ELISA Kits (R&D Systems). High-molecular-weight (HMW) adiponectin was measured with the HMW and Total Adiponectin ELISA Kit (ALPCO, Salem, NH), and CK18-M30 (apoptosis-associated capase-cleaved keratin 18, K18Asp396, or M30 neoepitope) and CK18-M65 (soluble keratin K18) were measured using the M30 Apopto-sense ELISA and M65 ELISA Kits (VLVbio, Nacka, Sweden).

### Outcomes

The primary efficacy end point was defined as the difference in change of LFC (in %) between EMPA and placebo from baseline to 24 weeks of treatment. Secondary end points comprised the differences in changes of measures of whole-body/skeletal muscle (M value,  $R_d$ ) and hepatic insulin sensitivity (HIR, insulin-stimulated EGP suppression, fasting EGP) measures between EMPA and placebo from baseline to 24 weeks. All assessments except LFC were exploratory. Safety was monitored by assessment of vital signs, physical examination, electrocardiogram, adverse events, and laboratory results (blood chemistry, hematological and coagulation parameters) at each visit.

### Power Calculation

An ~3% reduction from baseline in body weight was observed for EMPA 25 mg in a phase 3 study with patients with T2D (20). In patients with T2D with a short disease duration and excellent glycemic

control, an ~5% reduction in body weight corresponded to an ~7% reduction in LFC (19). Thus, the current study required a sample size of 30 patients/arm to detect a 4% absolute decrease in LFC from baseline with a pairwise comparison within a 95% CI, assuming an SD of 5.4% and a power of at least 80%. An estimated dropout rate of 15% resulted in 36 participants/arm.

### Statistical Analyses

All analyses for efficacy parameters were performed in the intention-to-treat population, including all patients, of which at least the baseline and 12-week and/or 24-week LFC data were available. For patient characteristics, data are shown as mean with SD for normally distributed data and median with first and third quartiles for log-normally distributed parameters. Values of parameters at week 0 in both treatment arms are presented as means for normally distributed data and geometric means for log-normally distributed data with 95% CIs. Placebo-corrected changes from baseline to 24 weeks for normally distributed parameters are presented as absolute changes and for log-normally distributed data, as relative changes with corresponding 95% CIs adjusted for age, sex, BMI, and respective baseline parameter (least square means). Comparison of changes between treatments was done by an ANCOVA adjusted for age, sex, BMI, and the baseline value of the respective parameter. Calculations were performed with SAS 9.4 TS1M2 (SAS Institute, Cary, NC). No data monitoring committee was foreseen for this small-scale phase 4 trial.

### RESULTS

Between 4 March 2016 and 1 February 2018, 84 patients were randomized to EMPA ( $n = 42$ ) or placebo ( $n = 42$ ) and received at least one dose of the study medication. Of all randomized patients, 65 (77%) completed the trial (Fig. 1).

### Patient Characteristics

Baseline anthropometric and metabolic measures were all comparable between EMPA and placebo (Table 1). Physical activity and daily calorie intake neither differed at baseline nor changed from baseline to 24 weeks between the groups (data not shown).

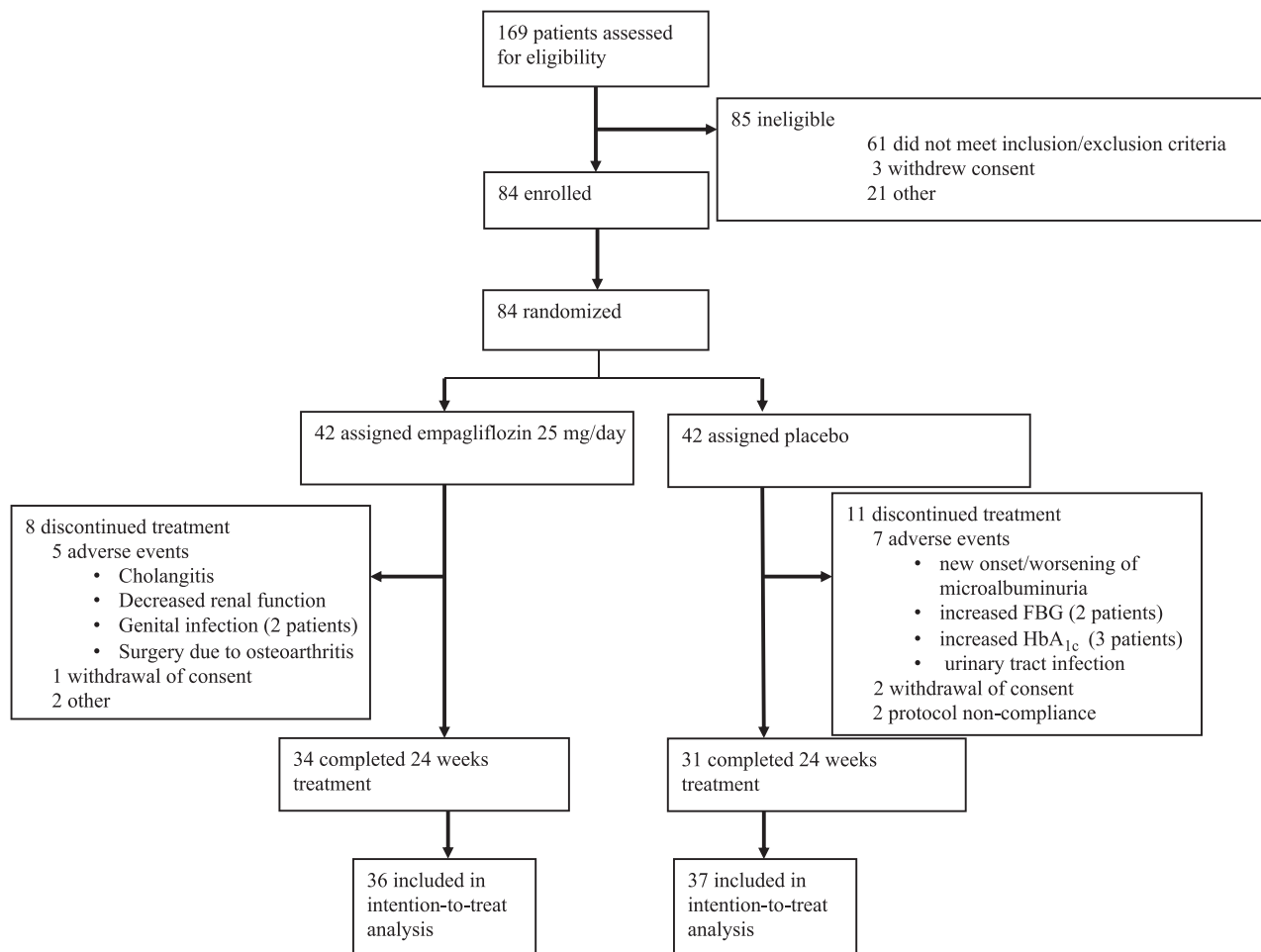


Figure 1—Trial profile.

### Effect of EMPA on LFC

In the intention-to-treat population, 29 (81%) of 36 patients in the EMPA arm and 29 (78%) of 37 in the placebo arm had NAFLD at week 0. LFC was comparable between groups (EMPA 9.6% [95% CI 7.3, 12.7]; placebo 11.3% [8.6, 14.7]) and decreased in both groups already at week 12 (relative reduction: EMPA  $-21\%$ , placebo  $-15\%$ ). At 24 weeks, a placebo-corrected absolute ( $-1.8\%$  [ $-3.4, -0.2$ ];  $P = 0.02$ ) and relative decrease in LFC ( $-22\%$  [ $-36, -7$ ];  $P = 0.009$ ) was observed, corresponding to a 2.3-fold higher relative reduction in EMPA (Fig. 2A and Supplementary Table 2). Further adjustment for change in body weight attenuated the difference in LFC reduction of EMPA and placebo (placebo-corrected decrease  $-6\%$  [ $-23, 14$ ];  $P = 0.50$ ).

Applying maximum likelihood methods to account for missing values for LFC at week 24 did not affect the results (data not shown). NAFLD resolution (LFC  $<5.56\%$

[21]) occurred in 5 (20%) of 25 patients in the EMPA group and 2 (8%) of 24 patients in the placebo group at 24 weeks.

To examine the impact of the presence of NAFLD on EMPA-mediated reduction of LFC, an interaction term of treatment and NAFLD status (yes/no) was added to the model. Interaction of NAFLD status and treatment was not significant ( $P = 0.94$ ).

The impact of sex on the EMPA-related reduction in LFC was examined by including an interaction term of treatment and sex in our model. There was a placebo-corrected decrease in LFC in males ( $-31\%$  [95% CI  $-44, -14$ ];  $P = 0.002$ ) but not in females ( $-1\%$  [ $-28, 37$ ];  $P = 0.96$ ). The test of interaction between sex and treatment did not achieve significance ( $P = 0.075$ ).

### Effect of EMPA on Skeletal Muscle and Hepatic and Adipose Tissue Insulin Sensitivity

During low-insulin clamp conditions, placebo-corrected whole-body/skeletal

muscle  $R_d$  increased by 30% (95% CI 9, 55;  $P = 0.005$ ) (Supplementary Table 1). However, there were no significant placebo-corrected changes in M value both at low (50% [0, 126];  $P = 0.05$ ) and high (12% [ $-12, 42$ ];  $P = 0.36$ ) insulin with EMPA (Fig. 2B and Supplementary Table 1). Changes in HIR and insulin-mediated suppression of EGP at low- and high-insulin conditions were also comparable between groups (Fig. 2C and Supplementary Table 1). Likewise, changes in adipose tissue insulin resistance and insulin-stimulated FFA suppression at low- and high-insulin conditions did not differ between groups (Fig. 2D and Supplementary Table 1).

### Effect of EMPA on Body Composition, Glycemia, and Lipidemia

EMPA resulted in a placebo-corrected weight loss of  $-2.5$  kg (95% CI  $-3.7, -1.4$ ;  $P < 0.001$ ) at 24 weeks (Fig. 3A and Supplementary Table 2). The body weight reduction occurred in 31 (86%)

**Table 1—Patient characteristics at week 0**

	EMPA (n = 42)	Placebo (n = 42)
Sex		
Male	29 (69)	29 (69)
Female	13 (31)	13 (31)
Age (years)	62.7 ± 7.0	61.5 ± 10.0
Ethnicity		
Caucasian	42 (100)	41 (98)
Hispanic/Latino	0 (0)	1 (2)
BMI (kg/m <sup>2</sup> )	32.1 ± 4.6	32.4 ± 4.2
Known diabetes duration (months)	36 ± 27	40 ± 27
Hepatic steatosis*	33 (79)	33 (79)
Concomitant medication		
Antihyperglycemic drugs#	28 (67)	26 (62)
Antihypertensive drugs	21 (50)	29 (69)
Lipid-lowering drugs	19 (45)	15 (36)
Glycemia		
HbA <sub>1c</sub>		
%	6.8 ± 0.5	6.7 ± 0.7
mmol/mol	51 ± 6	50 ± 8
FBG (mmol/L)	7.5 ± 1.4	7.2 ± 1.3
Serum lipid concentrations		
Triglycerides (mg/dL)	159 (122; 202)	181 (103; 251)
HDL cholesterol (mg/dL)	50 ± 15	48 ± 10
LDL cholesterol (mg/dL)	133 ± 40	120 ± 30
Liver transaminases		
ALT (μmol/s/L)	0.54 (0.42; 0.80)	0.62 (0.42; 0.88)
AST (μmol/s/L)	0.42 (0.36; 0.49)	0.43 (0.37; 0.55)

Data are mean ± SD for normally distributed parameters, median (25%; 75%) for log-normally distributed parameters, or n (%). ALT, alanine aminotransferase; AST, aspartate aminotransferase. \*LFC ≥5.56% measured by magnetic resonance–based methods. #Antihyperglycemic medication was stopped from at least 4 weeks before randomization until the end of the intervention period.

of 36 patients in the EMPA group and 18 (49%) of 37 patients in the placebo group. Weight loss of ≥5% occurred in 27% of patients on EMPA and in 16% on placebo. There were no placebo-corrected changes in VAT (−290 cm<sup>3</sup> [−694, 114]; *P* = 0.16) and SCAT (−2% [−10, 6]; *P* = 0.55) with EMPA. Of note, patients who underwent both VAT and SCAT measurements (*n* = 21 of 29) also exhibited a placebo-corrected decrease in body weight with EMPA (−2.6 kg [−4.0, −1.1]; *P* < 0.001).

EMPA led to a placebo-corrected change in FBG (−0.7 mmol/L [95% CI −1.3, −0.2]; *P* = 0.01) (Fig. 3B) but not in HbA<sub>1c</sub> (Supplementary Table 2). Placebo-corrected changes in fasting insulin, C-peptide, and FFA levels did not reach significance (all *P* > 0.2) (Supplementary Table 2). Also, serum HDL and LDL cholesterol, serum total cholesterol, and plasma triglycerides were unaffected by EMPA treatment (data not shown).

#### Effect of EMPA on Adiponectin and Inflammation- and Liver-Related Parameters

Serum uric acid markedly decreased (placebo-corrected change −74 mol/L [95% CI −108, −42]; *P* < 0.001), and HMW adiponectin concentrations increased (placebo-corrected change 36% [16, 60]; *P* < 0.001) from 0 to 24 weeks (Fig. 3C and D). Placebo-corrected changes in IL-1Ra, TNF-α, IL-6, and FGF-21 did not differ between groups (all *P* > 0.2) (Supplementary Table 3).

Serum alanine aminotransferase and γ-glutamyl transferase were reduced with similar effect sizes in EMPA and placebo after 24 weeks (Supplementary Table 3). CK18-M30 and -M65 numerically decreased in the EMPA group, but no placebo-corrected changes were detectable (Supplementary Table 3).

#### CONCLUSIONS

This trial provides evidence that empagliflozin effectively reduces LFC compared with placebo but has no major effects on

tissue-specific insulin sensitivity. Exploratory analyses revealed a marked decrease in serum uric acid and a rise in serum HMW adiponectin levels. Of interest, these effects occurred in the presence of moderate weight loss and despite only minor changes in glycemia in a cohort of metabolically well-controlled patients with T2D with a short disease duration.

#### Effects of SGLT2is on LFC and Body Weight

Recent randomized controlled trials demonstrated that SGLT2is can induce a reduction of LFC compared with baseline (6–9), but only one trial also reported a statistically significant effect on LFC compared with placebo (6). The magnitude of the reduction in LFC may depend on trial medication and design; duration of the intervention; cohort characteristics, such as NAFLD status, T2D duration, glycemic control, and sex distribution; and, finally, statistical power (22,23). The current study reports that EMPA leads to a nominally greater placebo-corrected decrease in LFC than dapagliflozin (6) but a slightly smaller decrease in change from baseline than canagliflozin (8). However, the absence of studies on dose dependency and head-to-head comparisons does not allow any conclusions about drug-specific effects at present. As indicated in other NAFLD trials (22,23), the guideline-based dietary counseling for all groups could have been responsible for the higher rates of LFC improvement observed in the placebo groups of this study and one previous (8) but not in other SGLT2i trials (6,9).

On the other hand, study duration may play a role as illustrated by the observation that alanine aminotransferase, as a crude surrogate marker of NAFLD, decreased only during the first 28 weeks of EMPA treatment (11). At the least, the nominally greater baseline-corrected decrease in LFC in the 24-week placebo-controlled trials (i.e., in one previous [8] and the current trial) than in the 8- and 12-week trials could support this contention (6,9).

As to cohort characteristics, the better metabolic control and shorter known diabetes duration compared with previous trials (6–9) and the possible inclusion of patients without NAFLD could have led to an underestimation of the efficacy of EMPA on LFC in our cohort (11). Indeed, incidence of NAFLD positively associates

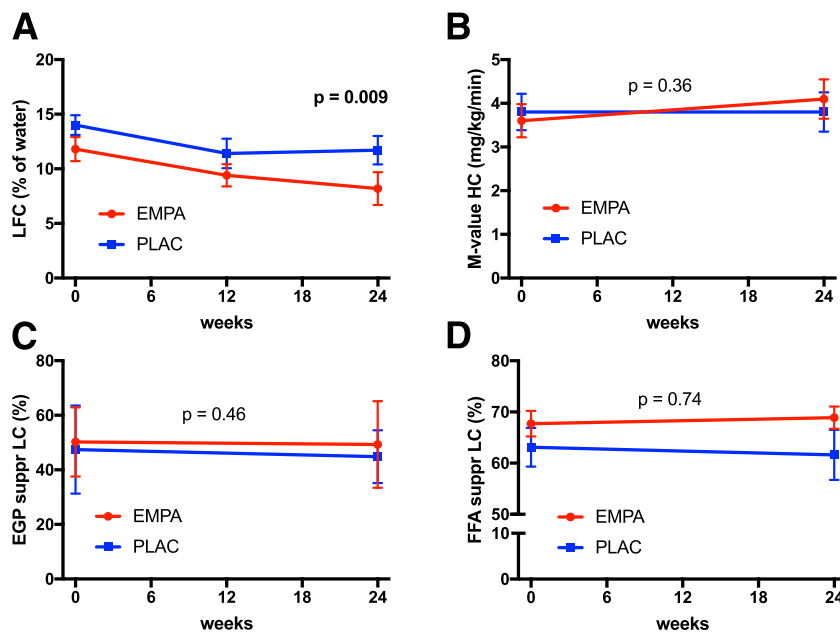


**Figure 2**—Effects of EMPA on LFC (A), whole-body insulin sensitivity (M value in high-insulin condition [40 IU/m<sup>2</sup> body surface area/min] [HC]) (B), hepatic insulin sensitivity as insulin-stimulated suppression of EGP under low-insulin conditions (20 IU/m<sup>2</sup> body surface area) (EGP suppression LC) (C), and adipose tissue insulin sensitivity as insulin-stimulated suppression of FFA under low-insulin conditions (FFA suppression LC) (D). Numbers of patients in EMPA and placebo (PLAC), respectively, of which week 0 and 24 data were obtained are as follows: 31 and 31 (A), 28 and 26 (B), 24 and 25 (C), and 27 and 27 (D). Unadjusted values of parameters are mean ± SEM. P values indicate significance level for PLAC-corrected EMPA effect and are based on ANCOVA with adjustment for age, sex, BMI, and the respective baseline parameter.

with higher HbA<sub>1c</sub> and most likely also longer diabetes duration (24), and NAFLD frequency may affect the magnitude of LFC reduction in T2D (8,11).

Finally, this study found a placebo-corrected reduction of LFC in males but not in females, although the interaction of sex and treatment was not significant and the number of females small. Given that the percentage of males ranged from 60 to 81% in the previous randomized SGLT2i studies (6–9), sex-dependent differences in metabolic effects on LFC cannot be excluded. In this context, a recent study suggested sex differences in the effects of EMPA on arterial stiffness (25), whereas a post hoc analysis of the BI 10773 (Empagliflozin) Cardiovascular Outcome Event Trial in Type 2 Diabetes Mellitus Patients (EMPA-REG OUTCOME) did not detect any changes in outcomes between females and males (26).

This study shows that the changes in LFC occur in parallel to the decline in body weight during SGLT2i treatment. While significant reduction in LFC was considered to require weight loss of ≥5% (8), studies have indicated that even minor weight loss up to 5% can initiate a decrease in LFC by 33% (3,27). Because a

body weight reduction of ≥5% was observed in only 27% of the EMPA group, the 34% decline in LFC underlines the role of minor weight loss for the effect of SGLT2is on LFC.

#### EMPA and Insulin Sensitivity

During low-insulin conditions, EMPA resulted in a borderline, but nonsignificant (M value) or significant (R<sub>d</sub>) increase in whole-body glucose disposal. Under these conditions, R<sub>d</sub> and M value represent the amount of glucose taken up not only by skeletal muscle but also by other organs like adipose tissue and the splanchnic bed (28). However, measures of adipose tissue (insulin-stimulated EGP suppression) or hepatic (insulin-stimulated EGP suppression) insulin sensitivity were not different between EMPA and placebo. Thus, the higher R<sub>d</sub> could have resulted from EMPA-induced glucosuria, but study medication was stopped at least 3 days before the clamps (to account for the half-life of EMPA [~10.7 h for EMPA 25 mg (29)]), rendering urinary glucose loss unlikely. Moderate increases in R<sub>d</sub> with SGLT2is have also been attributed to improvements in hyperglycemia and glucose toxicity (8,30). Thus, despite

the (very) good glucometabolic control and rather short known diabetes duration, the minor decrease in fasting glycemia with EMPA could have contributed to the small increase in R<sub>d</sub> during low-grade insulinemia. In contrast, the current study found no placebo-corrected effects of EMPA on R<sub>d</sub> and M value during high-insulin clamps, which is in line with the trials on dapagliflozin (6) and canagliflozin (8). Under these conditions, R<sub>d</sub> almost exclusively reflects insulin-stimulated skeletal muscle glucose uptake (28).

Interestingly, the decrease in LFC was not paralleled by improved hepatic insulin sensitivity, which is comparable to one dapagliflozin study (6) but in contrast to the canagliflozin trial (8). The latter study also reported lower HbA<sub>1c</sub> and discussed reduction of glucotoxicity by canagliflozin as the cause (8). The absence of changes in HbA<sub>1c</sub> in the current study supports this contention.

Previous studies demonstrated that the antihyperglycemic efficacy of SGLT2i is partly counteracted by a rise in EGP (31,32). This could result from a chronic SGLT2i-induced rise in plasma glucagon and decreased insulin concentrations. However, a recent clinical trial showed that canagliflozin still increases EGP when liraglutide prevents the changes in plasma insulin and glucagon levels (33). Similarly, hyperglucagonemia per se does not mediate the SGLT2i-induced increase in EGP (34). Of note, glycemia per se may regulate EGP in that a decrease in plasma glucose concentration can stimulate EGP independent of changes in plasma insulin and glucagon (35).

Finally, fasting FFA and insulin levels as well as adipose tissue insulin resistance were unchanged during this study. The previous placebo-controlled SGLT2i trials on LFC yielded contradictory results, showing elevated (8) or unchanged (8) or unchanged (6,9) fasting insulinemia. The previously reported SGLT2i-associated FFA elevation has been explained by glucosuria-induced relative hypoinsulinemia, which would reduce inhibition of lipolysis and tissue glucose uptake with a compensatory increase in lipid oxidation and hyperketonemia (4). In our cohort of patients with well-controlled, recent-onset T2D, EMPA did not decrease circulating insulin levels so that the ambient insulinemia

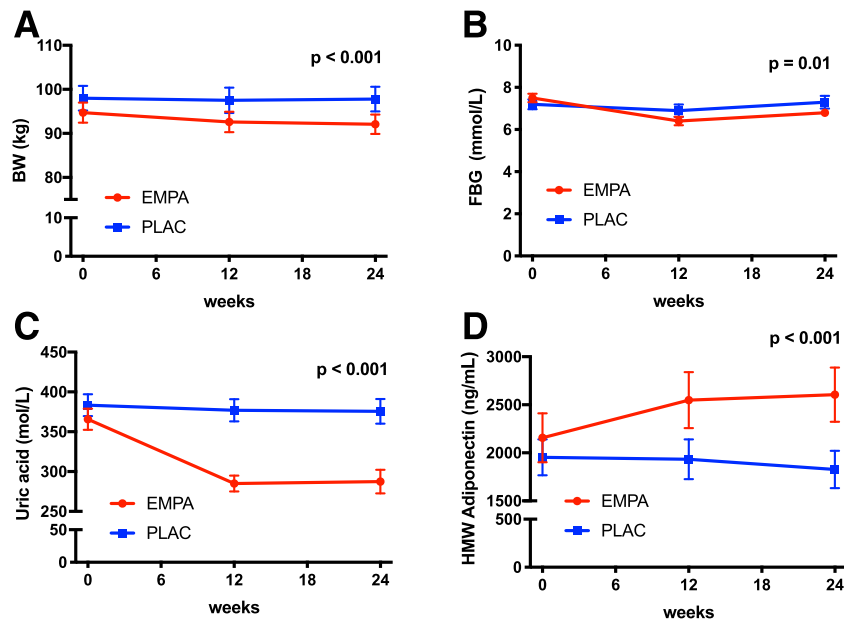


**Figure 3**—Effects of EMPA on body weight (BW) (A), FBG (B), serum uric acid levels (C), and serum HMW adiponectin levels (D). Comparison of changes in the respective parameters between treatment arms. Numbers of patients in EMPA and placebo (PLAC) groups, respectively, of which week 0 and 24 data were obtained are as follows: 32 and 32 (A), 31 and 31 (B), 31 and 31 (C), and 31 and 30 (D). Unadjusted values of parameters are mean  $\pm$  SEM. *P* values indicate significance level for PLAC-corrected EMPA effect and are based on ANCOVA with adjustment for age, sex, BMI, and the respective baseline parameter.

might have sufficed to inhibit lipolysis as shown in humans without diabetes (4).

#### Exploratory Analyses of Circulating Parameters

A recent uncontrolled pilot study provided some evidence that EMPA treatment for 24 weeks could improve histological components of NASH and its resolution despite a mean reduction in BMI of only  $-0.7$  kg/m<sup>2</sup> (36). The current trial did not observe placebo-corrected changes in circulating surrogate markers of liver injury, such as transaminases or CK18-M30 fragment. This is partly in line with some studies (6,7) but not in another that reported improvements in transaminases as well as CK18 fragments with dapagliflozin (9). The lack of an effect of EMPA could be due to the absence of NASH and fibrosis or masked by the greater decrease in LFC in the placebo group, which is a major trigger for reduction of these surrogate markers (27).

EMPA treatment markedly reduced serum uric acid and raised serum adiponectin concentrations. High uric acid levels trigger adipose tissue inflammation, insulin resistance, and hypo-adiponectinemia (37). Of note, increased uric acid and decreased adiponectin levels

associate with body weight; metabolic syndrome features, including T2D; and NAFLD (37–39).

#### Limitations

The patient cohort comprised exclusively metabolically well-controlled patients with T2D with short known disease duration with and without NAFLD. Thus, results cannot be necessarily extrapolated to the general population of patients with T2D, particularly to those with uncontrolled glycemia, longer disease duration, and more severe liver disease. On the other hand, this limitation represents a specific strength by showing that EMPA is effective in reducing LFC in the absence of major changes in glycemia. This trial provides no information about the efficacy and safety of EMPA in glucose-tolerant individuals with NAFLD, a collective at increased risk of T2D (2). Moreover, this study used detailed metabolic phenotyping with two-step euglycemic clamps but not mixed-meal tests, which would have allowed the assessment of postprandial  $\beta$ -cell function and metabolism, and did not include liver biopsies because of the expected early stages of NAFLD in these patients and the short duration of intervention. Finally, this study did not use multiple imputation

to account for missing values but performed maximum likelihood methods for the primary end point (40).

In conclusion, this proof-of-concept trial shows that the SGLT2i EMPA decreases LFC in near-normoglycemic patients with recent-onset T2D with and without NAFLD. EMPA induced minor weight loss and no effect on tissue-specific insulin sensitivity. The marked decrease in serum uric acid and the rise in HMW adiponectin levels with EMPA treatment calls for further studies on the clinical relevance of these observations. Because future NAFLD treatment in T2D will require strategies that simultaneously address the different mechanisms underlying metabolic liver disease, EMPA could serve as a partner for such combination treatments because of its favorable effects on liver fat and body weight.

**Acknowledgments.** The authors thank all the patients, investigators, and trial-site staff members involved in the conduct of the trial.

**Funding.** The study was supported by the German Diabetes Center (DDZ), which is funded by the German Federal Ministry of Health and the Ministry of Innovation, Science, and Research of the State North Rhine-Westphalia (Germany); the German Federal Ministry of Education and Research to the German Center for Diabetes Research (DZD e.V.); and Schmutzler Stiftung, Germany.

All funding bodies had no role in study design, data collection, data analysis, data interpretation, or writing of the report.

**Duality of Interest.** The study was supported by Boehringer Ingelheim through an Independent Research Grant. C.H. receives personal fees from Eli Lilly and Sanofi outside the submitted work. S.Kab. reports nonfinancial support and other from Sanofi, personal fees from Berlin-Chemie, and grants from the German Center of Diabetes Research and German Diabetes Association outside the submitted work. A.P. reports grants from the German Center for Diabetes Research during the conduct of this study and receives personal fees from Boehringer Ingelheim and Eli Lilly outside the submitted work. A.L.B. serves or has served on advisory boards for Novo Nordisk, Sanofi, AstraZeneca, and Boehringer Ingelheim and serves or has served on speakers bureaus for Novo Nordisk, Sanofi, Boehringer Ingelheim, and AstraZeneca. M.R. received investigator-initiated support from Boehringer Ingelheim during the conduct of the study; receives personal fees from Bristol-Myers Squibb, Boehringer Ingelheim, Eli Lilly, Fishawack Group, Gilead Sciences, Novo Nordisk, Poxel S.A. Société, Prosciento Inc., Servier Lab, Target Pharmsolutions, and Terra Firma outside of the submitted work; reports other from Sanofi, AstraZeneca, Nutricia/Danone, and Novartis outside the submitted work; and is on scientific advisory boards for Bristol-Myers Squibb, Eli Lilly, Gilead Sciences,

Novo Nordisk, Servier Laboratories, Target Pharmaceuticals, and Terra Firma. No other potential conflicts of interest relevant to this work were reported.

**Author Contributions.** S.Kah., S.G., K.S., C.H., J.M., H.K., S.Kab., E.H., S.Ko., M.L., K.K., Y.K., D.M., T.v.G., B.K., O.K., and J.-H.H. contributed to the acquisition and interpretation of data. M.F.W. contributed to the preparation and analysis of stable isotope tracers. S.R.B., C.K., N.S., A.P., A.L.B., and M.R. contributed to the study design and interpretation of data. S.Kah. and M.R. drafted the report. All authors contributed to the review of the report and approved the final version for submission. M.R. is the guarantor of this work and, as such, had full access to all the data in the study and takes responsibility for the integrity of the data and the accuracy of the data analysis.

**Prior Presentation.** Parts of this study were presented at the 79th Scientific Sessions of the American Diabetes Association, San Francisco, CA, 7–11 June 2019; the 2nd International Conference on Fatty Liver, Berlin, Germany, 27–29 June 2019; Diabetes Congress 2019, Berlin, Germany, 29 May–1 June 2019; and the 55th Annual Meeting of the European Association for the Study of Diabetes, Barcelona, Spain, 15–20 September 2019.

## References

- Tilg H, Moschen AR, Roden M. NAFLD and diabetes mellitus. *Nat Rev Gastroenterol Hepatol* 2017;14:32–42
- Mantovani A, Byrne CD, Bonora E, Targher G. Nonalcoholic fatty liver disease and risk of incident type 2 diabetes: a meta-analysis. *Diabetes Care* 2018;41:372–382
- Toplak H, Stauber R, Sourij H. EASL-EASD-EASO Clinical Practice Guidelines for the management of non-alcoholic fatty liver disease: guidelines, clinical reality and health economic aspects. *Diabetologia* 2016;59:1148–1149
- Ferrannini E. Sodium-glucose co-transporters and their inhibition: clinical physiology. *Cell Metab* 2017;26:27–38
- Zelinker TA, Wiviott SD, Raz I, et al. SGLT2 inhibitors for primary and secondary prevention of cardiovascular and renal outcomes in type 2 diabetes: a systematic review and meta-analysis of cardiovascular outcome trials. *Lancet* 2019;393:31–39
- Latva-Rasku A, Honka MJ, Kullberg J, et al. The SGLT2 inhibitor dapagliflozin reduces liver fat but does not affect tissue insulin sensitivity: a randomized, double-blind, placebo-controlled study with 8-week treatment in type 2 diabetes patients. *Diabetes Care* 2019;42:931–937
- Kuchay MS, Krishan S, Mishra SK, et al. Effect of empagliflozin on liver fat in patients with type 2 diabetes and nonalcoholic fatty liver disease: a randomized controlled trial (E-LIFT trial). *Diabetes Care* 2018;41:1801–1808
- Cusi K, Bril F, Barb D, et al. Effect of canagliflozin treatment on hepatic triglyceride content and glucose metabolism in patients with type 2 diabetes. *Diabetes Obes Metab* 2019;21:812–821
- Eriksson JW, Lundkvist P, Jansson PA, et al. Effects of dapagliflozin and n-3 carboxylic acids on non-alcoholic fatty liver disease in people with type 2 diabetes: a double-blind randomised placebo-controlled study. *Diabetologia* 2018;61:1923–1934
- Leiter LA, Forst T, Polidori D, Balis DA, Xie J, Sha S. Effect of canagliflozin on liver function tests in patients with type 2 diabetes. *Diabetes Metab* 2016;42:25–32
- Sattar N, Fitchett D, Hantel S, George JT, Zinman B. Empagliflozin is associated with improvements in liver enzymes potentially consistent with reductions in liver fat: results from randomised trials including the EMPA-REG OUTCOME® trial. *Diabetologia* 2018;61:2155–2163
- American Diabetes Association. Standards of medical care in diabetes—2014. *Diabetes Care* 2014;37(Suppl. 1):S14–S80
- Machann J, Thamer C, Schnoedt B, et al. Hepatic lipid accumulation in healthy subjects: a comparative study using spectral fat-selective MRI and volume-localized <sup>1</sup>H-MR spectroscopy. *Magn Reson Med* 2006;55:913–917
- Reeder SB, McKenzie CA, Pineda AR, et al. Water-fat separation with IDEAL gradient-echo imaging. *J Magn Reson Imaging* 2007;25:644–652
- Würslin C, Machann J, Rempp H, Claussen C, Yang B, Schick F. Topography mapping of whole body adipose tissue using a fully automated and standardized procedure. *J Magn Reson Imaging* 2010;31:430–439
- Machann J, Thamer C, Stefan N, et al. Follow-up whole-body assessment of adipose tissue compartments during a lifestyle intervention in a large cohort at increased risk for type 2 diabetes. *Radiology* 2010;257:353–363
- Phielix E, Brehm A, Bernroider E, et al. Effects of pioglitazone versus glimepiride exposure on hepatocellular fat content in type 2 diabetes. *Diabetes Obes Metab* 2013;15:915–922
- Baecke JA, Burema J, Frijters JE. A short questionnaire for the measurement of habitual physical activity in epidemiological studies. *Am J Clin Nutr* 1982;36:936–942
- Nowotny B, Zahiragic L, Bierwagen A, et al. Low-energy diets differing in fibre, red meat and coffee intake equally improve insulin sensitivity in type 2 diabetes: a randomised feasibility trial. *Diabetologia* 2015;58:255–264
- Roden M, Weng J, Eilbracht J, et al. EMPA-REG MONO trial investigators. Empagliflozin monotherapy with sitagliptin as an active comparator in patients with type 2 diabetes: a randomised, double-blind, placebo-controlled, phase 3 trial. *Lancet Diabetes Endocrinol* 2013;1:208–219
- Szczepaniak LS, Nurenberg P, Leonard D, et al. Magnetic resonance spectroscopy to measure hepatic triglyceride content: prevalence of hepatic steatosis in the general population. *Am J Physiol Endocrinol Metab* 2005;288:E462–E468
- Loomba R, Wesley R, Pucino F, Liang TJ, Kleiner DE, Lavine JE. Placebo in nonalcoholic steatohepatitis: insight into natural history and implications for future clinical trials. *Clin Gastroenterol Hepatol* 2008;6:1243–1248
- Han MAT, Altayar O, Hamdeh S, et al. Rates of and factors associated with placebo response in trials of pharmacotherapies for nonalcoholic steatohepatitis: systematic review and meta-analysis. *Clin Gastroenterol Hepatol* 2019;17:616–629.e26
- Hazlehurst JM, Woods C, Marjot T, Cobbold JF, Tomlinson JW. Non-alcoholic fatty liver disease and diabetes. *Metabolism* 2016;65:1096–1108
- Bosch A, Ott C, Jung S, et al. How does empagliflozin improve arterial stiffness in patients with type 2 diabetes mellitus? Sub analysis of a clinical trial. *Cardiovasc Diabetol* 2019;18:44
- Zinman B, Inzucchi SE, Wanner C, et al. EMPA-REG OUTCOME® investigators. Empagliflozin in women with type 2 diabetes and cardiovascular disease - an analysis of EMPA-REG OUTCOME®. *Diabetologia* 2018;61:1522–1527
- Romero-Gómez M, Zelber-Sagi S, Trenell M. Treatment of NAFLD with diet, physical activity and exercise. *J Hepatol* 2017;67:829–846
- Roden M. *Clinical Diabetes Research: Methods and Techniques*. Chichester, U.K., John Wiley & Sons, 2007
- Heise T, Seman L, Macha S, et al. Safety, tolerability, pharmacokinetics, and pharmacodynamics of multiple rising doses of empagliflozin in patients with type 2 diabetes mellitus. *Diabetes Ther* 2013;4:331–345
- O'Brien TP, Jenkins EC, Estes SK, et al. Correcting postprandial hyperglycemia in Zucker diabetic fatty rats with an SGLT2 inhibitor restores glucose effectiveness in the liver and reduces insulin resistance in skeletal muscle. *Diabetes* 2017;66:1172–1184
- Ferrannini E, Muscelli E, Frascerra S, et al. Metabolic response to sodium-glucose cotransporter 2 inhibition in type 2 diabetic patients. *J Clin Invest* 2014;124:499–508
- Merovci A, Solis-Herrera C, Daniele G, et al. Dapagliflozin improves muscle insulin sensitivity but enhances endogenous glucose production. *J Clin Invest* 2014;124:509–514
- Martinez R, Al-Jobori H, Ali AM, et al. Endogenous glucose production and hormonal changes in response to canagliflozin and liraglutide combination therapy. *Diabetes* 2018;67:1182–1189
- Perry RJ, Rabin-Court A, Song JD, et al. Dehydration and insulinopenia are necessary and sufficient for euglycemic ketoacidosis in SGLT2 inhibitor-treated rats. *Nat Commun* 2019;10:548
- Cherrington AD. Banting Lecture 1997. Control of glucose uptake and release by the liver in vivo. *Diabetes* 1999;48:1198–1214
- Lai LL, Vethakkan SR, Nik Mustapha NR, Mahadeva S, Chan WK. Empagliflozin for the treatment of nonalcoholic steatohepatitis in patients with type 2 diabetes mellitus. *Dig Dis Sci*. 25 January 2019 [Epub ahead of print]. DOI: 10.1007/s10620-019-5477-1
- Johnson RJ, Nakagawa T, Sanchez-Lozada LG, et al. Sugar, uric acid, and the etiology of diabetes and obesity. *Diabetes* 2013;62:3307–3315
- Gastaldelli A, Harrison SA, Belfort-Aguilar R, et al. Importance of changes in adipose tissue insulin resistance to histological response during thiazolidinedione treatment of patients with nonalcoholic steatohepatitis. *Hepatology* 2009;50:1087–1093
- Bellou V, Belbasis L, Tzoulaki I, Evangelou E. Risk factors for type 2 diabetes mellitus: an exposure-wide umbrella review of meta-analyses. *PLoS One* 2018;13:e0194127
- Schafer JL, Graham JW. Missing data: our view of the state of the art. *Psychol Methods* 2002;7:147–177



# Constant hepatic ATP concentrations during prolonged fasting and absence of effects of Cerbomed Nemos<sup>®</sup> on parasympathetic tone and hepatic energy metabolism

Sofiya Gancheva<sup>1,2,3</sup>, Alessandra Bierwagen<sup>1,2</sup>, Daniel F. Markgraf<sup>1,2</sup>, Gidon J. Bönhof<sup>1,2</sup>, Kevin G. Murphy<sup>4</sup>, Erifili Hatziagelaki<sup>5</sup>, Jesper Lundbom<sup>1,2</sup>, Dan Ziegler<sup>1,2,3</sup>, Michael Roden<sup>1,2,3,\*</sup>

## ABSTRACT

**Objective:** Brain insulin-induced improvement in glucose homeostasis has been proposed to be mediated by the parasympathetic nervous system. Non-invasive transcutaneous auricular vagus nerve stimulation (taVNS) activating afferent branches of the vagus nerve may prevent hyperglycemia in diabetes models. We examined the effects of 14-min taVNS vs sham stimulation by Cerbomed Nemos<sup>®</sup> on glucose metabolism, lipids, and hepatic energy homeostasis in fasted healthy humans (n = 10, age 51 ± 6 yrs, BMI 25.5 ± 2.7 kg/m<sup>2</sup>).

**Methods:** Heart rate variability (HRV), reflecting sympathetic and parasympathetic nerve activity, was measured before, during and after taVNS or sham stimulation. Endogenous glucose production was determined using [6,6-<sup>2</sup>H<sub>2</sub>]glucose, and hepatic concentrations of triglycerides (HCL), adenosine triphosphate (ATP), and inorganic phosphate (Pi) were quantified from <sup>1</sup>H/<sup>31</sup>P magnetic resonance spectroscopy at baseline and for 180 min following stimulation.

**Results:** taVNS did not affect circulating glucose, free fatty acids, insulin, glucagon, or pancreatic polypeptide. Rates of endogenous glucose production (P = 0.79), hepatic HCL, ATP, and Pi were also not different (P = 0.91, P = 0.48 and P = 0.24) between taVNS or sham stimulation. Hepatic HCL, ATP, and Pi remained constant during prolonged fasting for 3 h. No changes in heart rate or shift in cardiac autonomic function from HRV towards sympathetic or parasympathetic predominance were detected.

**Conclusion:** Non-invasive vagus stimulation by Cerbomed Nemos<sup>®</sup> does not acutely modulate the autonomic tone to the visceral organs and thereby does not affect hepatic glucose and energy metabolism. This technique is therefore unable to mimic brain insulin-mediated effects on peripheral homeostasis in humans.

© 2017 The Authors. Published by Elsevier GmbH. This is an open access article under the CC BY-NC-ND license (<http://creativecommons.org/licenses/by-nc-nd/4.0/>).

**Keywords** Vagus nerve stimulation; Hepatic insulin sensitivity; Hepatic energy metabolism; Liver fat content

## 1. INTRODUCTION

Insulin signaling in the central nervous system has been identified as an essential regulator of peripheral energy and glucose homeostasis in rodents and dogs [1–3]. Of note, brain insulin effects are abolished by hepatic vagotomy, suggesting that the brain–liver crosstalk is mediated by the vagus nerve [4]. Furthermore, brain insulin-induced suppression of endogenous glucose production (EGP) via hepatic IL-6/STAT3 activation has been suggested to depend on the inhibition of hepatic vagal branches [5]. Although these results indicate that the

vagal nerve may be key to controlling glucose homeostasis, its relevance in humans has not been determined.

Studies in humans using intranasal insulin for delivery to the brain provided support of the concept of central regulation of EGP, whole-body glucose uptake, and adipose tissue lipolysis [6–9]. We recently reported that intranasal insulin improves hepatic energy metabolism and reduces liver fat content in lean healthy humans but not in patients with type 2 diabetes (T2D) [10]. However, the mechanism of this brain–liver crosstalk remained unclear. Interestingly, parasympathetic tone, estimated from heart rate variability, was

<sup>1</sup>Institute for Clinical Diabetology, German Diabetes Center, Leibniz Center for Diabetes Research, Heinrich Heine University, Düsseldorf, Germany <sup>2</sup>German Center of Diabetes Research (DZD e.V.), München-Neuherberg, Germany <sup>3</sup>Division of Endocrinology and Diabetology, Medical Faculty, Heinrich-Heine University, Düsseldorf, Germany <sup>4</sup>Section of Endocrinology and Investigative Medicine, Division of Diabetes, Endocrinology and Metabolism, Imperial College Healthcare NHS Trust, London, United Kingdom <sup>5</sup>2nd Department of Internal Medicine, Research Institute and Diabetes Center, Athens University, “Attikon” University General Hospital, Athens, Greece

\*Corresponding author. Division of Endocrinology and Diabetology, Medical Faculty, Heinrich Heine University, c/o Auf'm Hennekamp 65, 40225 Düsseldorf, Germany. Fax: +49 211 3382 691. E-mail: [michael.roden@ddz.uni-duesseldorf.de](mailto:michael.roden@ddz.uni-duesseldorf.de) (M. Roden).

**Abbreviations:** ANOVA, analysis of variance; ATP, adenosine triphosphate; BRS, baroreflex sensitivity; EGP, endogenous glucose production; HCL, liver fat content; HF, high-frequency; HRV, heart rate variability; LF, low-frequency; MRS, magnetic resonance spectroscopy; NTS, nucleus tractus solitarius; Pi, inorganic phosphate; PP, pancreatic polypeptide; taVNS, transcutaneous auricular vagus nerve stimulation

Received July 19, 2017 • Revision received September 19, 2017 • Accepted October 1, 2017 • Available online 25 October 2017

<https://doi.org/10.1016/j.molmet.2017.10.002>

shown to correlate with the change in whole-body insulin sensitivity after intranasal insulin application [8], suggesting that vagal outputs also mediate brain-derived peripheral insulin sensitization in humans. Transcutaneous auricular vagus nerve stimulation (taVNS) can be applied in the external ear of humans to non-invasively activate the central projections of the auricular branch of the vagus nerve [11]. Thereby, taVNS induces an increase in the nucleus tractus solitarius (NTS) activity measured by functional magnetic resonance imaging [11]. Another human taVNS study found reduction in sympathetic outflow, as assessed using microneurography and increased heart rate variability, suggesting reduced sympathetic tone after vagal stimulation [12]. The mechanism behind this reduction of sympathetic output supposedly included taVNS induction of caudal ventrolateral medulla activity, which, in turn, inhibits rostral ventrolateral medulla and thus lowers sympathetic tone [13], suggesting that taVNS might act on the sympathetic nervous system independent of vagal activation. VNS is currently applied as adjunctive therapy in medically refractory epilepsy [14] but has also recently emerged as a promising treatment option for major depressive disorder [15], Alzheimer's disease [16,17], and inflammatory bowel disease [18] due to its anti-inflammatory potential [19]. The metabolic effects of vagal stimulation are not completely understood. Energy expenditure has been shown to increase [20] and postprandial insulin secretion is reduced after a single session of VNS in humans [21]. Evidence from Zucker diabetic fatty rats highlights the potential of taVNS to prevent hyperglycemia [22,23]. However, whether non-invasive taVNS in humans can modulate hepatic glucose and lipid metabolism is unknown.

Thus, we designed a randomized, controlled, crossover clinical study to assess the effects of taVNS on hepatic insulin sensitivity, lipid, and energy homeostasis in lean healthy humans. We further examined taVNS effects on cardiac autonomic function and circulating pancreatic polypeptide (PP) levels as readouts for vagal activation. We hypothesized that taVNS would increase parasympathetic tone and mimic intranasal insulin effects in healthy humans.

## 2. MATERIAL AND METHODS

### 2.1. Participants

Ten healthy humans not taking any medication and without any family history of diabetes were enrolled in this randomized controlled single-blind, cross-over, monocenter study between August 2015 and January 2017 (ClinicalTrials.gov registration no. NCT01479075). Participants exhibited normal glucose tolerance based on a standard 75-grams oral glucose tolerance test. The study was approved by the ethics board of Heinrich-Heine University Düsseldorf and written informed consent was obtained from each person prior to inclusion. Screening procedure included medical history, clinical exam and blood tests. None had clinical or laboratory signs of infection, cardiovascular, neurological, hepatic, renal, or endocrine disease. Patients with cardiac arrhythmia or peripheral neuropathy were excluded from participation. Female participants were postmenopausal. All volunteers refrained from caffeine-containing drinks consumption and exercise from 3 days before the study.

### 2.2. Study design

The volunteers arrived at 7:00 am at the German Diabetes Center after 10 h overnight fasting and remained fasted until the end of the study day. All participants were studied on two different days spaced by at least 7 days. Both cubital veins were catheterized for blood sampling and infusions. At time point  $-180$  min, the participants received a continuous infusion ( $0.036 \text{ mg} \cdot \text{min}^{-1} \cdot \text{kg} \cdot \text{body weight}^{-1}$ ) of

D-[6,6- $^2\text{H}_2$ ]glucose (99% enriched in  $^2\text{H}$  glucose; Cambridge Isotope Laboratories, Andover, MA) after a priming bolus of  $3.6 \text{ mg} \cdot \text{kg body weight}^{-1}$  fasting plasma glucose [ $\text{mg/dl}$ ]/90 [ $\text{mg/dl}$ ] for 5 min [7]. The tracer infusion lasted until  $+180$  min, and blood samples were drawn to measure tracer enrichment, metabolites, and hormones.

At time point zero, taVNS or sham stimulation using Cerbomed NEMOS<sup>®</sup> (Cerbomed, GmbH, Erlangen, Germany) device were applied for 14 min in the left external ear as described previously [11]. For taVNS, the earpiece of the device was positioned upright with the electrode in the cymba conchae of the left external ear. Sham stimulation (as a control) was conducted by positioning the earpiece upside down with the electrode on the earlobe of the left external ear. The stimulus intensity was adjusted for each participant starting from 0.1 mA and increasing in 0.1 mA until tingling sensation was achieved. Further increases in the intensity leading to pricking or burning sensations were avoided. All participants reported tingling sensation during all taVNS and sham stimulation procedures. The stimulation intensities that were selected in this way were 0.3–1.2 mA for the sham earlobe stimulation condition ( $0.8 \pm 0.1$  mA, mean  $\pm$  SEM) and 0.6–1.4 mA for the taVNS cymba conchae condition ( $0.9 \pm 0.1$  mA, mean  $\pm$  SEM), with no difference between conditions. The non-adjustable parameters of the device were continuous biphasic square pulses with 0.25 ms duration at 25 Hz.

### 2.3. Metabolites and hormones

Blood samples were chilled and centrifuged, and supernatants were stored at  $-80$  °C until analysis. The glucose oxidase method was used to measure venous blood glucose concentrations with EKF biosen C-Line glucose analyzer (EKF Diagnostic GmbH, Barleben, Germany). Serum triglycerides and plasma free fatty acids (FFA) were quantified enzymatically [10]. Serum C-peptide and insulin were measured chemoluminimetrically (Immulite 2000 Xpi; Siemens, Erlangen, Germany) [24]. Plasma glucagon was measured by radioimmunoassay (Millipore, St. Charles, Miss, USA). Serum PP was measured using an established radioimmunoassay in the Section of Investigative Medicine, Imperial College London [25]. Briefly, 100  $\mu\text{l}$  of sample were added to 600  $\mu\text{l}$  of 0.05 M phosphate buffer with 0.3% bovine serum albumin (BSA) w/v containing antibody (titer 1:860,000). The assay was incubated for 3 days at 4 °C. Bound and free radiolabeled PP were separated by charcoal adsorption of the free fraction using 4 mg of charcoal/tube suspended in 0.06 M phosphate buffer with gelatine. The samples were centrifuged at  $1500 \times g$  at 4 °C for 20 min, bound and free label separated by aspiration, and both pellet and supernatant counted in a gamma-counter (model NE1600, Thermo Electron Corporation). Gas chromatography-mass spectrometry for assessment of atom percent enrichment of  $^2\text{H}$  was performed on Hewlett–Packard 6890 gas chromatograph equipped with a 25-m CPSii5CB capillary column (0.2-mm inner diameter, 0.12- $\mu\text{m}$  film thickness; Chrompack/Varian, Middelburg, The Netherlands), interfaced to a Hewlett Packard 5975 mass selective detector (Hewlett Packard) as described previously [26]. Atom percent enrichment was calculated as mass ratio, corresponding to the tracer enrichment in plasma glucose.

### 2.4. $^1\text{H}/^{31}\text{P}$ magnetic resonance spectroscopy (MRS)

At time point  $-60$  min, the participants entered the 3-Tesla MR scanner (Achieva 3T Philips, Best, The Netherlands) for scans in the supine position at baseline, 30 min after taVNS or sham procedure and at time point  $+180$  min. A 14-cm circular  $^{31}\text{P}$  surface transmit-receive coil (Philips Healthcare, Best, The Netherlands) for  $^{31}\text{P}$ -MRS and the built-in  $^1\text{H}$  whole body coil for localization and proton spectroscopy were used as described before [27]. Participants were not allowed to

leave the scanner between measurements. Hepatic phosphorus metabolite concentrations (adenosine triphosphate, ATP, and inorganic phosphate, Pi) were corrected for the volume captured by lipid droplets within hepatocytes [28]. Intra- and inter-observer variability in spectral processing of  $^{31}\text{P}$ -MRS was reported previously [27].

### 2.5. Heart rate variability

Nine of the 10 volunteers underwent heart rate variability monitoring before, during, and after taVNS and sham stimulation on two additional test days. One volunteer did not want to participate further. Participants were again blinded to the random order of conditions. Stimulation intensities were similar to those on test days with MRS ( $1.0 \pm 0.1$  mA and  $1.1 \pm 0.1$  mA for sham and taVNS conditions, respectively;  $P > 0.05$  versus MRS test days for both sham and taVNS conditions). R–R intervals were recorded before and over 120 min after taVNS and sham stimulation using a digital SpiderView Holter with five electrodes to record two-channel ECG with ECG signal sampling rate of 200 Hz (Sorin Group, Munich, Germany). Heart rate variability (HRV) was analyzed using commercially available software (SyneScope version 3.00 analysis system; Sorin Group) as described before [29]. Frequency domain indices included the low frequency (LF) band (0.04–0.15 Hz), reflecting both sympathetic and parasympathetic modulation of heart rate and the high-frequency (HF) band (0.15–0.4 Hz), reflecting parasympathetic modulation of the heart rate. The low-frequency/high-frequency (LF/HF) ratio can be used as an index of cardiac autonomic balance such that a decrease in LF/HF ratio indicates a shift towards parasympathetic predominance. Additionally, R–R intervals were recorded with VariaCardio TF5 system (MIE Medical Research, Leeds, UK) with one-channel ECG over 10 min before, during and after taVNS or sham stimulation. Both VariaCardio and SpiderView were used for HRV measurements in supine position. They differed by the length of ECG recording (10 min and 2 h) thereby allowing us to assess both short- and long-term HRV, which are known not to be comparable [30].

### 2.6. Baroreflex sensitivity

Continuous plethysmographic arterial pressure and R–R intervals were recorded from the left middle finger before, during, and after each intervention in a supine position using a Finometer MIDI device and BeatScope Easy v02.10 software (Finapres Medical Systems, Enschede, The Netherlands). For the baroreflex sensitivity (BRS) assessment, time-domain and frequency-domain parameters were computed according to the Task Force of the European Society of Cardiology and the North American Society of Pacing and Electrophysiology [31], using commercially available software (BeatScope Easy; Nevrokard BRS Analysis v6.3.0, Nevrokard, Izola, Slovenia).

### 2.7. Calculations

BRS was determined using the sequence method for positive (BRS+ / +), negative (BRS– / –) and all (BRS-allSeq) sequences, spectral analysis (low-frequency, high-frequency and the average of the low- and high-frequency components), cross spectral analysis (transfer function BRS), or by dividing the standard deviation of R–R interval by the standard deviation of systolic blood pressure (BRS-SD) [32].

Rates of EGP were calculated by dividing the tracer ( $[6,6\text{-}^2\text{H}_2]$ glucose) infusion rate times tracer enrichment by the tracer enrichment in plasma glucose and subtracting the tracer infusion rate [28].

### 2.8. Statistical analysis

Data are presented as means  $\pm$  SEM. Two-way analysis of variance (ANOVA) was performed with the repeated measures factors time and

treatment followed by Tukey multiple comparisons test to determine source of differences. Spearman correlations were used to assess associations between changes in metabolite and hormone levels.  $P$  values  $< 0.05$  were defined to indicate significance of differences. All analyses were performed using Prism version 6.04 (GraphPad, La Jolla, CA) statistical software.

## 3. RESULTS

This study included healthy normal-to-overweight glucose tolerant individuals (Table 1).

### 3.1. taVNS does not alter heart rate variability

Data from nine participants were included in the heart rate variability analysis. There was no difference between HRV frequency domains (Figure 1) at baseline of the active taVNS and sham stimulation. No changes in HRV were seen during and after taVNS and sham stimulation (Figure 1). Both measurements from two-channel (SpiderView Holter) and one-channel (VariaCardio) ECG recordings revealed no effect of taVNS on LF/HF ratio (Figure 1A and B) (ANOVA  $P = 0.95$  and  $P = 0.49$ , respectively).

### 3.2. taVNS does not alter BRS

Data from nine participants were included in the BRS analysis. Heart rate (Figure 2D), blood pressure (Figure 2A, B), and baroreflex sensitivity (Table 2) at baseline of the active taVNS and sham stimulation did not differ. No changes in heart rate, systolic, diastolic, and mean blood pressure were found during or after taVNS and sham stimulation (Figure 2). There were no differences in BRS during or after taVNS and sham stimulation (Table 2).

### 3.3. taVNS does not affect circulating metabolites, hormones, and EGP, which change during fasting

Data from ten participants were included in this analysis. Baseline concentrations of blood glucose, serum triglycerides, FFA, insulin, c-peptide, glucagon, PP, and baseline EGP rates were comparable between taVNS and sham stimulation (Figure 3). ANOVA revealed no changes in any of these substrates or hormones for the factor treatment and treatment  $\times$  time interaction (180 min for blood glucose, serum triglycerides, FFA, insulin, c-peptide, glucagon, and EGP, 120 min for PP). EGP rates remained unaltered (Figure 3B) (ANOVA treatment  $P = 0.79$ , treatment  $\times$  time  $P = 0.22$ ).

Concentrations of glucose, FFA, insulin, c-peptide, and EGP changed over time (ANOVA time  $P < 0.001$ ,  $P < 0.001$ ,  $P = 0.02$ ,  $P < 0.001$  and

**Table 1** – Participants' characteristics.

Parameter	Mean $\pm$ SD
N (females)	10 (2)
Age (years)	51.1 $\pm$ 6.0
BMI ( $\text{kg}/\text{m}^2$ )	25.5 $\pm$ 2.7
Waist circumference (cm)	89 $\pm$ 10
Glucose (mg/dl)	77 $\pm$ 6
Insulin ( $\mu\text{U}/\text{ml}$ )	8.2 $\pm$ 5.2
C-peptide (ng/ml)	1.8 $\pm$ 0.6
HbA1c (%)	5.4 $\pm$ 0.3
GOT (U/l)	24 $\pm$ 12
GPT (U/l)	28 $\pm$ 16
Triglycerides (mg/dl)	95 $\pm$ 33
Free fatty acids ( $\mu\text{mol}/\text{l}$ )	299 $\pm$ 35

Data are mean  $\pm$  SD, GOT – glutamate oxaloacetate transaminase, GPT – glutamate pyruvate transaminase.

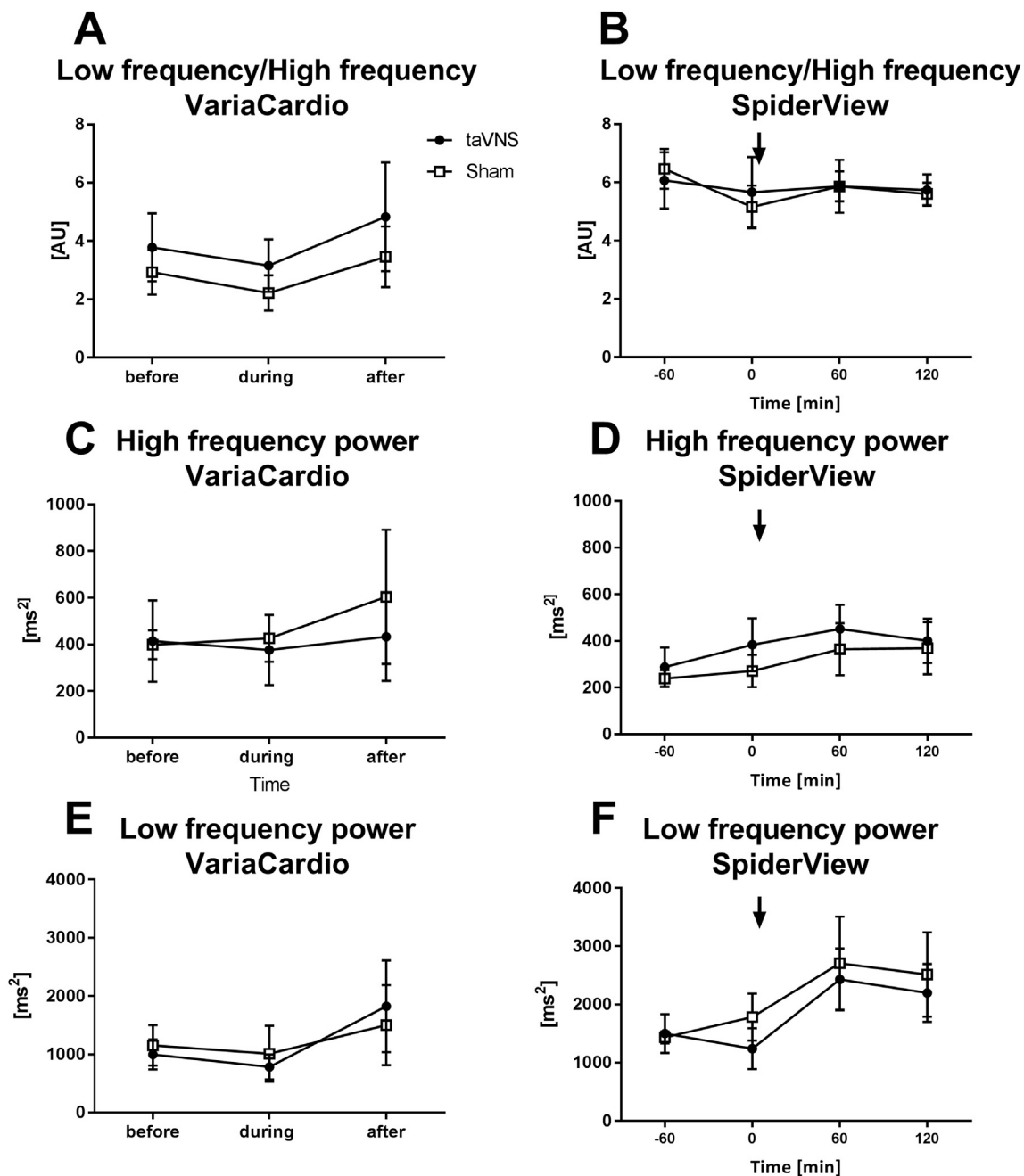


**Figure 1:** Heart rate variability frequency domains for sham and active taVNS stimulation. Stimulation denoted by an arrow. Mean  $\pm$  SEM.

$P < 0.001$ , respectively). During the 3 h, glucose decreased by 4% after both taVNS and sham procedure, while FFA increased by 40% after taVNS and by 20% after sham stimulation. Serum insulin decreased by 19% and 21% and c-peptide by 17% and 19% during this time period after taVNS and sham stimulation, respectively. Rates of EGP decreased by 19% and 21% after taVNS and sham stimulation, respectively.

#### 3.4. taVNS does not alter hepatic lipid and energy metabolism

Data from ten participants were included in this analysis. Baseline liver fat content and hepatic ATP and Pi concentrations were comparable on taVNS and sham stimulation days at baseline (Figure 4). There was no effect of taVNS on hepatic lipid, ATP and Pi content at 30 and 180 min

(Figure 4) (ANOVA treatment  $\times$  time  $P = 0.91$ ,  $P = 0.48$  and  $P = 0.24$ , respectively).

No changes in hepatic lipid, ATP, and Pi content over time were found (ANOVA time  $P = 0.49$ ,  $P = 0.48$ ,  $P = 0.27$ , respectively).

#### 3.5. Correlation analyses of hepatic phosphorus compounds with changes in circulating metabolites and hormones

The change in serum insulin between 180 min and baseline related positively to hepatic ATP after taVNS ( $P = 0.01$ ), but not after sham intervention ( $P = 0.78$ ). No associations between changes in FFA, glucose, c-peptide, EGP, and hepatic lipid, ATP and Pi content were found after taVNS and sham stimulation.

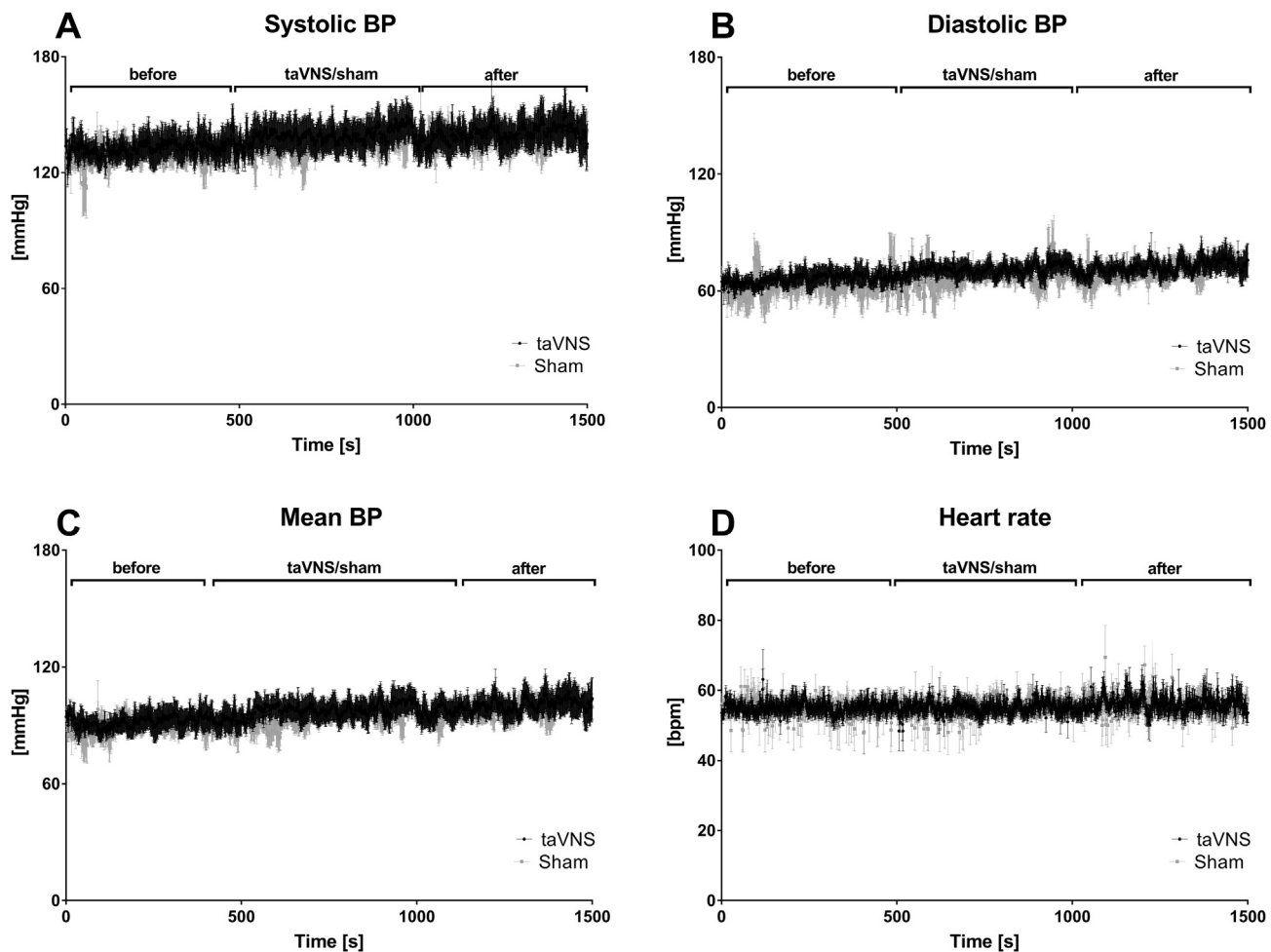


**Figure 2:** Systolic (A), diastolic (B), mean blood pressure (C), and heart rate (D) before, during and after sham and active taVNS stimulation. Mean  $\pm$  SEM.

**Table 2** — Baroreflex sensitivity (BRS) before, during and after transcutaneous auricular vagus nerve stimulation (taVNS).

Parameter	Condition	Before	During	After
BRS-SD (ms/mmHg)	taVNS	5.6 $\pm$ 2.9	5.1 $\pm$ 2.5	3.9 $\pm$ 2.0
	Sham	4.2 $\pm$ 1.5	3.7 $\pm$ 1.3	5.3 $\pm$ 2.6
BRS +/+ (ms/mmHg)	taVNS	12.3 $\pm$ 5.3	13.1 $\pm$ 5.7	16.6 $\pm$ 5.7
	Sham	11.9 $\pm$ 3.7	13.6 $\pm$ 5.6	14.5 $\pm$ 5.4
BRS -/- (ms/mmHg)	taVNS	18.3 $\pm$ 5.5	20.3 $\pm$ 10.1	13.9 $\pm$ 4.0
	Sham	13.0 $\pm$ 2.8	16.2 $\pm$ 4.2	17.5 $\pm$ 5.8
BRS-allSeq (ms/mmHg)	taVNS	16.7 $\pm$ 2.1	15.8 $\pm$ 6.2	14.9 $\pm$ 4.7
	Sham	15.9 $\pm$ 6.5	15.2 $\pm$ 4.5	17.8 $\pm$ 8.1

Data are mean  $\pm$  SD; BRS determined using the sequence method for positive (BRS+/+), negative (BRS-/-) and all (BRS-allSeq) sequences or by dividing the standard deviation of R-R interval by the standard deviation of systolic blood pressure (BRS-SD).

#### 4. DISCUSSION

This study found that non-invasive taVNS does not induce a shift in cardiac autonomic function and does not affect pancreatic polypeptide levels, suggesting no change in parasympathetic outflow to the pancreas and the heart in healthy humans. In accord with the lack of effect of taVNS on peripheral vagal tone, it also had no effect on hepatic

insulin sensitivity, lipid, and energy metabolism. These data indicate that taVNS is unable to mimic intranasal insulin effects and modulate hepatic glucose, lipid, and energy metabolism in humans, likely because it fails to alter visceral parasympathetic tone. Finally, this study shows that hepatic fat and phosphorous metabolite contents remain constant after prolonged fasting, at least in healthy non-obese humans.

Systemic glucose, insulin, c-peptide, glucagon, FFA, and triglyceride concentrations remained unaltered after taVNS in this study, which is in line with the findings on these substrates and hormones observed upon intranasal insulin under fasting conditions [10]. Previously observed transient reductions in glucose and FFA and the increase in serum insulin after intranasal insulin application in healthy humans are due to spillover of insulin into the circulation rather than to central insulin effects [10]. The lack of taVNS action on substrate and hormone levels in the present study could thus be interpreted as a match between intranasal insulin and vagus stimulation effects. Additionally, no difference in EGP was found after taVNS further supporting this concept. However, intranasal insulin acutely decreases liver lipids and increases hepatic ATP content, while the taVNS affected neither hepatic fat nor ATP concentrations [10]. The lack of taVNS effect on pancreatic polypeptide secretion suggests no changes in parasympathetic outflow to the visceral organs, which possibly explains this inconsistency. Even if intranasal insulin effects on peripheral

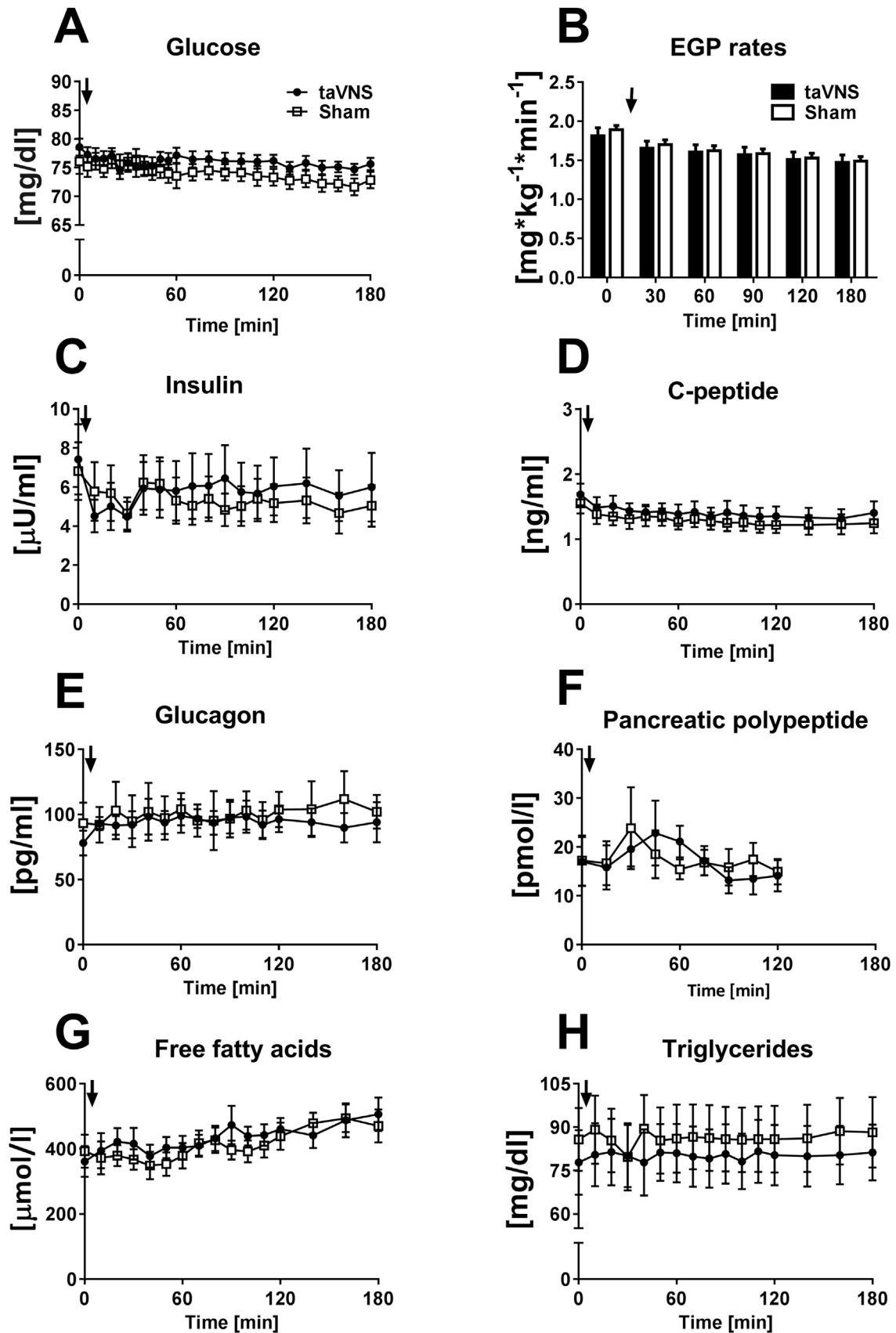


**Figure 3:** Concentrations of glucose (A), insulin (C), c-peptide (D), glucagon (E), pancreatic polypeptide (F), free fatty acids (G), triglycerides (H), and rates of endogenous glucose production (B) after sham and active taVNS stimulation. Stimulation denoted by an arrow. Mean  $\pm$  SEM.

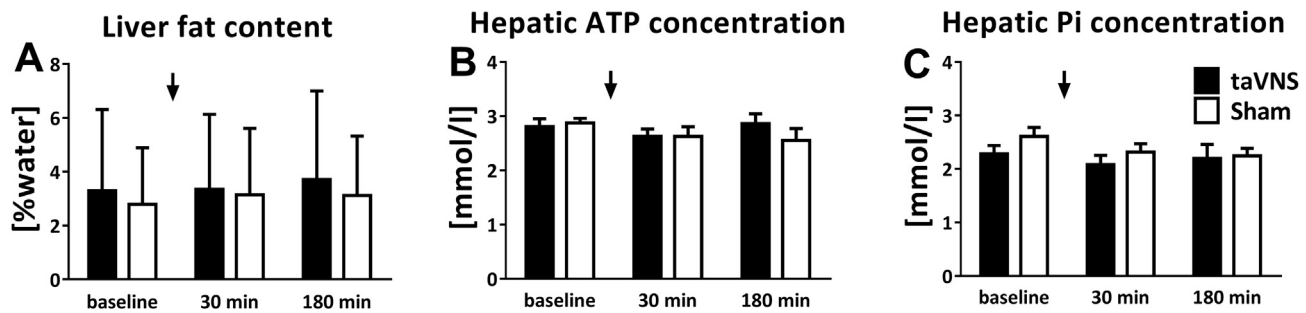


**Figure 4:** Liver fat content (A), hepatic concentrations of adenosine triphosphate (ATP) (B), and inorganic phosphate (Pi) (C) measured by  $^{31}\text{P}/^1\text{H}$  magnetic resonance spectroscopy before and after sham and active taVNS stimulation. Stimulation denoted by an arrow. Mean  $\pm$  SEM.

metabolism are mediated by the vagus nerve, as suggested previously [8], taVNS is not able to mimic these conditions, as it does not seem to modulate vagal tone to the abdominal viscera.

This study describes stable physiological levels of hepatic ATP and Pi concentrations over 3 h after overnight fasting, which adds to the understanding of the time course of basal ATP and Pi during prolonged fasting of healthy humans. Under these conditions, FFA increase by 20–40%, but do not affect hepatic lipid or energy substrate concentrations. The decrease in EGP rates by about 20% at 3 h is paralleled by a gradual reduction in blood glucose, but does not affect hepatic energy metabolism. These data demonstrate stable concentrations of hepatic phosphorus metabolites with prolonged fasting, in the face of alteration of circulating metabolites and hormones.

One previous report using the same stimulation procedure with NEMOS<sup>®</sup> device provided evidence for activation of the vagal viscerosensory NTS after taVNS from brain imaging [11]. NTS nuclei are structurally and functionally linked to the most important vagal nucleus for the efferent parasympathetic output to the visceral organs, the dorsal motor nucleus, which receives input from the NTS to directly innervate visceral structures [33]. Thus, NTS activation upon taVNS should translate to changes in vagal outflow to the periphery. Of note, the dorsal vagal complex has been identified as the site of central insulin action accounting for reduction in hepatic glucose production [34].

Furthermore, the role of the parasympathetic nervous system in human glucoregulatory physiology has been studied for over 20 years, providing evidence for direct muscarinic cholinergic inhibition of hepatic glucose production, which is offset by increased glucagon secretion stimulating hepatic glucose output [35]. The lack of any changes in insulin and glucagon secretion in our study point to the fact that taVNS does not elicit any autonomic system effects on the endocrine pancreas. Pancreatic polypeptide is a well-known readout for cholinergic activation [36], which was measured here continuously before, during and after taVNS. No differences were shown (Figure 3F), additionally supporting the concept that taVNS fails to modulate parasympathetic tone in humans.

Interestingly, vagal stimulation has been shown to modulate glucose metabolism in rheumatoid arthritis patients in the postprandial state [21]. Some differences between these and the present results could result from the different experimental settings, such as fasting versus postprandial conditions. Moreover, rheumatoid arthritis patients received invasive vagal stimulation using implanted devices, while participants in the present study underwent non-invasive taVNS in the outer ear. While cutaneous electrical stimulation with NEMOS<sup>®</sup> does not lead to peripheral metabolic effects, direct electric pulses to the

cervical vagus nerve fibers might indeed have the potential to modulate glucose homeostasis.

Of note, vagus nerve blockade has been found to cause no acute changes in hepatic glucose production or in insulin secretion and action in non-diabetic humans [37]. These data indicate that vagal tone modulation in the short-term does not have an effect on glucose metabolism. However, vagus modulation studies in diabetic humans, who are known to have impaired sympathovagal balance [38], have not been performed and remain a question of future investigation.

We further assessed the effects of taVNS on cardiac function and whether parasympathetic outflow to the cardiovascular system is modulated after vagal stimulation. In contrast to a previous report showing reduction in LF/HF ratio [12], this study found neither a change in HRV nor a shift in predominance of the autonomic regulation after taVNS. Of note, Clancy et al. examined two not-matched groups of different size with taVNS and sham stimulation without applying a crossover design. The present study performed simultaneous assessment of heart rate variability using two independent Holter methods with short- and long-term ECG recordings, which both showed no difference in any of the measured frequency domains, pointing to the lack of effect of taVNS on cardiac autonomic function. In line with previous report showing no acute effect of vagal nerve stimulation on cardiovascular autonomic and hemodynamic parameters [39], this study also did not observe alterations in BRS with taVNS (Table 2). Of note, vagus nerve stimulation has been suggested to improve autonomic imbalance in heart failure patients [40] and chronically increases BRS and elevates HF power of HRV [41], but, for this purpose, the stimulation parameters and dipole orientation are different from that used in epilepsy [39] and in the present study. Whether other stimulation parameters or vagus stimulation techniques such as neck vagus stimulation with gammaCore<sup>®</sup> [42] or VNS Therapy System implantation [20,21,39,40] will be able to affect the parasympathetic tone to the viscera and thereby might alter peripheral metabolism remains to be tested.

In conclusion, taVNS applied non-invasively in the outer ear neither affects hepatic glucose metabolism nor hepatocellular lipid and ATP content in healthy humans. Of note, prolonged fasting does not affect liver lipids and ATP in this cohort. No differences in circulating glucoregulatory hormones and pancreatic polypeptide levels between active and sham stimulation indicate a lack of parasympathetic tone modulation with taVNS, which is confirmed by the absence of alterations in cardiac autonomic function. These data suggest that encouraging results from rodent studies using taVNS on glucose metabolism are not translatable to humans and do not hold promise for the future treatment of T2D patients.

## FUNDING

This work was supported by the Ministry of Science and Research of the State of North Rhine-Westphalia (MIWF NRW) and the German Federal Ministry of Health (BMG). This study was supported in part by a grant of the Federal Ministry for Research (BMBF) to the German Center for Diabetes Research (DZD), by a grant of the Helmholtz Alliance Imaging and Curing Environmental Metabolic Diseases (ICEMED), by the German Research Foundation (DFG, SFB 1116) and by the Schmutzler-Stiftung.

The funding sources had no input in the design and conduct of this study, in the collection, analysis, and interpretation of the data; or in the preparation, review or approval of the article.

## CONTRIBUTION STATEMENT

S.G. researched, collected and analyzed data and wrote the manuscript. A.B., D.F.M., G.J.B., and K.G.M. collected data, contributed to the interpretation of results, and revised the article. J.L., D.Z., and E.H. contributed to the manuscript. M.R. designed the study, interpreted the data, and wrote the manuscript. M.R. is the guarantor of this work and, as such, had full access to all the data in the study and takes responsibility for the integrity of the data and the accuracy of the data analysis.

## ACKNOWLEDGMENTS

The authors have no potential conflicts of interest relevant to this article.

We thank Andrea Nagel, Nicole Achterath, Kai Tinnes, Myrko Eßer, David Höhn, Andrea Sparla, and Francesco Battiato (Institute for Clinical Diabetology, German Diabetes Center, Düsseldorf) for their excellent help with the experiments.

## CONFLICT OF INTEREST

The authors have no potential conflicts of interest relevant to this article.

## REFERENCES

- Vogt, M.C., Bruning, J.C., 2013. CNS insulin signaling in the control of energy homeostasis and glucose metabolism — from embryo to old age. *Trends in Endocrinology and Metabolism* 24(2):76–84.
- Scherer, T., Buettner, C., 2011. Yin and Yang of hypothalamic insulin and leptin signaling in regulating white adipose tissue metabolism. *Reviews in Endocrine & Metabolic Disorders* 12(3):235–243.
- Ramnanan, C.J., Saraswathi, V., Smith, M.S., Donahue, E.P., Farmer, B., Farmer, T.D., et al., 2011. Brain insulin action augments hepatic glycogen synthesis without suppressing glucose production or gluconeogenesis in dogs. *The Journal of Clinical Investigation* 121(9):3713–3723.
- Pocai, A., Lam, T.K., Gutierrez-Juarez, R., Obici, S., Schwartz, G.J., Bryan, J., et al., 2005. Hypothalamic K(ATP) channels control hepatic glucose production. *Nature* 434(7036):1026–1031.
- Kimura, K., Tanida, M., Nagata, N., Inaba, Y., Watanabe, H., Nagashimada, M., et al., 2016. Central insulin action activates Kupffer cells by suppressing hepatic vagal activation via the nicotinic Alpha 7 Acetylcholine receptor. *Cell Reports* 14(10):2362–2374.
- Heni, M., Wagner, R., Kullmann, S., Gancheva, S., Roden, M., Peter, A., et al., 2017. Hypothalamic and striatal insulin action suppresses endogenous glucose production and may stimulate glucose uptake during hyperinsulinemia in lean but not in overweight men. *Diabetes*.
- Iwen, K.A., Scherer, T., Heni, M., Sayk, F., Wellnitz, T., Machleidt, F., et al., 2014. Intranasal insulin suppresses systemic but not subcutaneous lipolysis in healthy humans. *The Journal of Clinical Endocrinology and Metabolism* 99(2):E246–E251.
- Heni, M., Wagner, R., Kullmann, S., Veit, R., Mat-Husin, H., Linder, K., et al., 2014. Central insulin administration improves whole-body insulin sensitivity via hypothalamus and parasympathetic outputs in men. *Diabetes*.
- Scherer, T., Wolf, P., Smajis, S., Gaggini, M., Hackl, M., Gastaldelli, A., et al., 2017. Chronic intranasal insulin does not affect hepatic lipids but lowers circulating BCAAs in healthy male subjects. *The Journal of Clinical Endocrinology and Metabolism* 102(4):1325–1332.
- Gancheva, S., Koliaki, C., Bierwagen, A., Nowotny, P., Heni, M., Fritsche, A., et al., 2015. Effects of intranasal insulin on hepatic fat accumulation and energy metabolism in humans. *Diabetes* 64(6):1966–1975.
- Frangos, E., Elrich, J., Komisaruk, B.R., 2015. Non-invasive access to the vagus nerve central projections via electrical stimulation of the external ear: fMRI evidence in humans. *Brain Stimulation* 8(3):624–636.
- Clancy, J.A., Mary, D.A., Witte, K.K., Greenwood, J.P., Deuchars, S.A., Deuchars, J., 2014. Non-invasive vagus nerve stimulation in healthy humans reduces sympathetic nerve activity. *Brain Stimulation* 7(6):871–877.
- Guyenet, P.G., 2006. The sympathetic control of blood pressure. *Nature Reviews Neuroscience* 7(5):335–346.
- Panebianco, M., Rigby, A., Weston, J., Marson, A.G., 2015. Vagus nerve stimulation for partial seizures. *The Cochrane Database of Systematic Reviews* 4:Cd002896.
- Rong, P., Liu, J., Wang, L., Liu, R., Fang, J.-L., Zhao, J., et al., 2016. Effect of transcutaneous auricular vagus nerve stimulation on major depressive disorder: a nonrandomized controlled pilot study. *Journal of Affective Disorders* 195:172–179.
- Sjogren, M.J., Hellstrom, P.T., Jonsson, M.A., Runnerstam, M., Silander, H.C., Ben-Menachem, E., 2002. Cognition-enhancing effect of vagus nerve stimulation in patients with Alzheimer's disease: a pilot study. *The Journal of Clinical Psychiatry* 63(11):972–980.
- Merrill, C.A., Jonsson, M.A., Minthon, L., Ejnell, H., C-son Silander, H., Blennow, K., et al., 2006. Vagus nerve stimulation in patients with Alzheimer's disease: additional follow-up results of a pilot study through 1 year. *The Journal of Clinical Psychiatry* 67(8):1171–1178.
- Bonaz, B., Sinniger, V., Pellissier, S., 2017. Vagus nerve stimulation: a new promising therapeutic tool in inflammatory bowel disease. *Journal of Internal Medicine*.
- Bonaz, B., Sinniger, V., Pellissier, S., 2016. Anti-inflammatory properties of the vagus nerve: potential therapeutic implications of vagus nerve stimulation. *The Journal of Physiology* 594(20):5781–5790.
- Vijgen, G.H.E.J., Bouvy, N.D., Leenen, L., Rijkers, K., Cornips, E., Majoie, M., et al., 2013. Vagus nerve stimulation increases energy expenditure: relation to brown adipose tissue activity. *PLoS One* 8(10):e77221.
- Tang, M.W., van Nierop, F.S., Koopman, F.A., Eggink, H.M., Gerlag, D.M., Chan, M.W., et al., 2017. Single vagus nerve stimulation reduces early postprandial C-peptide levels but not other hormones or postprandial metabolism. *Clinical Rheumatology*, 1–10.
- Li, S., Zhai, X., Rong, P., McCabe, M.F., Wang, X., Zhao, J., et al., 2014. Therapeutic effect of vagus nerve stimulation on depressive-like behavior, hyperglycemia and insulin receptor expression in Zucker fatty rats. *PLoS One* 9(11):e112066.
- Wang, S., Zhai, X., Li, S., McCabe, M.F., Wang, X., Rong, P., 2015. Transcutaneous vagus nerve stimulation induces tidal melatonin secretion and has an antidiabetic effect in Zucker fatty rats. *PLoS One* 10(4):e0124195.
- Szendroedi, J., Saxena, A., Weber, K.S., Strassburger, K., Herder, C., Burkart, V., et al., 2016. Cohort profile: the German diabetes study (GDS). *Cardiovascular Diabetology* 15:59.
- Sam, A.H., Sleeth, M.L., Thomas, E.L., Ismail, N.A., Mat Daud, N., Chambers, E., et al., 2015. Circulating pancreatic polypeptide concentrations

- predict visceral and liver fat content. *The Journal of Clinical Endocrinology and Metabolism* 100(3):1048–1052.
- [26] Nowotny, B., Zahiragic, L., Krog, D., Nowotny, P.J., Herder, C., Carstensen, M., et al., 2013. Mechanisms underlying the onset of oral lipid-induced skeletal muscle insulin resistance in humans. *Diabetes* 62(7):2240–2248.
- [27] Laufs, A., Livingstone, R., Nowotny, B., Nowotny, P., Wickrath, F., Giani, G., et al., 2014. Quantitative liver 31P magnetic resonance spectroscopy at 3T on a clinical scanner. *Magnetic Resonance in Medicine* 71(5):1670–1675.
- [28] Szendroedi, J., Chmelik, M., Schmid, A.I., Nowotny, P., Brehm, A., Krssak, M., et al., 2009. Abnormal hepatic energy homeostasis in type 2 diabetes. *Hepatology* 50(4):1079–1086.
- [29] Herder, C., Schamarek, I., Nowotny, B., Carstensen-Kirberg, M., Strassburger, K., Nowotny, P., et al., 2017. Inflammatory markers are associated with cardiac autonomic dysfunction in recent-onset type 2 diabetes. *Heart* 103(1):63–70.
- [30] Stuckey, M.I., Tulppo, M.P., Kiviniemi, A.M., Petrella, R.J., 2014. Heart rate variability and the metabolic syndrome: a systematic review of the literature. *Diabetes/Metabolism Research and Reviews* 30(8):784–793.
- [31] Heart rate variability: standards of measurement, physiological interpretation and clinical use. Task Force of the European Society of Cardiology and the North American Society of Pacing and Electrophysiology. *Circulation* 93(5), 1996:1043–1046.
- [32] Bernardi, L., De Barbieri, G., Rosengård-Bärlund, M., Mäkinen, V.P., Porta, C., Groop, P.H., 2010. New method to measure and improve consistency of baroreflex sensitivity values. *Clinical Autonomic Research* 20(6):353–361.
- [33] Dorsal Vagal Complex (DVC). In: Binder, M.D., Hirokawa, N., Windhorst, U. (Eds.), *Encyclopedia of neuroscience*. Berlin, Heidelberg: Springer Berlin Heidelberg. p. 998–9.
- [34] Filippi, B.M., Yang, C.S., Tang, C., Lam, T.K., 2012. Insulin activates Erk1/2 signaling in the dorsal vagal complex to inhibit glucose production. *Cell Metabolism* 16(4):500–510.
- [35] Boyle, P.J., Liggett, S.B., Shah, S.D., Cryer, P.E., 1988. Direct muscarinic cholinergic inhibition of hepatic glucose production in humans. *The Journal of Clinical Investigation* 82(2):445–449.
- [36] Schwartz, T.W., Holst, J.J., Fahrenkrug, J., Jensen, S.L., Nielsen, O.V., Rehfeld, J.F., et al., 1978. Vagal, cholinergic regulation of pancreatic polypeptide secretion. *The Journal of Clinical Investigation* 61(3):781–789.
- [37] Sathananthan, M., Ikramuddin, S., Swain, J.M., Shah, M., Piccinini, F., Dalla Man, C., et al., 2014. The effect of vagal nerve blockade using electrical impulses on glucose metabolism in nondiabetic subjects. *Diabetes, Metabolic Syndrome and Obesity: Targets and Therapy* 7:305–312.
- [38] Vinik, A.I., Ziegler, D., 2007. Diabetic cardiovascular autonomic neuropathy. *Circulation* 115(3):387–397.
- [39] Garamendi, I., Acera, M., Agundez, M., Galbarriatu, L., Marinas, A., Pomposo, I., et al., 2017. Cardiovascular autonomic and hemodynamic responses to vagus nerve stimulation in drug-resistant epilepsy. *Seizure* 45: 56–60.
- [40] Premchand, R.K., Sharma, K., Mittal, S., Monteiro, R., Dixit, S., Libbus, I., et al., 2014. Autonomic regulation therapy via left or right cervical vagus nerve stimulation in patients with chronic heart failure: results of the ANTHEM-HF trial. *Journal of Cardiac Failure* 20(11):808–816.
- [41] Libbus, I., Nearing, B.D., Amurthur, B., KenKnight, B.H., Verrier, R.L., 2016. Autonomic regulation therapy suppresses quantitative T-wave alternans and improves baroreflex sensitivity in patients with heart failure enrolled in the ANTHEM-HF study. *Heart Rhythm* 13(3):721–728.
- [42] Silberstein, S.D., Mechtler, L.L., Kudrow, D.B., Calhoun, A.H., McClure, C., Saper, J.R., et al., 2016. Non-invasive vagus nerve stimulation for the ACute treatment of cluster headache: findings from the randomized, double-blind, sham-controlled ACT1 study. *Headache* 56(8):1317–1332.



Sofiya Gancheva,<sup>1,2</sup> Alessandra Bierwagen,<sup>1,2</sup> Kirti Kaul,<sup>1,2</sup> Christian Herder,<sup>1,2</sup> Peter Nowotny,<sup>1,2</sup> Sabine Kahl,<sup>1,2,3</sup> Guido Giani,<sup>2,4</sup> Birgit Klueppelholz,<sup>2,4</sup> Birgit Knebel,<sup>2,5</sup> Paul Begovatz,<sup>1,2</sup> Klaus Strassburger,<sup>2,4</sup> Hadi Al-Hasani,<sup>2,5</sup> Jesper Lundbom,<sup>1,2</sup> Julia Szendroedi,<sup>1,2,3</sup> and Michael Roden,<sup>1,2,3</sup> for the German Diabetes Study (GDS) Group\*

## Variants in Genes Controlling Oxidative Metabolism Contribute to Lower Hepatic ATP Independent of Liver Fat Content in Type 1 Diabetes



Diabetes 2016;65:1849–1857 | DOI: 10.2337/db16-0162

**Type 1 diabetes has been recently linked to nonalcoholic fatty liver disease (NAFLD), which is known to associate with insulin resistance, obesity, and type 2 diabetes. However, the role of insulin resistance and hyperglycemia for hepatic energy metabolism is yet unclear. To analyze early abnormalities in hepatic energy metabolism, we examined 55 patients with recently diagnosed type 1 diabetes. They underwent hyperinsulinemic-normoglycemic clamps with [6,6-<sup>2</sup>H<sub>2</sub>]glucose to assess whole-body and hepatic insulin sensitivity. Hepatic  $\gamma$ ATP, inorganic phosphate (Pi), and triglyceride concentrations (hepatocellular lipid content [HCL]) were measured with multinuclei magnetic resonance spectroscopy (<sup>31</sup>P/<sup>1</sup>H-MRS). Glucose-tolerant humans served as control (CON) (*n* = 57). Whole-body insulin sensitivity was 44% lower in patients than in age- and BMI-matched CON. Hepatic  $\gamma$ ATP was 15% reduced ( $2.3 \pm 0.6$  vs.  $2.7 \pm 0.6$  mmol/L, *P* < 0.001), whereas hepatic Pi and HCL were similar in patients when compared with CON. Across all participants, hepatic  $\gamma$ ATP correlated negatively with glycemia and oxidized LDL. Carriers of the *PPARG* G allele (rs1801282) and noncarriers of *PPARGC1A* A allele (rs8192678) had 21 and 13% lower hepatic ATP concentrations. Variations in genes controlling oxidative metabolism contribute to a reduction in hepatic**

**ATP in the absence of NAFLD, suggesting that alterations in hepatic mitochondrial function may precede diabetes-related liver diseases.**

Nonalcoholic fatty liver disease (NAFLD) tightly relates to insulin resistance, the hallmark of type 2 diabetes (1). Only recently, type 1 diabetes has been also linked to NAFLD with similar adverse outcomes compared with patients with type 2 diabetes (2). Likewise, the role of insulin resistance in the development of type 1 diabetes has gained more interest (3–5). Insulin resistance in type 1 diabetes was described more than 30 years ago (4) and originally accounted for by long-term glucose toxicity (6). But mitochondrial function may also be impaired as shown by lower muscle ATP synthase flux (7). Interestingly, muscle ATP synthesis inversely correlates with hepatocellular lipid content (HCL) (8), suggesting a tight link between liver and muscle energy metabolism.

In overt type 2 diabetes, lower hepatic concentrations of energy-rich substrates such as inorganic phosphate (Pi) and ATP synthesis associate with increased fat content and insulin resistance in the liver (9,10). However, hepatic respiratory capacity was transiently elevated and followed

<sup>1</sup>Institute for Clinical Diabetology, German Diabetes Center, Leibniz Center for Diabetes Research, Heinrich Heine University, Düsseldorf, Germany

<sup>2</sup>German Center of Diabetes Research (DZD e.V.), München-Neuherberg, Germany

<sup>3</sup>Department of Endocrinology and Diabetology, Medical Faculty, Heinrich Heine University, Düsseldorf, Germany

<sup>4</sup>Institute for Biometrics and Epidemiology, German Diabetes Center, Leibniz Center for Diabetes Research, Heinrich Heine University, Düsseldorf, Germany

<sup>5</sup>Institute for Clinical Biochemistry and Pathobiochemistry, German Diabetes Center, Leibniz Center for Diabetes Research, Heinrich Heine University, Düsseldorf, Germany

Corresponding author: Michael Roden, michael.roden@ddz.uni-duesseldorf.de.

Received 2 February 2016 and accepted 12 April 2016.

Clinical trial reg. no. NCT01055093, clinicaltrials.gov.

This article contains Supplementary Data online at <http://diabetes.diabetesjournals.org/lookup/suppl/doi:10.2337/db16-0162/-/DC1>.

S.G. and A.B. contributed equally to this study.

\*A complete list of the members of the German Diabetes Study Group can be found in the APPENDIX.

© 2016 by the American Diabetes Association. Readers may use this article as long as the work is properly cited, the use is educational and not for profit, and the work is not altered.

by augmented production of lipid peroxides in the NOD mouse, a model of human type 1 diabetes (11). Recent studies provided further evidence for enhanced hepatic energy metabolism and oxidative stress in human obesity and NAFLD (12,13). It is therefore unclear whether hepatic energy homeostasis is altered only in the context of diabetes-related NAFLD and which factors contribute to such abnormalities.

Specifically, the impact of inherited or acquired factors possibly involved in hepatic energy metabolism has not been investigated. Genetic variants in regulators of oxidative phosphorylation like peroxisome proliferator-activated receptor- $\gamma$  and  $\Delta$  (genes *PPARG* and *PPARD*), *PPARG* coactivator-1 $\alpha$  (gene *PPARGC1A*), respiratory chain complex 1 (gene *NDUFB6*), and fat mass- and obesity-associated gene (gene *FTO*) also modulate glucose and lipid metabolism (14–18). Several cytokines, such as adiponectin, fetuin A, and fibroblast growth factor 21 (FGF21), can be altered in insulin-resistant states, but also in human (19–21) and rodent type 1 diabetes (11).

Thus, this study tests the hypothesis that hepatic energy metabolism is already lower in young nonobese near-normoglycemic patients with type 1 diabetes than in age- and BMI-matched healthy individuals and that it associates with impaired hepatic and peripheral insulin sensitivity independent of liver fat content. Highly sensitive magnetic resonance spectroscopy (MRS) was used to assess hepatic energy metabolism from hepatic ATP concentrations (22), which tightly correlate with unidirectional flux through hepatic ATP synthase (23).

## RESEARCH DESIGN AND METHODS

### Participants

Fifty-five patients with type 1 diabetes of the German Diabetes Study (GDS), a prospective observational study aiming at characterization of subphenotypes and monitoring of disease progression (clinicaltrials.gov registration no. NCT01055093) (24), fulfilled the following inclusion criteria: 1) age 18–69 years, 2) known diabetes duration of <12 months, and 3) type 1 diabetes diagnosis based on ketoacidosis with immediate insulin substitution, detection of at least one islet cell-directed autoantibody (islet cell autoantibody, glutamic acid decarboxylase autoantibody, or islet antigen-2 antibody), or C-peptide below the detection limit. Exclusion criteria were pregnancy, malignancies, and severe chronic diseases, including liver disease other than NAFLD. Healthy normoglycemic individuals from the GDS, the German National Cohort Study (25), and a pilot study at the German Diabetes Center (clinicaltrials.gov registration no. NCT01736202) served as the control group (CON) ( $n = 57$ ). These volunteers fulfilled the inclusion and exclusion criteria of GDS except for the presence of diabetes. Particularly, they did not have a family history of diabetes and had normal glucose tolerance based on a standard 75-g oral glucose tolerance test. All participants were screened, including medical history, physical examination, and routine blood test. Self-reported

alcohol consumption was <20 g/day. Informed consent was obtained from all volunteers prior to inclusion after approval of the trial by the ethics board of Heinrich Heine University.

### Study Design

All 112 participants had fasting blood samples and  $^{31}\text{P}/^{1}\text{H}$ -MRS measurements. All 55 patients with type 1 diabetes and 20 of all 57 CON, matched for age and BMI to 20 patients with type 1 diabetes of the larger patient group, underwent the modified Botnia clamp test on a separate day. They refrained from physical activity and any alcohol ingestion for 3 days prior to visits and remained fasted overnight for 10–12 h before the tests. Patients with type 1 diabetes withdrew their regular insulin dose in the morning of the tests.

### Hyperinsulinemic-Euglycemic Clamp

The modified Botnia clamps were performed as previously described and validated (26). In brief, an intravenous infusion of [6,6- $^2\text{H}_2$ ]glucose was started at –120 min and continued until +240 min. At 0 min, an intravenous glucose bolus (1 mg/kg body weight [BW] in a 30% [weight for volume] solution containing 1.98% [6,6- $^2\text{H}_2$ ]glucose) was administered followed by the clamp test using an insulin dose of 1.5 mU \* (BW in kg) $^{-1}$  \* min $^{-1}$  (Insuman Rapid; Sanofi, Frankfurt, Germany) from +60 until +240 min. Blood glucose concentrations were maintained at 5 mmol/L using a variable intravenous 20% glucose infusion.

### Blood Analyses

Blood samples were immediately chilled and centrifuged and supernatants stored at –20°C until analysis. Venous blood glucose concentrations were measured with the Biosen C-Line glucose analyzer (EKF Diagnostics, Barleben, Germany) (27). Serum triglycerides (TGs), cholesterol, aspartate aminotransferase (AST), alanine aminotransferase (ALT), and  $\gamma$ -glutamyl transpeptidase (GGT) were analyzed using a Cobas c311 analyzer (Roche Diagnostics, Mannheim, Germany) (27). Free fatty acids (FFAs) were quantified enzymatically (Wako, Neuss, Germany) in samples containing orlistat to prevent ex vivo lipolysis (27). Serum C-peptide, insulin, and plasma glucagon were measured radioimmunochemically (Millipore, St. Charles, MO) (27). Circulating FGF21, fetuin A, selenoprotein P (SepP), and high-molecular-weight adiponectin were determined by ELISA (13,27). Peroxidation of endogenous lipids and nucleic acid oxidation were assessed from thiobarbituric acid reactive substances (TBARS) and 8-hydroxydeoxyguanosine (8-OHdG), respectively (11,13). Protein carbonyl products and oxidized LDL (oxLDL) were measured with ELISA (Biocat, Heidelberg, Germany; intra-assay coefficient of variation: 1.6 and 2.5%, respectively). Antioxidative capacity was assessed colorimetrically from measurement of plasma glutathione (GSH) (USBio, Boston, MA; intra-assay coefficient of variation: 1.6%). Atom percent enrichment of  $^2\text{H}$  in glucose was determined after deproteinization and derivatization to the aldonitrile-pentaacetate as previously described (26).

## Genotyping

Genomic DNA was extracted from whole blood with the Qiagen Blood and Tissue Kit (Qiagen, Hilden, Germany). Genotyping was performed using real-time PCR-based allelic discrimination with TaqMan predesigned single nucleotide polymorphism (SNP) genotyping assays and chemistry (Thermo Fisher Scientific, Darmstadt, Germany) on a StepOnePlus Real-Time PCR System (Thermo Fisher Scientific).

## <sup>31</sup>P/<sup>1</sup>H-MRS and MRI

All measurements were performed in a 3-T magnetic resonance scanner (Achieva 3T; Philips Healthcare, Best, the Netherlands) using a 14-cm circular <sup>31</sup>P surface transmit-receive coil (Philips Healthcare) for <sup>31</sup>P-MRS and the built-in <sup>1</sup>H whole-body coil for localization and <sup>1</sup>H-MRS. Absolute quantification of  $\gamma$ ATP and Pi was performed as previously described (22). Data from localized <sup>1</sup>H-MRS were analyzed to assess fat content as previously described (28), and absolute concentrations were expressed as percent HCL relative to water content. Concentrations of phosphorus metabolites were corrected for the volume captured by lipid droplets within hepatocytes (9). Phosphocreatine contamination in the liver spectra was avoided by an MR localization technique excluding signals from abdominal wall muscle. Truncal subcutaneous and visceral adipose tissue contents were assessed by MRI as previously described (27).

## Calculations

Whole-body insulin sensitivity was calculated as *M* value from the mean glucose infusion rate during the last 30 min of the clamp test. Rates of glucose appearance were calculated by dividing the tracer infusion rate times tracer enrichment by percent of tracer enrichment in plasma and subtracting tracer infusion rate (26). Endogenous glucose production (EGP) was calculated from the difference between rates of glucose appearance and mean glucose infusion rates. Hepatic insulin sensitivity was calculated as percent EGP suppression by insulin during clamp steady state (iEGP).

## Statistical Analysis

Normally distributed data, given as means  $\pm$  SEM, were compared with the two-tailed unpaired Student *t* test. Nonnormally distributed data, given as median (25th; 75th percentiles), were compared with the Mann-Whitney *U* test. Pearson correlation analyses were used to describe the associations between parameters of anthropometry, glycemic control, insulin sensitivity, and lipid availability with hepatic ATP or Pi concentrations in the total study population. AST, ALT, HCL, FFAs, TGs, high-sensitivity C-reactive protein (hsCRP), oxLDL, and *M* values were not normally distributed and were therefore log transformed before analyses. Partial correlation analysis was performed by adjusting first for diabetes diagnosis and then for study, age, sex, and BMI. Multivariable linear regression analysis unadjusted as well as adjusted for age, sex, and BMI as potential confounders was used to assess interactions between variant allele carrier status and

hepatic ATP concentrations. Differences and correlations were considered significant at *P* < 0.05. All statistical analyses were performed using SAS version 9.4 software (SAS Institute, Cary, NC).

## RESULTS

### Participant Characteristics

Participants of the whole cohort had comparable age, sex, BMI, fasting lipids, and hsCRP (Table 1). Patients with type 1 diabetes exhibited higher fasting blood glucose and HbA<sub>1c</sub> than CON but had near-normal glucometabolic control and short known diabetes duration. Waist circumference was higher and AST was slightly lower in patients with type 1 diabetes. Among the age- and BMI-matched subgroups, whole-body insulin sensitivity was 44% lower in the patients with type 1 diabetes (*M* value 7.5 mg \* kg BW<sup>-1</sup> \* min<sup>-1</sup> [6.3; 10.4] vs. 13.4 mg \* kg BW<sup>-1</sup> \* min<sup>-1</sup> [9.1; 16.5] in CON, *P* = 0.001), whereas basal EGP (bEGP) and iEGP were comparable to CON (Supplementary Table 1). Differences in waist circumference and glycemic control were similar to those of the whole cohort.

### Hepatic Phosphorus Metabolites and Fat Content

Hepatocellular ATP content was 15% lower in patients with type 1 diabetes than in CON (2.27  $\pm$  0.07 vs. 2.66  $\pm$  0.07 mmol/L in CON, *P* < 0.001), whereas Pi concentrations were comparable (1.94  $\pm$  0.07 vs. 2.03  $\pm$  0.07 mmol/L, *P* = 0.49) (Fig. 1A and B). The subgroup comparison confirmed the results of lower hepatic ATP concentration (2.30  $\pm$  0.10 vs. 2.72  $\pm$  0.12 mmol/L, *P* = 0.018) but comparable hepatic Pi and HCL content in type 1 diabetes compared with CON (Supplementary Table 1).

**Table 1—Participant characteristics**

Parameter	Type 1 diabetes	CON
<i>n</i> (females)	55(21)	57(23)
Known diabetes duration (days)	190 $\pm$ 13	—
Age (years)	34.3 $\pm$ 1.2	33.3 $\pm$ 1.3
BMI (kg/m <sup>2</sup> )	24.9 $\pm$ 0.5	23.9 $\pm$ 0.3
Waist (cm)	87 $\pm$ 2	<b>80 <math>\pm</math> 1*</b>
Blood glucose (mg/dL)	104 $\pm$ 4	<b>75 <math>\pm</math> 1*</b>
HbA <sub>1c</sub> (%)	6.2 $\pm$ 0.1	<b>5.1 <math>\pm</math> 0.0*</b>
HbA <sub>1c</sub> (mmol/mol)	45 $\pm$ 1	<b>33 <math>\pm</math> 1*</b>
AST (units/L)	21 (16; 23)	<b>22 (19; 30)*</b>
ALT (units/L)	20 (15; 26)	21 (16; 28)
GGT (units/L)	18 $\pm$ 1	25 $\pm$ 5
Plasma FFAs ( $\mu$ mol/L)	326 (244; 522)	400 (317; 652)
Plasma TGs (mg/dL)	66 (50; 78)	67 (53; 110)
Serum cholesterol (mg/dL)	185 $\pm$ 5	194 $\pm$ 4
hsCRP (mg/dL)	0.11 (0.05; 0.18)	0.07 (0.03; 0.08)

Data are mean  $\pm$  SEM or median (Q1; Q3). \**P* < 0.05 CON vs. type 1 diabetes, unpaired Student *t* test or Mann-Whitney *U* test.

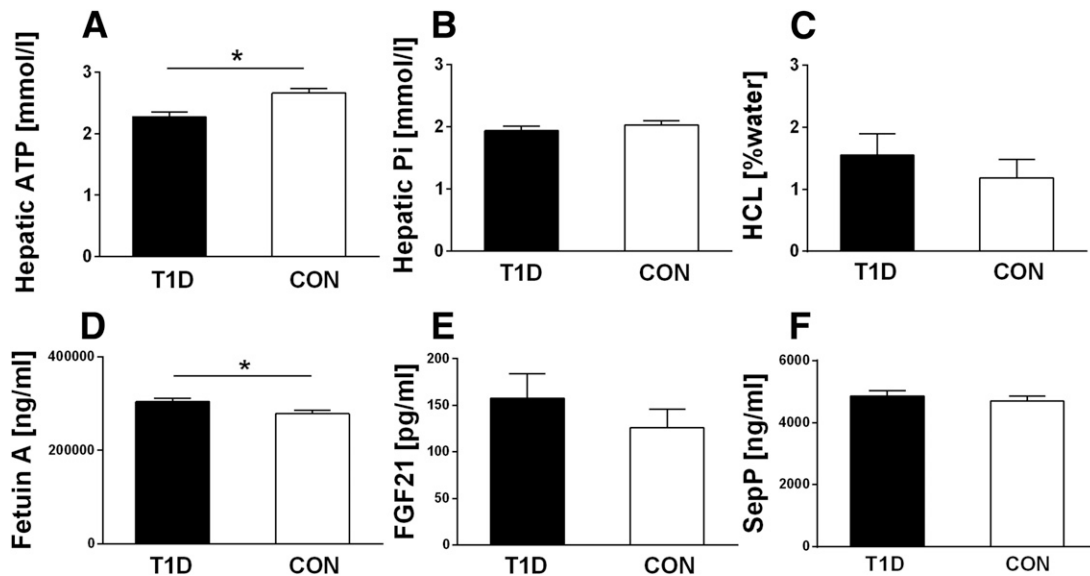


**Figure 1**—Hepatic concentrations of phosphorus metabolites and TGs. Hepatic concentrations of ATP (A), Pi (B), and HCL (C) and plasma concentrations of the hepatokines fetuin A (D), FGF21 (E), and SepP (F) in healthy participants (CON) and patients with type 1 diabetes (T1D). Data are mean  $\pm$  SEM; T1D  $n = 55$ , CON  $n = 57$  for hepatic ATP, Pi, and HCL; T1D  $n = 34$  and CON  $n = 27$  for hepatokines. \* $P < 0.001$  CON vs. T1D, unpaired Student  $t$  test or Mann-Whitney  $U$  test.

Across the whole cohort, HCL content did not differ between type 1 diabetes and CON (0.48% [0.26; 1.47] vs. 0.48% [0.20; 1.34],  $P = 0.55$ ) (Fig. 1C). The distribution of the individual HCL values covered a range from  $<1$  to 13% across the groups, with values  $>5.56\%$  in four patients with type 1 diabetes and two healthy humans.

#### Circulating Cytokines and Oxidative Stress Markers

Patients with type 1 diabetes exhibited higher fetuin A ( $305 \pm 7$  vs.  $279 \pm 7$  mg/mL,  $P = 0.01$ ) (Fig. 1D), whereas FGF21, SepP (Fig. 1E and F), and adiponectin (2,359 ng/mL [1,387; 5,213] vs. 2,681 ng/mL [1,608; 4,052] in CON,  $P = 0.88$ ) levels were similar to CON. OxLDL was 39% higher in patients with type 1 diabetes ( $43.9 \mu\text{g/mL}$  [24.3; 110.0] vs.  $31.4 \mu\text{g/mL}$  [17.1; 49.3],  $P = 0.038$ ) (Fig. 2A), whereas TBARS, 8OH-dG, and GSH levels (Fig. 2B–D) and protein carbonyl products ( $21.5 \text{ nmol/mL}$  [19.2; 35.3] vs.  $22.6 \text{ nmol/mL}$  [17.7; 35.3] in CON,  $P = 0.62$ ) were not different from CON.

#### Correlation Analyses

In an unadjusted analysis across all participants, hepatic ATP related negatively to HbA<sub>1c</sub>, fasting glucose, and oxLDL (Table 2). After adjustments for diabetes status, study, sex, age, and BMI, these correlations were no longer present. There were no associations between hepatic phosphorus metabolites and FFAs, TGs, total cholesterol, or hsCRP. Hepatic Pi correlated negatively with BMI ( $r = -0.20$ ,  $P = 0.03$ ), which remained significant after adjustment for diabetes status (data not shown). In the patients with type 1 diabetes, HCL content correlated positively with FGF21 ( $r = 0.67$ ,  $P < 0.001$ ), GGT ( $r = 0.56$ ,  $P < 0.001$ ), TGs ( $r = 0.55$ ,  $P < 0.001$ ), and visceral fat content ( $r = 0.41$ ,  $P < 0.01$ ) but negatively with

$M$  value ( $r = -0.52$ ,  $P < 0.001$ ) and adiponectin ( $r = -0.63$ ,  $P < 0.001$ ), which remained significant after adjustment for age, sex, and BMI (data not shown), whereas no association was observed between hepatic ATP and peripheral or hepatic insulin sensitivity (Supplementary Table 2).

#### Genetic Analyses

Among the patients with type 1 diabetes, carriers of the *PPARG* type 2 diabetes protective G allele (rs1801282) and noncarriers of *PPARGC1A* type 2 diabetes high-risk A allele (rs8192678) had 21% ( $P = 0.018$ ) and 13% lower ( $P = 0.028$ ) hepatic ATP concentrations compared with the corresponding noncarriers and carriers, respectively (Table 3). Multivariate linear regression analysis showed that the effect of variant allele carrier status of *PPARG* on hepatic ATP content is different at different carrier status of *PPARG* ( $P = 0.03$  unadjusted,  $P = 0.04$  adjusted for age, sex, and BMI) (Fig. 3). In carriers of the minor G allele in *PPARG* (rs2267668), related to reduced response in mitochondrial function to lifestyle intervention (18), no differences in hepatic ATP and Pi concentrations were found. The high-risk A allele in *FTO* (rs9939609) did not influence hepatic ATP and Pi levels (Table 3). Carriers of the A allele of *NDUFB6* gene polymorphism (rs540467) also exhibited no differences in hepatic phosphorous metabolites.

#### DISCUSSION

The main finding of this study is that patients with recent-onset type 1 diabetes already exhibit impaired hepatic energy metabolism independent of liver fat content, but in

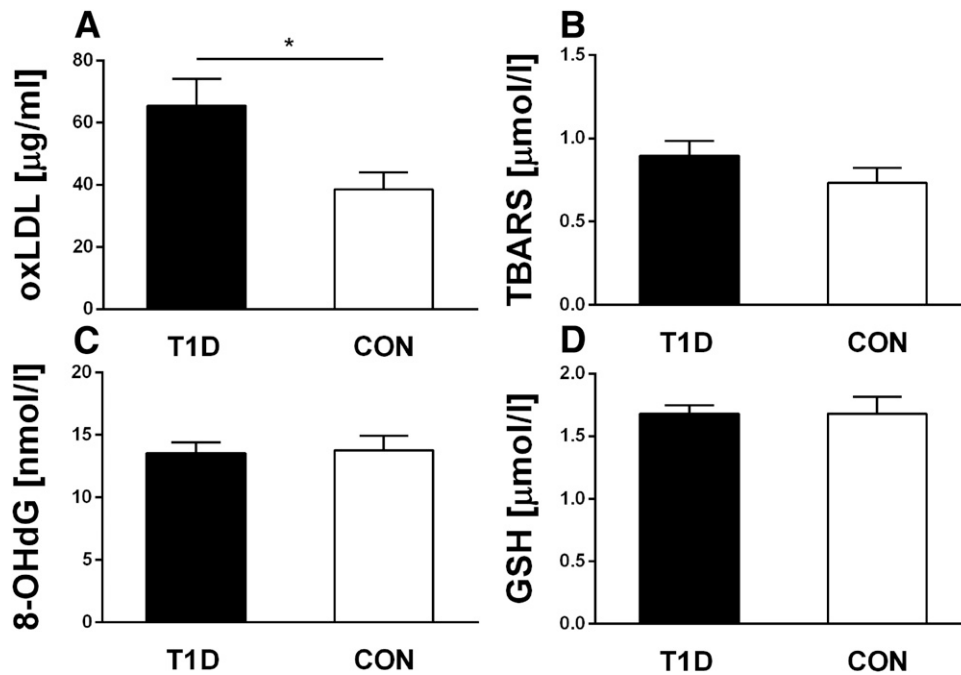


**Figure 2**—Plasma concentrations of the oxidative stress and antioxidant defense markers. OxLDL (A), TBARS (B), 8-OHdG (C), and GSH (D) in patients with type 1 diabetes (T1D,  $n = 34$ ) and healthy humans (CON,  $n = 27$ ). Data are means  $\pm$  SEM. \* $P < 0.05$  CON vs. T1D, Mann-Whitney  $U$  test.

the setting of increased peripheral insulin resistance and circulating fetuin A levels. Absolute concentrations of hepatic ATP may be further modulated by variations in genes known to control mitochondrial biogenesis. Of note, lower hepatic ATP levels in these near-normoglycemic patients are present early in the course of the disease, when hepatic insulin resistance and NAFLD are absent.

Recent data revealed that biopsy-proven NAFLD has similar liver-related adverse outcomes in type 1 diabetes compared with patients with type 2 diabetes (2). However, the risk factors and methods for early detection in type 1 diabetes remained unknown. Decreased hepatic ATP levels have been previously reported not only in obesity (29) but also in alcoholic hepatitis (30) and during postsurgical

**Table 2**—Pearson correlation analysis with hepatic ATP concentrations in total cohort of patients with type 1 diabetes and healthy participants

Variable	$n$	Unadjusted		Adjusted for status		Adjusted for status, study, sex, age, BMI	
		$r$	$P$	$r$	$P$	$r$	$P$
Age	112	0.10	0.28	0.13	0.17		
BMI	112	-0.01	0.87	0.04	0.71		
Waist	95	0.01	0.89	0.12	0.21	0.19	0.07
Glucose	101	<b>-0.22</b>	<b>0.02</b>	-0.08	0.45	-0.11	0.29
HbA <sub>1c</sub>	100	<b>-0.27</b>	<b>0.007</b>	-0.13	0.21	-0.14	0.16
AST (ln)	111	0.07	0.47	-0.03	0.72	-0.27	0.78
TGs (ln)	97	0.13	0.19	0.10	0.34	0.16	0.12
Cholesterol	111	0.14	0.14	0.01	0.28	0.15	0.11
FFAs (ln)	100	0.07	0.49	0.02	0.83	0.10	0.32
hsCRP (ln)	74	-0.10	0.38	0.03	0.81	-0.00	0.95
HCL (ln)	105	0.02	0.81	0.07	0.49	-0.03	0.77
oxLDL (ln)	61	<b>-0.29</b>	<b>0.02</b>	-0.22	0.09	-0.21	0.12
Fetuin A	61	0.02	0.87	0.14	0.27	0.12	0.38

ln, log transformed. Statistically significant results appear in boldface.

**Table 3—Hepatic ATP and Pi concentrations and HCL in variant allele carriers and noncarriers**

Variable	Carrier status	<i>NDUFB6</i> rs540467	<i>PPARGC1A</i> rs8192678	<i>PPARD</i> rs2267668	<i>PPARG</i> rs1801282	<i>FTO</i> rs9939609
Hepatic ATP (mmol/L)	0	2.36 ± 0.55	2.10 ± 0.46	2.26 ± 0.60	2.36 ± 0.54	2.38 ± 0.51
	1	2.12 ± 0.52	2.40 ± 0.57*	2.31 ± 0.44	1.87 ± 0.41*	2.23 ± 0.56
Hepatic Pi (mmol/L)	0	2.01 ± 0.53	1.86 ± 0.52	2.01 ± 0.52	1.94 ± 0.56	1.97 ± 0.49
	1	1.80 ± 0.48	2.01 ± 0.53	1.80 ± 0.54	1.94 ± 0.31	1.93 ± 0.54
Ln HCL (%)	0	−0.49 ± 1.60	−0.69 ± 1.66	−0.71 ± 1.43	−0.50 ± 1.45	−0.10 ± 1.10
	1	−0.73 ± 1.11	−0.49 ± 1.28	−0.30 ± 1.46	−0.94 ± 1.43	−0.79 ± 1.54

Data are means ± SD. 1, carrier; 0, noncarrier; ln HCL, log-transformed HCL. \**P* < 0.05 Wilcoxon rank sum test.

recovery in liver cirrhosis (31). There is evidence for a metabolic shift from oxidative phosphorylation to glycolysis at an early stage of liver injury, supporting the central role of mitochondrial function in liver adaptation to disease (32). Lower hepatic ATP could result from compromised production, i.e., oxidative phosphorylation, or from increased utilization by energy-consuming processes like lipogenesis. The patients of the current study exhibited low HCL in line with previous studies in humans (33) and comparable circulating lipids, excluding enhanced lipogenesis. Breakdown of ATP would also result in increased Pi levels, suggesting a reduced phosphorylation state (34), as observed in obesity (29), virus-induced cirrhosis (35), and hepatic malignancies (36). In contrast to type 2 diabetes (9), patients with type 1 diabetes had unchanged hepatic Pi concentrations. Of note, ATP content is a major discriminator for the degree of liver injury in NAFLD (37). In the current study, hepatic ATP concentrations were corrected for hepatocellular lipid volume (22) and still remained lower in type 1 diabetes, indicating reduced energy metabolism independent of liver

fat content. The absence of any clinical or biochemical signs of liver disease in these patients suggests that impaired switching between energy-demanding and energy-producing processes, but not loss of functional hepatocytes, is responsible for the observed abnormality in hepatic energy status.

Human as well as mouse models showed that glycemia, lipid availability, and oxidative stress are major determinants of hepatic mitochondrial function, with the latter considered at the same time a cause and a consequence of alterations in hepatic energy metabolism. Previous studies investigating hepatic energy metabolism with  $^{31}\text{P}/^1\text{H}$ -MRS have shown reduced hepatic ATP and Pi concentrations as well as lower flux through ATP synthase in type 2 diabetes (9,10). Our finding of decreased hepatic ATP content in type 1 diabetes (Fig. 1) shows that abnormal liver energy homeostasis is also a feature of the early course of type 1 diabetes and could therefore be associated with common hallmarks like hyperglycemia or muscle and hepatic insulin resistance (38). Previous studies demonstrated similar results and correlations of hepatic absolute ATP concentrations and hepatic ATP synthase flux with insulin resistance and liver fat content in patients with type 2 diabetes (9,10). Thus, hepatic absolute ATP content likely reflects ATP synthase flux, further suggesting that the lower ATP concentrations reflect diminished hepatic ATP synthesis in type 1 diabetes. In muscle of nonobese patients with type 1 diabetes, insulin-stimulated flux through muscle ATP synthase is reduced and associates with long-term glycemic control, as measured by HbA<sub>1c</sub> (7). In the current study, hepatic ATP associates negatively with fasting glycemia but only before adjustment for diabetes status, age, sex, and BMI, suggesting that other factors might be at play.

Recent studies in mouse models of type 1 diabetes described greater mitochondrial biogenesis by increased transcript levels of PGC1 $\alpha$  and TFAM and respiratory chain complex activity as adaptation to the increased lipid and glucose flux at diabetes onset and compensation for mitochondrial energetic deficit due to enhanced gluconeogenesis (11,39). Liver biopsy samples were not available in the current study, rendering direct measurements of mitochondrial function and biogenesis impossible. Depletion of hepatic ATP in humans with type 1 diabetes could result from chronically increased rates of energy-consuming processes, such as increased and unrestrained hepatic gluconeogenesis under conditions of portal hypoinsulinemia

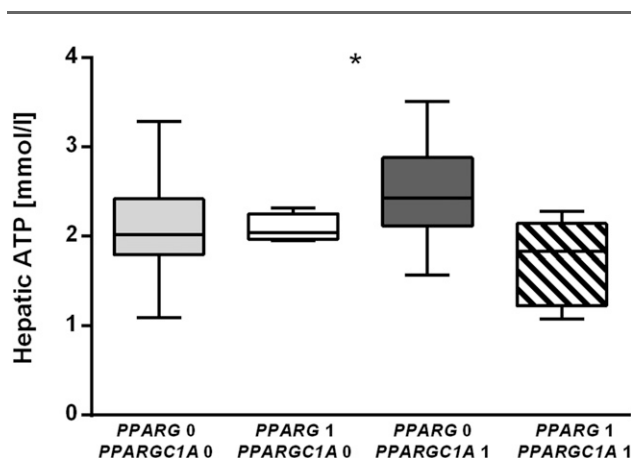


**Figure 3—Hepatic ATP concentrations and *PPARG* and *PPARG* coactivator-1 $\alpha$  (*PPARGC1A*) gene polymorphisms.** Hepatic ATP concentrations in patients carrying no *PPARG* and *PPARGC1A* variant alleles (light gray bar), carrying *PPARG* G allele and not carrying *PPARGC1A* A allele (white bar), not carrying *PPARG* G allele and carrying *PPARGC1A* A allele (dark gray bar), and carrying both *PPARG* and *PPARGC1A* variant alleles (hatched bar). 1, variant allele carriers; 0, variant allele noncarriers. \**P* < 0.05 for interaction, multivariable linear regression analysis.

(33). Nevertheless, the patients with type 1 diabetes of this study exhibited no increase in fasting EGP, suggesting no relevant increase in gluconeogenic flux. Higher hepatic or systemic lipids could also impair hepatic mitochondrial function by lipotoxicity (40), but again operation of this mechanism is unlikely in the absence of changes in plasma TGs, FFAs, and HCL.

Recent clinical trials in obese humans confirmed the concept of hepatic mitochondrial adaptation and mitochondrial flexibility at early stages of NAFLD but reported declining hepatic respiratory capacity along with augmented oxidative stress in nonalcoholic steatohepatitis (12,13). Higher systemic levels of oxidative stress and lipid peroxidation, along with the reduced antioxidant capacity in type 1 diabetes (41), could contribute to impaired mitochondrial function and reduced hepatic ATP content. The current study found no differences between lipid peroxidation assessed by TBARS, DNA oxidative damage measured by 8-OHdG, and protein carbonyl products or antioxidant defense, as assessed from GSH concentrations, between humans with and without type 1 diabetes. This could be due to the short duration of disease and excellent glucometabolic control of the patients. Interestingly, oxLDL reflecting susceptibility of LDL to oxidative modification was increased in patients with type 1 diabetes of the current study compared with CON, which has previously been linked to reduced plasma antioxidant levels and atherosclerosis in type 1 diabetes (42). Indeed, the finding that hepatic ATP concentrations correlated negatively with oxLDL supports a close relationship between early changes in oxidative stress and impaired hepatic energy metabolism but does not allow conclusions as to causality. Moreover, association with oxLDL was lost after adjustment for status, sex, age, and BMI, suggesting that observed changes are not necessarily related.

In patients with type 2 diabetes, hepatic insulin resistance is an independent predictor explaining lower absolute hepatic ATP and Pi contents (9) and ATP synthesis (10). In the current study, hepatic ATP concentrations did not correlate with any anthropometric or insulin sensitivity measures in patients with type 1 diabetes despite substantially lower peripheral insulin sensitivity and higher waist circumference compared with CON. Of note, no relation between subcutaneous and visceral fat content and hepatic ATP concentrations was detected, implying that fat mass and depot distribution do not play a major role for hepatic energy homeostasis in type 1 diabetes. Moreover, comparable iEGP between the two subgroups and the lack of association with hepatic ATP further suggest no effect of hepatic insulin sensitivity on hepatic energy status at this early stage of type 1 diabetes development. This implies that factors different from fat mass and insulin sensitivity underlie the abnormal hepatic energy metabolism.

A number of circulating adipo-/hepatokines are known to be altered and play a role in insulin resistance and lipid homeostasis in humans with type 1 diabetes (19–21) and rodent models (11). Indeed, we confirmed higher

fetuin A concentrations in patients with type 1 diabetes, as previously observed in rodent models of type 1 diabetes (11) and in human type 1 diabetes, where it relates to early markers of atherosclerosis and obesity (20). Concentrations of FGF21, a modulator of mitochondrial oxidative phosphorylation (43), did not differ between patients and CON, in contrast to one previous study, probably due to lower age and markedly worse glycemic control of those patients (21). Also, concentrations of the hepatokine SepP, which may be increased in obesity and NAFLD (44) and interfere with insulin signaling by inhibiting phosphorylation of key mediators in energy metabolism such as protein kinase B and AMP-activated protein kinase (45), were unchanged in patients with type 1 diabetes.

Abnormalities in glucose and energy homeostasis have also been related to SNPs in genes regulating metabolism. The common polymorphism Pro12Ala (rs1801282) of the *PPARG* gene associates with reduced type 2 diabetes risk through modulation of the production and release of adipose-derived insulin-sensitizing factors (14) and represents an important genetic link between type 2 and type 1 diabetes (46). The *PPAR* $\gamma$  coactivator-1 $\alpha$  regulates oxidative phosphorylation, and the variant serine-encoding allele (Gly482Ser) in the *PPARGC1A* gene associates with increased obesity and oxidative stress risk (47). Unexpectedly, we found reduced hepatic ATP concentrations in Ala allele carriers (*PPARG* rs1801282) and in Ser allele noncarriers (*PPARGC1A* rs8192678). As hepatic energy metabolism is augmented in obesity and insulin resistance (12), our present finding might suggest that in nonobese patients with type 1 diabetes with normal hepatic insulin sensitivity, these type 2 diabetes protective gene variants contribute to the absence of any increase in hepatic ATP concentrations.

Finally, a variant in the *NDUFB6* gene, encoding a subunit of complex I of the respiratory chain, associates with increased type 2 diabetes risk, relates to insulin resistance (48), and predicts the response of muscle energy metabolism to exercise training (16,17). However, no difference in hepatic phosphorous metabolites and HCL between carriers of the A allele in *NDUFB6* polymorphism rs540467 and noncarriers was found (Table 3).

In conclusion, hepatic ATP concentrations are reduced independently of hepatic lipid content and influenced by variants in genes controlling oxidative metabolism in type 1 diabetes. Our data underline the importance of liver mitochondrial function and energy homeostasis as early and sensitive markers in metabolic liver disease progression.

---

**Acknowledgments.** The authors thank Andrea Nagel, Nicole Achterath, Ulrike Partke, Gabi Gornitzka, Kai Tinnes, and Myrko Eßer (Institute for Clinical Diabetology, German Diabetes Center) for their excellent help with the experiments. **Funding.** This work was supported by the Ministry of Innovation, Science and Research of the State of North Rhine-Westphalia and the German Federal Ministry of Health. This study was supported in part by a grant from the Federal Ministry of Education and Research (BMBF) to the German Center for Diabetes Research,

by a grant from the Helmholtz Alliance Imaging and Curing Environmental Metabolic Diseases (ICEMED), and by the Schmutzler-Stiftung. Part of this project was conducted in the context of the pretest studies of the German National Cohort ([www.nationale-kohorte.de](http://www.nationale-kohorte.de)). These were funded by the BMBF (Förder Kennzeichen 01ER1001A-I) and supported by the Helmholtz Association as well as by the participating universities and institutes of the Leibniz Association.

The funding sources had no input in the design and conduct of this study, in the collection, analysis, and interpretation of the data, or in the preparation, review, or approval of the article.

**Duality of Interest.** No potential conflicts of interest relevant to this article were reported.

**Author Contributions.** S.G. wrote the manuscript and researched and collected data. A.B. contributed to the manuscript and collected data. K.K., C.H., P.N., S.K., G.G., B.Kl., B.Kn., P.B., and J.L. collected data. K.S. and H.A.-H. contributed to the manuscript and data analysis. J.S. and M.R. designed the study, researched data, and contributed to the manuscript. M.R. is the guarantor of this work and, as such, had full access to all the data in the study and takes responsibility for the integrity of the data and the accuracy of the data analysis.

## Appendix

The GDS Group consists of Michael Roden (speaker), Hadi Al-Hasani, Annette Buyken, Juergen Eckel, Gerd Geerling, Christian Herder, Andrea Icks, Joerg Kotzka, Oliver Kuss, Eckhard Lammert, Jesper Lundbom, Karsten Muessig, Peter Nowotny, Wolfgang Rathmann, Julia Szendroedi, and Dan Ziegler.

## References

- Saponaro C, Gaggini M, Gastaldelli A. Nonalcoholic fatty liver disease and type 2 diabetes: common pathophysiologic mechanisms. *Curr Diab Rep* 2015;15:607
- Harman DJ, Kaye PV, Harris R, Suzuki A, Gazis A, Aithal GP. Prevalence and natural history of histologically proven chronic liver disease in a longitudinal cohort of patients with type 1 diabetes. *Hepatology* 2014;60:158–168
- Bergman BC, Howard D, Schauer IE, et al. Features of hepatic and skeletal muscle insulin resistance unique to type 1 diabetes. *J Clin Endocrinol Metab* 2012;97:1663–1672
- DeFronzo RA, Hendler R, Simonson D. Insulin resistance is a prominent feature of insulin-dependent diabetes. *Diabetes* 1982;31:795–801
- Kacerovsky M, Jones J, Schmid AI, et al. Postprandial and fasting hepatic glucose fluxes in long-standing type 1 diabetes. *Diabetes* 2011;60:1752–1758
- Yki-Järvinen H. Glucose toxicity. *Endocr Rev* 1992;13:415–431
- Kacerovsky M, Brehm A, Chmelik M, et al. Impaired insulin stimulation of muscular ATP production in patients with type 1 diabetes. *J Intern Med* 2011;269:189–199
- Szendroedi J, Kaul K, Kloock L, et al. Lower fasting muscle mitochondrial activity relates to hepatic steatosis in humans. *Diabetes Care* 2014;37:468–474
- Szendroedi J, Chmelik M, Schmid AI, et al. Abnormal hepatic energy homeostasis in type 2 diabetes. *Hepatology* 2009;50:1079–1086
- Schmid AI, Szendroedi J, Chmelik M, Krssák M, Moser E, Roden M. Liver ATP synthesis is lower and relates to insulin sensitivity in patients with type 2 diabetes. *Diabetes Care* 2011;34:448–453
- Jelenik T, Séquaris G, Kaul K, et al. Tissue-specific differences in the development of insulin resistance in a mouse model for type 1 diabetes. *Diabetes* 2014;63:3856–3867
- Fritsch M, Koliaki C, Livingstone R, et al. Time course of postprandial hepatic phosphorus metabolites in lean, obese, and type 2 diabetes patients. *Am J Clin Nutr* 2015;102:1051–1058
- Koliaki C, Szendroedi J, Kaul K, et al. Adaptation of hepatic mitochondrial function in humans with non-alcoholic fatty liver is lost in steatohepatitis. *Cell Metab* 2015;21:739–746
- Stumvoll M, Häring H. The peroxisome proliferator-activated receptor-gamma2 Pro12Ala polymorphism. *Diabetes* 2002;51:2341–2347
- Grunnet LG, Brøns C, Jacobsen S, et al. Increased recovery rates of phosphocreatine and inorganic phosphate after isometric contraction in oxidative muscle fibers and elevated hepatic insulin resistance in homozygous carriers of the A-allele of FTO rs9939609. *J Clin Endocrinol Metab* 2009;94:596–602
- Kacerovsky-Bielez G, Chmelik M, Ling C, et al. Short-term exercise training does not stimulate skeletal muscle ATP synthesis in relatives of humans with type 2 diabetes. *Diabetes* 2009;58:1333–1341
- Kacerovsky-Bielez G, Kacerovsky M, Chmelik M, et al. A single nucleotide polymorphism associates with the response of muscle ATP synthesis to long-term exercise training in relatives of type 2 diabetic humans. *Diabetes Care* 2012;35:350–357
- Stefan N, Thamer C, Staiger H, et al. Genetic variations in PPAR $\alpha$  and PPAR $\gamma$ 1A determine mitochondrial function and change in aerobic physical fitness and insulin sensitivity during lifestyle intervention. *J Clin Endocrinol Metab* 2007;92:1827–1833
- Perseghin G, Lattuada G, Danna M, et al. Insulin resistance, intramyocellular lipid content, and plasma adiponectin in patients with type 1 diabetes. *Am J Physiol Endocrinol Metab* 2003;285:E1174–E1181
- Abd El Dayem SM, Battah AA, El Bohy AelM, El Shehaby A. Evaluation of fetuin-A and carotid intima-media thickness in adolescent type 1 diabetic patients. *J Pediatr Endocrinol Metab* 2015;28:287–292
- Xiao Y, Xu A, Law LS, et al. Distinct changes in serum fibroblast growth factor 21 levels in different subtypes of diabetes. *J Clin Endocrinol Metab* 2012;97:E54–E58
- Laufs A, Livingstone R, Nowotny B, et al. Quantitative liver  $^{31}\text{P}$  magnetic resonance spectroscopy at 3T on a clinical scanner. *Magn Reson Med* 2014;71:1670–1675
- Schmid AI, Chmelik M, Szendroedi J, et al. Quantitative ATP synthesis in human liver measured by localized  $^{31}\text{P}$  spectroscopy using the magnetization transfer experiment. *NMR Biomed* 2008;21:437–443
- Weber KS, Nowotny B, Strassburger K, et al.; GDS Group. The role of markers of low-grade inflammation for the early time course of glycemic control, glucose disappearance rate, and  $\beta$ -cell function in recently diagnosed type 1 and type 2 diabetes. *Diabetes Care* 2015;38:1758–1767
- German National Cohort (GNC) Consortium. The German National Cohort: aims, study design and organization. *Eur J Epidemiol* 2014;29:371–382
- Kahl S, Nowotny B, Piepel S, et al. Estimates of insulin sensitivity from the intravenous-glucose-modified-clamp test depend on suppression of lipolysis in type 2 diabetes: a randomised controlled trial. *Diabetologia* 2014;57:2094–2102
- Nowotny B, Zahiragic L, Bierwagen A, et al. Low-energy diets differing in fibre, red meat and coffee intake equally improve insulin sensitivity in type 2 diabetes: a randomised feasibility trial. *Diabetologia* 2015;58:255–264
- Hamilton G, Yokoo T, Bydder M, et al. In vivo characterization of the liver fat  $^1\text{H}$  MR spectrum. *NMR Biomed* 2011;24:784–790
- Nair S, P Chacko V, Arnold C, Diehl AM. Hepatic ATP reserve and efficiency of replenishing: comparison between obese and nonobese normal individuals. *Am J Gastroenterol* 2003;98:466–470
- Meyerhoff DJ, Boska MD, Thomas AM, Weiner MW. Alcoholic liver disease: quantitative image-guided P-31 MR spectroscopy. *Radiology* 1989;173:393–400
- Mann DV, Lam WW, Hjelm NM, et al. Human liver regeneration: hepatic energy economy is less efficient when the organ is diseased. *Hepatology* 2001;34:557–565
- Nishikawa T, Bellance N, Damm A, et al. A switch in the source of ATP production and a loss in capacity to perform glycolysis are hallmarks of hepatocyte failure in advanced liver disease. *J Hepatol* 2014;60:1203–1211
- Perseghin G, Lattuada G, De Cobelli F, et al. Reduced intrahepatic fat content is associated with increased whole-body lipid oxidation in patients with type 1 diabetes. *Diabetologia* 2005;48:2615–2621
- Solga SF, Horska A, Clark JM, Diehl AM. Hepatic  $^{31}\text{P}$  magnetic resonance spectroscopy: a hepatologist's user guide. *Liver Int* 2005;25:490–500
- Menon DK, Sargentoni J, Taylor-Robinson SD, et al. Effect of functional grade and etiology on in vivo hepatic phosphorus-31 magnetic resonance spectroscopy

- in cirrhosis: biochemical basis of spectral appearances. *Hepatology* 1995;21:417–427
36. Leij-Halfwerk S, Dagneli PC, Kappert P, Oudkerk M, Sijens PE. Decreased energy and phosphorylation status in the liver of lung cancer patients with weight loss. *J Hepatol* 2000;32:887–892
37. Abrigo JM, Shen J, Wong VW, et al. Non-alcoholic fatty liver disease: spectral patterns observed from an in vivo phosphorus magnetic resonance spectroscopy study. *J Hepatol* 2014;60:809–815
38. DeFronzo RA, Simonson D, Ferrannini E. Hepatic and peripheral insulin resistance: a common feature of type 2 (non-insulin-dependent) and type 1 (insulin-dependent) diabetes mellitus. *Diabetologia* 1982;23:313–319
39. Franko A, von Kleist-Retzow JC, Neschen S, et al. Liver adapts mitochondrial function to insulin resistant and diabetic states in mice. *J Hepatol* 2014;60:816–823
40. Cusi K. Role of obesity and lipotoxicity in the development of nonalcoholic steatohepatitis: pathophysiology and clinical implications. *Gastroenterology* 2012;142:711.e6–725.e6
41. Vessby J, Basu S, Mohsen R, Berne C, Vessby B. Oxidative stress and antioxidant status in type 1 diabetes mellitus. *J Intern Med* 2002;251:69–76
42. Tsai EC, Hirsch IB, Brunzell JD, Chait A. Reduced plasma peroxy radical trapping capacity and increased susceptibility of LDL to oxidation in poorly controlled IDDM. *Diabetes* 1994;43:1010–1014
43. Chau MD, Gao J, Yang Q, Wu Z, Gromada J. Fibroblast growth factor 21 regulates energy metabolism by activating the AMPK-SIRT1-PGC-1alpha pathway. *Proc Natl Acad Sci U S A* 2010;107:12553–12558
44. Choi HY, Hwang SY, Lee CH, et al. Increased selenoprotein p levels in subjects with visceral obesity and nonalcoholic fatty liver disease. *Diabetes Metab J* 2013;37:63–71
45. Steinbrenner H. Interference of selenium and selenoproteins with the insulin-regulated carbohydrate and lipid metabolism. *Free Radic Biol Med* 2013;65:1538–1547
46. Raj SM, Howson JM, Walker NM, et al. No association of multiple type 2 diabetes loci with type 1 diabetes. *Diabetologia* 2009;52:2109–2116
47. Weng SW, Lin TK, Wang PW, et al. Gly482Ser polymorphism in the peroxisome proliferator-activated receptor gamma coactivator-1alpha gene is associated with oxidative stress and abdominal obesity. *Metabolism* 2010;59:581–586
48. Ling C, Poulsen P, Simonsson S, et al. Genetic and epigenetic factors are associated with expression of respiratory chain component NDUFB6 in human skeletal muscle. *J Clin Invest* 2007;117:3427–3435



# Impaired Hepatic Mitochondrial Capacity in Nonalcoholic Steatohepatitis Associated With Type 2 Diabetes

*Diabetes Care* 2022;45:928–937 | <https://doi.org/10.2337/dc21-1758>

Sofiya Gancheva,<sup>1–3</sup> Sabine Kahl,<sup>1–3</sup> Dominik Pesta,<sup>2,3</sup> Lucia Mastroiuto,<sup>2,3</sup> Bedair Dewidar,<sup>2–4</sup> Klaus Strassburger,<sup>3,5</sup> Ehsan Sabah,<sup>6</sup> Irene Esposito,<sup>7</sup> Jürgen Weiß,<sup>3,8</sup> Theresia Sarabhai,<sup>1–3</sup> Martin Wolkersdorfer,<sup>9</sup> Thomas Fleming,<sup>10</sup> Peter Nawroth,<sup>10</sup> Marcel Zimmermann,<sup>11</sup> Andreas S. Reichert,<sup>11</sup> Matthias Schlensak,<sup>6</sup> and Michael Roden<sup>1–3</sup>

## OBJECTIVE

Individuals with type 2 diabetes are at higher risk of progression of nonalcoholic fatty liver (steatosis) to steatohepatitis (NASH), fibrosis, and cirrhosis. The hepatic metabolism of obese individuals adapts by upregulation of mitochondrial capacity, which may be lost during the progression of steatosis. However, the role of type 2 diabetes with regard to hepatic mitochondrial function in NASH remains unclear.

## RESEARCH DESIGN AND METHODS

We therefore examined obese individuals with histologically proven NASH without (OBE) ( $n = 30$ ; BMI  $52 \pm 9$  kg/m<sup>2</sup>) or with type 2 diabetes (T2D) ( $n = 15$ ;  $51 \pm 7$  kg/m<sup>2</sup>) as well as healthy individuals without liver disease (CON) ( $n = 14$ ;  $25 \pm 2$  kg/m<sup>2</sup>). Insulin sensitivity was measured by hyperinsulinemic-euglycemic clamps with D-[6,6-<sup>2</sup>H<sub>2</sub>]glucose. Liver biopsies were used for assessing mitochondrial capacity by high-resolution respirometry and protein expression.

## RESULTS

T2D and OBE had comparable hepatic fat content, lobular inflammation, and fibrosis. Oxidative capacity in liver tissue normalized for citrate synthase activity was 59% greater in OBE than in CON, whereas T2D presented with 33% lower complex II-linked oxidative capacity than OBE and higher H<sub>2</sub>O<sub>2</sub> production than CON. Interestingly, those with NASH and hepatic fibrosis score  $\geq 1$  had lower oxidative capacity and antioxidant defense than those without fibrosis.

## CONCLUSIONS

Loss of hepatic mitochondrial adaptation characterizes NASH and type 2 diabetes or hepatic fibrosis and may thereby favor accelerated disease progression.

Recent findings challenge the paradigm of diabetes classification by proposing diabetes subtypes (1). Specifically, the severe insulin-resistant diabetes subtype features increased prevalence of hepatic steatosis at diagnosis and hepatic fibrosis at 5 years of follow-up (2). Of note, hepatic fibrosis affects at least one of six individuals with type 2 diabetes (3). These data suggest tight links between insulin resistance and nonalcoholic fatty liver disease (NAFLD) progression. Abnormal adipose tissue function, lipotoxicity (4), and glucose toxicity, as well as abnormal mitochondrial function (5), have been implicated as possible mechanisms underlying insulin resistance. Notably, rapid

<sup>1</sup>Department of Endocrinology and Diabetology, Medical Faculty and University Hospital, Heinrich Heine University, Düsseldorf, Germany

<sup>2</sup>Institute for Clinical Diabetology, German Diabetes Center, Leibniz Center for Diabetes Research, Heinrich Heine University, Düsseldorf, Germany

<sup>3</sup>German Center for Diabetes Research, Partner Düsseldorf, München-Neuherberg, Germany

<sup>4</sup>Department of Pharmacology and Toxicology, Faculty of Pharmacy, Tanta University, Tanta, Egypt

<sup>5</sup>Institute for Biometrics and Epidemiology, German Diabetes Center, Leibniz Center for Diabetes Research, Heinrich Heine University, Düsseldorf, Germany

<sup>6</sup>Obesity and Reflux Center, Neuwerk Hospital, Mönchengladbach, Germany

<sup>7</sup>Institute of Pathology, Heinrich Heine University, Düsseldorf, Germany

<sup>8</sup>Institute for Clinical Biochemistry and Pathobiochemistry, German Diabetes Center, Leibniz Center for Diabetes Research, Heinrich Heine University, Düsseldorf, Germany

<sup>9</sup>Landesapothek Salzburg, Salzburg, Austria

<sup>10</sup>Department of Internal Medicine I, University Hospital Heidelberg, Heidelberg, Germany

<sup>11</sup>Institute of Biochemistry and Molecular Biology I, Medical Faculty and University Hospital Düsseldorf, Heinrich Heine University, Düsseldorf, Germany

Corresponding author: Michael Roden, michael.roden@ddz.de

Received 20 August 2021 and accepted 13 January 2022

This article contains supplementary material online at <https://doi.org/10.2337/figshare.18409844>.

© 2022 by the American Diabetes Association. Readers may use this article as long as the work is properly cited, the use is educational and not for profit, and the work is not altered. More information is available at <https://www.diabetesjournals.org/journals/pages/license>.

increases in liver fat content during the early course of type 2 diabetes have been related to deterioration of hepatic energy metabolism (6).

Indeed, type 2 diabetes has been associated with altered hepatic energy metabolism, including reduced hepatic ATP concentrations (7). Individuals with nonalcoholic steatohepatitis (NASH) also exhibit hepatic mitochondrial structural defects and impaired ATP repletion upon fructose challenge (8,9). However, recent studies have shown that mitochondrial function is not uniformly impaired in insulin resistance or NAFLD, with obese individuals with or without hepatic steatosis exhibiting up to fivefold higher maximal oxidative capacity than lean individuals, indicating hepatic mitochondrial adaptation to augmented lipid availability (10). Whether type 2 diabetes triggers loss of hepatic mitochondrial adaptation in states of severe obesity and insulin resistance is currently unclear.

Individuals with NASH also feature abnormal hepatic mitochondrial redox homeostasis, with higher generation of reactive oxygen species (ROS) paralleled by reduced antioxidant defense (10), possibly because of lipotoxicity and glucotoxicity (11). Increased lipid availability enhances oxidative metabolism and amplifies anaplerosis and cataplerosis, which is required for gluconeogenesis but also causes oxidative and endoplasmic reticulum (ER) stress (12,13). Type 2 diabetes leads not only to elevated lipid peroxidation but also to hyperglycemia-mediated increases in advanced glycation end products (AGE) (14,15). However, data on a contribution of oxidative stress and glyoxal- and methylglyoxal-induced cytotoxicity to liver injury in individuals with NASH and type 2 diabetes have not yet been reported.

Therefore, we combined *in vivo* measurement of hepatic insulin sensitivity with direct *ex vivo* analysis of mitochondrial functionality and oxidative stress from intraoperative liver samples to test the hypothesis that oxidative stress and AGEs from hyperglycemia drive the loss of hepatic mitochondrial adaptation in obese individuals with type 2 diabetes and NASH.

## RESEARCH DESIGN AND METHODS

### Study Population

The prospective cohort study, BARIA-DDZ, investigates obese Caucasians before and

at timed intervals for at least 1 year after bariatric (metabolic) surgery (Clinical trial reg. no. NCT01477957, ClinicalTrials.gov). All participants receive information about all procedures and risks before providing their written consent to the experimental protocol, which was approved by the ethics board of Heinrich Heine University and University Hospital Düsseldorf (Düsseldorf, Germany) and the ethics board of the North Rhine regional physicians' association (Düsseldorf, Germany).

This cross-sectional analysis comprised 45 obese individuals with NASH (30 without [OBE] and 15 with type 2 diabetes [T2D]) as well as 14 nonobese individuals undergoing elective surgery, such as cholecystectomy or herniotomy, serving as controls (CON). Data of four OBE, three T2D, and 12 CON had been reported previously (10,16). All participants were nonsmokers and engaged only in light physical activity. T2D had no antihyperglycemic medication ( $n = 10$ ), metformin only ( $n = 1$ ), metformin and glucagon-like peptide 1 receptor agonist (GLP-1ra) ( $n = 1$ ), DPP4 inhibitor (DPP4i) and GLP-1ra ( $n = 1$ ), metformin, GLP-1ra, and short-acting insulin ( $n = 1$ ), or short-acting insulin ( $n = 1$ ). Metformin and DPP4i were discontinued for 3 days, GLP-1ra for 1 week, and insulin for at least 10 h prior to the tests. The participants underwent 3-h hyperinsulinemic-euglycemic clamps (primed continuous insulin infusion:  $80 \text{ mU} \cdot \text{m}^{-2} \cdot \text{min}^{-1}$  for 10 min, followed by  $40 \text{ mU} \cdot \text{m}^{-2} \cdot \text{min}^{-1}$ ) (Insuman Rapid; Sanofi, Frankfurt am Main, Germany) combined with  $\text{D-}[6,6\text{-}^2\text{H}_2]\text{glucose}$  for measuring whole-body or peripheral ( $M$  value, calculated from steady-state glucose infusion rate with glucose space correction) and hepatic insulin sensitivities (hepatic insulin sensitivity index, calculated as  $100 \times$  the inverse of the product of fasting endogenous glucose production [EGP] and fasting serum insulin concentration) (17). Rates of glucose appearance ( $R_a$ ) were calculated by multiplying the tracer infusion rate by tracer enrichment, dividing by percentage of tracer enrichment in plasma, and subtracting the tracer infusion rate (17). Clamp- $R_a$  was calculated using Steele steady-state equations. EGP was calculated from the difference between  $R_a$  and mean glucose infusion rate. Adipose tissue insulin resistance was assessed by the adipose tissue insulin resistance index, as calculated from the product of fasting serum free

fatty acids (FFA) and insulin concentrations (18). Blood samples were collected before and during the clamp for measuring hormones and metabolites. NASH was defined by the steatosis, activity, and fibrosis score (19). Because T2D were older than OBE, all analyses were age adjusted in order to avoid the confounding effect of age.

### Mitochondrial Function and Oxidative Stress

Respiration rates and maximum oxidative capacity were assessed using *ex vivo* high-resolution respirometry in liver tissue and isolated hepatic mitochondria (Oxygraph 2k; Oroboros Instruments, Innsbruck, Austria) upon sequential titration of substrates and normalization for mitochondrial citrate synthase activity (CSA) as a marker of mitochondrial content (10,13). The protocol for tricarboxylic acid (TCA) cycle-linked respiration included addition of malate, glutamate, ATP, succinate, cytochrome C, and carbonylcyanide *p*-trifluoromethoxyphenylhydrazone for assessment of maximum uncoupled respiration. Additionally, for testing glycolysis-linked TCA respiration and  $\beta$ -oxidation-linked TCA respiration, pyruvate and octanoyl-carnitine were added to the protocols, respectively. Hepatic  $\text{H}_2\text{O}_2$  emission in isolated mitochondria was measured fluorimetrically using Amplex Red, reflecting ROS production mainly from complexes I and III as reported previously (10). Catalase activity was measured colorimetrically in hepatic lysates (Cayman Chemical Company, Ann Arbor, MI). Thiobarbituric acid reactive species (TBARS) were measured fluorimetrically (BioTek Instruments, Bad Friedrichshall, Germany) in liver homogenates (13).

### Mitochondrial DNA

DNA was extracted from liver tissue using the DNeasy Blood & Tissue Kit (Qiagen, Düsseldorf, Germany) following the manufacturer's instructions. Briefly, liver tissue was lysed using ATL plus buffer and proteinase K at  $56^\circ\text{C}$  for 2 h. Later, DNA was purified using a DNeasy Mini Spin Column and dissolved in  $50 \mu\text{L}$  AE buffer. DNA concentration and purity were assessed by a nanoplatform reader (Tecan, Männedorf, Switzerland) and diluted to  $5 \text{ ng}/\mu\text{L}$  using PCR-grade  $\text{H}_2\text{O}$ . Mitochondrial DNA (mtDNA) copy number was quantified with the StepOne

Plus PCR System (Applied Biosystems, Foster City, CA) using primers for nuclear gene lipoprotein lipase (*LPL*) (forward primer CGAGTCGCTTTCTCCTGATGAT; reverse primer TTCTGGATTCCAATGCTTCGA) and mitochondrial gene NADH dehydrogenase subunit 1 (*ND1*) (forward primer CCCTAAAACCCGCCACATCT; reverse primer GAGCGATGGTGAGAGCTAAGGT). A melting curve was created to ensure primer specificity. Each sample was measured in duplicate, and the ratio of mtDNA to nuclear DNA was calculated as described (20).

### Blood Analyses

Metabolites, insulin, and hs-CRP were assessed as described previously (10). FFA were assayed microfluorimetrically (Wako Chem USA Inc. Osaka, Japan) after collecting blood into ice-cold orlistat-containing vials (21).

### Western Blotting

Protein of mitofusin 1 (MFN1) and MFN2, mitochondrial fission 1 protein (FIS1), mitochondrial fission factor (MFF), DRP1, phosphorylated Ser616-DRP1 (phospho-Ser616-DRP1), PINK1, phospho-Thr257-PINK1, ubiquitin E3 ligase parkin (PARKIN), phospho-Ser65-PARKIN, protein kinase RNA-like endoplasmic reticulum (ER) kinase (PERK), activating transcription factor 4 (ATF4), and electron transport chain (ETC) complexes I–V (NDUFB8 [NADH:ubiquinone oxidoreductase subunit B8], SDHB [succinate dehydrogenase complex iron sulfur subunit B], UQCRC2 [ubiquinol-cytochrome C reductase core protein 2], COXIV [cytochrome c oxidase subunit IV], and ATP5A [ATP synthase F1 subunit  $\alpha$ ]) were quantified in total liver protein lysates (22) and normalized to GAPDH as loading control (23). Antibodies were obtained from Abcam (Cambridge, U.K.) (MFN1, MFN2, PINK1, and total OXPHOS rodent antibody cocktail, including NDUFB8, SDHB, UQCRC2, COXIV, and ATP5A), Cell Signaling Technology (Frankfurt, Germany) (DRP1, phospho-DRP1, GAPDH, COX IV, PARKIN, PERK, ATF4, and eIF2), Ubiquigent (Dundee, U.K.) (phospho-PINK and phospho-PARKIN), and Merck (FIS1).

For the quantification of optic atrophy protein (OPA1) long and short isoforms, tissue lysates (equivalent of 40  $\mu$ g protein) were mixed with 4 $\times$  Laemmli buffer

and heated at 95°C for 5 min, loaded onto a 10% SDS gel (24). SDS-PAGE was run for 2.5 h at 40 mA per gel (20 mA per gel in the stacking gel) to achieve maximum separation of OPA1 bands. Western blotting was performed in the semidry procedure for 2.5 h at 60 mA per gel. Gels were ponceau stained, imaged, cut into stripes at 70 kDa, blocked with 5% milk in Tris-buffered saline, and incubated with their respective antibodies OPA1 (1:1,000) (self-purified antibody produced in rabbit by Pineda, Berlin, Germany) and Tubulin (1:2,000) (RRID:AB\_2210370) overnight at 4°C. After second antibody incubation, blots were imaged with the Peqlab Fusion Imaging System. Blots were quantified manually in Fiji (based on ImageJ 1.53f51) by selecting bands and appropriate adjacent areas for background correction.

### AGE

Plasma free AGE and hepatic protein-bound AGE were measured by isotope dilution tandem mass spectrometry as described (25). Briefly, for protein-bound AGE, total protein extracts from the liver (~10 mg) were prepared by homogenization in 10 mmol/L Na-phosphate buffer (pH 7.4). The soluble protein fraction was retained and then concentrated by microspin ultrafiltration (10-kDa cutoff) at 14,000 rpm for 30 min at 4°C and then washed by five cycles of concentration. An aliquot of the washed protein (100  $\mu$ g/20  $\mu$ L) was then hydrolyzed by serial enzymatic digestion using pepsin, pronase E, aminopeptidase, and prolidase (25). For free AGE, 20  $\mu$ L plasma was diluted to 500  $\mu$ L with H<sub>2</sub>O and filtered by microspin ultrafiltration (10-kDa cutoff) at 14,000 rpm for 30 min at 4°C. The ultrafiltrate was then retained for the free adduct analysis. Approximately 30  $\mu$ L sample was spiked with an equal volume of 0.2% trifluoroacetic acid in H<sub>2</sub>O containing the isotopic standards. Samples were analyzed by liquid chromatography–tandem mass spectrometry using an ACQUITY ultrahigh-performance liquid chromatography system with a Xevo-TQS liquid chromatography–tandem mass spectrometry spectrometer (Waters Corporation, Milford, MA). AGE, including oxidation and nitration markers, were detected by electrospray positive ionization with multiple reaction monitoring. Molecular ion and fragment ion masses,

as well as cone voltage and collision energies, were optimized to  $\pm 0.1$  Da and  $\pm 1$  eV for multiple reaction monitoring detection of the analytes. Acquisition and quantification were completed with MassLynx 4.1 and TargetLynx 2.7 (Waters Corporation).

### Transmission Electron Microscopy

Liver samples were fixed immediately after preparation for 2 h at room temperature by immersion in 2.5% glutaraldehyde in 190 mmol/L Na-cacodylate buffer (pH 7.4). Subsequently, they were post-fixed in 1% reduced osmium tetroxide in double-distilled H<sub>2</sub>O for 60 min and afterward stained with 2% uranyl acetate in maleate buffer (pH 4.7). The specimens were dehydrated in graded ethanol and embedded in epoxy resin. Ultrathin sections (70–80 nm) were picked up onto formvar carbon-coated grids, stained with lead citrate, and viewed in a 910 transmission electron microscope (Zeiss Elektronenmikroskopie, Oberkochen, Germany). Images of one CON, three OBE, and three T2D were included in this analysis.

### Statistical Analyses

Normally distributed data are given as mean and SD or SEM or otherwise as median (interquartile range). Nonnormally distributed data were log<sub>e</sub> transformed to achieve near-normal distribution. To enhance power and avoid type I errors, residual variances were allowed to be different between groups. Statistical analyses using one-way ANCOVA adjusted for age with Tukey correction for multiple comparisons were performed using SAS (version 9.4; SAS Institute, Cary, NC). Covariate-adjusted Spearman correlation analyses in obese patients with NASH with and without type 2 diabetes were adjusted for age, sex, and BMI. Significance of differences was set at *P* values  $\leq 0.05$ .

## RESULTS

### Individuals With Type 2 Diabetes and NASH Have Greater Hepatic Insulin Resistance Than Those Without Liver Disease

Despite good glycemic control, T2D were more hyperglycemic and older than OBE, so all analyses were adjusted for age. Both T2D and OBE had similar degrees of obesity (class III), fasting hyperinsulinemia, whole-body (*M* value) and adipose tissue insulin resistance,

and low-grade inflammation (hs-CRP) (Table 1). Hepatic insulin sensitivity index was decreased in T2D and tended to be lower in OBE ( $P = 0.08$ ) than in CON. In T2D, serum AST was higher than in CON and OBE, whereas FFA, triglycerides,  $\gamma$ -glutamyl transferase, ALT, and alkaline phosphatase were not different between all groups.

OBE and T2D had  $\sim 20$ -fold greater liver fat content. Lobular inflammation was present in 90% and 100% of OBE and T2D, ballooning grade  $\geq 1$  in all OBE and T2D, and fibrosis stage  $\geq 1$  in 63% and 53% of OBE and T2D, respectively (Supplementary Table 1).

### Individuals With Type 2 Diabetes and NASH Lose Adaptation of Hepatic Oxidative Capacity Independently of Markers of Mitochondrial Content

In liver tissue, maximum uncoupled mitochondrial respiration (i.e., maximum oxidative capacity) linked to TCA cycle was increased by 34% in OBE compared with CON (Fig. 1A). An increase of 59% was seen after normalization by CSA (Fig. 1C) but not by mtDNA (Fig. 1E and F). Of

note, isolated mitochondria showed 182% and 170% higher oxidative capacity linked to TCA cycle and  $\beta$ -oxidation, respectively, in OBE than in CON (Fig. 1G and H). In contrast, T2D exhibited comparable respiration rates as CON and even a trend toward 30% lower TCA-linked oxidative capacity than OBE (Fig. 1C) ( $P = 0.14$ ), while ETC complex II-linked respiration was 33% reduced versus OBE (Supplementary Fig. 1A).

Biomarkers of hepatic mitochondrial content were assessed from CSA, mtDNA copy number, and ETC complex. CSA (Fig. 2A) and ETC complexes I, III, IV, and V were comparable between groups (Supplementary Figure 1B–E), while mtDNA and complex II were lower in OBE than in CON (Fig. 2B and C).

### Individuals With Type 2 Diabetes and NASH Exhibit Higher Hepatic Oxidative Stress and Ultrastructural Changes

T2D presented with 96% greater hepatic  $H_2O_2$  emission than CON (Fig. 3A) and gradually higher  $H_2O_2$  emission than OBE ( $P = 0.15$ ). Hepatic catalase

activity (Fig. 3B) and TBARS (data not shown) were similar between all groups.

Hepatic content of the mitochondrial fusion marker MFN2 was lower in T2D and OBE compared with CON (Fig. 3E). There were differences neither in total OPA1 (Fig. 3C) nor in ratios of long OPA1 isoforms to total OPA1 (Fig. 3D) or of short OPA1 isoforms to total OPA1 (data not shown) between all groups. The marker of mitochondrial fission MFF was also comparable between groups (Fig. 3G), and no differences were found after normalization to mtDNA (data not shown).

The ER stress markers PERK and ATF4 were lower in the livers of OBE and T2D compared with those of CON (all  $P < 0.001$ ), while eIF2 was higher in OBE and T2D ( $P = 0.001$  and  $P < 0.001$  vs. CON, respectively), and phospho-eIF2 did not differ between groups (data not shown).

Transmission electron microscopy revealed mitochondrial swelling and megamitochondria in both OBE and T2D but not in CON (Fig. 2D–F). Also, autophagosomes

**Table 1—Participant characteristics**

Parameter	CON	OBE	T2D
Total N	14	30	15
Female sex	8	26	9
Age, years	40 $\pm$ 10	39 $\pm$ 10	49 $\pm$ 8*
BMI, kg/m <sup>2</sup>	25 $\pm$ 2	52 $\pm$ 9†	51 $\pm$ 7†
Fasting glucose, mg/dL	79 $\pm$ 7	87 $\pm$ 11†	139 $\pm$ 30*†
Fasting insulin, $\mu$ U/mL	8.5 (5.8; 12.0)	26.2 (17.5; 30.3)†	28.9 (18.2; 48.2)†
HbA <sub>1c</sub> , %	5.1 $\pm$ 1.3	5.1 $\pm$ 1.1	7.3 $\pm$ 1.2*†
HbA <sub>1c</sub> , mmol/mol	32 $\pm$ 14	32 $\pm$ 12	56 $\pm$ 13*†
Fasting FFA, $\mu$ mol/L	436 (358; 612)	639 (572; 781)	728 (555; 791)
Fasting triglycerides, mg/dL	126 $\pm$ 94	152 $\pm$ 60	165 $\pm$ 58
AdipoIR, AU	5,845 (3,110; 7,171)	16,737 (10,466; 19,155)†	16,690 (14,214; 32,298)†
hs-CRP, mg/dL	0.2 $\pm$ 0.2	1.3 $\pm$ 1.5†	1.1 $\pm$ 1.1†
ALT, units/L	28 $\pm$ 25	31 $\pm$ 18	36 $\pm$ 19
AST, units/L	30 $\pm$ 41	44 $\pm$ 32	51 $\pm$ 17*†
GGT, units/L	45 $\pm$ 86	30 $\pm$ 20	50 $\pm$ 27
AP, units/L	68 $\pm$ 45	80 $\pm$ 16	77 $\pm$ 19
M value, mg/kg BW/min	8.8 (6.5; 10.9)	2.3 (1.9; 3.0)†	1.5 (1.4; 1.8)†
HIS, dL * min * kg BW/mg/ $\mu$ U	6.0 (4.4; 9.4)	3.7 (3.1; 5.0)	3.0 (1.9; 3.9)†

Data are presented as mean  $\pm$  SD or median (quartile 1; quartile 3). AdipoIR, adipose tissue insulin resistance index (fasting FFA \* fasting insulin); AP, alkaline phosphatase; BW, body weight; GGT, serum  $\gamma$ -glutamyl transferase; HIS, hepatic insulin sensitivity index (100/[fasting EGP \* fasting insulin]). \* $P < 0.05$  vs. OBE from one-way ANCOVA. † $P < 0.05$  vs. CON from one-way ANCOVA.

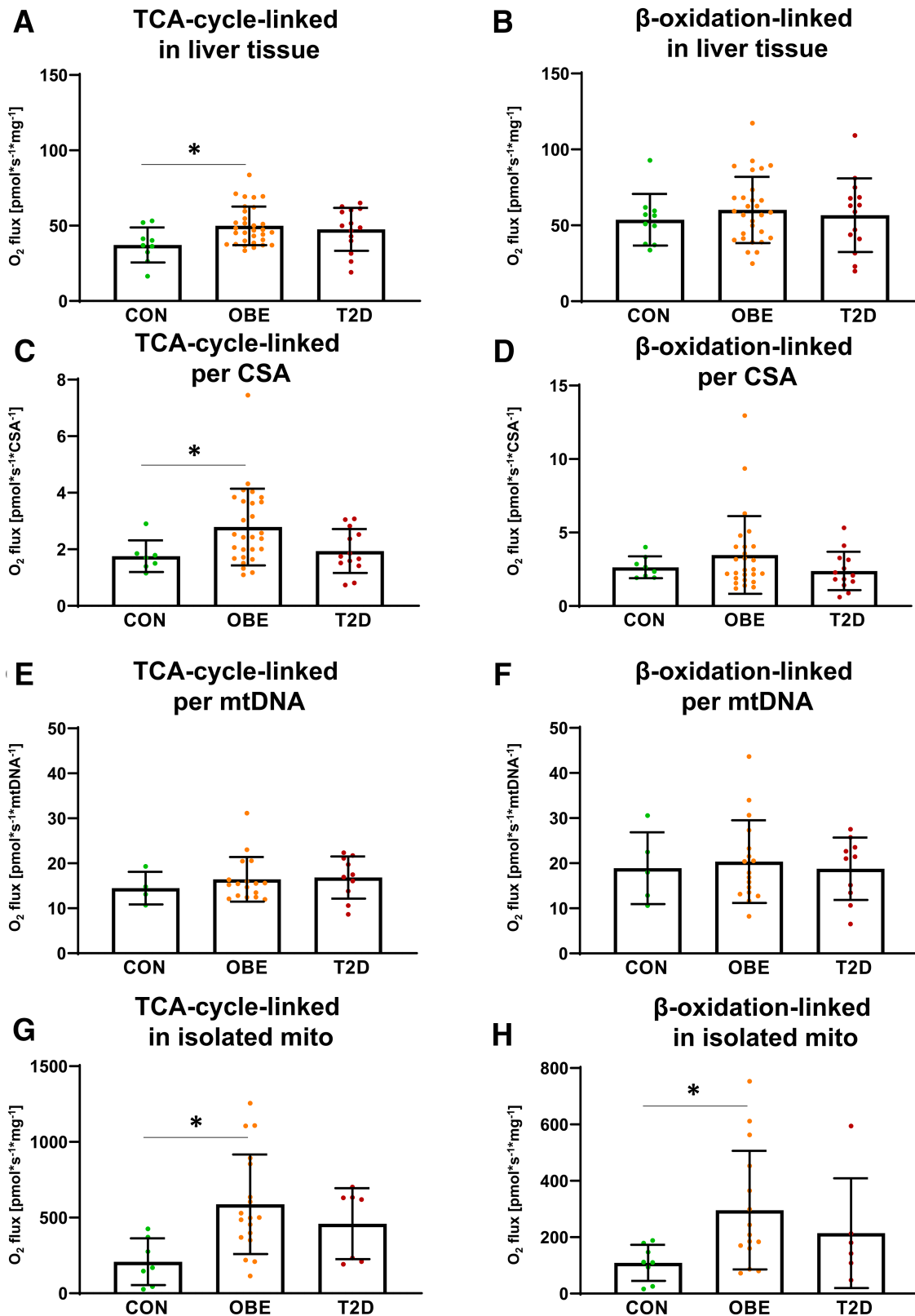


**Figure 1**—Maximum mitochondrial respiration. *A–H*: Maximum uncoupled mitochondrial respiration rates in liver tissue (*A* and *B*), liver tissue per mitochondrial content from CSA (*C* and *D*), liver tissue per mitochondrial content from mtDNA (*E* and *F*), and isolated mitochondria (mito) (*G* and *H*) in CON, OBE, and T2D. Data are mean ± SD. \**P* < 0.05 from one-way ANCOVA.

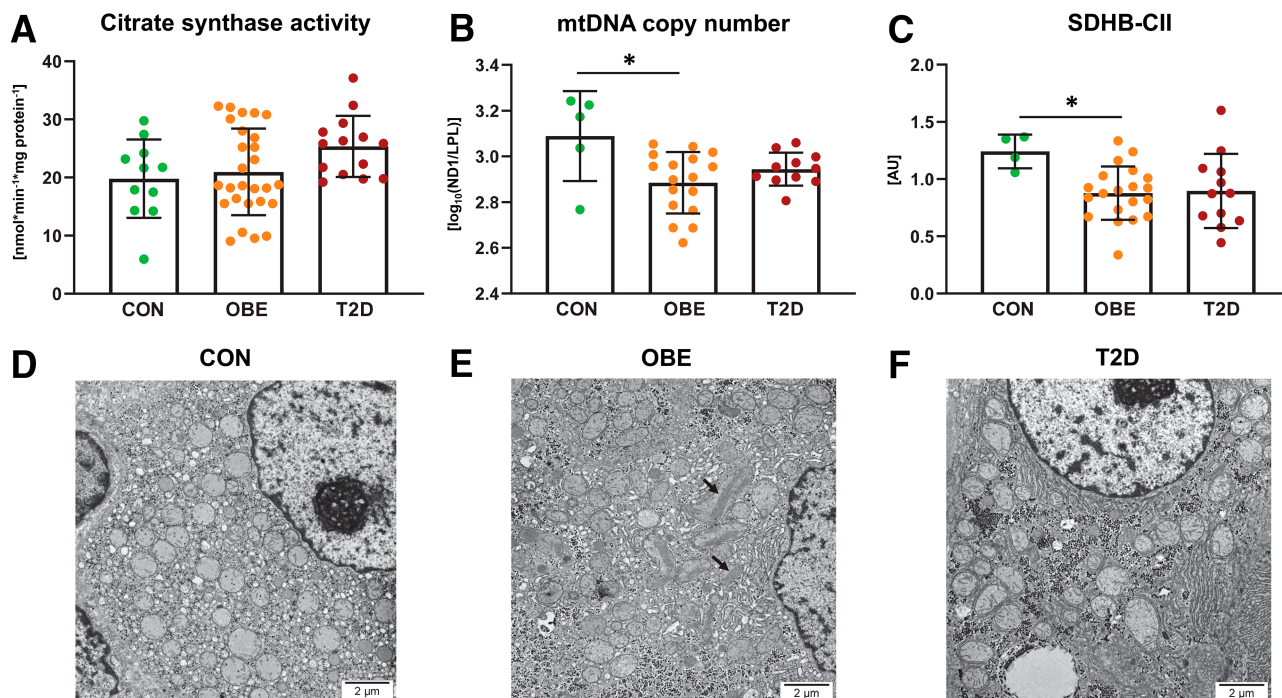


**Figure 2**—Hepatic mitochondrial content. *A–C*: Hepatic CSA (*A*), mtDNA copy number (*B*), and content of mitochondrial ETC complex II (*C*) in CON, OBE, and T2D. *D–F*: Representative images from transmission electron microscopy in hepatocytes from CON (*D*), OBE (*E*), and T2D (*F*). Paracrystalline inclusions are marked with an arrow. Data are mean  $\pm$  SD. \* $P < 0.05$  from one-way ANCOVA. SDHB, succinate dehydrogenase complex iron sulfur subunit B.

and inhomogeneous mitochondrial degeneration were found in both NASH groups, while only OBE also presented with paracrystalline inclusions.

### T2D Have Higher Hepatic Levels of Certain AGE Independent of Hepatic Oxidative Capacity

Hepatic methylglyoxal-derived hydroimidazolone isomer 1 (MG-1H) was higher in OBE compared with CON but not T2D, whereas fructosyl-lysine or fructosamine was higher in T2D compared with CON (Supplementary Table 2). Glyoxal-derived hydroimidazolone isomer 1, carboxyethyl-lysine, carboxymethyl-lysine, 3-nitrotyrosine, and argpyrimidine were not different between groups (Supplementary Table 2).

Plasma fructosyl-lysine was lower in OBE compared with CON, whereas plasma concentrations of other AGE were not different between groups (Supplementary Table 2).

Of note, Spearman correlation analysis across all patients with NASH with or without type 2 diabetes revealed a positive association between plasma MG-1H and fasting blood glucose and a negative association between hepatic

carboxymethyl-lysine and hepatic oxidative capacity (Supplementary Table 3).

### Association of Hepatic Insulin Resistance and Oxidative Stress With Impaired Mitochondrial Function in Patients With NASH

Covariate-adjusted Spearman correlation analysis, adjusted for age, sex, and BMI, revealed negative relationships of hepatic oxidative capacity with fasting blood glucose, fasting EGP, and hepatic TBARS (Supplementary Tables 3 and 4). Lower hepatic mitochondrial content, as assessed from ETC complexes II, III, and V, was related to increased hepatic  $H_2O_2$  emission (Supplementary Tables 3 and 4).

### Individuals With Hepatic Fibrosis Exhibit Loss of Adaptation of Hepatic Mitochondrial Function

To further analyze the impact of fibrosis itself, the NASH cohort was stratified into those without any histological fibrosis (F0) and those with any fibrosis (F1+) and then compared with CON. Despite similar ages, F1+ exhibited severe peripheral and adipose tissue insulin resistance when compared with CON and F0

(Supplementary Table 5). Mitochondrial content from hepatic CSA and mtDNA was increased in F1+ compared with F0 (Supplementary Fig. 2A and B). Hepatic mitochondrial oxidative capacity, with and without correction for CSA, was 67% and 28% lower in F1+ than in F0, respectively (Supplementary Fig. 2C and D). Hepatic content of ETC complexes I, III, IV, and V was lower in F1+ and F0 compared with CON (Supplementary Fig. 3).

Catalase activity in F1+ was increased compared with CON but reduced compared with F0 (Supplementary Fig. 4). Hepatic MG-1H was higher in F1+ than in CON, while other hepatic AGE were similar between groups (Supplementary Fig. 5). F1+ presented with lower MFN1, MFN2, FIS1, and MFF (Supplementary Fig. 6), as well as lower PARKIN and phospho-PARKIN, than CON (Supplementary Fig. 6).

### CONCLUSIONS

This study provides direct evidence from intraoperative human liver samples that 1) hepatic oxidative capacity is not upregulated in obese individuals with NASH and type 2 diabetes when

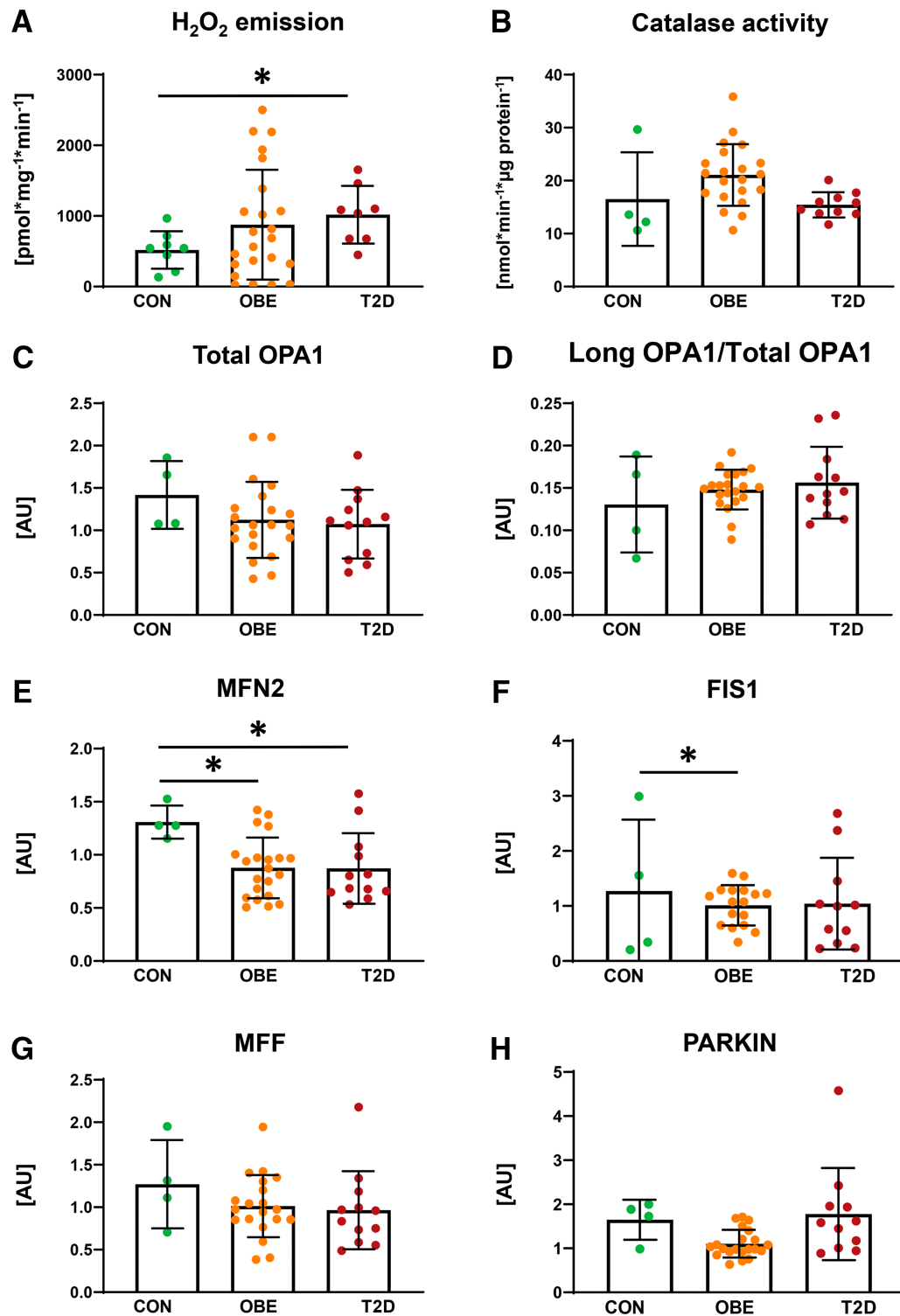


**Figure 3**—Oxidative stress and mitochondrial fusion and fission. *A–H*: Hepatic oxidative stress (H<sub>2</sub>O<sub>2</sub> emission) (*A*), antioxidant capacity (catalase activity) (*B*), total OPA1 content (*C*), ratio of long OPA1 isoforms to total OPA1 (*D*), MFN2 (*E*), fission markers FIS1 (*F*) and MFF (*G*), and PARKIN (*H*) in CON, OBE, and T2D. Data are mean ± SD. \**P* < 0.05 from one-way ANCOVA.

compared to obese nondiabetic individuals with NASH with type 2 diabetes, which is possibly related to hyperglycemia, and 2) early hepatic fibrosis is also linked to lower hepatic mitochondrial

oxidative capacity in the setting of enhanced AGE formation. These mechanisms may contribute to accelerated NAFLD progression and thereby determine worsening of its prognosis.

The strikingly higher mitochondrial oxidative capacity in obese individuals with NASH without type 2 diabetes, observed both in liver tissue and isolated liver mitochondria, is not explained by higher

mitochondrial content because mtDNA and ETC complex II were also reduced in this group, in agreement with our previous findings of upregulated oxidative capacity in obesity and hepatic steatosis (10). While mouse model studies also support the concept of increased mitochondrial respiration and TCA cycle activity in the early stages of NAFLD (26,27), in NASH models oxidative capacity and content are diminished (28), and with the development of hyperglycemia, ketogenesis is blunted (29). Thus, alterations in hepatic mitochondrial function represent a promising treatment target in models of NASH and hepatic fibrosis (30,31). Here, our findings suggest that loss of adaptation of hepatic mitochondrial function can be possibly explained by the presence of type 2 diabetes in individuals with NASH.

Of note, the decline of mitochondrial function does not seem to be related to insulin sensitivity, because both NASH groups exhibited comparable peripheral, hepatic, and adipose tissue insulin resistance. Surprisingly, oxidative capacity was not uniformly downregulated in all NASH livers. Higher lipid peroxidation and hyperglycemia independent of age, sex, and BMI were related to the reduction of hepatic oxidative capacity in NASH and type 2 diabetes. Hepatic mitochondrial  $H_2O_2$  release was increased in NASH with type 2 diabetes, which might reflect higher mitochondrial respiration, but not necessarily augmented ROS production, because TBARS and 3-nitro-tyrosine were not increased. Thus, our findings do not clearly support a contribution of hepatic oxidative stress to altered mitochondrial function. These findings are in contrast to evidence of unaltered muscle mitochondrial function in obesity (32). In addition, no changes in skeletal muscle mitochondrial respiration were found in the settings of lipid-induced ROS production (12) or of reduced lipid availability and lower ROS (33), suggesting organ-specific mitochondrial differences.

Mitochondrial dynamics have been shown to play a vital role in NAFLD development (34). The current study found reductions for the hepatic mitochondrial fusion marker MFN2 but not for the long OPA1 isoforms. Consequently, changes in hepatic mitochondrial fusion cannot explain the changes in oxidative phosphorylation. Similarly, mitochondrial ultrastructural alterations,

such as swelling, autophagosome activity, and matrix degeneration, were found in both NASH groups, in line with previous reports (8), independent of the presence of diabetes. Although activation of ER stress represents a possible link between mitochondrial dynamics and oxidative stress (35), we found no consistent evidence of elevated ER stress, because hepatic ATF4 and PERK were not increased in the NASH groups.

Aging may lead to impaired mitochondrial functionality in skeletal muscle (36,37) or altered mitochondrial morphology in the liver (38). However, the present findings were observed to be independent of age, because age adjustment did not affect the differences in the various measures of oxidative capacity. The finding of reduced mitochondrial functionality exclusively in combined NASH and type 2 diabetes, is in agreement with previous *in vivo* studies showing lower hepatic ATP concentrations in individuals with type 2 diabetes compared with obese individuals with a comparable degree of steatosis (7). Of note, recent longitudinal findings show doubling of hepatocellular lipids over the first 5 years after type 2 diabetes diagnosis, which is, however, paralleled by constant hepatic ATP content (6). These prospective data suggest failure of hepatic mitochondria to adapt to increased lipid availability in the setting of hyperglycemia and act as a bridge to the present cross-sectional analysis demonstrating the key role of type 2 diabetes in alterations in mitochondrial function in metabolic liver disease.

Of note, one other study using high-resolution respirometry in intraoperative liver biopsies found no differences in hepatic oxidative phosphorylation capacity between lean and obese individuals with or without type 2 diabetes (39). This is likely due to the very small cohort size, broad variation in liver fat content, and lower severity of disease (based on lower BMI and better glucometabolic control) compared with the current study. Likewise, the unchanged hepatic mitochondrial oxidation, derived from *in vivo*  $^{13}C$  magnetic resonance spectroscopy (40) or plasma 3-hydroxybutyrate measurements (41), may be the result of the inclusion of normal to overweight individuals without histological NAFLD staging or of the distinct

methods assessing other features of mitochondrial function.

In type 2 diabetes, hyperglycemia leads to formation of reactive dicarbonyls, such as glyoxal and methylglyoxal, which can cause protein and nucleic carbonylation and oxidative stress in hepatocytes, among other cells (42,43). This study showed that fasting blood glucose are negatively related to hepatic oxidative capacity, even after adjustments for age, sex, and BMI, underlining a role of hyperglycemia and glucotoxicity in impaired hepatic energy metabolism in NAFLD, as suggested previously for type 1 diabetes (44). Still, liver MG-1H was only increased in individuals with NASH without type 2 diabetes, whereas plasma MG-1H levels were higher in T2D versus OBE. Furthermore, a majority of hepatic and plasma AGE were comparable between groups. Thus, these findings do not support the concept that hepatic accumulation of AGE significantly contributes to enhanced oxidative stress or loss of mitochondrial adaptation in combined NASH and type 2 diabetes. Moreover, plasma MG-1H levels were closely related to fasting glycemia but not to findings on hepatic metabolism.

Hepatic fibrosis rather than inflammation is the key histological feature of NAFLD, defining the progression of disease, especially in insulin-resistant cohorts (45,46). Our findings suggest that the reduction of hepatic oxidative capacity is also key for hepatic fibrosis and loss of mitochondrial adaptation in NASH, because individuals exhibiting any degree of hepatic fibrosis had lower mitochondrial respiration rates than those showing no signs of fibrosis. These data further corroborate the relevance of hepatic mitochondria in the progression of NAFLD as well as in metabolic liver injury. Along these lines, individuals with any hepatic fibrosis (F1+) showed lower hepatic oxidative capacity as well as reduced hepatic catalase activity, possibly reflecting declining antioxidant defense capacity. Of note, hepatic MG-1H was increased in patients with fibrosis, suggesting that AGE formation related to failing mitochondria along with hyperglycemia might be associated with the progression of fibrosis. This is in agreement with the key role of ROS in the development of liver fibrosis (47). A possible contribution of hyperglycemia could not

be excluded here, because F1+ patients exhibited slightly increased HbA<sub>1c</sub>.

Several limitations must be mentioned, such as the low availability of intraoperative liver samples from healthy individuals without liver disease, which was due to ethical considerations. Of note, the small number of samples from this control group may explain some of the inconsistencies between expression data and functional data. In addition, the design of a cross-sectional study does not allow us to draw conclusions as to the time course of changes in the different groups. Nevertheless, the comprehensive phenotyping provides novel insights into pathophysiological alterations. Finally, the absence of a uniformly accepted reference method impedes the assessment of mitochondrial content.

Taken together, this study shows evidence of mitochondrial function decline as a common feature of patients with NASH who also have type 2 diabetes or hepatic fibrosis, representing different axes of hepatic metabolic disease. In type 2 diabetes, increased ROS formation along with hyperglycemia might be linked to derangements of mitochondrial respiration. Liver fibrosis is characterized by reductions in the content of ETC complexes and increased AGE formation. Thus, loss of mitochondrial adaptation seems to be closely related to metabolic liver disease and is possibly linked to its progression.

**Acknowledgments.** The authors thank all volunteers for their participation in this study and also thank Drs. Tomas Jelenik, Chrysi Koliaki, Daniel Markgraf, and Julia Szendroedi for contributions to clinical examination and/or laboratory assessments as well as Kai Tinnes, Myrko Esser, David Höhn, Andrea Sparla, Kerstin Förster, Fariba Zivehe, Jan-Marc Leonhard, Michelle Reina Do Fundo, Gisela Pansegrau, and Sandra Schmidt for excellent technical assistance.

**Funding.** This study was supported in part by the German Diabetes Center, which is funded by the Ministry of Culture and Science of the State of North Rhine-Westphalia and the German Federal Ministry of Health, through grants of the Federal Ministry for Research to the German Center for Diabetes Research (grant 2016). Parts of the study were also supported by grants from the European Funds for Regional Development (EFRE-0400191), EUREKA Eurostars-2 (E! 113230 DIA-PEP), the German Research Foundation (SFB 1116/2 and GRK 2576), the German Diabetes Association, and Schmutzler Stiftung.

The funding sources had no role in study design, data collection, data analysis, data interpretation, or writing of the report.

**Duality of Interest.** M.R. is on scientific advisory boards of Allergan, AstraZeneca, Bristol-Myers Squibb, Eli Lilly, Gilead Sciences, Inventiva, Intercept Pharma, Novartis, Novo Nordisk, Servier Laboratories, Target NRW, and Terra Firma and has received support for investigator-initiated studies from Boehringer Ingelheim, Nutricia/Danone, and Sanofi. No other potential conflicts of interest relevant to this article were reported.

**Author Contributions.** S.G. performed the clinical experiments, collected and analyzed data, and wrote, edited, and reviewed the manuscript. S.K. and T.S. performed clinical experiments and edited and reviewed the manuscript. D.P., L.M., B.D., M.W., M.Z., and A.S.R. performed laboratory analyses and edited and reviewed the manuscript. K.S. performed statistical analyses and edited and reviewed the manuscript. E.S. and M.S. performed bariatric surgery procedures and edited and reviewed the manuscript. I.E. performed liver histology and edited and reviewed the manuscript. J.W. performed transmission electron microscopic measurements and edited and reviewed the manuscript. T.F. and P.N. performed analysis of AGE and edited and reviewed the manuscript. M.R. initiated the investigation, designed and led the clinical experiments, and wrote, reviewed, and edited the manuscript. All authors gave final approval of the version to be published. M.R. is the guarantor of this work and, as such, had full access to all the data in the study and takes responsibility for the integrity of the data and the accuracy of the data analysis.

## References

- Ahlqvist E, Storm P, Käräjämäki A, et al. Novel subgroups of adult-onset diabetes and their association with outcomes: a data-driven cluster analysis of six variables. *Lancet Diabetes Endocrinol* 2018;6:361–369
- Zaharia OP, Strassburger K, Strom A, et al.; German Diabetes Study Group. Risk of diabetes-associated diseases in subgroups of patients with recent-onset diabetes: a 5-year follow-up study. *Lancet Diabetes Endocrinol* 2019;7:684–694
- Lomonaco R, Godinez Leiva E, Bril F, et al. Advanced liver fibrosis is common in patients with type 2 diabetes followed in the outpatient setting: the need for systematic screening. *Diabetes Care* 2021;44:399–406
- Rosso C, Kazankov K, Younes R, et al. Crosstalk between adipose tissue insulin resistance and liver macrophages in non-alcoholic fatty liver disease. *J Hepatol* 2019;71:1012–1021
- Roden M, Shulman GI. The integrative biology of type 2 diabetes. *Nature* 2019;576:51–60
- Kupriyanova Y, Zaharia OP, Bobrov P, et al.; GDS Group. Early changes in hepatic energy metabolism and lipid content in recent-onset type 1 and 2 diabetes mellitus. *J Hepatol* 2021;74:1028–1037
- Szendroedi J, Chmelik M, Schmid AI, et al. Abnormal hepatic energy homeostasis in type 2 diabetes. *Hepatology* 2009;50:1079–1086
- Sanyal AJ, Campbell-Sargent C, Mirshahi F, et al. Nonalcoholic steatohepatitis: association of

insulin resistance and mitochondrial abnormalities. *Gastroenterology* 2001;120:1183–1192

- Cortez-Pinto H, Chatham J, Chacko VP, Arnold C, Rashid A, Diehl AM. Alterations in liver ATP homeostasis in human nonalcoholic steatohepatitis: a pilot study. *JAMA* 1999;282:1659–1664
- Koliaki C, Szendroedi J, Kaul K, et al. Adaptation of hepatic mitochondrial function in humans with non-alcoholic fatty liver is lost in steatohepatitis. *Cell Metab* 2015;21:739–746
- Mota M, Banini BA, Cazanave SC, Sanyal AJ. Molecular mechanisms of lipotoxicity and glucotoxicity in nonalcoholic fatty liver disease. *Metabolism* 2016;65:1049–1061
- Anderson EJ, Lustig ME, Boyle KE, et al. Mitochondrial H<sub>2</sub>O<sub>2</sub> emission and cellular redox state link excess fat intake to insulin resistance in both rodents and humans. *J Clin Invest* 2009;119:573–581
- Jelenik T, Kaul K, Séquaris G, et al. Mechanisms of insulin resistance in primary and secondary nonalcoholic fatty liver. *Diabetes* 2017;66:2241–2253
- Satapati S, Kucejova B, Duarte JA, et al. Mitochondrial metabolism mediates oxidative stress and inflammation in fatty liver [published correction appears in *J Clin Invest* 2016;126:1605]. *J Clin Invest* 2015;125:4447–4462
- Brings S, Fleming T, Freichel M, Muckenthaler MU, Herzig S, Nawroth PP. Dicarboxyls and advanced glycation end-products in the development of diabetic complications and targets for intervention. *Int J Mol Sci* 2017;18:984
- Apostolopoulou M, Gordillo R, Koliaki C, et al. Specific hepatic sphingolipids relate to insulin resistance, oxidative stress, and inflammation in nonalcoholic steatohepatitis. *Diabetes Care* 2018;41:1235–1243
- Matsuda M, DeFronzo RA. Insulin sensitivity indices obtained from oral glucose tolerance testing: comparison with the euglycemic insulin clamp. *Diabetes Care* 1999;22:1462–1470
- Gastaldelli A, Gaggini M, DeFronzo RA. Role of adipose tissue insulin resistance in the natural history of type 2 diabetes: results from the San Antonio Metabolism Study. *Diabetes* 2017;66:815–822
- Bedossa P, Poitou C, Veyrie N, et al. Histopathological algorithm and scoring system for evaluation of liver lesions in morbidly obese patients. *Hepatology* 2012;56:1751–1759
- Rooney JP, Ryde IT, Sanders LH, et al. PCR based determination of mitochondrial DNA copy number in multiple species. *Methods Mol Biol* 2015;1241:23–38
- Nowotny B, Zahiragic L, Krog D, et al. Mechanisms underlying the onset of oral lipid-induced skeletal muscle insulin resistance in humans. *Diabetes* 2013;62:2240–2248
- Zhou T, Chang L, Luo Y, Zhou Y, Zhang J. Mst1 inhibition attenuates non-alcoholic fatty liver disease via reversing Parkin-related mitophagy [published correction appears in *Redox Biol* 2020;28:101299]. *Redox Biol* 2019;21:101120
- Gancheva S, Ouni M, Jelenik T, et al. Dynamic changes of muscle insulin sensitivity after metabolic surgery. *Nat Commun* 2019;10:4179
- Duvezin-Caubet S, Jagasia R, Wagener J, et al. Proteolytic processing of OPA1 links mitochondrial dysfunction to alterations in

- mitochondrial morphology. *J Biol Chem* 2006; 281:37972–37979
25. Rabbani N, Shaheen F, Anwar A, Masania J, Thornalley PJ. Assay of methylglyoxal-derived protein and nucleotide AGEs. *Biochem Soc Trans* 2014;42:511–517
26. Satapati S, Sunny NE, Kucejova B, et al. Elevated TCA cycle function in the pathology of diet-induced hepatic insulin resistance and fatty liver. *J Lipid Res* 2012;53:1080–1092
27. Patterson RE, Kalavalapalli S, Williams CM, et al. Lipotoxicity in steatohepatitis occurs despite an increase in tricarboxylic acid cycle activity. *Am J Physiol Endocrinol Metab* 2016;310:E484–E494
28. Krishnan A, Abdullah TS, Mounajjed T, et al. A longitudinal study of whole body, tissue, and cellular physiology in a mouse model of fibrosing NASH with high fidelity to the human condition. *Am J Physiol Gastrointest Liver Physiol* 2017; 312:G666–G680
29. Fletcher JA, Deja S, Satapati S, Fu X, Burgess SC, Browning JD. Impaired ketogenesis and increased acetyl-CoA oxidation promote hyperglycemia in human fatty liver. *JCI Insight* 2019; 5:e127737
30. Boland ML, Laker RC, Mather K, et al. Resolution of NASH and hepatic fibrosis by the GLP-1R/GcgR dual-agonist Cotadutide via modulating mitochondrial function and lipogenesis. *Nat Metab* 2020;2:413–431
31. Perry RJ, Kim T, Zhang X-M, et al. Reversal of hypertriglyceridemia, fatty liver disease, and insulin resistance by a liver-targeted mitochondrial uncoupler. *Cell Metab* 2013;18:740–748
32. Konopka AR, Asante A, Lanza IR, et al. Defects in mitochondrial efficiency and H<sub>2</sub>O<sub>2</sub> emissions in obese women are restored to a lean phenotype with aerobic exercise training. *Diabetes* 2015;64:2104–2115
33. Phielix E, Jelenik T, Nowotny P, Szendroedi J, Roden M. Reduction of non-esterified fatty acids improves insulin sensitivity and lowers oxidative stress, but fails to restore oxidative capacity in type 2 diabetes: a randomised clinical trial. *Diabetologia* 2014;57:572–581
34. Galloway CA, Lee H, Brookes PS, Yoon Y. Decreasing mitochondrial fission alleviates hepatic steatosis in a murine model of nonalcoholic fatty liver disease. *Am J Physiol Gastrointest Liver Physiol* 2014;307:G632–G641
35. Schneeberger M, Dietrich MO, Sebastián D, et al. Mitofusin 2 in POMC neurons connects ER stress with leptin resistance and energy imbalance. *Cell* 2013;155:172–187
36. Johnson ML, Robinson MM, Nair KS. Skeletal muscle aging and the mitochondrion. *Trends Endocrinol Metab* 2013;24:247–256
37. Coen PM, Jubrias SA, Distefano G, et al. Skeletal muscle mitochondrial energetics are associated with maximal aerobic capacity and walking speed in older adults. *J Gerontol A Biol Sci Med Sci* 2013;68:447–455
38. Sastre J, Pallardó FV, Plá R, et al. Aging of the liver: age-associated mitochondrial damage in intact hepatocytes. *Hepatology* 1996;24: 1199–1205
39. Lund MT, Kristensen M, Hansen M, et al. Hepatic mitochondrial oxidative phosphorylation is normal in obese patients with and without type 2 diabetes. *J Physiol* 2016;594:4351–4358
40. Petersen KF, Befroy DE, Dufour S, Rothman DL, Shulman GI. Assessment of hepatic mitochondrial oxidation and pyruvate cycling in NAFLD by (13)C magnetic resonance spectroscopy. *Cell Metab* 2016;24:167–171
41. Kotronen A, Seppälä-Lindroos A, Vehkavaara S, et al. Liver fat and lipid oxidation in humans. *Liver Int* 2009;29:1439–1446
42. Shangari N, Chan TS, Popovic M, O'Brien PJ. Glyoxal markedly compromises hepatocyte resistance to hydrogen peroxide. *Biochem Pharmacol* 2006;71:1610–1618
43. Thornalley PJ, Jahan I, Ng R. Suppression of the accumulation of triosephosphates and increased formation of methylglyoxal in human red blood cells during hyperglycaemia by thiamine in vitro. *J Biochem* 2001;129:543–549
44. Gancheva S, Bierwagen A, Kaul K, et al.; German Diabetes Study (GDS) Group. Variants in genes controlling oxidative metabolism contribute to lower hepatic ATP independent of liver fat content in type 1 diabetes. *Diabetes* 2016;65:1849–1857
45. McPherson S, Hardy T, Henderson E, Burt AD, Day CP, Anstee QM. Evidence of NAFLD progression from steatosis to fibrosing-steatohepatitis using paired biopsies: implications for prognosis and clinical management. *J Hepatol* 2015;62:1148–1155
46. Pais R, Charlotte F, Fedchuk L, et al.; LIDO Study Group. A systematic review of follow-up biopsies reveals disease progression in patients with non-alcoholic fatty liver. *J Hepatol* 2013;59:550–556
47. Parola M, Robino G. Oxidative stress-related molecules and liver fibrosis. *J Hepatol* 2001;35: 297–306

Copyright of Diabetes Care is the property of American Diabetes Association and its content may not be copied or emailed to multiple sites or posted to a listserv without the copyright holder's express written permission. However, users may print, download, or email articles for individual use.

# Cardiometabolic risk factor clustering in patients with deficient branched-chain amino acid catabolism: A case-control study

Sofiya Gancheva<sup>1,2,3</sup> | Daria Caspari<sup>4</sup> | Alessandra Bierwagen<sup>2,3</sup> |  
 Tomas Jelenik<sup>2,3</sup> | Sonia Caprio<sup>5</sup> | Nicola Santoro<sup>5,6</sup> | Maik Rothe<sup>2,3</sup> |  
 Daniel F. Markgraf<sup>2,3</sup> | Diran Herebian<sup>4</sup> | Jong-Hee Hwang<sup>2,3</sup> |  
 Soner Öner-Sieben<sup>4</sup> | Jasmin Mennenga<sup>4</sup> | Giovanni Pacini<sup>7</sup> | Eva Thimm<sup>4</sup> |  
 Andrea Schlune<sup>4</sup> | Thomas Meissner<sup>4</sup> | Stephan vom Dahl<sup>8</sup> | Dirk Klee<sup>9</sup> |  
 Ertan Mayatepek<sup>4</sup> | Michael Roden<sup>1,2,3</sup> | Regina Ensenuer<sup>4,10</sup>

<sup>1</sup>Division of Endocrinology and Diabetology, Medical Faculty, Heinrich Heine University Düsseldorf, Düsseldorf, Germany

<sup>2</sup>Institute for Clinical Diabetology, German Diabetes Center, Leibniz Institute for Diabetes Research, Heinrich Heine University Düsseldorf, Düsseldorf, Germany

<sup>3</sup>German Center for Diabetes Research (DZD e.V.), München-Neuherberg, Germany

<sup>4</sup>Department of General Pediatrics, Neonatology, and Pediatric Cardiology, University Children's Hospital, Medical Faculty, Heinrich Heine University Düsseldorf, Düsseldorf, Germany

<sup>5</sup>Department of Pediatrics, Magnetic Resonance Research Center, Yale University School of Medicine, New Haven, Connecticut

<sup>6</sup>Department of Medicine and Health Sciences, "V.Tiberio" University of Molise Via de Sanctis, Campobasso, Italy

<sup>7</sup>Metabolic Unit, CNR Institute of Neuroscience, Padova, Italy

<sup>8</sup>Division of Gastroenterology, Hepatology and Infectious Diseases, Medical Faculty, Heinrich Heine University Düsseldorf, Düsseldorf, Germany

<sup>9</sup>Department of Diagnostic and Interventional Radiology, Medical Faculty, Heinrich Heine University Düsseldorf, Düsseldorf, Germany

<sup>10</sup>Institute of Child Nutrition, Max Rubner-Institut, Karlsruhe, Germany

## Correspondence

Regina Ensenuer, Department of General Pediatrics, Neonatology, and Pediatric Cardiology, University Children's Hospital, Medical Faculty, Heinrich Heine University Düsseldorf, c/o

## Abstract

Classical organic acidemias (OAs) result from defective mitochondrial catabolism of branched-chain amino acids (BCAAs). Abnormal mitochondrial function relates to oxidative stress, ectopic lipids and insulin resistance (IR). We

**Abbreviations:** AHA, American Heart Association; ANOVA, analysis of variance; BCAA, branched-chain amino acid; CKD, chronic kidney disease; HCL, hepatocellular lipids; HDL, high-density lipoprotein; IDF, International Diabetes Federation; IMCL, intramyocellular lipids; IR, insulin resistance; IVA, isovaleric acidemia; MRS, magnetic resonance spectroscopy; MetS, metabolic syndrome; MMA, methylmalonic acidemia; MMA CBL, methylmalonic acidemia due to cobalamin-synthesis defect; mtDNA, mitochondrial DNA; OA, organic acidemia; OGIS, oral glucose insulin sensitivity; OGTT, oral glucose tolerance test; OxRedox, oxidation reduction; PA, propionic acidemia; PCr, phosphocreatine; Pi, inorganic phosphate; QUICKI, quantitative insulin-sensitivity check index; ROS, reactive oxygen species; SD, standard deviation; TBARS, thiobarbituric acid reactive substances; TCA, tricarboxylic acid; TE, echo time; TG, triglycerides; TR, repetition time.

Sofiya Gancheva and Daria Caspari share first-authorship.

Michael Roden and Regina Ensenuer share last-authorship.

This is an open access article under the terms of the Creative Commons Attribution-NonCommercial-NoDerivs License, which permits use and distribution in any medium, provided the original work is properly cited, the use is non-commercial and no modifications or adaptations are made.

© 2020 The Authors. *Journal of Inherited Metabolic Disease* published by John Wiley & Sons Ltd on behalf of SSIEM

Moorenstrasse 5, 40225 Düsseldorf,  
Germany.

Email: regina.ensenauer@med.uni-  
duesseldorf.de

Michael Roden, Division of Endocrinology  
and Diabetology, Medical Faculty,  
Heinrich Heine University, c/o Auf'm  
Hennekamp 62, 40225 Düsseldorf,  
Germany.

Email: michael.roden@ddz.de

**Communicating Editor:** Manuel Schiff

#### Funding information

Association of the Rhine-Westphalia;  
European Funds for Regional  
Development, Grant/Award Number:  
EFRE-0400191; German Federal Ministry  
of Education and Research (BMBF);  
German Center for Diabetes Research  
(DZD e.V.); Ministry of Culture and  
Science of the state North Rhine-  
Westphalia; German Federal Ministry of  
Health

investigated whether genetically impaired function of mitochondrial BCAA catabolism associates with cardiometabolic risk factors, altered liver and muscle energy metabolism, and IR. In this case-control study, 31 children and young adults with propionic acidemia (PA), methylmalonic acidemia (MMA) or isovaleric acidemia (IVA) were compared with 30 healthy young humans using comprehensive metabolic phenotyping including *in vivo*  $^{31}\text{P}/^1\text{H}$  magnetic resonance spectroscopy of liver and skeletal muscle. Among all OAs, patients with PA exhibited abdominal adiposity, IR, fasting hyperglycaemia and hypertriglyceridemia as well as increased liver fat accumulation, despite dietary energy intake within recommendations for age and sex. In contrast, patients with MMA more frequently featured higher energy intake than recommended and had a different phenotype including hepatomegaly and mildly lower skeletal muscle ATP content. In skeletal muscle of patients with PA, slightly lower inorganic phosphate levels were found. However, hepatic ATP and inorganic phosphate concentrations were not different between all OA patients and controls. In patients with IVA, no abnormalities were detected. Impaired BCAA catabolism in PA, but not in MMA or IVA, was associated with a previously unrecognised, metabolic syndrome-like phenotype with abdominal adiposity potentially resulting from ectopic lipid storage. These findings suggest the need for early cardiometabolic risk factor screening in PA.

#### KEYWORDS

cardiometabolic, fatty liver, metabolic syndrome, mitochondria, organic acidemia, oxidative stress

## 1 | INTRODUCTION

Organic acidemias (OAs) are caused by deficiencies of mitochondrial enzymes or co-factors involved in branched-chain amino acid (BCAA) catabolism.<sup>1</sup> Accumulation of specific metabolites in propionic acidemia (PA), isovaleric acidemia (IVA) and methylmalonic acidemia (MMA) have been suggested to exert 'toxic' effects.<sup>2-4</sup> Isolated MMA is due to either a deficiency of methylmalonyl-CoA mutase, a defect in the transport or synthesis of its cofactor adenosylcobalamin, or a deficiency of the enzyme methylmalonyl-CoA epimerase.<sup>5</sup> In PA and MMA, accumulation of propionyl-CoA inhibits tricarboxylic acid (TCA) and urea cycle activities,<sup>6</sup> but also methylmalonic acid and isovaleric acid may impair mitochondrial morphology and function.<sup>7-10</sup> In addition, the reduced flux of substrates to the TCA cycle may potentially contribute to abnormal mitochondrial functionality.

Abnormal mitochondrial function associates with the production of reactive oxygen species (ROS). Post-mortem studies in brain synaptosomes from patients with PA and MMA showed that methylmalonic acid, but not propionic acid, induces lipid peroxidation and protein

oxidative damage due to generation of ROS.<sup>11</sup> Exposure to isovaleric acid reduces  $\text{Na}^+/\text{K}^+$ -ATPase activity in synaptic membranes of rat cerebral cortex, likely via free radical formation.<sup>9</sup> Furthermore, fibroblasts of patients with PA exhibit increased ROS levels, possibly related to the severity of the gene defect.<sup>12</sup> In line, antioxidant treatment can reduce ROS levels and oxidative damage, at least in fibroblasts of patients with PA and in a mouse model of PA.<sup>13</sup>

Common states of insulin resistance (IR), such as obesity and type 2 diabetes, may be also characterised by abnormal mitochondrial function along with oxidative stress and ectopic lipid storage.<sup>14-16</sup> In both adults and children, accumulation of hepatocellular and intramyocellular lipids (HCL, IMCL) is tightly linked to IR.<sup>17,18</sup> Furthermore, metabolites such as free fatty acids and BCAAs can directly induce IR via substrate signaling in liver and skeletal muscle.<sup>17</sup> Thus, one might hypothesise that abnormal mitochondrial function – as observed in patients with branched-chain OAs – might lead to IR or its clinical correlates, the metabolic syndrome (MetS) or cardiometabolic risk factor clustering.<sup>19-22</sup> 'Cardiometabolic risk factor clustering' is defined by the accumulation of risk factors that are closely

related to type 2 diabetes and/or cardiovascular disease and, as recently recommended by the American Academy of Pediatrics, should be in the focus for clinical screening in children and adolescents.<sup>21</sup> Those risk factors comprise central obesity, fasting hyperglycaemia, dyslipidemia (high triglycerides [TG], low HDL cholesterol) and high blood pressure. Interestingly, patients with OAs feature a broad range of symptoms of largely unexplained origin<sup>23–26</sup> and those with PA and MMA appear to have less favourable long-term outcome compared to those with IVA.<sup>27–29</sup>

This study therefore examined whether genetically altered mitochondrial function due to abnormal BCAA catabolism is related to abnormal tissue-specific energy metabolism, IR and MetS by employing in-depth metabolic phenotyping with frequent sampling oral glucose tolerance tests (OGTT) and <sup>31</sup>P/<sup>1</sup>H magnetic resonance spectroscopy (MRS) of liver and skeletal muscle.

## 2 | MATERIALS AND METHODS

### 2.1 | Participants

This case-control study enrolled patients with OAs and sex-, age- and BMI-matched healthy humans serving as controls (ClinicalTrials.gov registration number NCT03917212). Inclusion criteria for patients were age  $\geq 5$  years and diagnosis of OA based on biochemical, enzymatic and/or molecular genetic findings. The group of patients with OAs consisted of 9 patients with PA, 6 with IVA, 10 with classical MMA and 6 with an adenosylcobalamin synthesis defect comprising cobalamin A or B deficiency (MMA CBL) based on cellular functional (CBL A/B  $n = 4$ ) or molecular genetic analyses (CBL B  $n = 2$ ). Exclusion criteria for the OGTT comprised chronic gastrointestinal diseases, which could affect glucose absorption, and allergy to red currant, which is contained in the glucose test solution. Patients regularly attending the Division of Metabolic Diseases at the University Children's Hospital Düsseldorf were recruited by phone call. In total, 31 patients with OAs, comprising 23 minors and 8 adults were included. Due to low compliance, OGTT and MRS measurement could not be performed in four and three patients with OAs, respectively (OGTT: PA  $n = 3$ , MMA  $n = 1$ ; MRS: PA  $n = 1$ , MMA  $n = 1$ , MMA CBL  $n = 1$ ). Additionally, OGTT and MRS data were not available from three and three patients with OAs, respectively, because of technical reasons (OGTT:  $n = 1$  patient each with PA, MMA and IVA; MRS:  $n = 1$  patient each with PA, MMA CBL and IVA).

Healthy individuals were recruited among the patients' siblings and through convenience sampling.

Twenty-one healthy children, five of whom were siblings of patients, and 9 healthy adults underwent MRS measurements as a control group. In addition, 11 healthy children of comparable age, sex and BMI from the Yale Pathophysiology of Type 2 Diabetes in Youth Study<sup>30</sup> and 5 healthy adults from a previous study at the German Diabetes Center<sup>31</sup> served as controls for OGTT data. The study was approved by the ethics board of the Medical Faculty, Heinrich Heine University Düsseldorf (protocol no. 3778). Written informed consent was obtained from the participants and their parents, when participants were minors.

### 2.2 | Study design

The study was performed at the Department of General Pediatrics, Neonatology and Pediatric Cardiology of the University Children's Hospital Düsseldorf for clinical and metabolic examinations and at the German Diabetes Center for MRS measurements. The study took place between August 2015 and February 2017. Participants were admitted to the hospital 1 day prior to measurements and advised to avoid exhaustive physical activity for two days before admission.

### 2.3 | Clinical parameters

Height and weight were measured in underwear, and BMI values of children and adolescents were plotted on age- and sex-specific percentiles<sup>32</sup> and defined as "high normal" if values were  $\geq 75$ th percentile.<sup>33</sup> Blood pressure and waist circumference were determined in children and adults and defined as high according to national and international reference values,<sup>34,35</sup> respectively. The absolute daily intake of energy and macronutrients of patients with PA and MMA, who were on a defined and controlled dietary therapy (Table 1), was extracted from their medical records. MetS was defined for children according to Goodman et al<sup>20</sup> and for adults according to Alberti et al<sup>19</sup> and diagnosed, if any 3 or more of 5 MetS components were present (Table S1). For children, MetS components were: fasting glucose  $\geq 100$  mg/dL, systolic blood pressure  $\geq 90$ th percentile and/or diastolic blood pressure  $\geq 90$ th percentile, waist circumference  $\geq 90$ th percentile, HDL cholesterol  $\leq 10$ th percentile and TG  $\geq 110$  mg/dL. For adults, MetS components were: fasting glucose  $\geq 100$  mg/dL; systolic blood pressure  $\geq 130$  mm Hg and/or diastolic blood pressure  $\geq 85$  mm Hg; waist circumference  $\geq 94$  cm for men,  $\geq 80$  cm for women; HDL cholesterol  $< 40$  mg/dL in men,  $< 50$  mg/dL in women; TG  $\geq 150$  mg/dL.

**TABLE 1** Daily energy and macronutrient intake in patients with PA and MMA at the time of study

Disease	Age years	Weight kg	Sex	Protein g/kg d	Carbohydrate		Fat		Energy kcal/kg d	Age- and sex-specific recommendation for energy intake <sup>36 a</sup> kcal/kg d	
					g/kg d	% energy <sup>37</sup>	g/kg d	% energy <sup>37</sup>			
PA <sup>b</sup>	12	61.6	f	0.7	4.7	49.6	1.8	43.1	37.5	40.4	
	12	56.5	m	0.9	3.9	51.8	1.2	36.2	29.2	46.3	
	13	38.5	m	0.9	6.6	59.3	1.6	32.6	44.9	41.4	
	16	44.4	m	1.2	6.4	57.0	1.6	32.3	44.6	37.6	
	17	58.1	f	1.1	4.2	50.9	1.3	35.7	32.1	33.6	
	17	57.8	m	0.7	5.1	58.3	1.3	33.7	35.1	37.6	
	18	69.1	m	n/a <sup>c</sup>	n/a <sup>c</sup>	n/a <sup>c</sup>	n/a <sup>c</sup>	n/a <sup>c</sup>	n/a <sup>c</sup>	n/a <sup>c</sup>	37.6
	23	71.3	m	n/a <sup>c</sup>	n/a <sup>c</sup>	n/a <sup>c</sup>	n/a <sup>c</sup>	n/a <sup>c</sup>	n/a <sup>c</sup>	n/a <sup>c</sup>	33.9
MMA	6	20.0	f	1.0	10.1	59.4	2.6	34.7	68.1	64.7	
	9	43.5	m	1.0	6.7	58.0	1.7	33.4	46.1	58.0	
	10	35.0	m	0.9	8.0	58.6	2.1	34.9	54.6	46.3	
	11	30.8	f	0.8	10.3	67.8	1.8	26.9	59.4	40.4	
	11	29.2	m	1.2	11.6	57.8	3.2	36.2	80.1	46.3	
	12	38.9	f	0.8	6.0	57.5	1.6	34.8	40.8	40.4	
	12	43.0	m	0.9	7.6	58.3	2.0	34.8	51.9	46.3	
	14	42.2	f	0.8	6.6	58.6	1.7	34.3	45.2	35.2	
	14	50.6	f	0.7	n/a <sup>c</sup>	n/a <sup>c</sup>	n/a <sup>c</sup>	n/a <sup>c</sup>	39.5	35.2	
	19	50.0	f	0.9	5.8	53.8	1.8	37.9	43.1	31.4	

Abbreviations: MMA, methylmalonic acidemia; n/a, not available, PA, propionic acidemia.

<sup>a</sup>Guiding values based on lowest physical activity level (PAL) 1.4: absolute values were divided by reference body weights of the respective 50th percentile based on the German KiGGS study.<sup>32,38</sup>

<sup>b</sup>Data was available from 8 of 9 patients with PA.

<sup>c</sup>Patients did not follow a calculated dietary therapy.

## 2.4 | Oral glucose tolerance test

Eight hours prior to their first blood draw, all patients were given a standardised night meal (200 kcal) to prevent metabolic decompensation that may occur after prolonged fasting. Adults received 75 g glucose and children received 1.75 g/kg body weight glucose (Accu-Check O.G.T Dextrose, Roche Diagnostics, Mannheim, Germany) orally or through a feeding tube between 08:30 and 9:00 AM. Blood sampling was done before (0) and 30, 60 and 120 minutes after glucose intake. Fasting insulin sensitivity was assessed from the quantitative insulin-sensitivity check index, whereas dynamic insulin sensitivity was assessed from the oral glucose insulin sensitivity index (OGIS).<sup>39</sup> Insulin secretion was described by fasting beta-cell function, adaptation index, disposition index, ratio of change in C-peptide and glucose at 30 minutes ( $\Delta C_{p30}/\Delta G_{30}$ ), while insulin kinetics were assessed from hepatic insulin extraction.<sup>39</sup>

## 2.5 | Biochemical analyses

Glucose, total cholesterol, LDL and HDL cholesterol, glutamate-oxaloacetate transaminase, glutamate-pyruvate transaminase, gamma-glutamyl transferase, C-reactive protein, creatinine, uric acid and cystatin C were measured photometrically (Cobas 8000 c702 chemistry analyzer, Roche Diagnostics, Mannheim, Germany), and haemoglobin A1c was analysed by a turbidimetric inhibition immunoassay (Cobas 6000 c501 analyzer). For TG measurements, blood samples were drawn into a vial containing orlistat to prevent in vitro lipolysis and immediately chilled on ice for 30 minutes, as described.<sup>31</sup> Insulin and C-peptide were analysed by radioimmunoassays (Millipore, St. Charles, CO). Serum thiobarbituric acid reactive substances (TBARS), oxidation reduction (OxRedox) potential and antioxidative capacity were measured to estimate oxidative stress.<sup>40</sup> Details on the biochemical analyses of the Yale cohort were reported previously.<sup>30</sup>

**TABLE 2** Participants' clinical and biochemical characteristics, insulin sensitivity and secretion, liver and muscle energy metabolism according to disease group and respective control group

Parameter	PA	CON PA	MMA	CON MMA	MMA CBL A/B <sup>a</sup>	CON MMA CBL A/B	IVA	CON IVA
n	9	9	10	10	6	6	6	6
Sex (male)	6 (67)	6 (67)	4 (40)	4 (40)	5 (83)	5 (83)	2 (33)	2 (33)
Age (years)	15.7 ± 3.6	17.2 ± 4.0	11.8 ± 3.5	12.4 ± 3.9	14.8 ± 7.4	14.5 ± 7.7	19.0 ± 11.9	18.8 ± 11.2
BMI (kg/m <sup>2</sup> )	23.7 ± 3.7	20.4 ± 3.8	19.6 ± 2.7	19.2 ± 2.6	20.3 ± 4.0	19.7 ± 4.3	21.2 ± 6.8	21.3 ± 8.8
Overweight or high normal weight (≥P75) <sup>b</sup>	5 (56)	2 (22)	3 (30)	2 (20)	2 (33)	2 (33)	2 (33)	1 (17)
Normal weight <sup>c</sup>	4 (44)	7 (78)	7 (70)	7 (70)	4 (67)	4 (67)	4 (67)	4 (67)
Underweight <sup>d</sup>	0 (0)	0 (0)	0 (0)	1 (10)	0 (0)	0 (0)	0 (0)	1 (17)
Fasting glucose (mg/dL)	98.2 ± 19.1	84.4 ± 20.8	95.3 ± 12.4	92.8 ± 12.0	85.8 ± 13.7	85.8 ± 18.5	86.2 ± 7.7	85.1 ± 19.6
HOMA-IR (mg/dL)	3.4 ± 1.8	2.1 ± 1.8	3.2 ± 0.2	3.6 ± 1.0	2.1 ± 1.3	2.8 ± 1.7	1.0 ± 0.1	2.5 ± 2.0
QUICKI	0.4 ± 0.1	0.5 ± 0.1	0.4 ± 0.1	0.4 ± 0.0	0.4 ± 0.1	0.4 ± 0.1	0.5 ± 0.1	0.4 ± 0.1
Matsuda index	3.1 ± 2.0	8.0 ± 7.1	4.3 ± 3.4	2.3 ± 0.4	6.4 ± 4.8	5.5 ± 5.6	9.1 ± 6.0	7.1 ± 7.7
OGIS (mL min <sup>-1</sup> /m <sup>2</sup> )	<b>364 ± 83</b>	488 ± 83	403.4 ± 34.5	389.6 ± 36.9	408.8 ± 71.4	470.0 ± 75.9	421.3 ± 62.3	438.5 ± 106.5
Fasting beta-cell-function	170.8 ± 40.1	121.8 ± 64.5	234.4 ± 131.2	113.6 ± 39.2	154.8 ± 91.2	119.8 ± 57.4	80.9 ± 49.1	105.4 ± 23.6
ΔCp <sub>30</sub> /ΔG <sub>30</sub>	0.6 ± 0.4	1.0 ± 0.5	1.78 ± 1.05	0.70 ± 0.53	0.67 ± 0.22	0.85 ± 0.47	<b>0.38 ± 0.20</b>	0.75 ± 0.19
Adaptation index	0.4 ± 0.1	0.4 ± 0.2	0.6 ± 0.2	0.4 ± 0.1	0.4 ± 0.2	0.4 ± 0.1	0.3 ± 0.1	0.4 ± 0.1
Disposition index	2.9 ± 1.0	2.9 ± 1.5	3.4 ± 1.6	4.1 ± 0.8	2.3 ± 1.2	3.4 ± 1.3	2.4 ± 1.4	3.4 ± 1.8
Hepatic extraction (%)	58.5 ± 8.7	66.0 ± 7.8	<b>61.8 ± 6.7</b>	42.3 ± 5.3	61.0 ± 1.1	65.7 ± 9.0	69.2 ± 12.1	62.0 ± 14.2
Liver γ-ATP (mmol/L)	2.63 ± 0.58	2.61 ± 0.41	2.74 ± 0.42	2.96 ± 0.32	3.43 ± 1.77	3.88 ± 1.09	2.47 ± 0.48	2.88 ± 0.75
Liver Pi (mmol/L)	2.19 ± 0.60	1.53 ± 0.23	2.47 ± 0.55	2.14 ± 0.62	2.78 ± 1.45	2.70 ± 1.23	1.88 ± 0.50	2.09 ± 0.63
Muscle γ-ATP/TP	0.17 ± 0.01	0.16 ± 0.01	<b>0.16 ± 0.01</b>	0.17 ± 0.01	0.17 ± 0.03	0.17 ± 0.01	0.16 ± 0.01	0.16 ± 0.01
Muscle PCr/TP	0.78 ± 0.01	0.77 ± 0.03	0.76 ± 0.01	0.76 ± 0.01	0.77 ± 0.04	0.74 ± 0.02	0.76 ± 0.02	0.77 ± 0.02
Muscle Pi/TP	<b>0.06 ± 0.01</b>	0.07 ± 0.01	0.08 ± 0.01	0.07 ± 0.01	0.06 ± 0.02	0.09 ± 0.02	0.08 ± 0.01	0.07 ± 0.02

Note: Data are mean ± SD or n (%); unpaired Student's *t* test, Mann-Whitney *U* test or Fisher's exact test; bold value indicates statistical significance (*P* < .05 vs CON group). ATP, adenosine triphosphate; BMI, body mass index; CON, control; ΔCp<sub>30</sub>/ΔG<sub>30</sub>, early phase of C-peptide secretion function; HDL, high density lipoprotein; HOMA-IR, homeostatic model assessment insulin resistance; IVA, isovaleric acidemia; MMA, methylmalonic acidemia; MMA CBL, adenosylcobalamin synthesis defect; OGIS, oral glucose insulin sensitivity index; PA, propionic acidemia; PCr, phosphocreatine; Pi, inorganic phosphate; QUICKI, quantitative insulin-sensitivity check index; TP, total phosphorus. Fasting glucose was available in PA n = 6, MMA n = 9, MMA CBL n = 6, IVA n = 6 and respective matched controls. HOMA-IR, OGIS, QUICKI and Matsuda index were available in PA n = 5, MMA n = 7, MMA CBL n = 6, IVA n = 5 and respective matched controls. Fasting β-cell function, adaptation and disposition index were available in PA n = 5, MMA n = 7, MMA CBL n = 6, IVA n = 5 and respective matched controls. Hepatic insulin extraction was available in PA n = 4, MMA n = 4, MMA CBL n = 3, IVA n = 3 and respective matched controls. ΔCp<sub>30</sub>/ΔG<sub>30</sub> was available in PA n = 5, MMA n = 6, MMA CBL n = 3, IVA n = 5 and respective matched controls. Liver γATP and Pi were available in PA n = 4, MMA n = 5, MMA CBL n = 4, IVA n = 5 and respective matched controls. Muscle γATP/TP, PCr/TP and Pi/TP were available in PA n = 6, MMA n = 7, MMA CBL n = 3, IVA n = 5 and respective matched controls.

<sup>a</sup>Cobalamin A/B defect (n = 4), cobalamin B defect (n = 2).

<sup>b</sup>BMI ≥ 25 kg/m<sup>2</sup> (≥18 years) or BMI ≥ P75 (<18 years).<sup>33</sup>

<sup>c</sup>BMI 18.5-24.9 kg/m<sup>2</sup> (≥18 years) or BMI P3 ≤ P75 (<18 years).

<sup>d</sup>BMI < 18.5 kg/m<sup>2</sup> (≥18 years) or BMI < P3 (<18 years).<sup>32</sup>

## 2.6 | Liver ultrasound

All patients underwent liver ultrasound by experienced radiologists on an Aplio 400, Aplio XG, Xario (all from Canon Medical Systems, Neuss, Germany) or a S2000 (Siemens AG, Erlangen, Germany). For children, liver size was measured in the anterior axillary line and compared to standard percentiles.<sup>41</sup> Steatosis was defined by hyperechogenicity of liver tissue and increased posterior beam attenuation.

## 2.7 | Liver and skeletal muscle <sup>1</sup>H- and <sup>31</sup>P-MRS

Four hours prior to measurements, patients received a meal according to their dietary protocol, and controls were provided an age-appropriate meal of similar energy

content (280-460 kcal) to ensure comparable nutritional conditions. All measurements were performed in a 3-T magnet (Achieva, Philips Healthcare, Best, The Netherlands). IMCL was measured in vastus lateralis muscle by <sup>1</sup>H-MRS using the point resolved spectroscopy sequence from a localised volume of interest (VOI: 1 × 1 × 2 cm<sup>3</sup>) with a repetition time of 2000 ms and an echo time of 32 ms. The signal averages of non-water-suppressed and water-suppressed MRS were 16 and 96, respectively. Spectra were analysed using LCmodel with build-in eddy-current correction to obtain a measure of IMCL relative to tissue water content. HCL was measured with <sup>1</sup>H-MRS using the stimulated echo acquisition mode sequence. Briefly, non-water-suppressed spectra were acquired from a VOI of 3 × 3 × 2 cm<sup>3</sup> with water and fat peaks integrated using the jMRUI v4.0 software.

Liver and skeletal muscle ATP and inorganic phosphate (Pi) contents were measured using <sup>31</sup>P-MRS.<sup>42</sup>

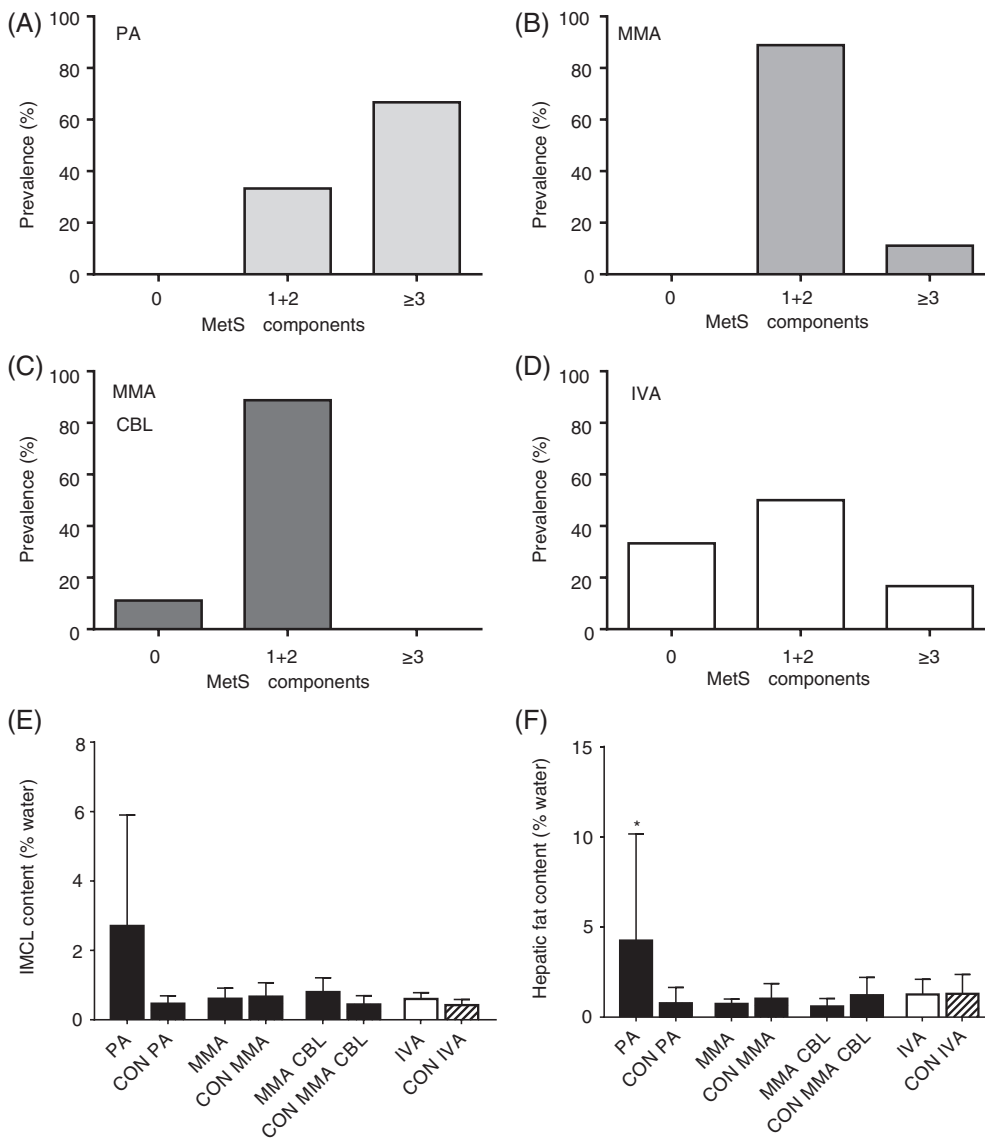


**FIGURE 1** Prevalence of the MetS and MetS components as well as ectopic lipid storage in patients with organic acidemias. A-D, Prevalence of MetS components, according to Goodman et al<sup>20</sup> for children and according to Alberti et al<sup>19</sup> for adults. E, Intramyocellular lipid content and F, hepatic fat content. Data are mean ± SD, \**P* < .05 vs CON. CON, control; IMCL, intramyocellular lipids; IVA, isovaleric acidemia; MetS, metabolic syndrome; MMA, methylmalonic acidemia; MMA CBL, adenosylcobalamin synthesis defect; PA, propionic acidemia. MetS components available in PA *n* = 7, MMA *n* = 10, MMA CBL *n* = 6, IVA *n* = 6 and respective controls. IMCL available in PA *n* = 7, MMA *n* = 5, MMA CBL *n* = 4, IVA *n* = 6 and respective controls. Liver fat content available in PA *n* = 7, MMA *n* = 6, MMA CBL *n* = 4, IVA *n* = 5 and respective controls

Briefly, liver spectra were acquired using a 14-cm circular  $^{31}\text{P}$  surface coil (Philips Healthcare), using the  $^1\text{H}$  body coil for  $^1\text{H}$ -decoupling and nuclear Overhauser enhancement. Localised liver spectra were obtained with VOIs of  $4 \times 4 \times 4 \text{ cm}^3$  for children and  $6 \times 6 \times 6 \text{ cm}^3$  for adolescents and adults. The resulting spectra were analysed for absolute concentration of ATP and Pi using the jMRUI v4.0 software. For skeletal muscle, a 6-cm surface coil (PulseTeq Ltd, Chobham, UK) was positioned on 2 cm into the medial head of the right gastrocnemius muscle. From non-localised  $^{31}\text{P}$  spectra, muscle ATP, Pi and phosphocreatine (PCr) content were assessed and expressed relative to the total phosphorus content (TP = ATP + Pi+PCr).

## 2.8 | Statistical analysis

Descriptive statistics are reported as mean  $\pm$  SD for normally distributed continuous variables and median (interquartile range) for skewed data. Categorical variables are expressed as proportions above defined cut-off values.<sup>19,20</sup> Differences between patients and respective control groups were analysed using unpaired Student's *t* test for normally distributed continuous variables and the Mann-Whitney *U* test for skewed data. Categorical data was compared

using Fisher's exact test. OGTT data was subjected to two-way analysis of variance (ANOVA) with repeated-measures factors time and group, and *P*-values were multiplicity-adjusted for each comparison using Sidak's multiple comparisons test. One-way ANOVA was used for comparisons between OA patient groups for serum TBARS, serum OxRedox potential and serum antioxidative capacity data.

## 3 | RESULTS

### 3.1 | Patients' clinical characteristics

Table 2 shows the clinical and biochemical data of the groups of patients with PA, MMA, MMA CBL, IVA and the control groups matched to the respective disease groups. The prevalence of MetS and its components for the various OA groups are presented in Figure 1A-D. MetS defined as having  $\geq 3$  of 5 components<sup>19,20</sup> was present in nearly 70% of patients with PA (Figure 1A). The majority had an increased waist circumference and dyslipidemia, 50% showed fasting hyperglycaemia ( $\geq 100 \text{ mg/dL}$ ),<sup>19,20</sup> and approximately one-third had arterial hypertension (Table 3). Four out of five PA patients with a severe phenotype (Table S1) presented with MetS and the same

**TABLE 3** Metabolic syndrome components in patients according to disease group

Parameter	PA	MMA	MMA CBL A/B <sup>a</sup>	IVA
Increased waist circumference <sup>b</sup>	5 (71)	4 (50)	2 (33)	2 (33)
Fasting glucose (mg/dL)	98.2 $\pm$ 19.1	95.3 $\pm$ 12.4	85.8 $\pm$ 13.7	86.2 $\pm$ 7.7
Fasting hyperglycaemia <sup>c</sup>	3 (50)	3 (33)	0 (0)	0 (0)
Triglycerides (mg/dL)	262.9 $\pm$ 234.4	263.6 $\pm$ 121.5	97.3 $\pm$ 24.8	75.0 $\pm$ 23.9
Hypertriglyceridemia <sup>d</sup>	4 (67)	9 (100)	0 (0)	0 (0)
HDL cholesterol (mg/dL)	33.3 $\pm$ 16.4	30.7 $\pm$ 7.7	48.6 $\pm$ 10.3	51.0 $\pm$ 15.3
Low HDL cholesterol <sup>e</sup>	5 (83)	8 (89)	1 (17)	2 (40)
SBP (mm Hg)	112.9 $\pm$ 23.5	110.5 $\pm$ 11.5	128.5 $\pm$ 28.6	116.8 $\pm$ 12.0
Systolic hypertension <sup>f</sup>	2 (29)	4 (40)	4 (67)	2 (33)
DBP (mm Hg)	68.4 $\pm$ 16.7	69.4 $\pm$ 10.8	78.3 $\pm$ 29.9	63.2 $\pm$ 7.3
Diastolic hypertension <sup>g</sup>	2 (29)	3 (30)	3 (50)	0 (0)

Note: Data are mean  $\pm$  SD or n (%). DBP, diastolic blood pressure; HDL, high density lipoprotein; IVA, isovaleric acidemia; MMA, methylmalonic acidemia; MMA CBL, adenosylcobalamin synthesis defect; PA, propionic acidemia; SBP, systolic blood pressure. **Respective reference values for healthy children are given in the table legend.** Reference values established in populations of German or European children were used for HDL cholesterol ( $\leq \text{P10}$ ) and TG.<sup>43</sup> Weight circumference was available in PA n = 7, MMA n = 8, MMA CBL n = 6, IVA n = 6. Triglycerides were available in PA n = 6, MMA n = 9, MMA CBL n = 6, IVA n = 5. Fasting glucose was available in PA n = 6, MMA n = 9, MMA CBL n = 6, IVA n = 6. Systolic and diastolic blood pressure was available in PA n = 7, MMA n = 10, MMA CBL n = 6, IVA n = 6.

<sup>a</sup>Cobalamin A/B defect (n = 4), cobalamin B defect (n = 2).

<sup>b</sup> $\geq 94 \text{ cm}$  for males ( $\geq 16$  years),  $\geq 80 \text{ cm}$  for females ( $\geq 16$  years)<sup>19</sup> or  $\geq \text{P90}$  ( $< 16$  years, according to age, sex, race/ethnicity).<sup>20</sup>

<sup>c</sup>Elevated  $\geq 100 \text{ mg/dL}$ .<sup>19,20</sup>

<sup>d</sup>Elevated  $\geq 150 \text{ mg/dL}$  ( $\geq 16$  years)<sup>19</sup> or  $\geq 110 \text{ mg/dL}$  ( $< 16$  years).<sup>20</sup>

<sup>e</sup>Decreased  $< 40 \text{ mg/dL}$  for males ( $\geq 16$  years),  $< 50 \text{ mg/dL}$  for females ( $\geq 16$  years)<sup>19</sup> or  $\leq \text{P10}$  ( $< 16$  years, according to sex and race).<sup>20</sup>

<sup>f</sup>Systolic hypertension  $\geq 130 \text{ mm Hg}$  ( $\geq 16$  years)<sup>19</sup> or  $\geq \text{P90}$  ( $< 16$  years, according to age, sex, height).<sup>20</sup>

<sup>g</sup>Diastolic hypertension  $\geq 85 \text{ mm Hg}$  ( $\geq 16$  years)<sup>19</sup> or  $\geq \text{P90}$  ( $< 16$  years, according to age, sex, height).<sup>20</sup>

proportion of them exhibited pre-diabetes or overt type 2 diabetes. Dyslipidemia was found in the majority and hypertension in more than one-third of patients with MMA (Table 3). Chronic kidney disease (CKD) stage  $\geq$ G3b<sup>44</sup> was present in 89% of patients with MMA (Table S1). But even upon exclusion of hypertension and hypertriglyceridemia, which are also features of CKD,<sup>44</sup> 60% of patients with MMA still showed 2 to 3 MetS components (Table S1). Conversely, no patient with MMA CBL fulfilled the criteria for MetS (Figure 1C and Table S1), but systolic and/or diastolic hypertension was present in 83%, with only one of these patients having CKD stage  $\geq$ G3b.

### 3.2 | Dietary factors

Individual daily energy and macronutrient intake by the calculated dietary treatment prescribed for patients with PA or MMA are presented in Table 1. Compared to age- and sex-specific recommendations for energy intake,<sup>36</sup> only 33% of patients with PA but 80% of patients with MMA were above the recommended energy intakes. Percentages of energy from fat and carbohydrates were within standard recommendations (30%-35% and >50%, respectively)<sup>37</sup> in the vast majority of patients of either group.

### 3.3 | Glucose metabolism

During OGTT, blood glucose concentrations were markedly higher at 60 and 120 minutes in patients with PA, but lower at 60 minutes in patients with MMA as compared to the respective controls (Figure 2A,B). No differences were found for patients with MMA CBL or IVA (Figure 2C,D). Although fasting insulin sensitivity was not different, OGIS was lower in patients with PA than in controls (Table 2). Hepatic insulin extraction was higher in patients with MMA, and  $\Delta$ Cp<sub>30</sub>/ $\Delta$ G<sub>30</sub> was lower in patients with IVA, compared to the respective controls.

### 3.4 | Skeletal muscle energy metabolism

Compared to controls, IMCL in the gastrocnemius muscle was not different for all OA groups (Figure 1E). Patients with MMA had slightly lower ATP ( $P < .05$ ), while patients with PA featured slightly lower Pi compared to respective controls ( $P < .05$ ) (Table 2). Muscle phosphocreatine content was comparable between patients with OAs and their controls (Table 2).

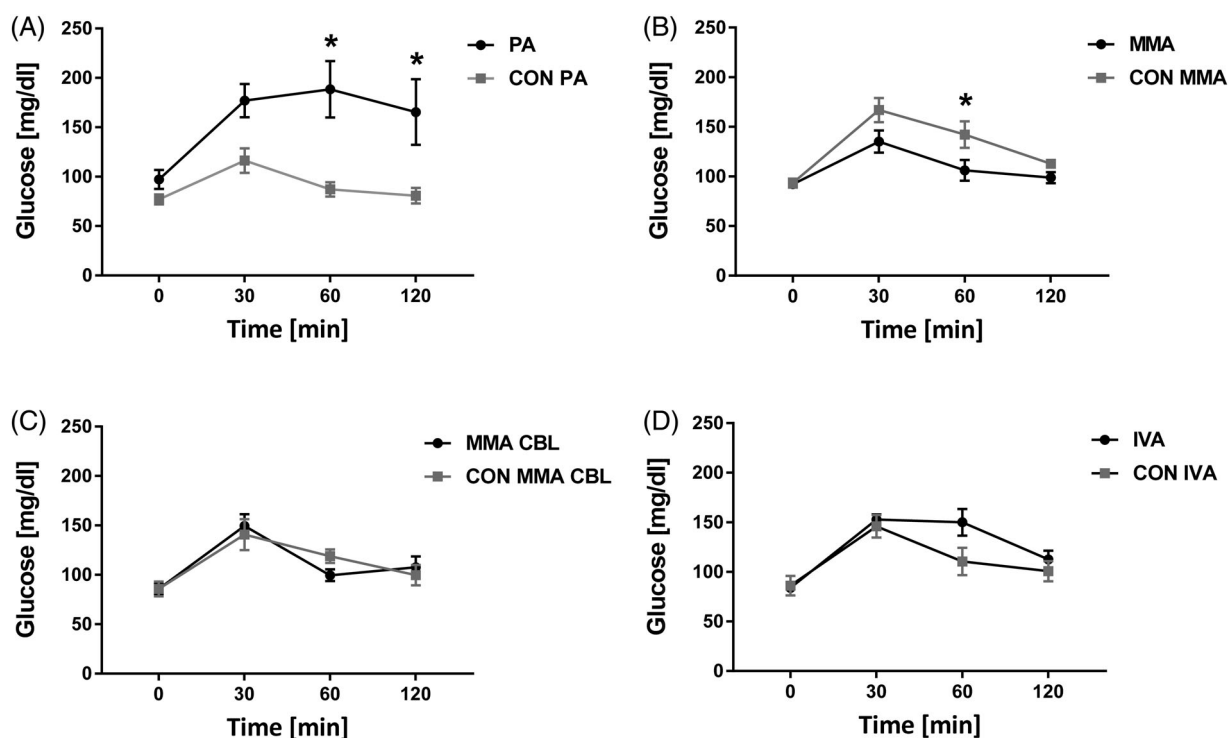


**FIGURE 2** Blood glucose concentrations during an oral glucose tolerance test in patients with organic acidemias and controls. A, PA  $n = 5$ ; B, MMA  $n = 8$ ; C, MMA CBL  $n = 6$  and D, IVA  $n = 5$ . Data are mean  $\pm$  SD, \* $P < .05$  vs CON. CON, control; IVA, isovaleric acidemia; MMA, methylmalonic acidemia; MMA CBL, adenosylcobalamin synthesis defect; PA, propionic acidemia

### 3.5 | Liver morphology and energy metabolism

Sonographically, 75% (6/8) of PA, 80% (8/10) of MMA and 67% (4/6) of MMA CBL patients, but only 17% (1/6) of IVA patients featured hepatomegaly. While ultrasound suggested hepatic steatosis in 38% (3/8) of patients with PA and in one patient each of the remaining groups (data not shown), two-thirds of them showing hepatomegaly, <sup>1</sup>H-MRS identified only one patient with PA and steatosis who also had hepatomegaly (Figure 1F). Of note, neither hepatic ATP nor Pi differed between OA patients and matched controls (Table 2).

### 3.6 | Oxidative stress

Serum OxRedox potential (Figure S1A) and serum antioxidative capacity (Figure S1B) were similar in all patient groups. Serum TBARS were higher in patients with PA than in those with IVA (Figure S1C).

## 4 | DISCUSSION

Here, we provide evidence for cardiometabolic risk factor clustering in PA from a case-control study in patients with branched-chain OAs. Patients with PA exhibit an accumulation of cardiometabolic risk factors with abdominal adiposity and IR already at young age predisposing for MetS. On the other hand, the data suggest an early adaptation of substrate fluxes in all OAs as shown by unchanged hepatic ATP levels.

### 4.1 | Propionic acidemia

Among all patients with OAs, children and adolescents with PA showed the highest percentage of abdominal obesity, postprandial hyperglycaemia, dyslipidemia, and hepatic fat accumulation, along with lower insulin sensitivity. Their daily macronutrient and energy intake was medically controlled by a calculated diet as an essential feature of treatment.<sup>27</sup> Of note, PA participants did not follow a more calorie-dense diet compared to standard recommendations,<sup>36</sup> and both carbohydrate and fat contents were within recommended ranges (Table 1). Therefore, the specific metabolic phenotype of patients with PA is not related to an excessive dietary energy intake.<sup>36</sup> Furthermore, the family histories did not identify a higher incidence and/or other causes of dyslipidemia or MetS in first-degree relatives of our participants, and thus, this factor likely does not affect the findings.

Compared to other OAs and controls, high proportions of children and adolescents with PA exhibited fasting hyperglycaemia and dyslipidemia consistent with the definitions of paediatric MetS or cardiometabolic risk factor clustering.<sup>21</sup> Indeed, early-onset PA may manifest with abnormal glucose metabolism, even mimicking diabetic ketoacidosis,<sup>45,46</sup> although patients have so far not been reported to present with forms of diabetes.<sup>47,48</sup> Patients with PA also showed lower insulin sensitivity, which tightly associates with MetS, cardiometabolic risk and ultimately type 2 diabetes, potentially manifesting in childhood or adolescence. In our study, nearly 70% of children and adolescents with PA presented with MetS and the remaining approximately 30% had at least one MetS component.<sup>20</sup> This seems markedly higher than the prevalence of MetS ranging from 1% to 11% in European children aged 2 to 11 years<sup>49</sup> and approximately 30% in obese children and adolescents.<sup>50</sup> Consequently, early screening for MetS components in childhood appears to be of clinical relevance for this group of patients. Notably, the severity of the PA phenotype seems to relate to the prevalence of MetS or pre-diabetes/type 2 diabetes, suggesting a previously unrecognised link between PA and impairment of glucose and lipid metabolism. The strongly increased prevalence of paediatric MetS or cardiometabolic risk factor clustering in PA may further support the hypothesis that severe mitochondrial derangements can indeed lead to abnormalities of glucose and lipid metabolism, as suggested for other mitochondriopathies such as Friedreich's ataxia<sup>51</sup> or mitochondrial abnormalities in first-degree relatives of type 2 diabetes patients.<sup>52</sup> A higher frequency of cardiovascular insults in patients with PA has so far not been described.

Defective mitochondrial catabolism in PA also results in accumulation of propionyl-CoA-related metabolites, potentially leading to hyperammonemia through inhibition of N-acetylglutamate synthetase and inhibition of energy metabolism.<sup>53</sup> This leads to mitochondrial abnormalities including reductions in mitochondrial (mt)DNA, expression of respiratory chain complexes and oxidative phosphorylation in skeletal muscle as reported for PA patients.<sup>54</sup> In the present study, patients with PA showed altered muscle energy metabolism based on mildly reduced Pi levels, further confirming mitochondrial abnormalities in PA using non-invasive in vivo MRS measurements.

### 4.2 | MMA and MMA CBL

In contrast to the identified metabolic alterations in PA, patients with MMA had even lower post-glucose challenge glycaemia accompanied by altered hepatic insulin kinetics,

but no changes in fasting glucose, insulin sensitivity or secretion. Alterations in glucose regulation have been reported in infants and young children with MMA mimicking diabetic ketoacidosis.<sup>55,56</sup> Overall, 60% of patients with MMA in our study still had 2 to 3 cardiometabolic risk factors even after exclusion of high blood pressure and hypertriglyceridemia from the panel of MetS components for those with CKD  $\geq$  stage G3b.<sup>44</sup> On the other hand, none of the children and adolescents with MMA CBL fulfilled criteria for MetS, and the majority had 1 to 2 risk factors. These findings underscore the differences in clinical presentation between the two entities MMA and MMA CBL despite the common biochemical finding of methylmalonic acid accumulation.<sup>5</sup> Patients with MMA also exhibited hepatomegaly in accordance with previous findings.<sup>25</sup> However, hepatomegaly was present without hepatic steatosis and might be related to abnormal liver regeneration as suggested previously by increased alpha-fetoprotein concentrations in patients with MMA and PA.<sup>25</sup> In this regard, a recent report points to the development of liver neoplasms in patients with MMA as an emerging liver complication.<sup>57</sup> Also, hepatomegaly was not accompanied by changes in ATP concentrations, which differs from a previous study in rodents reporting abnormal hepatic mitochondrial morphology and lower hepatic mitochondrial complex IV activity from *ex vivo* measurements.<sup>7</sup> The present study measured hepatic ATP concentrations non-invasively *in vivo*, which reflects resting flux through ATP synthase.<sup>16</sup> Thus, the discrepancies might be due to the methodology and the distinct feature of mitochondrial function measured (*ex vivo* vs *in vivo*). Mechanisms of differences in steatosis development in PA and MMA have not been fully elucidated, but toxicity of specific metabolites, besides depletion of coenzyme A pools, might be responsible for the hepatic abnormalities.<sup>25</sup>

Interestingly, we detected slightly lower skeletal muscle ATP content in MMA compared to controls, suggestive of abnormal muscle energy metabolism. Of note, muscle hypotonia and decreased muscle mass have been reported as a common clinical feature.<sup>58</sup> Nevertheless, the absence of any alterations in insulin sensitivity is in line with the concept that abnormal muscle mitochondrial function does not generally relate to IR.<sup>16</sup>

### 4.3 | IVA and comparison with other OAs

In opposite to PA and MMA, patients with IVA did not show any relevant alterations in energy metabolism, insulin sensitivity or secretion. This possibly reflects the clinically milder and intermittent phenotype of IVA which results from a defect of leucine catabolism that is located more proximally in the BCAA catabolic pathway than the enzymes defective in PA and MMA. In contrast

to the impairment of acetyl-CoA formation in IVA, both PA and MMA enzyme defects lead to shortage of succinyl-CoA for TCA cycle function, possibly contributing to the more severe energy deficiency than in IVA.<sup>24,29</sup> It seems likely that mechanisms involving the defective pathways in OAs and/or disease-specific metabolites affect certain features of mitochondrial function, thereby exhibiting different degrees of mitochondrial toxicity and thus influencing metabolic phenotypes. Such differences, for example, in anaplerotic pathways, might underlie the changes in muscle energy metabolism of patients with PA and MMA, but not of those with IVA. Similarly, hepatomegaly was present in the majority of patients with PA, MMA and MMA CBL, potentially due to increased liver regeneration,<sup>25</sup> but only in one patient with IVA. Accumulation of propionate and propionyl CoA-derived metabolites both in PA and MMA and subsequent depletion of coenzyme A pools might possibly explain the observed hepatic involvement, based on data showing direct toxic effects on mitochondrial function in liver.<sup>59-61</sup>

While patients with PA exhibited increased cardiometabolic risk factor clustering and IR, there were no such changes in glucose metabolism or MetS in the groups of MMA and IVA participants. Whether severe impairment of TCA cycle function in PA might lead to reduced rates of glycolysis with lower acetyl-CoA flux to the TCA cycle and might possibly contribute to postprandial hyperglycaemia, remains speculative. However, cardiometabolic risk factor clustering in PA cannot be explained by more frequent anabolic therapies, as we found a nearly 9-fold increase in hospital admissions due to metabolic decompensations in our group of MMA patients compared to PA patients within the last 2 years prior to study.

### 4.4 | Strengths and limitations

This study has several limitations. The relatively small group size and wide spectrum of clinical presentation within this group of deeply phenotyped patients with OAs results in higher intragroup variation and decreases statistical power. Nevertheless, the group size of these patients with OAs as ultra rare conditions<sup>62</sup> and commonly functional limitations, which could hinder them from participating in research, is larger than in previous studies. The control groups were carefully recruited for each OA, but some variables (serum oxidative stress) are not available in the healthy children due to investigator consideration regarding blood sampling in minors (Figure S1). Also, some control participants were used from a study at a different site and time.<sup>30</sup> While acute effects of physical activity can be largely excluded for all

patients by the recommendation of refraining from exercising for 48 hours prior to admission and for another 24 hours before metabolic tests, habitual physical activity has not been formally assessed, and thereby a possible confounding effect of long-term exercise cannot be excluded. In addition, as 6 out of 9 participants with PA were young adults of 16 years of age and older, puberty may have affected the prevalence of IR in this cohort. All of these factors may introduce some variation and limit the generalisability of the results. On the other hand, our work offers novel data on in vivo organ energy metabolism in children and adolescents and can now serve as a basis for future studies in minors using repetitive measurements in prospective cohorts or intervention trials such as testing adjuvant treatment with antioxidants in PA.<sup>13</sup>

In conclusion, PA increases the risk of MetS and cardiometabolic risk factor clustering potentially suggesting that genetic mitochondrial derangements may contribute to the development of further metabolic abnormalities. Alterations in muscle energy metabolism of patients with PA or MMA might underlie or contribute to their IR and ectopic lipid accumulation. From a clinical perspective, these findings would suggest regular screening for cardiometabolic risk factor clustering particularly in patients with PA to prevent additional disease burden. Nevertheless, prospective studies are needed for identifying the longitudinal time course of alterations and testing treatment strategies addressing liver and muscle energy metabolism.

## ACKNOWLEDGMENTS

Part of this work is the basis for the doctoral thesis of Daria Caspari. The authors would like to thank Nora Schmitz, Tjark Engelhardt, Kateryna Fuks, Delphina Gomes, Thi Thu Thuy Nguyen and Anne-Kathrin Neugebauer from the Department of General Pediatrics, Neonatology, and Pediatric Cardiology, University Children's Hospital Dusseldorf, and Kai Tinnes, Myrko Esser and Andrea Nagel from the Institute for Clinical Diabetology, German Diabetes Center Dusseldorf for their excellent help with the experiments. The work of MR and SG was funded by a grant to the German Diabetes Center (DDZ) from the German Federal Ministry of Health and the Ministry of Culture and Science of the state North Rhine-Westphalia. M.R. also received funding by the German Center for Diabetes Research (DZD e.V.) from the German Federal Ministry of Education and Research (BMBF) and by the European Funds for Regional Development (EFRE-0400191). This study was supported in part by a grant of the Association of the Rhine-Westphalia paediatricians and paediatric surgeons.

## CONFLICT OF INTEREST

The authors declare no conflicts of interest.

## AUTHOR CONTRIBUTIONS

S.G. and D.C. collected and analyzed analysed data and wrote the manuscript, A.B. researched and analyzed analysed data, T.J., N.S. and S.C. collected data, Ma.R. collected and researched data, G.P. calculated indices of insulin sensitivity and beta cell function, D.M. and D.H. collected and analyzed analysed data, J-H.H. reviewed and edited the manuscript, S.Ö., J.M., S.v.D., D.K., A.S., E.T., T.M. and E.M. collected data, R.E. and M.R. designed the study, researched data and reviewed and edited the manuscript. All authors reviewed and approved the final manuscript. R.E. and M.R. are the guarantors of the work and, as such, had full access to all the data in the study and take responsibility for the integrity of the data and the accuracy of the data analysis.

## REFERENCES

- Baumgartner MR, Horster F, Dionisi-Vici C, et al. Proposed guidelines for the diagnosis and management of methylmalonic and propionic acidemia. *Orphanet J Rare Dis*. 2014;9:130.
- Ando T, Rasmussen K, Nyhan WL, Donnell GN, Barnes ND. Propionic acidemia in patients with ketotic hyperglycinemia. *J Pediatr*. 1971;78:827-832.
- Oberholzer VG, Levin B, Burgess EA, Young WF. Methylmalonic aciduria. An inborn error of metabolism leading to chronic metabolic acidosis. *Arch Dis Child*. 1967;42:492-504.
- Tanaka K, Budd MA, Efron ML, Isselbacher KJ. Isovaleric acidemia: a new genetic defect of leucine metabolism. *Proc Natl Acad Sci U S A*. 1966;56:236-242.
- Fowler B, Leonard JV, Baumgartner MR. Causes of and diagnostic approach to methylmalonic acidurias. *J Inher Metab Dis*. 2008;31:350-360.
- Longo N, Price LB, Gappmaier E, et al. Anaplerotic therapy in propionic acidemia. *Mol Genet Metab*. 2017;122:51-59.
- Chandler RJ, Zervas PM, Shanske S, et al. Mitochondrial dysfunction in mut methylmalonic acidemia. *FASEB J*. 2009;23:1252-1261.
- de Keyzer Y, Valayannopoulos V, Benoist JF, et al. Multiple OXPHOS deficiency in the liver, kidney, heart, and skeletal muscle of patients with methylmalonic aciduria and propionic aciduria. *Pediatr Res*. 2009;66:91-95.
- Ribeiro CA, Balestro F, Grando V, Wajner M. Isovaleric acid reduces Na<sup>+</sup>, K<sup>+</sup>-ATPase activity in synaptic membranes from cerebral cortex of young rats. *Cell Mol Neurobiol*. 2007;27:529-540.
- Wajner M, Goodman SI. Disruption of mitochondrial homeostasis in organic acidurias: insights from human and animal studies. *J Bioenerg Biomembr*. 2011;43:31-38.
- Fernandes CG, Borges CG, Seminotti B, et al. Experimental evidence that methylmalonic acid provokes oxidative damage and compromises antioxidant defenses in nerve terminal and striatum of young rats. *Cell Mol Neurobiol*. 2011;31:775-785.

12. Gallego-Villar L, Perez-Cerda C, Perez B, et al. Functional characterization of novel genotypes and cellular oxidative stress studies in propionic acidemia. *J Inherit Metab Dis*. 2013; 36:731-740.
13. Rivera-Barahona A, Alonso-Barroso E, Perez B, Murphy MP, Richard E, Desviat LR. Treatment with antioxidants ameliorates oxidative damage in a mouse model of propionic acidemia. *Mol Genet Metab*. 2017;122:43-50.
14. Ebner S, Mange H, Langhof H, et al. Mitochondrial haplogroup T is associated with obesity in austrian juveniles and adults. *PLoS One*. 2015;10:e0135622.
15. Koliaki C, Szendroedi J, Kaul K, et al. Adaptation of hepatic mitochondrial function in humans with non-alcoholic fatty liver is lost in steatohepatitis. *Cell Metab*. 2015;21:739-746.
16. Szendroedi J, Phielix E, Roden M. The role of mitochondria in insulin resistance and type 2 diabetes mellitus. *Nat Rev Endocrinol*. 2011;8:92-103.
17. Gancheva S, Jelenik T, Alvarez-Hernandez E, Roden M. Interorgan Metabolic Crosstalk in Human Insulin Resistance. *Physiol Rev*. 2018;98:1371-1415.
18. Larson-Meyer DE, Newcomer BR, Ravussin E, et al. Intrahepatic and intramyocellular lipids are determinants of insulin resistance in prepubertal children. *Diabetologia*. 2011;54:869-875.
19. Alberti KG, Eckel RH, Grundy SM, et al. Harmonizing the metabolic syndrome: a joint interim statement of the International Diabetes Federation Task Force on Epidemiology and Prevention; National Heart, Lung, and Blood Institute; American Heart Association; World Heart Federation; International Atherosclerosis Society; and International Association for the Study of Obesity. *Circulation*. 2009;120:1640-1645.
20. Goodman E, Daniels SR, Meigs JB, Dolan LM. Instability in the Diagnosis of Metabolic Syndrome in Adolescents. *Circulation*. 2007;115:2316-2322.
21. Magge SN, Goodman E, Armstrong SC. The metabolic syndrome in children and adolescents: shifting the focus to cardiometabolic risk factor clustering. *Pediatrics*. 2017;140:e20171603.
22. Zimmet P, Alberti KG, Kaufman F, et al. The metabolic syndrome in children and adolescents – an IDF consensus report. *Pediatr Diabetes*. 2007;8:299-306.
23. Cappuccio G, Atwal PS, Donti TR, et al. Expansion of the phenotypic spectrum of propionic acidemia with isolated elevated propionylcarnitine. *JIMD Rep*. 2016;35:33-37.
24. Ensenaer R, Vockley J, Willard JM, et al. A common mutation is associated with a mild, potentially asymptomatic phenotype in patients with isovaleric acidemia diagnosed by newborn screening. *Am J Hum Genet*. 2004;75:1136-1142.
25. Imbard A, Garcia Segarra N, Tardieu M, et al. Long-term liver disease in methylmalonic and propionic acidemias. *Mol Genet Metab*. 2018;123:433-440.
26. Kolker S, Garcia-Cazorla A, Valayannopoulos V, et al. The phenotypic spectrum of organic acidurias and urea cycle disorders. Part 1: the initial presentation. *J Inherit Metab Dis*. 2015a;38:1041-1057.
27. Fraser JL, Venditti CP. Methylmalonic and propionic acidemias: clinical management update. *Curr Opin Pediatr*. 2016;28:682-693.
28. Grunert SC, Mullerleile S, De Silva L, et al. Propionic acidemia: clinical course and outcome in 55 pediatric and adolescent patients. *Orphanet J Rare Dis*. 2013;8:6.
29. Grunert SC, Wendel U, Lindner M, et al. Clinical and neurocognitive outcome in symptomatic isovaleric acidemia. *Orphanet J Rare Dis*. 2012;7:9.
30. Giannini C, Weiss R, Cali A, et al. Evidence for early defects in insulin sensitivity and secretion before the onset of glucose dysregulation in obese youths: a longitudinal study. *Diabetes*. 2012;61:606-614.
31. Gancheva S, Koliaki C, Bierwagen A, et al. Effects of intranasal insulin on hepatic fat accumulation and energy metabolism in humans. *Diabetes*. 2015;64:1966-1975.
32. Rosario AS, Kurth BM, Stolzenberg H, Ellert U, Neuhauser H. Body mass index percentiles for children and adolescents in Germany based on a nationally representative sample (KiGGS 2003–2006). *Eur J Clin Nutr*. 2010;64:341-349.
33. Riedel C, von Kries R, Buyken AE, et al. Overweight in adolescence can be predicted at age 6 years: a CART analysis in German cohorts. *PLoS One*. 2014;9:e93581.
34. McCarthy HD, Jarrett KV, Crawley HF. The development of waist circumference percentiles in British children aged 5.0–16.9 y. *Eur J Clin Nutr*. 2001;55:902-907.
35. Neuhauser HK, Thamm M, Ellert U, Hense HW, Rosario AS. Blood pressure percentiles by age and height from non-overweight children and adolescents in Germany. *Pediatrics*. 2011;127(124):e978-e188.
36. DGE. New reference values for energy intake. *Ann Nutr Metab*. 2015;66:219-223.
37. Prentice A, Branca F, Decsi T, et al. Energy and nutrient dietary reference values for children in Europe: methodological approaches and current nutritional recommendations. *Br J Nutr*. 2004;92(Suppl 2):S83-S146.
38. Kurth BM, Kamtsiuris P, Holling H, et al. The challenge of comprehensively mapping children's health in a nation-wide health survey: design of the German KiGGS-Study. *BMC Public Health*. 2008;8:196.
39. Pacini G. Assessment of insulin sensitivity from steady-state and dynamic tests. In: Roden M, ed. *Clinical Diabetes Research: Methods and Techniques*. Chichester, West Sussex: John Wiley & Sons, Ltd; 2007:27-41.
40. Jelenik T, Kaul K, Sequaris G, et al. Mechanisms of insulin resistance in primary and secondary nonalcoholic fatty liver. *Diabetes*. 2017;66:2241-2253.
41. Dittrich M, Milde S, Dinkel E, Baumann W, Weitzel D. Sonographic biometry of liver and spleen size in childhood. *Pediatr Radiol*. 1983;13:206-211.
42. Laufs A, Livingstone R, Nowotny B, et al. Quantitative liver 31P magnetic resonance spectroscopy at 3T on a clinical scanner. *Magn Reson Med*. 2014;71:1670-1675.
43. Dortschy R, Rosario AS, Scheidt-Nave C, et al. Bevölkerungsbezogene Verteilungswerte ausgewählter Laborparameter aus der Studie zur Gesundheit von Kindern und Jugendlichen in Deutschland (KiGGS). *Bevölkerungsbezogene Verteilungswerte ausgewählter Laborparameter aus der Studie zur Gesundheit von Kindern und Jugendlichen in Deutschland (KiGGS)*. Berlin, Germany: Robert Koch-Institut; 2009.
44. Ketteler M, Block GA, Evenepoel P, et al. Diagnosis, evaluation, prevention, and treatment of chronic kidney disease-mineral and bone disorder: synopsis of the kidney disease: improving global outcomes 2017 clinical practice guideline update. *Ann Intern Med*. 2018;168:422-430.

45. Dweikat IM, Naser EN, Abu Libdeh AI, et al. Propionic acidemia mimicking diabetic ketoacidosis. *Brain Dev.* 2011;33:428-431.
46. Joshi R, Phatarpekar A. Propionic acidemia presenting as diabetic ketoacidosis. *Indian Pediatr.* 2011;48:164-165.
47. Alfadhel M, Babiker A. Inborn errors of metabolism associated with hyperglycaemic ketoacidosis and diabetes mellitus: narrative review. *Sudanese Journal of Paediatrics.* 2018;18:10-23.
48. Vantyghem MC, Dobbelaere D, Mention K, Wemeau JL, Saudubray JM, Douillard C. Endocrine manifestations related to inherited metabolic diseases in adults. *Orphanet J Rare Dis.* 2012;7:11.
49. Ahrens W, Pigeot I, Pohlabein H, et al. Prevalence of overweight and obesity in European children below the age of 10. *International Journal of Obesity (2005).* 2014;38(suppl 2):S99-S107.
50. Friend A, Craig L, Turner S. The prevalence of metabolic syndrome in children: a systematic review of the literature. *Metab Syndr Relat Disord.* 2013;11:71-80.
51. Vorgerd M, Schols L, Hardt C, Ristow M, Eppelen JT, Zange J. Mitochondrial impairment of human muscle in Friedreich ataxia in vivo. *Neuromuscular Disorders.* 2000;10:430-435.
52. Befroy DE, Petersen KF, Dufour S, et al. Impaired mitochondrial substrate oxidation in muscle of insulin-resistant offspring of type 2 diabetic patients. *Diabetes.* 2007;56:1376-1381.
53. Gregersen N. The specific inhibition of the pyruvate dehydrogenase complex from pig kidney by propionyl-CoA and isovaleryl-Co-A. *Biochem Med.* 1981;26:20-27.
54. Schwab MA, Sauer SW, Okun JG, et al. Secondary mitochondrial dysfunction in propionic aciduria: a pathogenic role for endogenous mitochondrial toxins. *Biochem J.* 2006;398:107-112.
55. Dejkhamron P, Wejapikul K, Unachak K, Sawangareetrakul P, Tanpaiboon P, Wattanasirichaigoon D. Isolated methylmalonic acidemia with unusual presentation mimicking diabetic ketoacidosis. *Journal of Pediatric Endocrinology & Metabolism.* 2016;29:373-378.
56. Guven A, Cebeci N, Dursun A, Aktekin E, Baumgartner M, Fowler B. Methylmalonic acidemia mimicking diabetic ketoacidosis in an infant. *Pediatr Diabetes.* 2012;13:e22-e25.
57. Forny P, Hochuli M, Rahman Y, et al. Liver neoplasms in methylmalonic aciduria: An emerging complication. *J Inherit Metab Dis.* 2019;42:793-802.
58. Kolker S, Valayannopoulos V, Burlina AB, et al. The phenotypic spectrum of organic acidurias and urea cycle disorders. Part 2: the evolving clinical phenotype. *J Inherit Metab Dis.* 2015b;38:1059-1074.
59. Brass EP, Beyerinck RA. Effects of propionate and carnitine on the hepatic oxidation of short- and medium-chain-length fatty acids. *Biochem J.* 1988;250:819-825.
60. Kolker S, Schwab M, Horster F, et al. Methylmalonic acid, a biochemical hallmark of methylmalonic acidurias but no inhibitor of mitochondrial respiratory chain. *J Biol Chem.* 2003;278:47388-47393.
61. Matsushita T, Stumpf DA, Seliem M, Eguren LA, Chrislip K. Propionate mitochondrial toxicity in liver and skeletal muscle: acyl CoA levels. *Biochem Med Metab Biol.* 1991;45:244-253.
62. Almasi T, Guey LT, Lukacs C, Csetneki K, Voko Z, Zelei T. Systematic literature review and meta-analysis on the epidemiology of methylmalonic acidemia (MMA) with a focus on MMA caused by methylmalonyl-CoA mutase (mut) deficiency. *Orphanet J Rare Dis.* 2019;14:84.

## SUPPORTING INFORMATION

Additional supporting information may be found online in the Supporting Information section at the end of this article.

**How to cite this article:** Gancheva S, Caspari D, Bierwagen A, et al. Cardiometabolic risk factor clustering in patients with deficient branched-chain amino acid catabolism: A case-control study. *J Inherit Metab Dis.* 2020;43:981–993. <https://doi.org/10.1002/jimd.12231>

# Dynamic changes of muscle insulin sensitivity after metabolic surgery

Sofiya Gancheva<sup>1,2,3,11</sup>, Meriem Ouni <sup>3,4,11</sup>, Tomas Jelenik<sup>2,3</sup>, Chrysi Koliaki<sup>1,2,3,5</sup>, Julia Szendroedi<sup>1,2,3</sup>, Frederico G.S. Toledo<sup>6</sup>, Daniel F. Markgraf <sup>2,3</sup>, Dominik H. Pesta <sup>2,3</sup>, Lucia Mastrototaro<sup>2,3</sup>, Elisabetta De Filippo<sup>2,3</sup>, Christian Herder <sup>1,2,3</sup>, Markus Jähnert <sup>3,4</sup>, Jürgen Weiss<sup>3,7</sup>, Klaus Strassburger <sup>3,8</sup>, Matthias Schlensak<sup>9</sup>, Annette Schürmann <sup>3,4,10,12</sup> & Michael Roden <sup>1,2,3,12</sup>

The mechanisms underlying improved insulin sensitivity after surgically-induced weight loss are still unclear. We monitored skeletal muscle metabolism in obese individuals before and over 52 weeks after metabolic surgery. Initial weight loss occurs in parallel with a decrease in muscle oxidative capacity and respiratory control ratio. Persistent elevation of intramyocellular lipid intermediates, likely resulting from unrestrained adipose tissue lipolysis, accompanies the lack of rapid changes in insulin sensitivity. Simultaneously, alterations in skeletal muscle expression of genes involved in calcium/lipid metabolism and mitochondrial function associate with subsequent distinct DNA methylation patterns at 52 weeks after surgery. Thus, initial unfavorable metabolic changes including insulin resistance of adipose tissue and skeletal muscle precede epigenetic modifications of genes involved in muscle energy metabolism and the long-term improvement of insulin sensitivity.

<sup>1</sup>Division of Endocrinology and Diabetology, Medical Faculty, Heinrich-Heine University, Düsseldorf, Germany. <sup>2</sup>Institute for Clinical Diabetology, German Diabetes Center, Leibniz Center for Diabetes Research, Heinrich Heine University, Düsseldorf, Germany. <sup>3</sup>German Center for Diabetes Research (DZD e.V.), Neuherberg, Germany. <sup>4</sup>German Institute of Human Nutrition, Department of Experimental Diabetology, German Institute of Human Nutrition, Potsdam-Rehbruecke, Germany. <sup>5</sup>Laikon University Hospital, Athens, Greece. <sup>6</sup>Division of Endocrinology and Metabolism, Department of Medicine, University of Pittsburgh School of Medicine, Pittsburgh, PA, USA. <sup>7</sup>Institute for Clinical Biochemistry and Pathobiochemistry, German Diabetes Center, Leibniz Center for Diabetes Research, Heinrich Heine University, Düsseldorf, Germany. <sup>8</sup>Institute for Biometrics and Epidemiology, German Diabetes Center, Leibniz Center for Diabetes Research, Heinrich Heine University, Düsseldorf, Germany. <sup>9</sup>General Surgery Department, Schön Clinics, Düsseldorf, Germany. <sup>10</sup>Institute of Nutritional Sciences, University of Potsdam, Nuthetal, Germany. <sup>11</sup>These authors contributed equally: Sofiya Gancheva, Meriem Ouni. <sup>12</sup>These authors jointly supervised this work: Annette Schürmann, Michael Roden. Correspondence and requests for materials should be addressed to M.R. (email: [michael.roden@ddz.uni-duesseldorf.de](mailto:michael.roden@ddz.uni-duesseldorf.de))

Obesity-related insulin resistance associates with greater availability of free fatty acids (FFA), mitochondrial alterations and inflammation<sup>1,2</sup>. Bariatric or metabolic surgery improves whole body insulin sensitivity on the long term<sup>3</sup>, while the early metabolic effects and underlying mechanisms remain elusive<sup>4-7</sup>.

Recently, we showed upregulation of both hepatic mitochondrial capacity and oxidative stress in obese individuals undergoing metabolic surgery<sup>8</sup>. Skeletal muscle mainly accounts for whole body insulin sensitivity and insulin resistant humans generally exhibit reduced muscle mitochondrial capacity<sup>1,9</sup>. Recent studies convincingly demonstrated that diet-induced weight loss rapidly improves hepatic, but not muscle insulin resistance in humans<sup>10</sup>. Metabolic surgery seems to exert variable effects on mitochondria<sup>11,12</sup> and may also affect lipolysis<sup>4</sup> and intracellular lipid mediators, but the time course of effects on skeletal muscle is unclear.

Gastric bypass surgery results in epigenetic alterations, but current data on DNA methylation are conflicting<sup>13</sup>. Specifically, it is unknown whether epigenetic alterations occur very early or rather late after metabolic surgery and relate to gene expression.

Here, we report the distinct epigenetic, transcriptional and metabolic changes in skeletal muscle and their dynamic temporal relationships during the improvement of insulin sensitivity by combined monitoring of systemic and cellular metabolism after metabolic surgery in obese humans (OB) and by comparing the pattern with that of healthy nonobese humans (CON).

## Results

### Obese humans feature higher muscle lipid intermediates.

Before surgery (baseline), OB had higher fasting glucose, insulin, ultrasensitive CRP (usCRP), and interleukin-6 (IL-6) than CON (Table 1). Insulin sensitivity at the level of adipose tissue (Adipo-IR) assessed from fasting FFA and insulin concentrations (Fig. 1a) and of whole body/skeletal muscle (*M*-value assessed from hyperinsulinemic-euglycemic clamps at steady state insulinemia of  $58 \pm 14 \mu\text{U/ml}$ ; Fig. 1b) was lower in OB than in CON. OB also exhibited impaired metabolic flexibility ( $\Delta\text{RQ}$ ) (Table 1).

Insulin resistance can result from accumulation of lipid mediators such as diacylglycerol (DAG), which activate novel protein kinase C (PKC) isoforms, or from sphingolipids, which

stimulate c-Jun N-terminal kinase (JNK)<sup>14,15</sup>. In muscle of OB, specific DAG species were increased in membranes (18:1 18:1), lipid droplets (18:1 18:1, 18:2 18:2 and 16:0 18:1) and cytosol (16:0 18:1) (Fig. 1c, Suppl. Fig. 1a, c). Also, membrane/cytosolic ratios were markedly elevated for PKC $\epsilon$  ( $2.1 \pm 1.9 \text{ AU}$  vs  $0.4 \pm 0.3 \text{ AU}$  in CON,  $p = 0.01$  using unpaired *t*-test) and there was a trend towards higher PKC $\theta$  ( $p = 0.227$  using unpaired *t*-test, Fig. 1d) indicating enzyme activation. However, neither ceramides nor the Thr183/Tyr185-phosphorylated JNK ratios were different between OB and CON at baseline (Fig. 1e, f, Suppl. Fig. 1b, d, f). High-resolution respirometry of vastus lateralis muscle revealed lower maximal uncoupled respiration, when expressed per mg tissue (Fig. 2a), but unchanged citrate synthase activity (CSA) in OB (Fig. 2b). Electron transport chain (ETC) complexes II and III were lower in OB, while I, IV and V were similar in both groups (Fig. 2c, Suppl. Fig. 2a–d). Respiratory control ratio was lower, while leak control ratio was similar in OB vs. CON (Fig. 2d, e). Of note, muscle mitofusin-2 (Mfn2) and optic atrophy type 1 (Opa1) were lower in OB at baseline indicating reduced mitochondrial fusion activity (Suppl. Fig. 3a, b), while the autophagy markers, microtubule-associated protein 1A/1B-light chain 3 (LC3:  $0.42 \pm 0.59$  vs  $0.52 \pm 0.20$  in CON,  $p = 0.22$  using unpaired *t*-test) and p62 protein (sequestosome 1, p62:  $2.14 \pm 0.69$  vs  $1.50 \pm 0.58$  in CON,  $p = 0.17$  using unpaired *t*-test) were comparable between groups. Also, serum oxidation-reduction potential, antioxidant capacity and lipid peroxidation from thiobarbituric acid reactive species (TBARS) were not different (Fig. 2f, Table 1).

**Transient decrease in adipose tissue insulin sensitivity.** Forty-nine OB were studied at 2, 12, 24, and 52 weeks after surgery. Surprisingly, despite rapid weight loss of  $10 \pm 3 \text{ kg}$  ( $6.8 \pm 1.6\%$  of body weight) within 2 weeks, fasting glucose, insulin, C-peptide and inflammatory markers remained unchanged (Table 1). Insulin sensitivity did not improve in skeletal muscle and even deteriorated in adipose tissue (Fig. 1a, b). Of note, adipose tissue insulin resistance (Adipo-IR) remained  $\approx 3$ -fold higher also at 12 and 24 weeks after surgery. The latter abnormality results from a rise in plasma FFA concentrations by 56% at 2 weeks compared to baseline (Table 1). The higher Adipo-IR occurred in the presence of marked increases in several muscle membrane and lipid

**Table 1 Participants' characteristics**

Parameter	CON	OB Baseline	OB 2 w	OB 12 w	OB 24 w	OB 52 w
N (male)	14 (9)	49 (14)	42 (13)	47 (13)	49 (14)	45 (12)
Age (years)	40.3 $\pm$ 7.3	40.4 $\pm$ 10.0				
BMI (kg/m <sup>2</sup> )	24.5 $\pm$ 3.7	51.4 $\pm$ 7.1 <sup>#</sup>	47.6 $\pm$ 6.8*	42.3 $\pm$ 6.6*	38.5 $\pm$ 6.6*	33.9 $\pm$ 6.1*
Body weight (kg)	75 $\pm$ 18	154 $\pm$ 27 <sup>#</sup>	143 $\pm$ 25*	127 $\pm$ 24*	115 $\pm$ 23*	101 $\pm$ 20*
Change in BW (%)	-	-	6.8 $\pm$ 1.6	17.4 $\pm$ 3.7	25.3 $\pm$ 5.5	33.0 $\pm$ 7.7
Glucose (mg/dl)	79 $\pm$ 8	98 $\pm$ 24 <sup>#</sup>	93 $\pm$ 26	84 $\pm$ 17*	83 $\pm$ 14*	80 $\pm$ 12*
Insulin ( $\mu\text{U/ml}$ )	6(3;8)	21(18;29) <sup>#</sup>	22(14;29)	12(8;17)*	10(7;14)*	9(5;11)*
C-peptide (ng/ml)	1.3(1.1;1.6)	3.3(2.7;4.7) <sup>#</sup>	3.8(2.4;4.5)	2.4(1.9;3.0)*	2.1(1.6;2.9)*	1.8(1.5;2.5)*
HbA1c (%)	5.2 $\pm$ 0.3	5.8 $\pm$ 0.8*	5.5 $\pm$ 0.8*	5.3 $\pm$ 0.5*	5.2 $\pm$ 0.5*	5.2 $\pm$ 0.4*
FFA ( $\mu\text{mol/l}$ )	492 $\pm$ 275	676 $\pm$ 161	1057 $\pm$ 263*	699 $\pm$ 220	643 $\pm$ 239	527 $\pm$ 221*
Triglycerides (mg/dl)	843(69;133)	131(88;177)	113(86;139)	106(87;131)*	97(75;130)*	92(72;113)*
usCRP (mg/dl)	0.1(0.1;0.2)	0.7(0.4;1.3) <sup>#</sup>	0.6(0.4;1.2)	0.5(0.3;0.7)*	0.3(0.2;0.7)*	0.1(0.1;0.3)*
IL-6 (pg/ml)	1.0(0.9;1.3)	3.6(2.4;4.7) <sup>#</sup>	3.0(2.1;4.4)	2.4(2.2;3.5)*	2.6(2.1;4.1)	1.6(1.0;2.0)*
HMW-adiponectin (ng/ml)	3181 (2491;4362)	1432 (1065;3069) <sup>#</sup>	2170 (1327;3346)*	2708 (1579;3394)*	3217 (1766;4211)*	4025 (3118;6709)*
TBARS ( $\mu\text{mol/mg}$ protein)	13(11;19)	11(8;16)	11(7;18)	8(6;14)	8(6;10)*	6(5;8)*
Static ORP (mV)	169 $\pm$ 11	162 $\pm$ 12	160 $\pm$ 8	161 $\pm$ 9	161 $\pm$ 8	164 $\pm$ 10
REE (kcal/d)	1550 (1346;1686)	2240 (2026;2692) <sup>#</sup>	1928 (1756;2201)*	1875 (1641;2067)*	1804 (1580;2065)*	1815 (1558;2015)*
$\Delta\text{RQ}$	0.12 $\pm$ 0.03	0.07 $\pm$ 0.07 <sup>#</sup>	0.05 $\pm$ 0.08	0.08 $\pm$ 0.05	0.12 $\pm$ 0.06*	0.16 $\pm$ 0.08*

Mean  $\pm$  SD or median(q1;q3)

CON lean humans, OB obese humans, BW body weight, TG-triglycerides, FFA free fatty acids, HMW adiponectin-high molecular weight adiponectin, TBARS thiobarbituric acid reactive substances, ORP oxidation-reduction potential, REE resting energy expenditure, RQ respiratory quotient,  $\Delta\text{RQ}$  RQ<sub>clamp</sub> - RQ<sub>baseline</sub>

\* $p < 0.05$  vs OB baseline using CPM for repeated measures analysis, <sup>#</sup> $p < 0.05$  vs CON using unpaired two-tailed *t*-test

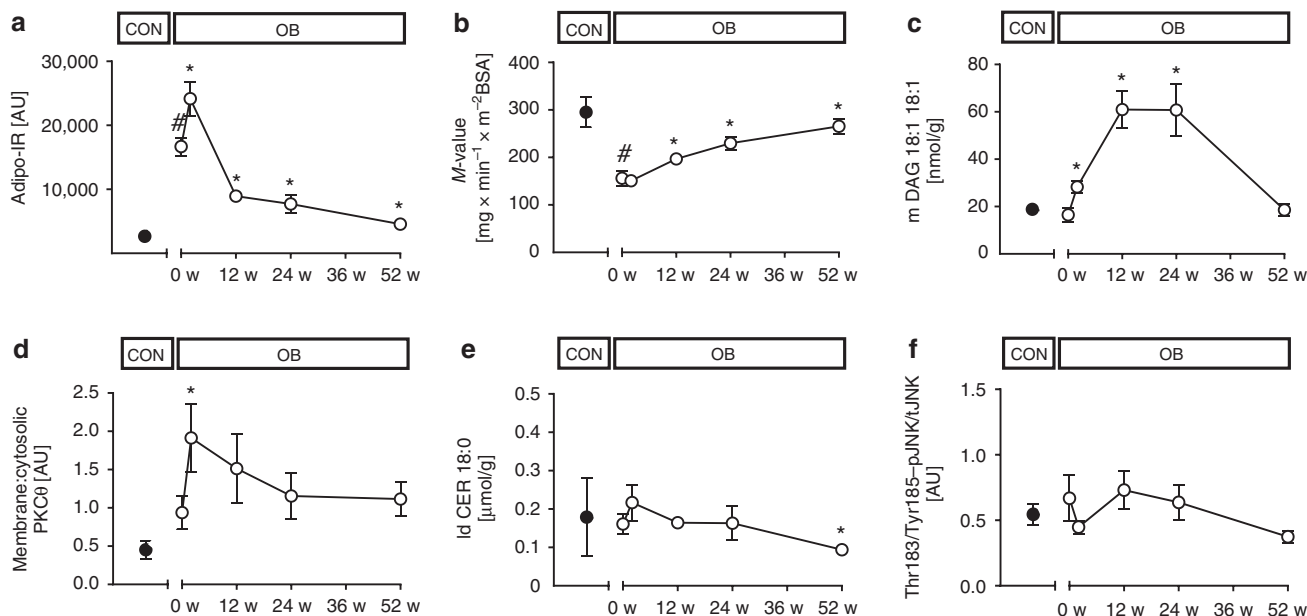


**Fig. 1** Time course of metabolic changes. Time course of changes in adipose tissue insulin sensitivity given as Adipo-IR (fasting free fatty acids\*fasting insulin) (CON *n* = 14, OB *n* = 47) **(a)**, muscle insulin sensitivity (CON *n* = 7, OB *n* = 43) **(b)**, muscle membrane DAG 18:1 18:1 (CON *n* = 4, OB *n* = 10) **(c)**, muscle protein kinase C (PKC)  $\theta$  activation (CON *n* = 4, OB *n* = 9) **(d)**, muscle lipid droplet ceramide 18:0 (CON *n* = 4, OB *n* = 10) **(e)** and muscle pJNK/tJNK ratio (CON *n* = 4, OB *n* = 8) **(f)** in obese (empty circles) and in nonobese humans at baseline (black circles). Mean  $\pm$  SEM, \**p* < 0.05 vs OB at baseline (0 w) using CPM for repeated measures analysis, #*p* < 0.05 vs CON using unpaired two-tailed *t*-test, CON nonobese humans, OB obese participants, BSA body surface area, LD lipid droplet, DAG diacylglycerol, pJNK phosphorylated c-Jun N-terminal kinase, tJNK total c-Jun N-terminal kinase

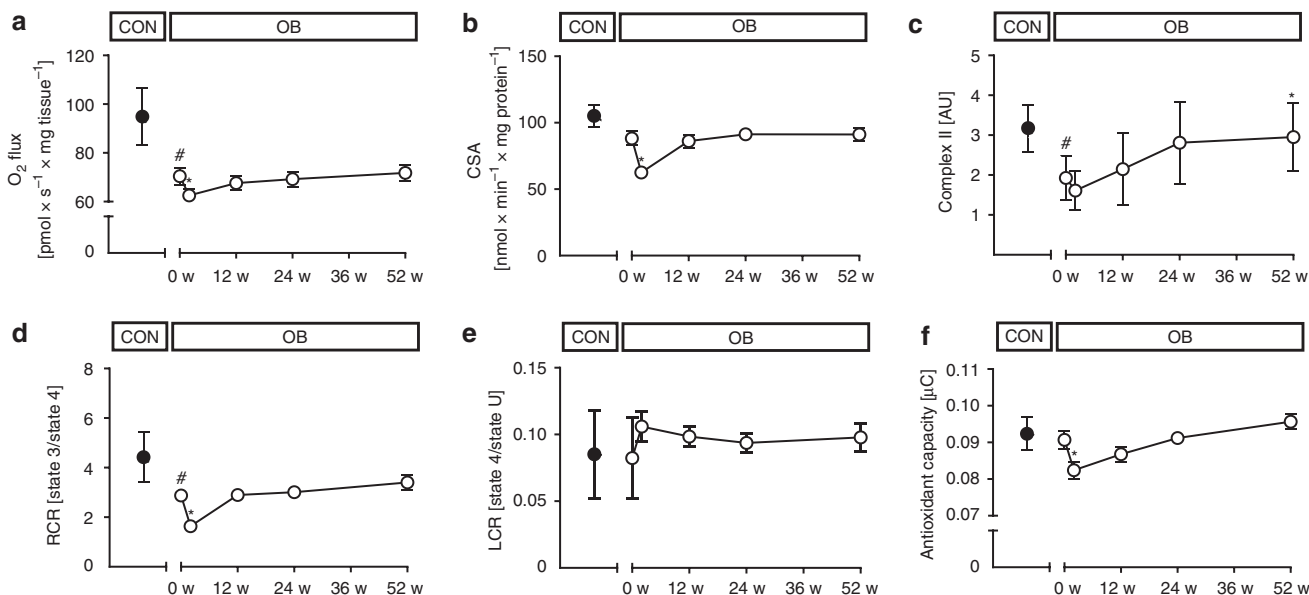


**Fig. 2** Time course of muscle changes. Time course of changes in muscle maximum uncoupled respiration (CON *n* = 14, OB *n* = 45) **(a)**, citrate synthase activity (CSA) (CON *n* = 13, OB *n* = 45) **(b)**, electron transport chain complex II succinate dehydrogenase complex iron sulfur subunit B protein content (CON *n* = 10, OB *n* = 15) **(c)**, respiratory control ratio (RCR) (CON *n* = 13, OB *n* = 43) **(d)**, leak control ratio (LCR) (CON *n* = 13, OB *n* = 44) **(e)** and serum antioxidant capacity (CON *n* = 6, OB *n* = 28) **(f)** in obese (empty circles) and nonobese humans at baseline (black circles). Mean  $\pm$  SEM, \**p* < 0.05 vs OB at baseline (0 w) using CPM for repeated measures analysis, #*p* < 0.05 vs CON using unpaired two-tailed *t*-test. CON nonobese humans, OB obese participants

droplet DAG species (Fig. 1c, Suppl. Fig. 1a, e). Muscle PKC $\theta$  activation doubled (*p* < 0.05 using a covariance pattern model for repeated measures analysis, CPM; Fig. 1d) and PKC $\epsilon$  also showed a trend towards higher values (1.5  $\pm$  1.5 vs 2.1  $\pm$  1.9 AU, *p* = 0.16, CPM) at 2 weeks. Membrane ceramide C18:1 and cytosolic ceramide 18:1 increased, while cytosolic and membrane ceramide 24:0 even decreased at 2 weeks (Suppl. Fig. 1b, d, f), all without

any changes in pJNK/tJNK (Fig. 1f). Maximum respiration per mg tissue decreased by 10% in the uncoupled state (Fig. 2a) and by 17% in state 3. At 2 weeks, measures of muscle mitochondrial content showed variable results with lower CSA and density from transmission electron microscopy (Fig. 2b, Suppl. Fig. 4), but unchanged ETC complexes I-IV (Fig. 2c, Suppl. Fig. 2a-d). Compared to baseline, ETC complex V increased already at

2 weeks (Suppl. Fig. 2d). This was paralleled by a 43% lower respiratory control ratio indicating impaired mitochondrial efficiency (Fig. 2d). At 2 weeks, muscle Mfn2, Opa1, Fis1, Pink1, phospho-Pink1, Parkin, phospho-Parkin, DRP-1, phospho-DRP1 (Suppl. Fig. 3) as well as LC3 ( $0.45 \pm 0.34$  vs.  $0.42 \pm 0.59$  AU,  $p = 0.26$  using CPM) and p62 did not differ from baseline ( $2.21 \pm 0.69$  vs.  $1.50 \pm 0.58$  AU,  $p = 0.15$ , using CPM). Serum antioxidant capacity was also decreased, while oxidation-reduction capacity and lipid peroxidation remained unchanged at 2 weeks (Fig. 2f, Table 1).

#### Metabolic abnormalities normalize at 52 weeks after surgery.

At 52 weeks, the total weight loss of  $50 \pm 14$  kg ( $33.0 \pm 7.7\%$  of initial body weight) was accompanied by progressive improvements in glycemia and insulinemia (Table 1). A subgroup comparison between patients undergoing gastric bypass and sleeve gastrectomy surgery did not suggest differences in the time course of changes in body weight and muscle insulin sensitivity. However, the relatively small subgroup size does not allow to draw firm conclusions on a possible metabolic difference between these surgical techniques. The transiently increased plasma FFA improved by 22% (Table 1) and adipose tissue insulin resistance (Adipo-IR) gradually decreased until 52 weeks, but remained higher in OB than in CON (Fig. 1a). Muscle insulin sensitivity reached values of CON at 52 weeks (Fig. 1b). Muscle membrane and lipid droplet DAG continued to rise until 24 weeks before decreasing to baseline values at 52 weeks (Fig. 1c, Suppl. Fig. 1). Membrane/cytosolic PKC $\theta$  translocation decreased in parallel at 12 and 24 weeks towards baseline values (Fig. 1d). PKC $\epsilon$  showed a trend towards lower values ( $1.19 \pm 0.94$  vs.  $2.14 \pm 1.86$  AU at baseline,  $p = 0.053$  using CPM). Measures of mitochondrial function and content returned towards baseline (Fig. 2a–d, Suppl. Fig. 4). Compared to baseline, ETC complexes I, III and IV started to increase at 12 weeks, followed by II at 52 weeks (Fig. 2c, Suppl. Fig. 2a–d). Of note, Mfn2, Opa1, Fis1 (Suppl. Fig. 3a–c), LC3 ( $0.6 \pm 0.4$  vs.  $0.4 \pm 0.6$  AU at baseline,  $p = 0.03$  using CPM) and p62 ( $2.0 \pm 0.5$  vs.  $1.5 \pm 0.6$  AU at baseline,  $p = 0.01$  using CPM) were increased at 52 weeks. There was no difference in phospho-Pink1, phospho-Parkin and phospho-DRP1 at 52 weeks (Suppl. Fig. 3). Of note, inflammatory markers decreased, while high-molecular-weight (HMW) adiponectin rose at 12 and 24 weeks (Table 1).

#### Rapid effects on gene expression after metabolic surgery.

To examine whether the metabolic differences reflect altered gene transcription, we initially compared the muscle transcriptome between OB before surgery (OB 0 w) and CON and detected 595 differentially expressed genes (Fig. 3a, Supplementary Data 1). Gene ontology (GO) analysis indicated that several genes are implicated in the regulation of apoptotic processes (GO:0042981), MAPK cascade (GO:0043410), inflammatory response (GO:0006954, GO:0050729), oxygen transport (GO:0015671) and others (Fig. 3b; Suppl. Table 3).

Comparing the muscle transcriptome of OB over the time course after surgery identified 937 out of 1,528 upregulated and 591 downregulated genes at 2 weeks (Fig. 3a, Supplementary Data 1). GO analysis showed significant enrichments in genes controlling transcriptional regulation (GO:0000398, GO:0010501), small GTPase-mediated signal transduction (GO:0051056) and negative regulation of insulin receptor signaling (GO:0046627) (Fig. 3c, Suppl. table 4). Among all transcripts, 1,244 were transiently altered at 2 weeks and then returned to baseline values (see also below), whereas 203 remained constantly changed (Fig. 3a). These transcripts comprise genes related to regulation of gene expression

(GO:0010467), calcium mediated signaling (GO:0019722) and negative regulation of insulin receptor signaling (GO:0046627) (Suppl. Fig. 5a, Suppl. table 5).

The genes exhibiting strongest changes at 2 weeks are involved in mitochondrial function (*HMGCS2*), lipid metabolism (*ANGPTL4*, *ABCA1*, *ABCG1*), calcium signaling (*PCDH15*), protein folding (*DNAJC28*), and inflammatory processes (*CISH*) (Suppl. Table 1). As altered mitochondrial functionality and lipid homeostasis were also the key metabolic abnormalities at 2 weeks (Figs. 1, 2) and because of the known association between abnormal mitochondrial, lipid and calcium homeostasis with insulin resistance, we further analyzed genes of these pathways over the entire post-surgical time period. This revealed 70 mitochondrial, 23 lipid metabolism and 60 calcium-related genes with significantly different expression levels (Fig. 3d). Importantly, several transiently regulated mitochondrial genes are coding for ribosomal RNA and tRNA or are known to modify mitochondrial tRNAs<sup>16</sup> suggesting that the mitochondrial transcription and translation machinery is highly active immediately after surgery.

At 12 weeks after surgery, 625 genes were significantly altered (341 up- and 284 downregulated), at 24 weeks 756 genes (519 up- and 237 downregulated) in comparison to their expression before surgery (Fig. 3a, Supplementary Data 1). The pathways affected at 12 weeks comprise—among others—glycogen metabolic process (GO:0005977), translation (GO:0006413 and GO:0006364) and transmembrane transport (GO:0055085) (Suppl. Fig. 5b; Suppl. table 6). At 24 weeks, genes related to transmembrane receptor protein tyrosine kinase signaling (GO:0007169), cytoskeleton organization (GO:0007010) and regulation of cell growth (GO:0001558) are mostly higher expressed than before surgery (Suppl. table 7).

At 52 weeks, 1,449 transcripts were significantly altered (Fig. 3a, Supplementary Data 1), which comprise genes involved in glycogen metabolic process (GO:0005977), protein polyubiquitination / destabilization (GO:0016567, GO:0031648), (Suppl. table 8) and including upregulation of those contributing to transcription (*BACH1*), cytoskeletal and tubulin reorganization (*MYH3*, *CCDC8*, *ACTC1*) (Suppl. table 2 and 8).

#### Alterations of DNA methylation occur later after surgery.

Mitochondria are also essential for providing metabolites for the generation and modification of epigenetic marks, which in turn modulate gene expression<sup>17</sup>. Thus, we examined whether the transient increase in muscle mitochondrial oxidative capacity could contribute to reprogramming of DNA methylation. Indeed, 107,325 CpG sites showed differential muscle DNA methylation between OB and CON. The methylation of individual CpG sites before and after metabolic surgery was compared by paired analysis. At 2 weeks, only 19 CpGs were different, of which 14 remained altered at 52 weeks (Fig. 4a). At 52 weeks, 109,105 CpGs were differentially methylated compared to baseline (Fig. 4a). Of note, most differentially methylated CpG sites (89% at 2 weeks and 70% at 52 weeks) were hypomethylated after surgery (Suppl. Fig. 6a, b). Changes in DNA methylation were very low (between  $-5$  and  $+4\%$ ) at 2 weeks, and higher ( $-14$  to  $+11\%$ ) at 52 weeks when compared to baseline. The number of differentially methylated CpG sites at 2 weeks was low and not enriched in a specific genomic region (Suppl. Fig. 6c). Changes in DNA methylation observed at 52 weeks occurred mostly outside CpG islands, particularly in open sea and shelf areas ( $p < 2 \times 10^{-16}$ ,  $p = 2.3 \times 10^{-8}$  Pearson's Chi-squared test). A significant enrichment was visible in intergenic regions and gene bodies at 52 weeks ( $p < 2 \times 10^{-16}$ , Chi-square test, Suppl. Fig. 6c). This enrichment explains the relatively small overlap between

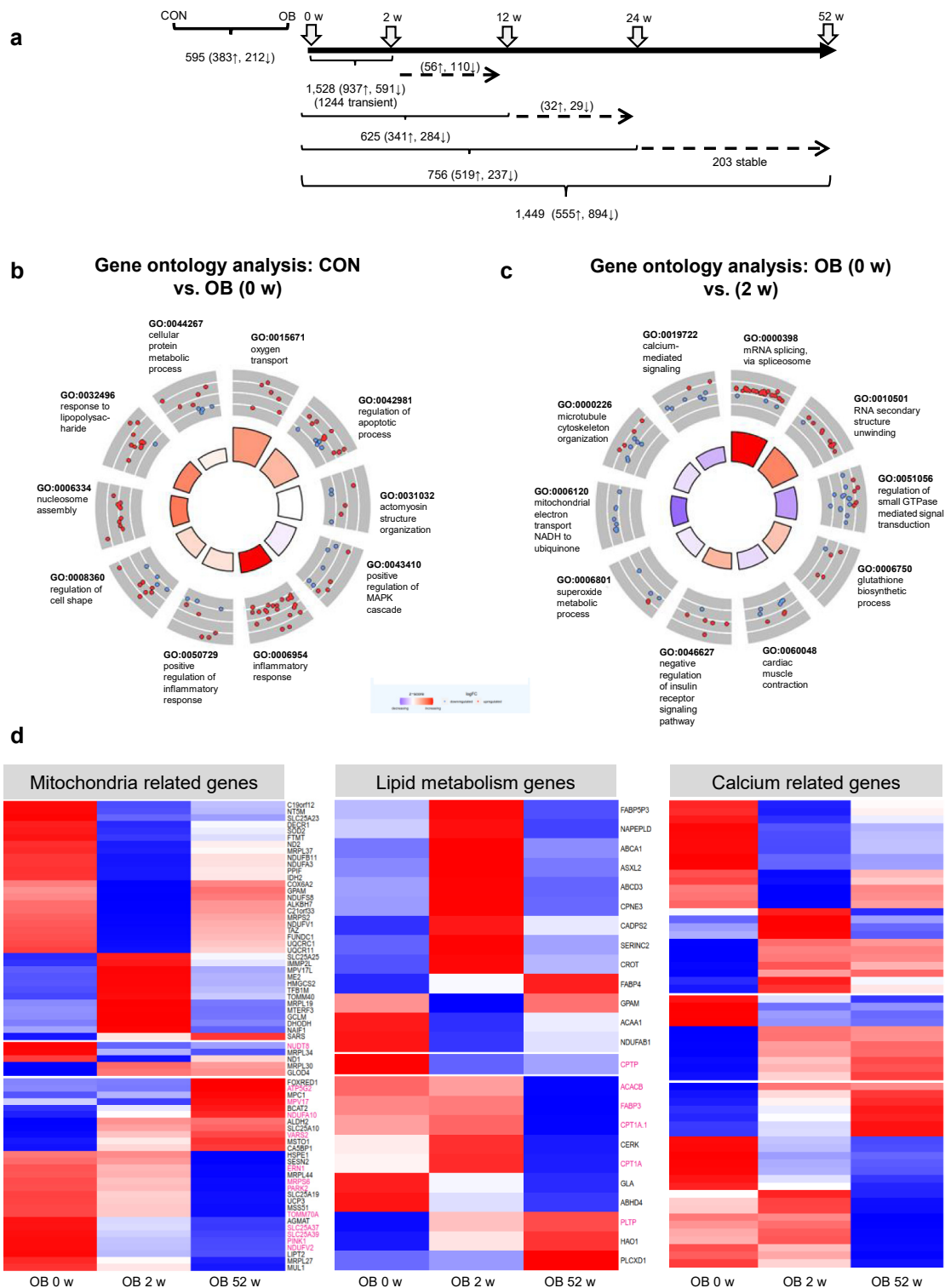


**Fig. 3** Differences in skeletal muscle transcriptome. Transcriptome analysis of skeletal muscle before (0 weeks), at 2, 12, 24 and 52 weeks after metabolic surgery. Data are given as number of differentially expressed transcripts between indicated groups and time points (**a**). Gene ontology analysis of genes differentially expressed between lean (CON) and obese (OB) participants. The inner circle depicts the main processes to be increased (blue) or decreased (red) in OB. The outer circle shows scaled scatter plots for affected genes and their regulation within the most-enriched biological pathway in OB at baseline (OB, 0 w) (**b**) and 2 weeks after the surgery (OB, 2 w) (**c**). Changes in mRNA expression of genes related to mitochondrial function, lipid metabolism and calcium signaling in skeletal muscle (**d**). Heat maps indicate expression levels of listed genes at 0 (baseline), 2 and 52 weeks after metabolic surgery. Each column represents the average expression level of 16 individuals and each row shows the expression profile of one single transcript with significant differences. Up- and downregulated genes are indicated by red and blue signals, respectively; the signal intensity corresponds to the log-transformed magnitude of the average of expression per group. All genes printed in bold magenta show differentially methylated CpGs at 52 weeks. For gene expression unadjusted p-value and DNA methylation data are adjusted for multiple testing with Benjamini Hochberg correction \* $p < 0.05$  (unpaired (CON vs OB) and paired (OB 0 vs 2 weeks/52 weeks two-tailed  $t$ -test; CON:  $n = 6$ , OB:  $n = 16$ )

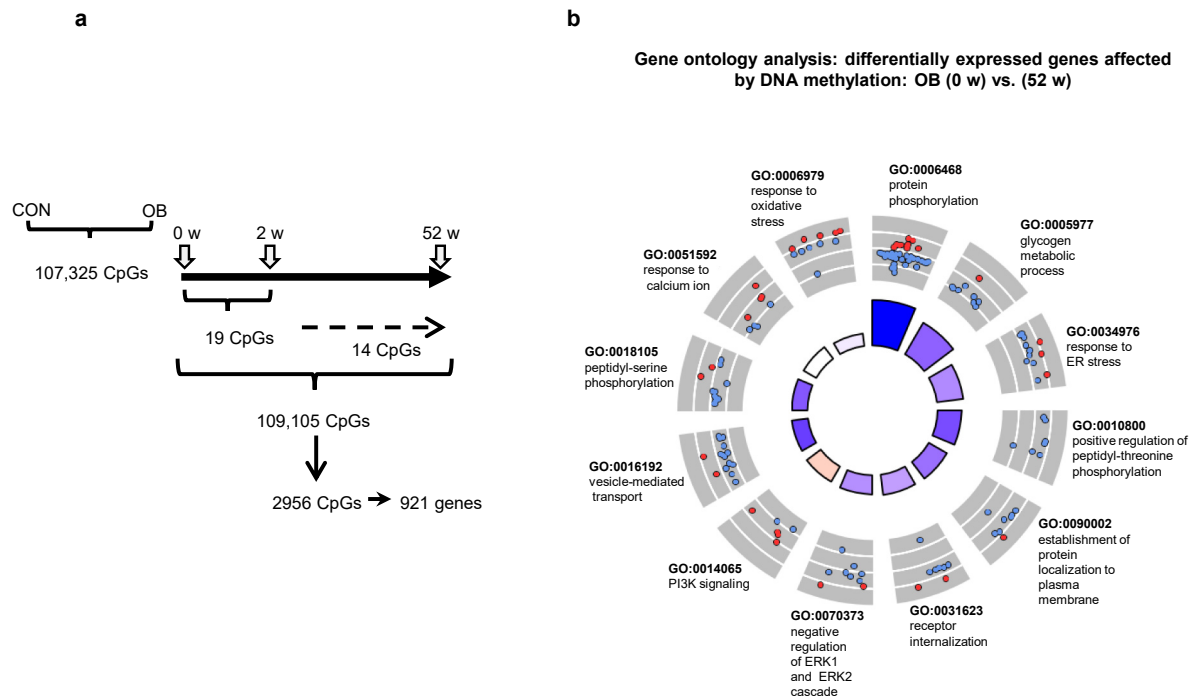


**Fig. 4** Genome wide DNA methylation analysis in skeletal muscle. The number of differentially methylated CpG sites between the indicated groups (**a**). A total of 2956 CpG sites are located in/or in close proximity of 921 genes exhibiting different expression between baseline and 52 weeks. Gene ontology analysis of 921 differentially expressed genes with altered levels of DNA methylation at 52 weeks (**b**). Up- and downregulated genes are indicated by red and blue signals, respectively. \* $p < 0.05$  (unadjusted  $p$ -value paired  $t$  test for gene expression,  $n = 16$ , methylation data with Benjamini Hochberg correction)

differentially methylated CpGs and differentially expressed genes, as only 2956 CpGs are located in/or close to regions of the 921 differentially expressed genes (Fig. 4a). Among differentially expressed genes involved in mitochondrial function, lipid metabolism and calcium signaling, we detected 13, 6 and 30, respectively, which were affected by DNA methylation at 52 weeks (Fig. 3d, highlighted in magenta).

**Changes in gene expression via altered DNA methylation.** DNA methylation in promoter and enhancer regions is associated with silencing of gene transcription, whereas elevated DNA methylation is typically found in the body of actively transcribed genes<sup>18</sup>. To further investigate the relationship between DNA methylation and gene expression, we compared all upregulated genes with hypomethylated CpGs in promoters and hypermethylated CpGs in gene bodies and vice versa for the downregulated genes. None of the differentially expressed genes detected at 2 weeks showed altered DNA methylation. However, at 52 weeks, 2956 CpGs were identified in 921 differentially expressed genes (Fig. 4a). GO analysis indicated enrichment in genes linked to several biological pathways, including protein phosphorylation, glycogen metabolic process (GO:0005977), protein localization to plasma membrane and vesicle-mediated transport (Fig. 4b, Suppl. table 9). Among those, 323 contain >2 differentially methylated CpGs and levels of altered DNA methylation higher than 5%. Only few genes (~20) were previously described to be epigenetically regulated in obese humans<sup>13,19</sup>. Taking genes with an altered expression and DNA methylation (>5%) of at least 2 CpG sites into account, which can also be linked to insulin sensitivity, we identified 94 gene candidates to be affected by epigenetic alterations (Suppl. Fig. 7). Examples are *PTPRE*, a negative regulator of insulin receptor (IR) signaling in skeletal muscle; *PIK3R1*, a regulator of the PI3-kinase; *MLXIP*, involved in transcriptional activation of glycolytic target genes, and *ACACB*, a mitochondrial enzyme playing a role

in fatty acid metabolism (Fig. 5a–d). A hypermethylation in the promoter region of *PTPRE* gene related to lower expression at 52 weeks (Fig. 5a). A lower DNA methylation in the promoter and a higher methylation in the gene body of *PIK3R1* is linked to its higher expression after the surgery (Fig. 5b), whereas a hypomethylation in the gene body of *MLXIP* and *ACACB* associated with their lower expression (Fig. 5c, d). In addition, the time course of the expression of the listed candidates was evaluated. *PTPRE* expression decreased already at 2 weeks, whereas the changes of the expression of *PIK3R1* occurred at 12 weeks and *ACACB* and *MLXIP* at 52 weeks (Suppl. Fig. 9).

**Correlation of altered expression and methylation.** In order to relate the differential expression and changes in DNA methylation to the primary metabolic phenotypes, e.g., body weight, insulin sensitivity, we calculated their correlation. Table 2 lists the expression levels of several genes associated with changes in  $M$ -value (27), fasting glucose (1219), HMW-adiponectin (73) and mitochondrial content (29). GO analysis of the 1219 affected genes, which correlated to glucose concentrations, can be linked to cytoskeleton organization (GO:0007010), calcium signaling (GO:0016338) and others (Suppl. table 10). The correlation analysis of the 921 differentially expressed and methylated genes (at 52 weeks) revealed 177 genes associated with BMI, 443 with  $M$ -value and 70 with HMW-adiponectin (Table 3). The correlations between methylation levels and  $M$ -value of the OB group for *PTPRE* ( $R^2 = 0.286$ ;  $p = 10^{-4}$ , Pearson correlation) and *PIK3R1* ( $R^2 = 0.312$ ;  $p = 5.10^{-5}$ , Pearson correlation) indicate that their interindividual epigenetic alterations are linked to the improvement in insulin sensitivity (Suppl. Fig. 10).

**Epigenetic reprogramming of transiently altered expression.** As 1150 mRNAs (encoded by 1126 genes) were only transiently differentially expressed at 2 weeks (Fig. 3a) and returned to

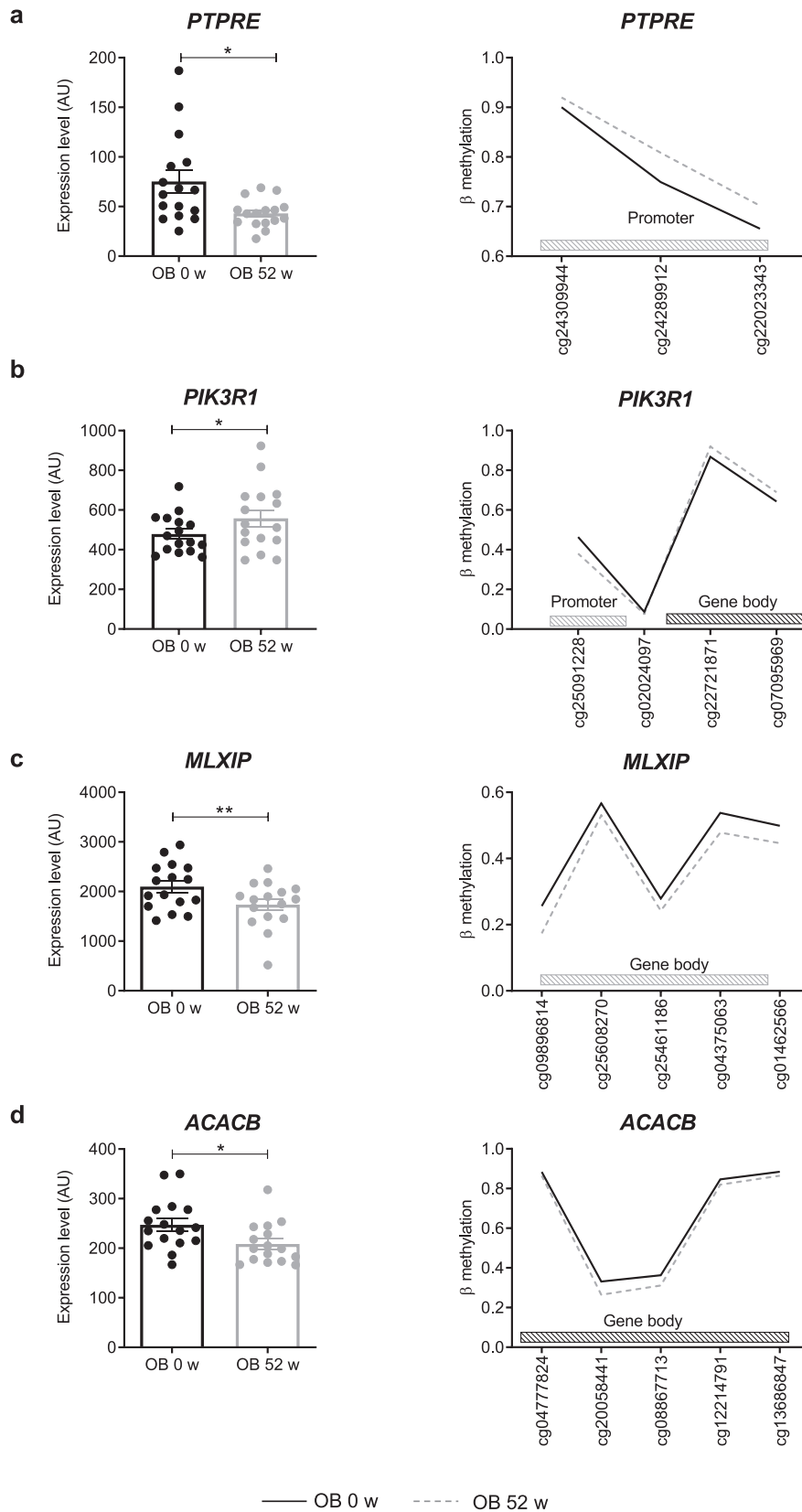


**Fig. 5** Gene candidates showing differences in expression and DNA methylation. Expression is shown in left panels and levels of DNA methylation in right panels. Differentially methylated CpGs are located at different positions of the genes, either in the promoter as shown for *PTPRE* (a), in the gene body as shown for *MLXIP* (c) and *ACACB* (d), or in both as depicted in *PIK3R1* (b). Mean  $\pm$  SEM (left panels). Obese humans given as black circles/lines at baseline and as gray circles/lines at 52 weeks. Only significantly differentially methylated CpGs are represented; \* $p < 0.05$  (Gene expression unadjusted  $p$ -value paired  $t$  test,  $n = 16$ , methylation data with Benjamini Hochberg correction)

**Table 2 Pearson correlations between gene expression levels and indicated clinical parameters**

	Body mass index	M-value	Fasting glucose	FFA suppression	HMW-adiponectin	Mitochondrial content (CSA)
Number of genes	25	27	1219	76	73	29

**Table 3 Number of genes differentially expressed and methylated at 52 and exhibiting at least one CpG significantly correlated to the indicated clinical parameters**

	Body mass index	M-value	Fasting glucose	FFA suppression	HMW-adiponectin	Mitochondrial content (CSA)
Number of genes	177	443	163	112	70	27

baseline expression levels, we tested whether epigenetic alterations were responsible for this effect. We therefore mapped the differentially methylated CpGs at 52 weeks to all transiently altered transcripts at 2 weeks. Indeed, 75% (849) of these genes showed changes in DNA methylation at 52 weeks (Fig. 6a; Chi-square  $p < 10^{-255}$ ), including genes involved in mitochondrial function ( $n = 12$ ), calcium signaling ( $n = 11$ ), lipid metabolism ( $n = 4$ ). Representative examples comprise *HMGCS2* (hydroxymethylglutaryl-CoA synthase<sup>20</sup>), and *IMMP2L* a mitochondrial inner membrane protease subunit 2 involved in peptides translocation into mitochondria<sup>21,22</sup> (Fig. 6b; Suppl. Fig. 9). Collectively, these data indicate that changes in methylation at 52 weeks associate with the reversal of altered expression of genes involved in mitochondrial functionality and lipid metabolism.

## Discussion

This study provides insights into the mechanisms, by which metabolic surgery sequentially affects systemic and tissue-specific metabolism and its epigenetic regulation in obese humans. In particular, surgically-induced weight loss (i) is not immediately followed by improved muscle insulin resistance, likely related to transiently augmented lipolysis resulting in accumulation of lipid intermediates, inadequate mitochondrial function and altered gene expression profiles, (ii) may subsequently modify DNA methylation of genes involved in muscle energy metabolism, and (iii) associate with changes in gene expression along with restoration of muscle metabolism within one year. We thereby provide evidence for a role of transient changes in the expression of specific genes, which may be reprogrammed by DNA methylation.

Generally, the impressive weight loss by metabolic surgery is believed to be responsible for the improvement of whole-body metabolism, and specifically of insulin sensitivity leading to remission of type 2 diabetes<sup>3,5,6</sup>. Surprisingly, this study demonstrates that the rapid loss of ~10 kg equaling ~7% of body weight within 2 weeks, does not translate into immediate improvement of muscle insulin resistance. Interestingly, analysis of the few previous studies on early effects of metabolic surgery also found no<sup>6,7</sup> or minor increases in insulin sensitivity<sup>4,23</sup>. Using a low-caloric dietary intervention, Taylor and colleagues reported marked improvements in hepatic fat content and glucose production, but also no changes in muscle insulin sensitivity after one week<sup>24,25</sup>. The present study now identifies sustained elevation of adipose lipolysis as underlying cause, resulting in initial doubling of fasting plasma FFA with persisting adipose tissue insulin resistance for up to 6 months after surgery and parallel intracellular accumulation of 18:1 18:1 DAG species and PKC $\theta$  stimulation. Thereby, it shows that dynamic changes in endogenous FFA associate with activation of the DAG/PKC pathway in humans, which has been previously only

demonstrated for high doses of exogenous lipid infusions<sup>15,26</sup>. The greater muscle PKC $\epsilon$  activation in OB before surgery suggests that also this PKC isoform relates to obesity-mediated muscle insulin resistance as suggested<sup>27</sup> and reported for hepatic insulin resistance<sup>28</sup>. Other lipid mediators like ceramides, previously associated with human muscle insulin resistance in some<sup>29</sup>, but not other studies<sup>26,30</sup>, were generally not altered in muscle of OB. Membrane and cytosolic C18:1 ceramides were also elevated at 2 and 12 weeks, but without concomitant changes in muscle JNK phosphorylation, and subsequently rapidly decreased during follow-up as reported in lower-degree obesity<sup>11</sup>. Of note, several DAG as well as ceramide species were decreased, when insulin sensitivity had increased at 52 weeks. This occurred in parallel with a trend towards decreased PKC $\epsilon$  activation and lower pJNK/tJNK at 52 weeks. The latter, however, could also be related to lower inflammatory activity<sup>15</sup> as supported by the lower usCRP and IL-6 levels. Taken together, these data indicate that the DAG-PKC pathway is primarily responsible for the initial lack of improvement in muscle insulin resistance upon metabolic surgery and along with reduced inflammatory activity underlies the later increase in insulin sensitivity.

Insulin resistance frequently, but not generally associates with impaired mitochondrial function<sup>12,27,31–33</sup>. The present study not only confirmed the lower muscle mitochondrial oxidative capacity and coupling efficiency and fusion activity in OB before surgery<sup>32–34</sup>, but also provides evidence for a dynamic regulation of mitochondria in humans. At 2 weeks, mitochondrial mass decreased, as measured independently by both biochemical and ultrastructural analyses. Moreover, no changes in ETC complexes I–III were detected at 2 weeks, possibly suggesting a transient delay in the improvement of mitochondrial abundance. Intracellular lipid accumulation likely accounts for the reduction of mitochondrial mass, oxidative capacity and coupling efficiency early after surgery as reported for C2C12-differentiated myotubes<sup>35</sup>. Decreased antioxidant capacity could result from augmented ROS quenching in the presence of elevated lipid peroxidation and higher lipid influx. The continued impairment of mitochondrial fusion activity at 2 weeks, suggests that altered mitochondrial functionality persists during elevated lipid availability and only reverses with improved insulin action at 52 weeks<sup>36</sup>. Paralleled by decreasing plasma FFA, lower muscle mitochondrial function returned to baseline values within 12 weeks and then remained unchanged until 52 weeks, despite continuous improvement of insulin sensitivity in line with normalization of mitochondrial function in other studies with limited time resolution<sup>12,37,38</sup>. Our findings are in concert with long-term caloric restriction data demonstrating no change in mitochondrial oxidative capacity despite improved insulin sensitivity<sup>39</sup>. This indicates that surgical weight loss—similar to that by caloric restriction<sup>40</sup> or by inhibition of lipolysis<sup>41</sup>—dissociates modulation of insulin sensitivity from muscle mitochondrial respiration.

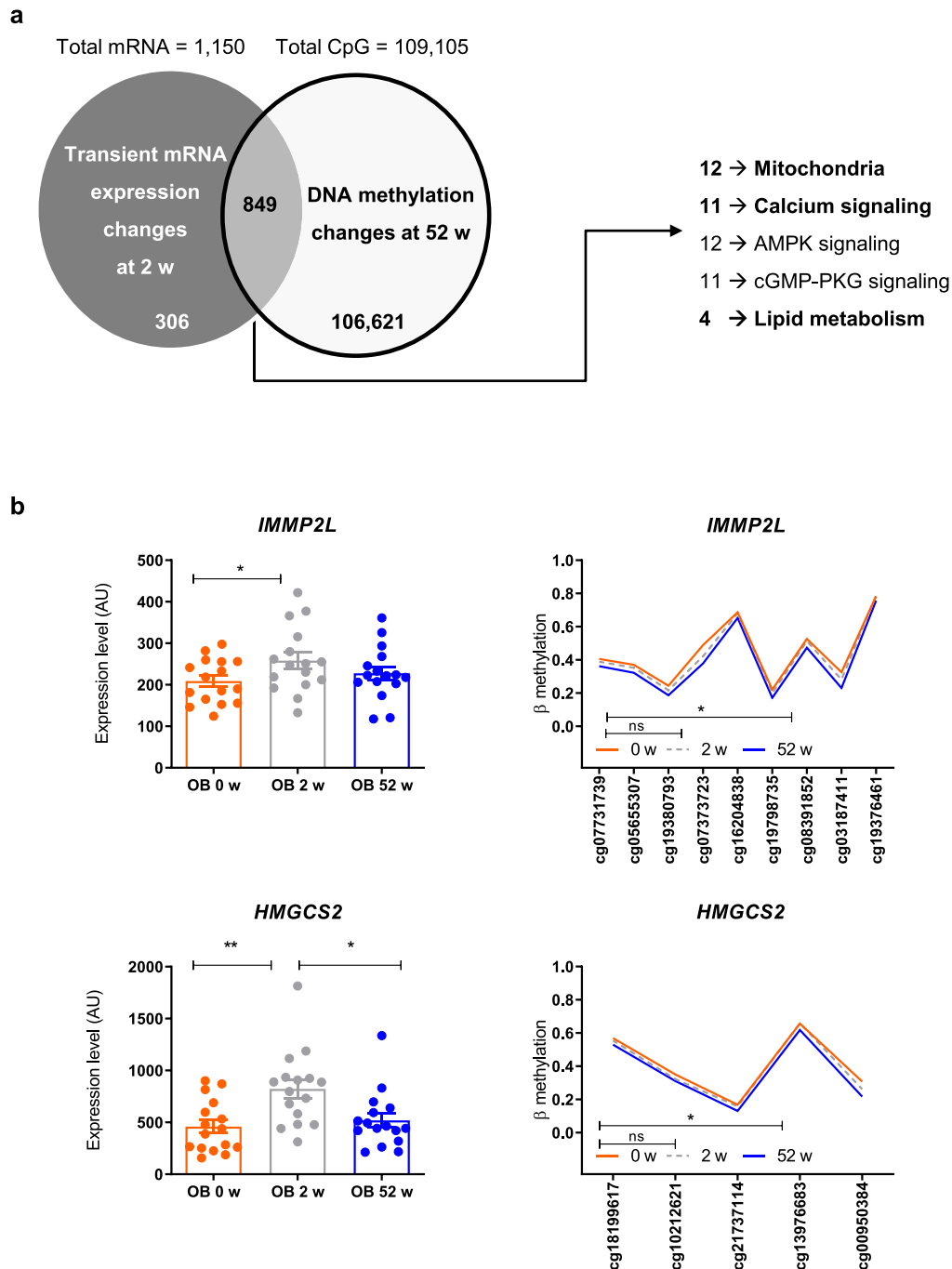


**Fig. 6** Reprogramming of gene transcripts by DNA methylation at 52 weeks. Seventy-five percent of genes exhibiting transient differences in expression at baseline show changes in DNA methylation at 52 weeks. Chi-square test  $p < 10^{-255}$ . Gene ontology analysis identified the indicated number of genes to be altered in the listed cellular processes (right panel) (a). Examples of changes in DNA methylation in *IMMP2L* (upper panel) and *HMGCS2* genes (lower panel). Both genes are only differentially expressed 2 weeks after the surgery (b). Mean  $\pm$  SEM, obese humans are shown as red circles/lines at baseline, as gray circles/lines at 2 weeks and as blue circles/lines at 52 weeks after surgery. \* $p < 0.05$  (Gene expression unadjusted  $p$ -value 2-tailed paired  $t$  test,  $n = 16$ , methylation data with Benjamini Hochberg correction)

However, in contrast to our findings, short-term caloric restriction for 60 h or 53 days did not affect muscle mitochondrial density<sup>42,43</sup>, suggesting acute intervention-specific effects of weight loss in humans. Nevertheless changes in diet and eating behavior, which have been extensively studied previously<sup>44</sup>, were not assessed in this observational study, thereby limiting conclusions as to their possible confounding effect on weight loss. In addition to the changes resulting from surgery, moderate changes

of measured variables could be also due to the repeated testing one year later.

Comprehensive analysis of muscle gene expression profiles reflected the observed metabolic alterations. Before surgery, as described previously<sup>13,19</sup> particularly genes involved in lipid metabolism, such as *FFAR4* (free fatty acid receptor 4), exhibited differential expression. At 2 weeks, the expression pattern mirrored the transient alterations of lipid metabolism and

mitochondrial function, which later returned to baseline or approached those of healthy humans. Elevated *ABCD3* (ATP-binding cassette sub-family D member 3) or *NAPEL2* (N-acylphosphatidylethanolamine-hydrolyzing phospholipase D) expression at 2 weeks likely reflects the higher FFA uptake<sup>45,46</sup>. Also genes related to mitochondria and calcium handling showed higher expression levels, such as *SLC25A25* (calcium-binding mitochondrial carrier protein SCA25), encoding a calcium-dependent mitochondrial solute carrier<sup>47</sup>. Of note, elevated mitochondrial  $\text{Ca}^{2+}$  increases activities of glycerol 3-phosphate dehydrogenase, pyruvate dehydrogenase phosphatase, NAD-isocitrate dehydrogenase and 2-oxoglutarate dehydrogenase, all of which increase the NADH production for oxidative phosphorylation<sup>48</sup>. Another set of transiently upregulated genes relates to small GTPase-mediated signaling, such as *ARHGAP24*, *RACGAP1*, *ITSN1* and to negative regulation of insulin signaling, such as *SOCS1*, *RPS6KB1*. The latest mediates TNF- $\alpha$ -induced insulin resistance by phosphorylating IRS1 at multiple serine residues, resulting in accelerated degradation of IRS1<sup>49–51</sup>. This points to a role of local inflammatory processes as cause of adipose tissue insulin resistance leading to enhanced lipolysis early after surgery. At 52 weeks, downregulated genes comprise interferon- $\gamma$  mediated signaling, in line with the time course of inflammatory markers of the present study and the lower expression of inflammation-related genes in a previous study<sup>52</sup>. Interestingly, interferon- $\gamma$  has recently been closely linked to skeletal muscle insulin resistance and derailed glucose metabolism in obesity<sup>53</sup>.

We also provide detailed description of time-dependent changes in muscle metabolism, transcriptome and methylome. At 2 weeks, several transient changes in skeletal muscle occurred in parallel, comprising augmented lipid availability, mitochondrial adaptation and altered expression of genes related to lipid metabolism and cAMP signaling. Interestingly, transcriptional changes at this time point are not linked to alterations in DNA methylation indicating that other regulatory mechanisms, e.g., activity of transcription factors, mediate the differences in gene expression. In contrast, at 52 weeks, many CpGs are differentially methylated, suggesting that alterations in the entire methylome may occur at a later stage<sup>13</sup>. However, in agreement with previous studies<sup>13,54,55</sup>, changes in DNA methylation of ~5% are relatively small. The functional relevance of such moderate differences has been proven for some genes by reporter assays<sup>56</sup>. The improvement of mitochondrial flexibility after surgery-induced weight loss might provide substrates for epigenetic changes in muscle at 52 weeks. Interestingly, recent reports provided supporting information on the role of oxidative capacity for epigenetic changes<sup>17,57,58</sup>. Nearly 3000 of the differentially methylated CpGs are associated with altered expression of the corresponding 921 genes, pointing towards the relevance of epigenetic mechanisms in response to weight loss. Metabolic surgery remodels DNA methylation of genes involved in insulin signaling, such as *PIK3R1* and *PTPRE* and *ACACB* (also designated *ACC2*), which is essential for fatty acid metabolism<sup>59</sup>. Mice lacking *Acc2* exhibit higher fatty acid oxidation rates in the soleus muscle than control mice<sup>60</sup>. Previous studies found only three genes with differences in expression linked to changes in DNA methylation after surgery, *SORBS3* (sorbin and SH3 domain containing 3), *PGC-1 $\alpha$*  (PPARG coactivator 1  $\alpha$ ) and *PKD4* (pyruvate dehydrogenase kinase 4)<sup>13</sup>. The present study identified close to 300 epigenetic changes associated with altered expression of important metabolic genes, likely contributing to improved insulin sensitivity and lipid metabolism. Pathway enrichment analysis of the 921 differentially expressed and methylated genes indicates that several genes are implicated in the regulation of glycogen metabolism,

intracellular signal transduction and cAMP biosynthesis, reflecting improved skeletal muscle activity and metabolism<sup>61</sup>.

Moreover, the present study found that changes in DNA methylation are associated with reprogramming up to 75% of the transiently altered genes, which possibly normalize their expression levels at 52 weeks (Fig. 6). Of note, genes undergoing such changes are involved in mitochondrial and lipid metabolism, again reflecting the early transient metabolic alterations. This data provides at least indirect evidence that DNA (de)methylation processes are possibly involved in the reprogramming of gene expression in response to metabolic surgery. The question is whether all changes in expression and DNA methylation are occurring in response to weight loss or if and to which extent weight-independent alterations contribute to observed phenotypes. The finding that the number of genes correlating with BMI is clearly lower than that of genes associating for instance with fasting glycemia or adiponectin levels indicates that not all observed effects are directly related to body weight loss (Tables 2 and 3). At present, no data are available on the time course of possible effects of a comparable diet-induced weight loss on epigenetic changes and alterations in energy metabolism. Consequently, the present data have to be interpreted in the context of surgical weight loss and cannot be generalized to weight loss by other interventions or causes. Taken together, surgically-induced weight loss induces several metabolic events leading to sustained improvement of insulin sensitivity. These effects involve transient dyslipidemia and lipotoxic insulin resistance as well as reduced mitochondrial mass associated with altered gene expression followed by long term metabolic reprogramming of gene expression possibly mediated by epigenetic mechanisms. These mechanisms underlie the dynamic changes of insulin sensitivity after bariatric surgery and point at mitochondrial function and lipid metabolism as key obesity treatment targets.

## Methods

**Study population.** We studied 49 obese Caucasian patients (OB) before and 2, 12, 24 and 52 weeks after sleeve gastrectomy or gastric bypass surgery (Suppl. Fig. 8). Healthy nonobese humans were examined once (controls, CON). The OB group included 13 patients with type 2 diabetes (T2D) presenting with good metabolic control (fasting glucose:  $139 \pm 24$  vs.  $92 \pm 16$  mg/dl,  $p < 0.01$ , unpaired two-sided  $t$ -test; HbA1c:  $7.2 \pm 1.0$  vs.  $5.6 \pm 0.5$  %,  $p < 0.01$ , unpaired two-sided  $t$ -test) and similar serum insulin, c-peptide and lipid levels as the glucose tolerant participants. T2D patients were drug naive ( $n = 3$ ) or treated with monotherapy (metformin:  $n = 3$ , DPP-4 inhibitor:  $n = 1$ , GLP-1 agonist:  $n = 1$ ) or combination therapy (metformin+insulin:  $n = 2$ , metformin+GLP-1 agonist:  $n = 2$ , metformin+GLP-1+insulin:  $n = 1$ ). Oral glucose-lowering medication and GLP-1 agonists were withdrawn 3 days, while long acting insulin analogues were replaced with NPH insulin for 7 days before the metabolic tests. If necessary, regular insulin was used during the night before the metabolic studies to avoid hyperglycemia. Participants were allowed to take thyroid hormones, oral contraceptives or antihypertensive treatment, but not immunomodulatory or other medications. All participants were non-smokers and engaged only in light physical activity and had no evidence for growth hormone deficiency, which has been shown to affect changes in lean mass and insulin sensitivity after bariatric surgery in other obese cohorts<sup>62</sup>. Six months prior to surgery patients underwent structured multimodal non-surgical weight-lowering treatment following the German guidelines for obesity management without achieving weight loss of >10%. Dietary and physical activity counselling was provided after the surgery according to local guidelines. Data of some participants were part of a previous report<sup>8</sup>. Each participant underwent 3-h hyperinsulinemic-euglycemic clamps using primed-continuous infusion of insulin ( $80 \text{ mU} \cdot \text{m}^{-2} \cdot \text{min}^{-1}$  for 8 min followed by  $40 \text{ mU} \cdot \text{m}^{-2} \cdot \text{min}^{-1}$ ; Insuman Rapid, Sanofi, Frankfurt am Main, Germany) combined with indirect calorimetry for assessment of insulin sensitivity and metabolic flexibility from the change in the respiratory quotient ( $\Delta\text{RQ}$ ) during the clamp ( $\text{RQ}_{\text{steady state}} - \text{RQ}_{\text{baseline}}$ )<sup>8</sup>. A variable infusion of 20% (w/v) glucose (B. Braun, Melsungen, Germany) was administered to maintain blood glucose at 90 mg/l, which was checked at 5-min intervals. Blood samples were collected before and during the clamp for measuring hormones and metabolites. All participants received information about all procedures and risks before providing their written consent to a protocol, approved by the ethics board of Heinrich-Heine University Düsseldorf (registered clinical trial, NCT01477957). The study was performed in compliance with all relevant ethical regulations for work with human participants.

**Mitochondrial content and function.** Mitochondrial respiration was assessed in permeabilized muscle fibers, obtained by biopsies from the vastus lateralis muscle<sup>30</sup>. Maximal oxidative phosphorylation (state 3) and resting respiration rates (state 4) were quantified upon sequential exposure to substrates followed by incremental titration steps of 1.0  $\mu$ l carbonyl cyanide p-[trifluoromethoxy]-phenylhydrazone (FCCP) until maximal uncoupled respiration (state u) was achieved in a 2-chamber Oxygraph-2k (OROBOROS Instruments, Innsbruck, Austria)<sup>41</sup>. Respiratory rates were expressed per mg tissue weight as well as per individual CSA<sup>1</sup>. Respiratory control ratio (RCR), defined as state 3/state 4, was used as an index of mitochondrial coupling, while leaking control ratio (LCR) was calculated from state 4/state u ratio, as a marker of the proton leak. Mitochondrial content was quantified by transmission electron microscopy and stereological principles using a 144-point grid overlaid on micrographs<sup>63,64</sup>. For each biopsy, 10–12 micrographs (6300 $\times$  and 25,000 $\times$  magnification) of longitudinally-sectioned tissue were analyzed in a blinded fashion.

**Blood analyses.** Metabolites, insulin, C-peptide and hsCRP<sup>33</sup> as well as IL-6 and HMW adiponectin were assessed<sup>65</sup>. Serum concentrations of TBARS were measured fluorometrically (BioTek, Bad Friedrichshall, Germany)<sup>66</sup>. Plasma static oxidation-reduction potential (sORP) and antioxidant capacity were determined in plasma as markers of systemic oxidative stress using the RedoxSYS (Luoxis Diagnostics, Inc., Englewood, CO, USA)<sup>66</sup>.

**Protein analysis.** Activities of PKC $\theta$  and PKC $\epsilon$  were assessed from the ratios of the protein contents in membrane and cytosol fractions upon differential centrifugation by Western blots<sup>66</sup>. Antibodies (BD Biosciences, catalogue Nr. 610090 and 610086) were diluted by 1:1000 for use. Total c-Jun N-terminal kinase (JNK) and Thr<sup>183</sup>/Tyr<sup>185</sup>-phosphorylated JNK were quantified using specific antibodies (Cell Signaling Technology, catalogue Nr. 9252 and 9255, dilution 1:1000). Protein of Mfn2 (Abcam, catalogue Nr. ab56889, dilution 1:1000), Opa1 (BD Biosciences, catalogue Nr. 612607, dilution 1:1000), Fis1 (Merckmillipore, catalogue Nr. ABC67, dilution 1:1000), LC3 (Cell Signaling technology, catalogue Nr. 4108, dilution 1:1000), p62 (BD Biosciences, catalogue Nr. 610833, dilution 1:1000), DRP1 (Cell Signaling technology, catalogue Nr. 5391, dilution 1:1000), phospho-Ser<sup>616</sup>-DRP1 (Cell Signaling technology, catalogue Nr. 3455, dilution 1:1000), Pink1 (Abcam, catalogue Nr. ab23707, dilution 1:1000), phospho-Thr<sup>257</sup>-Pink1 (Ubiquigent, catalogue Nr. 68-0057-100, dilution 1:200), Parkin (Abcam, catalogue Nr. ab15954, dilution 1:1000), phospho-Ser<sup>65</sup>-Parkin (Ubiquigent, catalogue Nr. 68-0056-100, dilution 1:200), ETC Complex I-V (NADH:ubiquinone oxidoreductase subunit B8, succinate dehydrogenase complex iron sulfur subunit B, ubiquinol-cytochrome C reductase core protein 2, cytochrome c oxidase subunit IV, ATP synthase F1 subunit alpha, antibodies from Abcam, catalogue Nr. ab110413, dilution 1:300) were quantified in total protein lysates and were normalized to GAPDH (Cell Signaling technology, catalogue Nr. 2118, dilution 1:20,000) as a loading control.

**Targeted lipidomics.** For quantification of lipid intermediates in subcellular muscle fractions, lipids were extracted, purified and analyzed from frozen tissue samples, using lipid chromatography mass spectrometry (LC-MS/MS)<sup>67</sup>. In brief, 50 mg of tissue was homogenized in 20 mM Tris/HCl, 1 mM EDTA 0.25 mM EGTA, pH 7.4, using a IKA T10 basic Ultra Turrax (IKA; Wilmington, NC, USA) and a tight-fitting glass douncer (Wheaton, Rochdale, UK). An internal standard (d517:0-DAG; Avanti Polar Lipids, Ala, USA) was added and samples were centrifuged for 1 h (100,000  $\times$  g, 4 °C). Lipid droplet, cytosol and membrane fractions were collected and lipids of each fraction were extracted according to Folch et al.<sup>68</sup>, followed by solid phase extraction (Sep Pak Diol Cartridges; Waters, Milford, MA, USA). The resulting lipid phase was dried under a gentle flow of nitrogen and resuspended in methanol. Lipid analytes were separated using a Phenomenex Luna Omega column (1.6  $\mu$ m 100A; Phenomenex, Torrance, CA, USA) on an Infinity 1290 HPLC system (Agilent Technologies, Santa Clara, CA, USA) and analyzed by multiple reaction monitoring on a triplequadrupole mass spectrometer (Agilent 6495; Agilent Technologies), operated in the positive ion mode.

**Gene expression analyses.** Total RNA was extracted from 5–10 mg of muscle biopsies from the same participants described above using miRNA micro kit (Qiagen, Hilden, Germany) as per the manufacturer's protocol, with additional DNase treatment. All RNA samples with RNA integrity number RIN  $\geq$  7 (Bioanalyzer, Agilent Technologies, Germany), were selected for microarray analysis. Transcriptome analysis was carried out by Oaklabs (Berlin, Germany) on their experimentally validated ArrayXS Human (design ID 079407, Agilent 60-mer SurePrint technology, Agilent Technologies). Gene ontology analysis was performed using David data base tools<sup>69</sup>, with cutoff enrichment score set above 1.7 and enriched  $p$  value < 0.05 (Fisher test).

**DNA methylation.** Genomic DNA was extracted from 5 mg of skeletal muscle biopsies using Invisorb® Genomic DNA Kit II according to the manufacturer's protocol. An amount of 500 ng of genomic DNA from each participant was bisulfite-converted using Zymo EZ DNA Methylation-Gold kit (Zymo Research Corporation, Irvine, CA, USA) and then hybridized on Infinium®

MethylationEPIC BeadChip, (Eurofins Genomics GmbH, Ebersberg, Germany). EPIC chip covered 890,703 cytosine positions located in TSS200, TSS1500, 5UTR, 1Exon, gene body, 3UTR and intergenic regions of the human genome. Pre-processing and normalization included steps of probe filtering, color bias correction, background subtraction and subset quantile normalization and was processed with "ChAMP" background as previously described<sup>70,71</sup>. Mean change in beta methylation was calculated for a specific CpG site with comparing mean of beta methylation before to those at 2 or 52 weeks after surgery. As our study included both male and female participants, probes annotated to chromosome Y and X were excluded. All probes annotated to contain SNPs were excluded for unpaired analysis, but included for all paired analysis.

**Statistical analyses.** Normally distributed parameters are presented as means  $\pm$  SD or means  $\pm$  SEM, otherwise as median (interquartile range [IQR]). Not-normally distributed data were log<sub>e</sub>-transformed to achieve near-normal distribution. Statistical analyses using covariance pattern model for repeated measures analysis based on patients with baseline and at least one follow-up muscle biopsy were performed. Analyses of the whole obese cohort were adjusted for age, sex, body mass index, surgery type and diabetes status at baseline and performed using SAS (version 9.4; SAS Institute, Cary, NC, USA). Phenotype traits were correlated to gene expression and DNA methylation by Pearson. Heat maps were generated with ggplots, R-package version 1.2.067. Programming and calculation of DNA methylation and transcripts were performed with R version 3.4.1 (2017-06-30).  $P$  values for transcriptome and methylation analysis were calculated by two-tailed Welch's  $t$ -test.  $P$  values of DNA methylation analysis were corrected by Benjamini Hochberg. Correction for multiple testing was performed for the methylome data and not for the transcriptome data. The reason for this is to avoid the number of false negatives and oversee relevant effects according to suggestions of John H. McDonald (McDonald, J.H. 2014. Handbook of Biological Statistics (3rd ed.). Sparky House Publishing, Baltimore, Maryland; p. 254–260). However, we provided the results of the multiple correction in the Supplementary Data 1 from A–E. A 4-field chi-square test was used for the enrichment analyses.

**Reporting summary.** Further information on research design is available in the Nature Research Reporting Summary linked to this article.

## Data availability

The metabolic dataset and all relevant western blots analyzed and reported in this study are included in the Source Data file. All array and methylation data analyzed and reported in this work have been deposited and are available at: (accession number GSE135066). R scripts used in this study have been uploaded to [https://git.connect.dzd-ev.de/markusjaehnert/pmid\\_31519890](https://git.connect.dzd-ev.de/markusjaehnert/pmid_31519890). Supplementary Data 1A–E are available at [https://git.connect.dzd-ev.de/markusjaehnert/pmid\\_31519890](https://git.connect.dzd-ev.de/markusjaehnert/pmid_31519890). All data are available from the corresponding author upon reasonable request.

Received: 28 October 2018 Accepted: 15 August 2019

Published online: 13 September 2019

## References

- Koliaki, C. & Roden, M. Alterations of Mitochondrial Function and Insulin Sensitivity in Human Obesity and Diabetes Mellitus. *Annual review of nutrition* **36**, 337–367 (2016).
- Cusi, K. The role of adipose tissue and lipotoxicity in the pathogenesis of type 2 diabetes. *Current diabetes reports* **10**, 306–315 (2010).
- Mingrone, G. & Cummings, D. E. Changes of insulin sensitivity and secretion after bariatric/metabolic surgery. *Surgery for obesity and related diseases : official journal of the American Society for Bariatric Surgery* **12**, 1199–1205 (2016).
- Gastaldelli, A. et al. Short-term Effects of Laparoscopic Adjustable Gastric Banding Versus Roux-en-Y Gastric Bypass. *Diabetes care* **39**, 1925–1931 (2016).
- Astiarraga, B. et al. Biliopancreatic diversion in nonobese patients with type 2 diabetes: impact and mechanisms. *The Journal of clinical endocrinology and metabolism* **98**, 2765–2773 (2013).
- Camasta, S. et al. Early and longer term effects of gastric bypass surgery on tissue-specific insulin sensitivity and beta cell function in morbidly obese patients with and without type 2 diabetes. *Diabetologia* **54**, 2093–2102 (2011).
- de Weijer, B. A. et al. Hepatic and peripheral insulin sensitivity do not improve 2 weeks after bariatric surgery. *Obesity (Silver Spring, Md.)* **21**, 1143–1147 (2013).
- Koliaki, C. et al. Adaptation of hepatic mitochondrial function in humans with non-alcoholic fatty liver is lost in steatohepatitis. *Cell metabolism* **21**, 739–746 (2015).

9. Toledo, F. G. & Goodpaster, B. H. The role of weight loss and exercise in correcting skeletal muscle mitochondrial abnormalities in obesity, diabetes and aging. *Molecular and cellular endocrinology* **379**, 30–34 (2013).
10. Taylor, R. et al. Remission of Human Type 2 Diabetes Requires Decrease in Liver and Pancreas Fat Content but Is Dependent upon Capacity for beta Cell Recovery. *Cell metabolism* **28**, 547–556.e543 (2018).
11. Coen, P. M. et al. Exercise and Weight Loss Improve Muscle Mitochondrial Respiration, Lipid Partitioning, and Insulin Sensitivity After Gastric Bypass Surgery. *Diabetes* **64**, 3737–3750 (2015).
12. Vijgen, G. H. et al. Impaired skeletal muscle mitochondrial function in morbidly obese patients is normalized one year after bariatric surgery. *Surgery for obesity and related diseases : official journal of the American Society for Bariatric Surgery* **9**, 936–941 (2013).
13. Barres, R. et al. Weight loss after gastric bypass surgery in human obesity remodels promoter methylation. *Cell reports* **3**, 1020–1027 (2013).
14. Gancheva, S., Jelenik, T., Alvarez-Hernandez, E. & Roden, M. Interorgan Metabolic Crosstalk in Human Insulin Resistance. *Physiol Rev* **98**, 1371–1415 (2018).
15. Petersen, M. C. & Shulman, G. I. Mechanisms of Insulin Action and Insulin Resistance. *Physiological reviews* **98**, 2133–2223 (2018).
16. Chujo, T. & Suzuki, T. Trmt61B is a methyltransferase responsible for 1-methyladenosine at position 58 of human mitochondrial tRNAs. *RNA (New York, N.Y.)* **18**, 2269–2276 (2012).
17. Matilainen, O., Quiros, P. M. & Auwerx, J. Mitochondria and Epigenetics - Crosstalk in Homeostasis and Stress. *Trends Cell Biol* **27**, 453–463 (2017).
18. Jones, P. A. Functions of DNA methylation: islands, start sites, gene bodies and beyond. *Nature reviews. Genetics* **13**, 484–492 (2012).
19. Davegardh, C. et al. Abnormal epigenetic changes during differentiation of human skeletal muscle stem cells from obese subjects. *BMC Med* **15**, 39 (2017).
20. Puisac, B. et al. Characterization of splice variants of the genes encoding human mitochondrial HMG-CoA lyase and HMG-CoA synthase, the main enzymes of the ketogenesis pathway. *Mol Biol Rep* **39**, 4777–4785 (2012).
21. Burri, L. et al. Mature DIABLO/Smac is produced by the IMP protease complex on the mitochondrial inner membrane. *Mol Biol Cell* **16**, 2926–2933 (2005).
22. Sica, V. & Kroemer, G. IMMP2L: a mitochondrial protease suppressing cellular senescence. *Cell Res* **28**, 607–608 (2018).
23. Guidone, C. et al. Mechanisms of recovery from type 2 diabetes after malabsorptive bariatric surgery. *Diabetes* **55**, 2025–2031 (2006).
24. Lim, E. L. et al. Reversal of type 2 diabetes: normalisation of beta cell function in association with decreased pancreas and liver triacylglycerol. *Diabetologia* **54**, 2506–2514 (2011).
25. Taylor, R., et al. Remission of Human Type 2 Diabetes Requires Decrease in Liver and Pancreas Fat Content but Is Dependent upon Capacity for beta Cell Recovery. *Cell Metab* (2018).
26. Itani, S. I., Ruderman, N. B., Schmieder, F. & Boden, G. Lipid-induced insulin resistance in human muscle is associated with changes in diacylglycerol, protein kinase C, and IkappaB-alpha. *Diabetes* **51**, 2005–2011 (2002).
27. Perreault, L., et al. Intracellular localization of diacylglycerols and sphingolipids influences insulin sensitivity and mitochondrial function in human skeletal muscle. *JCI insight* **3**, (2018).
28. Kumashiro, N. et al. Cellular mechanism of insulin resistance in nonalcoholic fatty liver disease. *Proceedings of the National Academy of Sciences of the United States of America* **108**, 16381–16385 (2011).
29. Adams, J. M. et al. Ceramide Content Is Increased in Skeletal Muscle From Obese Insulin-Resistant Humans. *Diabetes* **53**, 25–31 (2004).
30. Szendroedi, J. et al. Role of diacylglycerol activation of PKCtheta in lipid-induced muscle insulin resistance in humans. *Proceedings of the National Academy of Sciences of the United States of America* **111**, 9597–9602 (2014).
31. Szendroedi, J. et al. Muscle mitochondrial ATP synthesis and glucose transport/phosphorylation in type 2 diabetes. *PLoS medicine* **4**, e154 (2007).
32. Coen, P. M. et al. Reduced skeletal muscle oxidative capacity and elevated ceramide but not diacylglycerol content in severe obesity. *Obesity (Silver Spring, Md.)* **21**, 2362–2371 (2013).
33. Fritsch, M. et al. Time course of postprandial hepatic phosphorus metabolites in lean, obese, and type 2 diabetes patients. *The American journal of clinical nutrition* **102**, 1051–1058 (2015).
34. Bach, D. et al. Expression of Mfn2, the Charcot-Marie-Tooth neuropathy type 2A gene, in human skeletal muscle: effects of type 2 diabetes, obesity, weight loss, and the regulatory role of tumor necrosis factor alpha and interleukin-6. *Diabetes* **54**, 2685–2693 (2005).
35. Park, M. et al. A Role for Ceramides, but Not Sphingomyelins, as Antagonists of Insulin Signaling and Mitochondrial Metabolism in C2C12 Myotubes. *The Journal of biological chemistry* **291**, 23978–23988 (2016).
36. Lam, T. et al. Reversal of intramyocellular lipid accumulation by lipophagy and a p62-mediated pathway. *Cell death discovery* **2**, 16061 (2016).
37. Nijhawan, S., Richards, W., O’Hea, M. F., Audia, J. P. & Alvarez, D. F. Bariatric surgery rapidly improves mitochondrial respiration in morbidly obese patients. *Surgical endoscopy* **27**, 4569–4573 (2013).
38. Fernstrom, M. et al. Improved Muscle Mitochondrial Capacity Following Gastric Bypass Surgery in Obese Subjects. *Obesity surgery* **26**, 1391–1397 (2016).
39. Johnson, M. L. et al. Mechanism by Which Caloric Restriction Improves Insulin Sensitivity in Sedentary Obese Adults. *Diabetes* **65**, 74–84 (2016).
40. Toledo, F. G. et al. Mitochondrial capacity in skeletal muscle is not stimulated by weight loss despite increases in insulin action and decreases in intramyocellular lipid content. *Diabetes* **57**, 987–994 (2008).
41. Phielix, E., Jelenik, T., Nowotny, P., Szendroedi, J. & Roden, M. Reduction of non-esterified fatty acids improves insulin sensitivity and lowers oxidative stress, but fails to restore oxidative capacity in type 2 diabetes: a randomised clinical trial. *Diabetologia* **57**, 572–581 (2014).
42. Hoeks, J. et al. Prolonged fasting identifies skeletal muscle mitochondrial dysfunction as consequence rather than cause of human insulin resistance. *Diabetes* **59**, 2117–2125 (2010).
43. Rabol, R. et al. Reduced skeletal muscle mitochondrial respiration and improved glucose metabolism in nondiabetic obese women during a very low calorie dietary intervention leading to rapid weight loss. *Metabolism: clinical and experimental* **58**, 1145–1152 (2009).
44. Al-Najim, W., Docherty, N. G. & le Roux, C. W. Food Intake and Eating Behavior After Bariatric Surgery. *Physiological reviews* **98**, 1113–1141 (2018).
45. Morita, M. & Imanaka, T. Peroxisomal ABC transporters: structure, function and role in disease. *Biochim Biophys Acta* **1822**, 1387–1396 (2012).
46. Igarashi, M., Watanabe, K., Tsuduki, T., Kimura, I. & Kubota, N. NAPE-PLD controls OEA synthesis and fat absorption by regulating lipoprotein synthesis in an in vitro model of intestinal epithelial cells. *FASEB J* **33**, 3167–3179 (2019).
47. Fiermonte, G. et al. Identification of the mitochondrial ATP-Mg/Pi transporter. Bacterial expression, reconstitution, functional characterization, and tissue distribution. *J Biol Chem* **279**, 30722–30730 (2004).
48. Fink, B. D., Bai, F., Yu, L. & Sivitz, W. I. Regulation of ATP production: dependence on calcium concentration and respiratory state. *American journal of physiology. Cell physiology* **313**, C146–c153 (2017).
49. Raught, B. et al. Phosphorylation of eucaryotic translation initiation factor 4B Ser422 is modulated by S6 kinases. *EMBO J* **23**, 1761–1769 (2004).
50. Wang, X. et al. Regulation of elongation factor 2 kinase by p90(RSK1) and p70 S6 kinase. *EMBO J* **20**, 4370–4379 (2001).
51. Fleckenstein, D. S., Dirks, W. G., Drexler, H. G. & Quentmeier, H. Tumor necrosis factor receptor-associated factor (TRAF) 4 is a new binding partner for the p70S6 serine/threonine kinase. *Leuk Res* **27**, 687–694 (2003).
52. Tamboli, R. A. et al. Reduction in inflammatory gene expression in skeletal muscle from Roux-en-Y gastric bypass patients randomized to omentectomy. *PLoS one* **6**, e28577 (2011).
53. Sestan, M. et al. Virus-Induced Interferon-gamma Causes Insulin Resistance in Skeletal Muscle and Derails Glycemic Control in Obesity. *Immunity* **49**, 164–177.e166 (2018).
54. Day, S. E. et al. Next-generation sequencing methylation profiling of subjects with obesity identifies novel gene changes. *Clin Epigenetics* **8**, 77 (2016).
55. Leenen, F. A., Muller, C. P. & Turner, J. D. DNA methylation: conducting the orchestra from exposure to phenotype? *Clin Epigenetics* **8**, 92 (2016).
56. Kammel, A. et al. Early hypermethylation of hepatic Igf2p2 results in its reduced expression preceding fatty liver in mice. *Hum Mol Genet* **25**, 2588–2599 (2016).
57. Pietrocopa, F., Galluzzi, L., Bravo-San Pedro, J. M., Madeo, F. & Kroemer, G. Acetyl coenzyme A: a central metabolite and second messenger. *Cell Metab* **21**, 805–821 (2015).
58. Wallace, D. C. & Fan, W. Energetics, epigenetics, mitochondrial genetics. *Mitochondrion* **10**, 12–31 (2010).
59. Cheng, D. et al. Expression, purification, and characterization of human and rat acetyl coenzyme A carboxylase (ACC) isozymes. *Protein Expr Purif* **51**, 11–21 (2007).
60. Abu-Elheiga, L., Oh, W., Kordari, P. & Wakil, S. J. Acetyl-CoA carboxylase 2 mutant mice are protected against obesity and diabetes induced by high-fat/high-carbohydrate diets. *Proc Natl Acad Sci U S A* **100**, 10207–10212 (2003).
61. Berdeaux, R. & Stewart, R. cAMP signaling in skeletal muscle adaptation: hypertrophy, metabolism, and regeneration. *American journal of physiology. Endocrinology and metabolism* **303**, E1–17 (2012).
62. Savastano, S. et al. Growth hormone treatment prevents loss of lean mass after bariatric surgery in morbidly obese patients: results of a pilot, open, prospective, randomized, controlled study. *The Journal of clinical endocrinology and metabolism* **94**, 817–826 (2009).
63. Toledo, F. G. S. et al. Impact of prolonged overfeeding on skeletal muscle mitochondria in healthy individuals. *Diabetologia* **61**, 466–475 (2018).
64. Chomentowski, P., Coen, P. M., Radikova, Z., Goodpaster, B. H. & Toledo, F. G. Skeletal muscle mitochondria in insulin resistance: differences in

- intermyofibrillar versus subsarcolemmal subpopulations and relationship to metabolic flexibility. *The Journal of clinical endocrinology and metabolism* **96**, 494–503 (2011).
65. Hansen, C. S. et al. Adiponectin, biomarkers of inflammation and changes in cardiac autonomic function: Whitehall II study. *Cardiovascular diabetology* **16**, 153 (2017).
  66. Jelenik, T. et al. Mechanisms of Insulin Resistance in Primary and Secondary Nonalcoholic Fatty Liver. *Diabetes* **66**, 2241–2253 (2017).
  67. Preuss, C. et al. A New Targeted Lipidomics Approach Reveals Lipid Droplets in Liver, Muscle and Heart as a Repository for Diacylglycerol and Ceramide Species in Non-Alcoholic Fatty Liver. *Cells* **8**(2019).
  68. Folch, J., Lees, M. & Sloane Stanley, G. H. A simple method for the isolation and purification of total lipides from animal tissues. *J Biol Chem* **226**, 497–509 (1957).
  69. Huang, D. W., Sherman, B. T. & Lempicki, R. A. Systematic and integrative analysis of large gene lists using DAVID bioinformatics resources. *Nat Protoc* **4**, 44–57 (2009).
  70. Morris, T. J. & Beck, S. Analysis pipelines and packages for Infinium HumanMethylation450 BeadChip (450k) data. *Methods* **72**, 3–8 (2015).
  71. Butcher, L. M. & Beck, S. Probe Lasso: a novel method to rope in differentially methylated regions with 450K DNA methylation data. *Methods* **72**, 21–28 (2015).

## Acknowledgements

The authors would like to thank Kai Tinnes, Myrko Esser, Ilka Rokitta, David Höhn, Fariba Zivehe, and Andrea Sparla from the Institute for Clinical Diabetology, German Diabetes Center Dusseldorf for their excellent help with the experiments. This study was supported in part by the Ministry of Culture and Science of the State of North Rhine-Westfalia (MKW NRW), the German Federal Ministry of Health (BMG), by a grant of the Federal Ministry for Research (BMBF) to the German Center for Diabetes Research (DZD e.V., DZD Grant 2016), and by grants from the Helmholtz portfolio theme: Metabolic Dysfunction and Common Disease and the Helmholtz Alliance to Universities: Imaging and Curing Environmental Metabolic Diseases (ICEMED), the German Research Foundation (DFG, SFB 1116), German Diabetes Association (DDG) and the Schmutzler Stiftung.

## Author Contributions

S.G. performed the clinical experiments, analyzed data and wrote, edited, and reviewed the manuscript. M.O. performed gene expression and methylation analyses, analyzed data and wrote, edited, and reviewed the manuscript. C.K. and J.S. performed clinical experiments and edited and reviewed the manuscript. D.M. performed lipidomic analyses and edited and reviewed the manuscript. M.J. and K.S. performed statistics analyses

and edited and reviewed the manuscript. J.W. and F.G.S.T. performed electron microscopy analysis and edited and reviewed the manuscript. T.J., E.F. D.H.P., L.M., and C.H. performed laboratory analyses and edited and reviewed the manuscript. M.S. performed bariatric surgery procedures and edited and reviewed the manuscript. A.S. designed and led the gene transcription and methylation analysis and wrote, reviewed, and edited the manuscript. M.R. initiated the investigation, designed and led the clinical experiments, and wrote, reviewed, and edited the manuscript. All authors gave final approval of the version to be published. M.R. is the guarantor of this work and, as such, had full access to all the data in the study and takes responsibility for the integrity of the data and the accuracy of the data analysis.

## Additional information

**Supplementary Information** accompanies this paper at <https://doi.org/10.1038/s41467-019-12081-0>.

**Competing interests:** The authors declare no competing interests.

**Reprints and permission** information is available online at <http://npg.nature.com/reprintsandpermissions/>

**Peer review information** *Nature Communications* thanks Carel Le Roux and other anonymous reviewer(s) for their contribution to the peer review of this work. Peer reviewer reports are available.

**Publisher's note** Springer Nature remains neutral with regard to jurisdictional claims in published maps and institutional affiliations.



**Open Access** This article is licensed under a Creative Commons Attribution 4.0 International License, which permits use, sharing, adaptation, distribution and reproduction in any medium or format, as long as you give appropriate credit to the original author(s) and the source, provide a link to the Creative Commons license, and indicate if changes were made. The images or other third party material in this article are included in the article's Creative Commons license, unless indicated otherwise in a credit line to the material. If material is not included in the article's Creative Commons license and your intended use is not permitted by statutory regulation or exceeds the permitted use, you will need to obtain permission directly from the copyright holder. To view a copy of this license, visit <http://creativecommons.org/licenses/by/4.0/>.

© The Author(s) 2019, corrected publication 2022

<https://doi.org/10.1038/s41467-022-29350-0>

OPEN

# Author Correction: Dynamic changes of muscle insulin sensitivity after metabolic surgery

Sofiya Gancheva, Meriem Ouni , Tomas Jelenik, Chrysi Koliaki, Julia Szendroedi, Frederico G. S. Toledo, Daniel F. Markgraf , Dominik H. Pesta , Lucia Mastrototaro, Elisabetta De Filippo, Christian Herder , Markus Jähnert , Jürgen Weiss, Klaus Strassburger , Matthias Schlensak, Annette Schürmann  & Michael Roden 

Correction to: *Nature Communications* <https://doi.org/10.1038/s41467-019-12081-0>, published online 13 September 2019.

The original version of this article included errors in the Results and Supplementary information. During analysis of annotation of gene expression data, the skeletal muscle transcriptome data of the different microarrays used for the samples at different time points (before and after the surgery), was combined and normalized, but the command “merge” of the Software R was used incorrectly in this step. The incorrect R code used in the first submission was: “dataset1\_2 <- merge(dataset1[, 1:49], dataset2[, 1:9]) dataset<-merge (dataset1\_2,dataset3[,1:31],by=“TargetName”.

These two “merge” commands combined the expression values of all samples of three microarrays. The mistake was that the gene-annotation information-columns were not considered. The “merge” command has the argument “sort”, which by default is TRUE, leading to an alphabetical sorting of the “TargetName” column. This led to a wrong combining of the gene-annotation information-columns and the “TargetName” in a later step.

The data has now been reanalyzed, only columns with the expression data were used, and the command “inner\_join” was applied, because this command always keeps the row-order. The correct code is: “dataset1\_2 <- inner\_join(dataset1[, 1:49], dataset2[, 1:9], by=“TargetName”) dataset<-inner\_join(dataset1\_2,dataset3,by=“TargetName”. The corrected paper has been reviewed by the original reviewers #1 and #2, and by a new reviewer. The conclusions are not affected. The following changes have been made in the text and figures:

The sentence that read “To examine whether the metabolic differences reflect altered gene transcription, we initially compared the muscle transcriptome between OB before surgery (OB 0 w) and CON and detected 1037 differentially expressed genes (Fig. 3a). Gene ontology (GO) analysis indicated that several genes are implicated in the biosynthesis of long-chain fatty acyl-CoA and fatty acids as well as reactive oxygen species (ROS) metabolism (Fig. 3b; Supplementary Table 3)”. now reads “To examine whether the metabolic differences reflect altered gene transcription, we initially compared the muscle transcriptome between OB before surgery (OB 0 w) and CON and detected 595 differentially expressed genes (Fig. 3a). Gene ontology (GO) analysis indicated that several genes are implicated in the regulation of apoptotic processes (GO:0042981), MAPK cascade (GO:0043410), inflammatory response (GO:0006954, GO:0050729), oxygen transport (GO:0015671), and others (Fig. 3b; Supplementary Table 3).

The sentence that read “Comparing the muscle transcriptome of OB over the time course after surgery identified 783 out of 1287 upregulated and 504 downregulated genes at 2 weeks (Fig. 3a). GO analysis showed significant enrichments in genes controlling catabolic processes, lipid metabolism, and phosphorylation (GO:0016310; Fig. 3c, Supplementary Table 4). Among all transcripts, 1072 were transiently altered at 2 weeks and then returned to baseline values (see also below), whereas 215 remained constantly changed (Fig. 3a). These transcripts comprise genes related to the adenylate cyclase-modulating G-protein coupled receptor signaling pathway, lipid metabolism and regulation of gene expression (Supplementary Fig. 5a, Supplementary Table 5)”. now reads “Comparing the muscle transcriptome of OB over the time course after surgery identified 937 out of 1528 upregulated and 591 downregulated genes at 2 weeks (Fig. 3a). GO analysis showed significant enrichments in genes controlling transcriptional regulation (GO:0000398, GO:0010501), small GTPase-mediated signal transduction (GO:0051056), and negative regulation of insulin receptor signaling (GO:0046627) (Fig. 3c; Supplementary Table 4). Among all transcripts, 1244 were transiently altered at 2 weeks and then returned to

baseline values (see also below, Fig. 6b), whereas 203 remained constantly changed (Fig. 3a). These transcripts comprise genes related to regulation of gene expression (GO:0010467), calcium-mediated signaling (GO:0019722), and negative regulation of insulin receptor signaling (GO:0046627) (Supplementary Fig. 5a, Supplementary Table 5”).

The sentence that read “The genes exhibiting strongest changes at 2 weeks are involved in mitochondrial function (MTUS1, TRMT6), fatty acid metabolism (SLC27A4), calcium signaling (ATP2C2), transcriptional regulation (ZNF329, GTF2E2), protein transport (RAB3D), and inflammatory processes (IL18RAP) (Supplementary Table 1)”. now reads “The genes exhibiting strongest changes at 2 weeks are involved in mitochondrial function (*HMGCS2*), lipid metabolism (*ANGPTL4*, *ABCA1*, and *ABCG1*), calcium signaling (*PCDH15*), protein folding (*DNAJC28*), and inflammatory processes (*CISH*) (Supplementary Table 1)”.

The sentence that read “This revealed 49 mitochondrial, 24 lipid metabolism and 36 calcium-related genes with significantly different expression levels (Fig. 3d)”. now reads “This revealed 70 mitochondrial, 23 lipid metabolism and 60 calcium-related genes with significantly different expression levels (Fig. 3d)”.

The sentences that read “At 12 weeks after surgery, 868 genes were significantly altered (604 up- and 264 downregulated), at 24 weeks 709 genes (563 up- and 146 downregulated) in comparison to their expression before surgery (Fig. 3a). The pathways affected at 12 weeks comprise—among others—glucose homeostasis (GO0042593) and negative regulation of phosphate activity (GO:0006814) (Supplementary Fig. 5b, Supplementary Table 6). At 24 weeks, genes related to positive regulation of GTPase activity (GO:0043547) and protein autophosphorylation (GO:0046777) as well as ion transmembrane transport (GO:0034765) are mostly higher expressed than before surgery (Supplementary Fig. 5c, Supplementary Table 7). At 52 weeks, 1535 transcripts were significantly altered (Fig. 3a; Supplementary Table 6), which comprise genes involved in calcium and sodium transport and interferon- $\gamma$  signaling (Supplementary Fig. 5b) including upregulation of those contributing to transcription (*BACH1*), cytoskeletal and tubulin reorganization (*CCDC87*) (Supplementary Table 8)”. now read “At 12 weeks after surgery, 625 genes were significantly altered (341 up- and 284 downregulated), at 24 weeks 756 genes (519 up- and 237 downregulated) in comparison to their expression before surgery (Fig. 3a). The pathways affected at 12 weeks comprise—among others—glycogen metabolic process (GO:0005977), translation (GO:0006413 and GO:0006364), and transmembrane transport (GO:0055085) (Supplementary Fig. 5b, Supplementary Table 6). At 24 weeks, genes related to transmembrane receptor protein tyrosine kinase signaling (GO:0007169), cytoskeleton organization (GO:0007010), and regulation of cell growth (GO:0001558) are mostly higher expressed than before surgery (Supplementary Table 7). At 52 weeks, 1449 transcripts were significantly altered (Fig. 3a, Supplementary Table 8), which comprise genes involved glycogen metabolic process (GO:0005977), protein polyubiquitination/destabilization (GO:0016567, GO:0031648), (Supplementary Table 8) and including upregulation of those contributing to cytoskeletal and tubulin reorganization (*MYH3*, *CCDC87*, and *ACTC1*) (Supplementary Table 8)”.

The sentences that read “This enrichment explains the small overlap between differentially methylated CpGs and differentially expressed genes, as only 1467 CpGs are located in/or close to regions of the 430 differentially expressed genes (Fig. 4a). Among differentially expressed genes involved in mitochondrial function, lipid metabolism and calcium signaling, we detected 17, 4, and 15, respectively, which were affected by DNA methylation at 52 weeks (Fig. 3d, highlighted in magenta)”. now read “This enrichment explains the relatively small overlap between differentially methylated CpGs and differentially expressed genes, as only 2956 CpGs are located in/or close to regions of the 921 differentially expressed genes (Fig. 4a). Among differentially expressed genes involved in mitochondrial function, lipid metabolism, and calcium signaling, we detected 13, 6 and 30, respectively, which were affected by DNA methylation at 52 weeks (Fig. 3d, highlighted in magenta)”.

The sentence that read “However, at 52 weeks, 1467 CpGs were identified in 430 differentially expressed genes (Fig. 4a). GO analysis indicated enrichment in genes linked to 12 biological pathways, including cAMP biosynthesis, lysosomal organization, and muscle cell differentiation (Fig. 4b; Supplementary Table 9). Among those, 230 contain >2 differentially methylated CpGs and levels of altered DNA methylation ranging from 5 to 10%”. now reads “However, at 52 weeks, 2956 CpGs were identified in 921 differentially expressed genes (Fig. 4a). GO analysis indicated enrichment in genes linked to several biological pathways, including protein phosphorylation, glycogen metabolic process (GO:0005977), protein localization to plasma membrane, and vesicle-mediated transport (Fig. 4b; Supplementary Table 9). Among those, 323 contain >2 differentially methylated CpGs and levels of altered DNA methylation are higher than 5%”.

The sentences “Examples are *TBC1D1*, encoding a Rab-GTPase activating protein, *TBC1* domain family member 1, and *ASPSCR1*, encoding *UBX* domain-containing tether for *GLUT4*. Lower promoter methylation of *TBC1D1* associated with higher expression (Fig. 5a), whereas hypomethylation of *ASPSCR1* in the gene body related to lower expression at 52 weeks (Fig. 5b). Of note, both genes are involved in glucose transport via glucose transporter 4 (*GLUT4*)<sup>20,21</sup>. In addition, both *NR4A1* (nuclear receptor subfamily 4 group A member 1) and *ELOVL5* (*ELOVL* fatty acid elongase 5) exhibited hypermethylated promoters and hypomethylated gene bodies corresponding to lower expression (Fig. 5c, d). *ELOVL5* is involved in the elongation of long-chain polyunsaturated fatty acids 22 and upregulated upon high-fat feeding<sup>23</sup>, *NR4A1* encodes a nuclear receptor and transcription factor regulating the expression of genes involved in glucose metabolism<sup>24</sup>. In addition, the time course of the expression of the listed candidates was evaluated. *TBC1D1* expression increased and *ASPSCR1* decreased already at 2 weeks, whereas the changes of the expression of *ELOVL5* and *NR4A1* occurred only at 52 weeks (Supplementary Fig. 9)”. now read “Examples are *PTPRE*, a negative regulator of insulin receptor (IR) signaling in skeletal muscle; *PIK3R1*, a regulator of the PI3-kinase; *MLXIP*, involved in transcriptional activation of glycolytic target genes, and *ACACB*, a mitochondrial enzyme playing a role in fatty acid metabolism (Fig. 5a–d). A hypermethylation in the promoter region of *PTPRE* gene related to lower expression at 52 weeks (Fig. 5a). A lower DNA methylation in the promoter and a higher methylation in the gene body of *PIK3R1* is linked to its higher expression after the surgery (Fig. 5b), whereas a hypomethylation in the gene body of *MLXIP* and *ACACB* associated with their lower expression (Fig. 5c, d). In addition, the time course of the expression of

the listed candidates was evaluated. *PTPRE* expression decreased already at 2 weeks, whereas the changes of the expression of *PI3KR1* occurred at 12 weeks and *ACACB* and *MLXIP* at 52 weeks (Supplementary Fig. 9”).

The sentences that read “Table 2 lists the expression levels of several genes associated with changes in M-value (27), fasting glucose (231), HMW-adiponectin (61), and mitochondrial content (13). GO analysis of the 231 affected genes, which correlated to glucose concentrations, can be linked to regulation of DNA binding (GO:0043388), macromolecule catabolism (GO:0009057), exocytosis (GO:0006887), secretion (GO:0032940), and others (Supplementary Table 10). The correlation analysis of the 430 differentially expressed and methylated genes (at 52 weeks) revealed 43 genes associated with BMI, 189 with M-value, and 31 with HMW-adiponectin (Table 3). The correlations between methylation levels and M-value of the OB group for *ASPCSR1* ( $R_2 = 0.233$ ;  $p = 0.0009$ , Pearson correlation) and *ELOVL5* ( $R_2 = 0.234$ ;  $p = 0.0009$ , Pearson correlation) indicate that their interindividual epigenetic alterations are linked to the improvement in insulin sensitivity (Supplementary Fig. 10).” now read “In order to relate the differential expression and changes in DNA methylation to the primary metabolic phenotypes, e. g. body weight, insulin sensitivity, we calculated their correlation. Table 2 lists the expression levels of several genes associated with changes in M-value (27), fasting glucose (1219), HMW-adiponectin (73), and mitochondrial content (29). GO analysis of the 1219 affected genes, which correlated to glucose concentrations, can be linked to cytoskeleton organization (GO:0007010), calcium signaling (GO:0016338), and others (Supplementary Table 10). The correlation analysis of the 921 differentially expressed and methylated genes (at 52 weeks) revealed 177 genes associated with BMI, 443 with M-value, and 70 with HMW-adiponectin (Table 3). The correlations between methylation levels and M-value of the OB group for *PTPRE* ( $R_2 = 0.286$ ;  $p = 10^{-4}$ , Pearson correlation) and *PIK3R1* ( $R_2 = 0.312$ ;  $p = 5.10^{-5}$ , Pearson correlation) indicate that their interindividual epigenetic alterations are linked to the improvement in insulin sensitivity (Supplementary Fig. 10”).

The sentence “As 1072 transcripts (encoded by 468 genes) were only transiently differentially expressed at 2 weeks (Fig. 3a) and returned to baseline expression levels, we tested whether epigenetic alterations were responsible for this effect”. now reads “As 1150 mRNAs (encoded by 1126 genes) were only transiently differentially expressed at 2 weeks (Fig. 3a) and returned to baseline expression levels, we tested whether epigenetic alterations were responsible for this effect”.

The sentence “Indeed, 93% (438) of these genes showed changes in DNA methylation at 52 weeks (Fig. 6a; Chi-square  $p < 10^{-255}$ ), including genes involved in mitochondrial function ( $n = 22$ ), calcium signaling ( $n = 20$ ), lipid metabolism ( $n = 10$ ). Representative examples comprise *FTO*, an obesity-related gene encoding  $\alpha$ -ketoglutarate dependent dioxygenase 25, and *TOMM7*, a translocase of outer mitochondrial membrane 7 involved in translocation of pre-proteins into mitochondria 26,27 (Fig. 6b; Supplementary Fig. 9)”. now reads “Indeed, 75% (849) of these genes showed changes in DNA methylation at 52 weeks (Fig. 6a; Chi-square  $p < 10^{-255}$ ), including genes involved in mitochondrial function ( $n = 12$ ), calcium signaling ( $n = 11$ ), lipid metabolism ( $n = 4$ ). Representative examples comprise *HMGCS2* (hydroxymethylglutaryl-CoA synthase<sup>20</sup>, and *IMMP2L* a mitochondrial inner membrane protease subunit 2 involved in peptides translocation into mitochondria<sup>21,22</sup> (Fig. 6b; Supplementary Fig. 9)”.

The sentence “Before surgery, as described previously<sup>13,19</sup>, particularly genes involved in lipid metabolism, such as *SCD5* (stearoyl-CoA desaturase 5), exhibited differential expression” now reads “Before surgery, as described previously<sup>13,19</sup> particularly genes involved in lipid metabolism, such as *FFAR4* (free fatty acid receptor 4), exhibited differential expression”.

The sentence “Elevated *SLC27A4* (fatty acid transporter 4) expression at 2 weeks likely reflects the higher FFA uptake 50. Also, genes related to mitochondria and calcium handling showed higher expression levels, such as *ATP2C2*, encoding a manganese-transporting calcium ATPase 51, and *MCUR1*, a key regulator of oxidative phosphorylation 52, encoding a mitochondrial calcium uniporter protein required for calcium”. now reads “Elevated *ABCD3* (ATP-binding cassette sub-family D member 3) or *NAPELD* (N-acyl-phosphatidylethanolamine-hydrolyzing phospholipase D) expression at 2 weeks likely reflects the higher FFA uptake<sup>45,46</sup>. Also, genes related to mitochondria and calcium handling showed higher expression levels, such as *SLC25A25* (calcium-binding mitochondrial carrier protein SCaMC-2) encoding a calcium-dependent mitochondrial solute carrier<sup>47</sup>”.

The sentences “Consequently, elevated *MCUR1* expression can be linked to the evanescent stimulation of  $\beta$ -oxidation. Another set of transiently upregulated genes relates to inflammatory processes, such as *IL18RAP*, encoding the receptor accessory protein of the pro-inflammatory interleukin 18 (IL18)<sup>54</sup>. Interestingly, carriers of polymorphisms in the *IL18RAP* gene suffer from greater susceptibility to obesity<sup>54</sup>”. now read “Another set of transiently upregulated genes relates to small GTPase-mediated signaling, such as *ARHGAP24*, *RACGAP1*, *ITSN1* and to negative regulation of insulin signaling, such as *SOCS1*, *RPS6KB1*. The latest mediates TNF-alpha-induced insulin resistance by phosphorylating *IRS1* at multiple serine residues, resulting in accelerated degradation of *IRS1*<sup>49–51</sup>”.

The sentence that read “Likewise, *MTUS1*, possibly contributing to protection against pro-inflammatory response of endothelial cells 55, may be involved in the anti-inflammatory defense at 2 weeks. In addition, *MTUS1* has recently been shown to be involved in mitochondrial motility, fusion, and in the maintenance of mitochondrial morphology 56 and its reduction at 2 weeks may serve to support the evidence for alterations of mitochondrial content and function early after surgery.” has now been deleted.

The sentences “Nearly 1500 of the differentially methylated CpGs are associated with altered expression of the corresponding 430 genes, pointing towards the relevance of epigenetic mechanisms in response to weight loss. Metabolic surgery remodels DNA methylation of glucose and lipid metabolism-related genes, such as *TBC1D1*, contributing to *GLUT4* translocation<sup>20</sup>, *ASPCSR1*, a tethering protein sequestering *GLUT4*-containing vesicles<sup>21</sup> and *ELOVL5*, which is essential for fatty acid synthesis<sup>22</sup> and known to be upregulated in human skeletal muscle upon overfeeding<sup>23</sup>”. now read “Nearly 3000 of the differentially methylated CpGs are associated with altered expression of the corresponding 921 genes, pointing towards the relevance of epigenetic mechanisms in response to weight loss. Metabolic surgery remodels DNA methylation of genes involved in insulin signaling, such as *PIK3R1* and *PTPRE* and *ACACB*

(also designated *ACC2*), which is essential for fatty acid metabolism<sup>59</sup>. Mice lacking *Acc2* exhibit higher fatty acid oxidation rates in the soleus muscle than control mice<sup>60</sup>.

The sentences “The present study identified close to 100 epigenetic changes associated with altered expression of important metabolic genes, likely contributing to improved insulin sensitivity and lipid metabolism. Pathway enrichment analysis of the 430 differentially expressed and methylated genes indicates that several genes are implicated in the regulation of muscle cell differentiation, intracellular signal transduction, and cAMP biosynthesis, reflecting improved skeletal muscle activity and metabolism<sup>64</sup>.” now reads “The present study identified close to 300 epigenetic changes associated with altered expression of important metabolic genes, likely contributing to improved insulin sensitivity and lipid metabolism. Pathway enrichment analysis of the 921 differentially expressed and methylated genes indicate that several genes are implicated in the regulation of glycogen metabolism, intracellular signal transduction, and cAMP biosynthesis, reflecting improved skeletal muscle activity and metabolism<sup>61</sup>”.

The sentence “Moreover, the present study found that changes in DNA methylation are associated with reprogramming up to 70% of the transiently altered transcripts, which possibly normalize their expression levels at 52 weeks (Fig. 6).” now reads “Moreover, the present study found that changes in DNA methylation are associated with reprogramming up to 75% of the transiently altered transcripts, which possibly normalize their expression levels at 52 weeks (Fig. 6)”.

The original version of this Article contained an error in Tables 2 and 3. The correct version of the ‘Number of genes’ row in Table 2 states 25 for Body mass index, 1219 for Fasting glucose, 76 for FFA suppression, 73 for HMW-adiponectin, 29 for Mitochondria content, instead of the original values of 17, 231, 11, 61, and 13, respectively. The correct version of the row ‘Number of genes’ in Table 3 states 177 for Body mass index, 443 for M-value, 163 for Fasting glucose, 112 for FFA suppression, 70 for HMW-adiponectin, and 27 for Mitochondrial content, instead of the original values of 43, 189, 98, 38, 31, and 9, respectively.

The original version of the Supplementary Information associated with this Article contained errors in Supplementary Figs. 5, 7, 9, and 10. The HTML has been updated to include a corrected version of the Supplementary Information; the original incorrect versions of these Figures can be found as Supplementary Information associated with this Correction.

All gene ontology terms depicted in Supplementary Fig. 5 are corrected. In Supplementary Fig. 7, the numbers shown in the Venn diagram as well as the overlapping genes (*PIK3R1*, *HMGCS2*, *MAPK10*...) were changed.

Genes shown in Supplementary Fig. 9 “*ASPSCR1*, *NR4A1*, *Elovl5*, *TBC1D1*, *TOMM7* and *FTO*” are replaced by the correct candidates: “*ACACB*, *PTPRE*, *PI3KR1*, *MLXIP*, *IMML2P*, *HMGCS2*”. The correlation plots in Supplementary Fig. 10 were substituted with the corrected ones (from “*ASPSCR1*, *ELOVL5*” to “*PTPRE*, *PIK3R1*”).

All genes shown in Supplementary Tables 1–10 are corrected. We included the following information “Gene names given in italics” in the updated manuscript.

In the updated Supplementary Tables 3–10 the Go-terms used in dedicated figures are highlighted in green. Table annotations had been changed accordingly.

In addition, as part of the re-review to resolve this correction, it was also noticed that multiple correction was not applied to the data. This has now been addressed, and in the Statistical Analysis section of the “Methods”, the following text was added “Correction for multiple testing was performed for the methylome data and not for the transcriptome data. The reason for this is to avoid the number of false negatives and oversee relevant effects according to suggestions of John H. McDonald (McDonald, J.H. 2014. Handbook of Biological Statistics (3rd ed.). Sparky House Publishing, Baltimore, Maryland; p. 254–260). However, we provided the results of the multiple correction in the Supplementary Tables from S11 to 15” in the Statistical Analysis section of the “Methods”.

The current version of the manuscript also adds in the Legend of Fig. 3, the text “For gene expression unadjusted *p*-value and DNA methylation data are adjusted for multiple testing with Benjamini Hochberg correction”. In the legend for Fig. 4 the sentence that read “Up- and downregulated genes are indicated by red and blue signals, respectively. \**p* < 0.05 (paired t test, *n* = 16, methylation data with Benjamini Hochberg correction)” now reads “Up- and downregulated genes are indicated by red and blue signals, respectively. \**p* < 0.05 (unadjusted *p*-value paired t test for gene expression, *n* = 16, methylation data with Benjamini Hochberg correction)”. The legend of Fig. 5, where it read “Only significantly differentially methylated CpGs are represented; \**p* < 0.05 (paired t test, *n* = 16, methylation data with Benjamini Hochberg correction)” now reads “Only significantly differentially methylated CpGs are represented; \**p* < 0.05 (Gene expression unadjusted *p*-value paired t test, *n* = 16, methylation data with Benjamini Hochberg correction)”. The legend of Fig. 6, where it read “\**p* < 0.05 (two-tailed paired t test, *n* = 16, methylation data with Benjamini Hochberg correction)” now reads “\**p* < 0.05 (Gene expression unadjusted *p*-value two-tailed paired t test, *n* = 16, methylation data with Benjamini Hochberg correction) (b)”.

The results of the multiple correction testing, requested by the reviewers, are now included in Supplementary Data 1.

The original version of Table 2 and 3, and those of Figures 3, 4, 5, and 6 have now been replaced with corrected versions.

The previous version of Table 2 was:

<b>Table 2 Pearson correlations between gene expression levels and indicated clinical parameters.</b>						
	<b>Body mass index</b>	<b>M-value</b>	<b>Fasting glucose</b>	<b>FFA suppression</b>	<b>HMW-adiponectin</b>	<b>Mitochondrial content (CSA)</b>
Number of genes	17	27	231	11	61	13

The correct version appears as:

<b>Table 2 Pearson correlations between gene expression levels and indicated clinical parameters.</b>						
	<b>Body mass index</b>	<b>M-value</b>	<b>Fasting glucose</b>	<b>FFA suppression</b>	<b>HMW-adiponectin</b>	<b>Mitochondrial content (CSA)</b>
Number of genes	25	27	1219	76	73	29

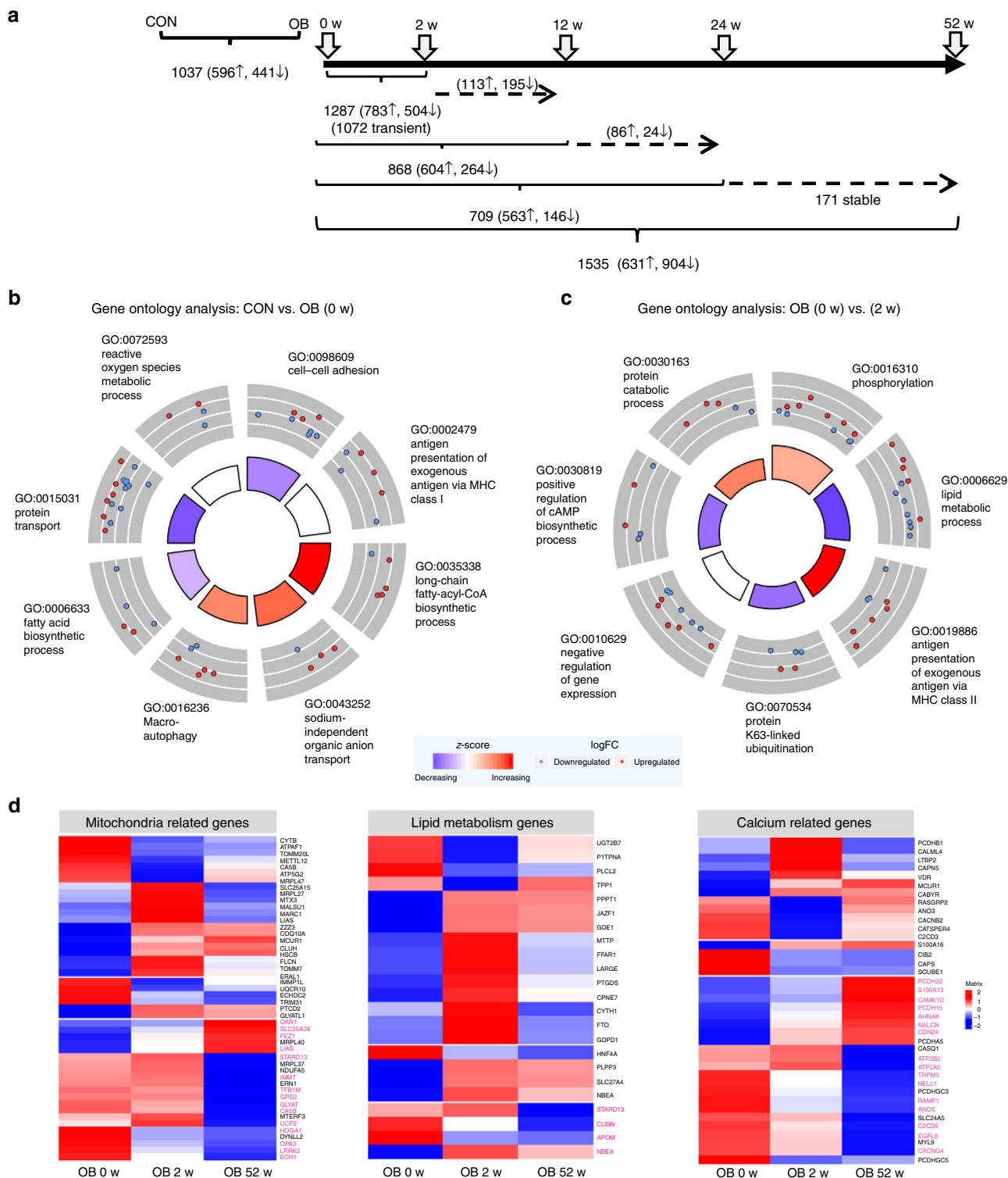
The previous version of Table 3 was:

<b>Table 3 Number of genes differentially expressed and methylated at 52 and exhibiting at least one CpG significantly correlated to the indicated clinical parameters.</b>						
	<b>Body mass index</b>	<b>M-value</b>	<b>Fasting glucose</b>	<b>FFA suppression</b>	<b>HMW-adiponectin</b>	<b>Mitochondrial content (CSA)</b>
Number of genes	43	189	98	38	31	9

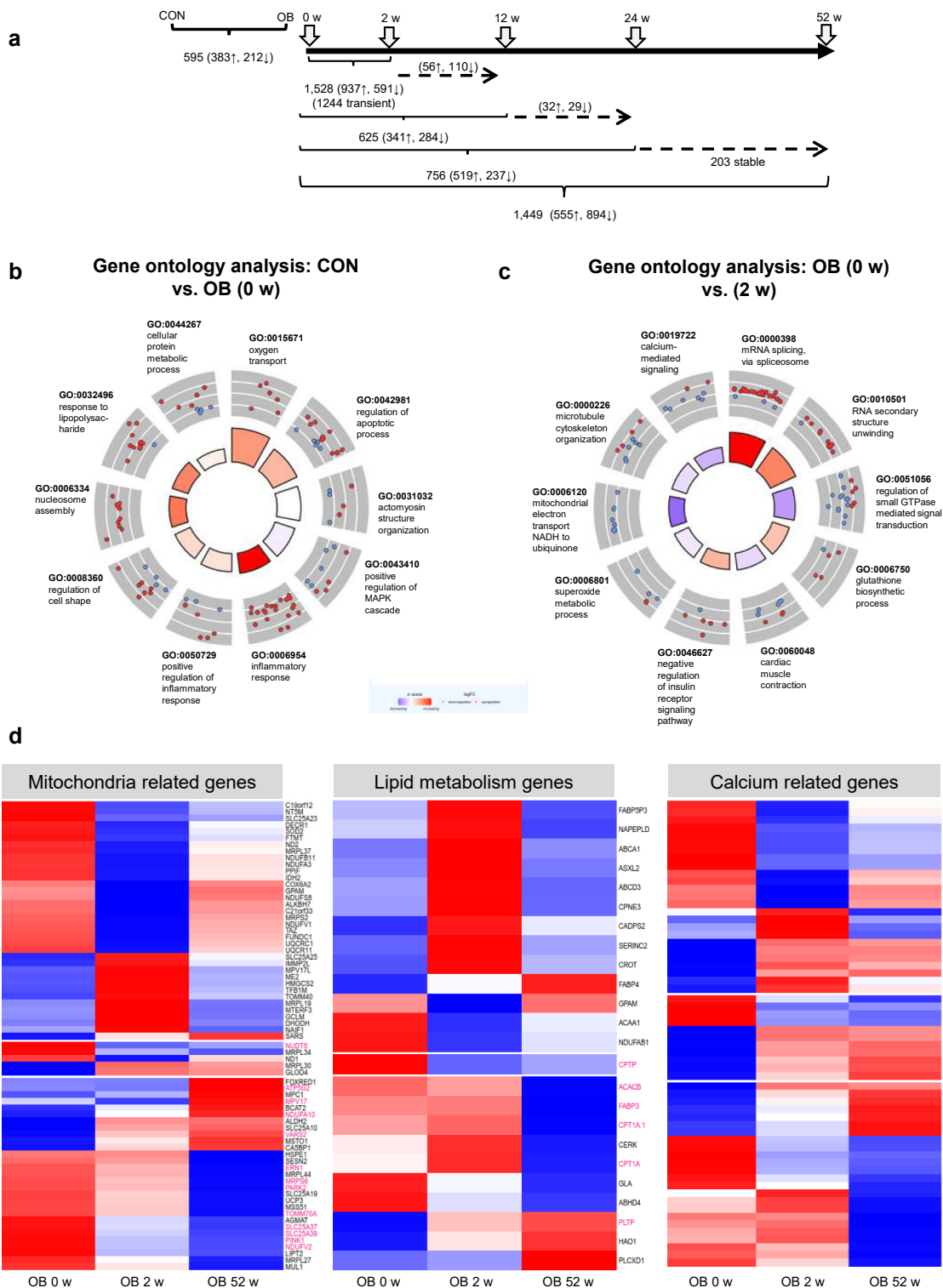
The correct version appears as:

<b>Table 3 Number of genes differentially expressed and methylated at 52 and exhibiting at least one CpG significantly correlated to the indicated clinical parameters.</b>						
	<b>Body mass index</b>	<b>M-value</b>	<b>Fasting glucose</b>	<b>FFA suppression</b>	<b>HMW-adiponectin</b>	<b>Mitochondrial content (CSA)</b>
Number of genes	177	443	163	112	70	27

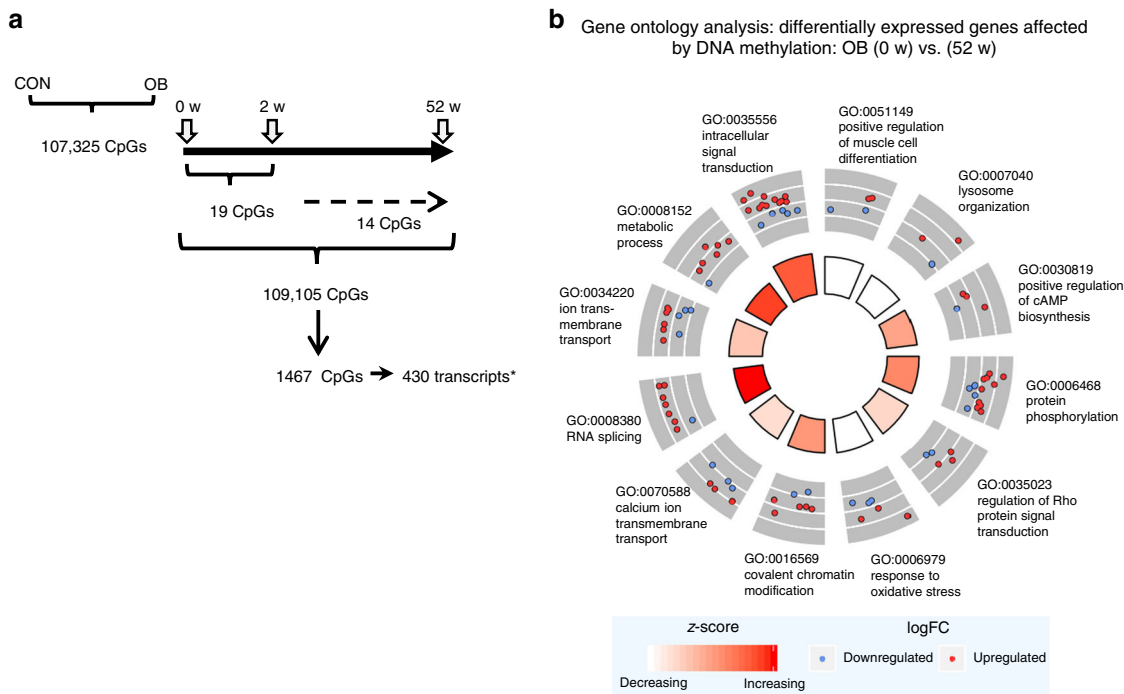
The previous version of Figure 3 was:



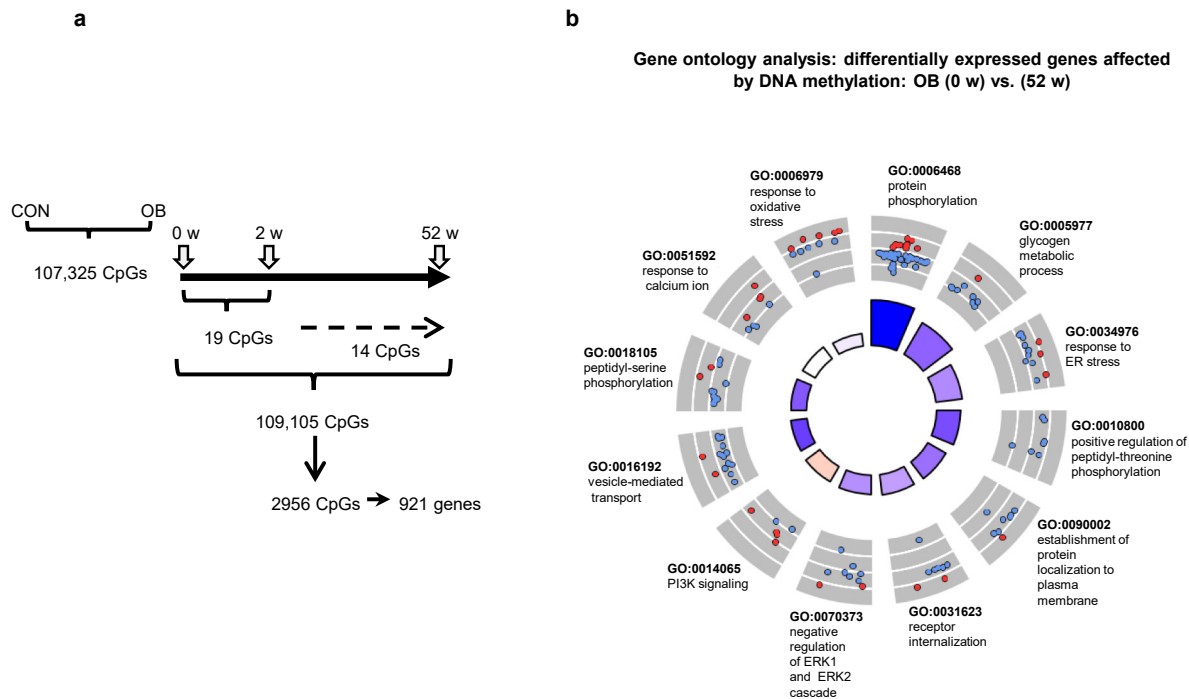
The correct version appears as:



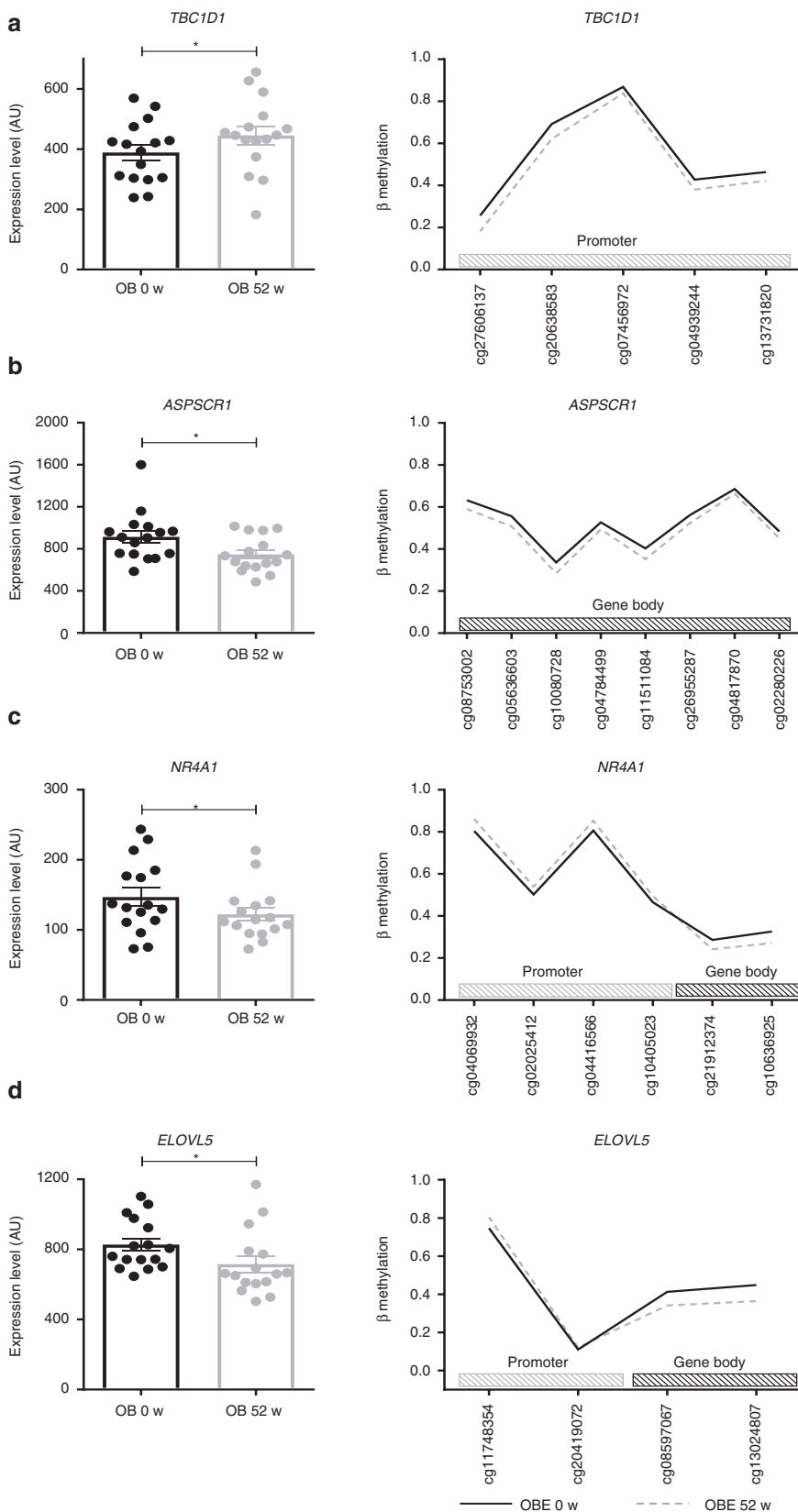
The previous version of Figure 4 was:



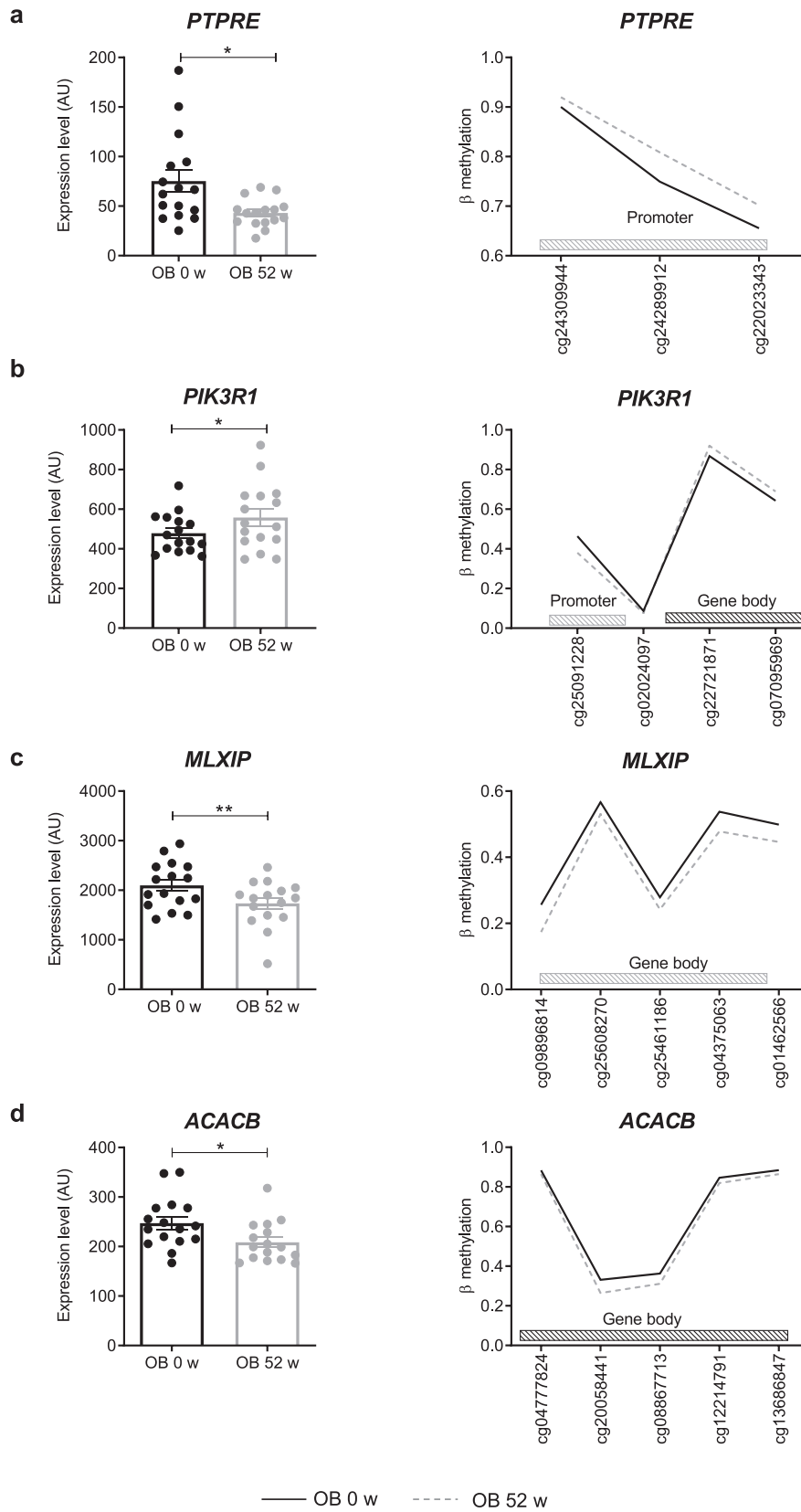
The correct version appears as:



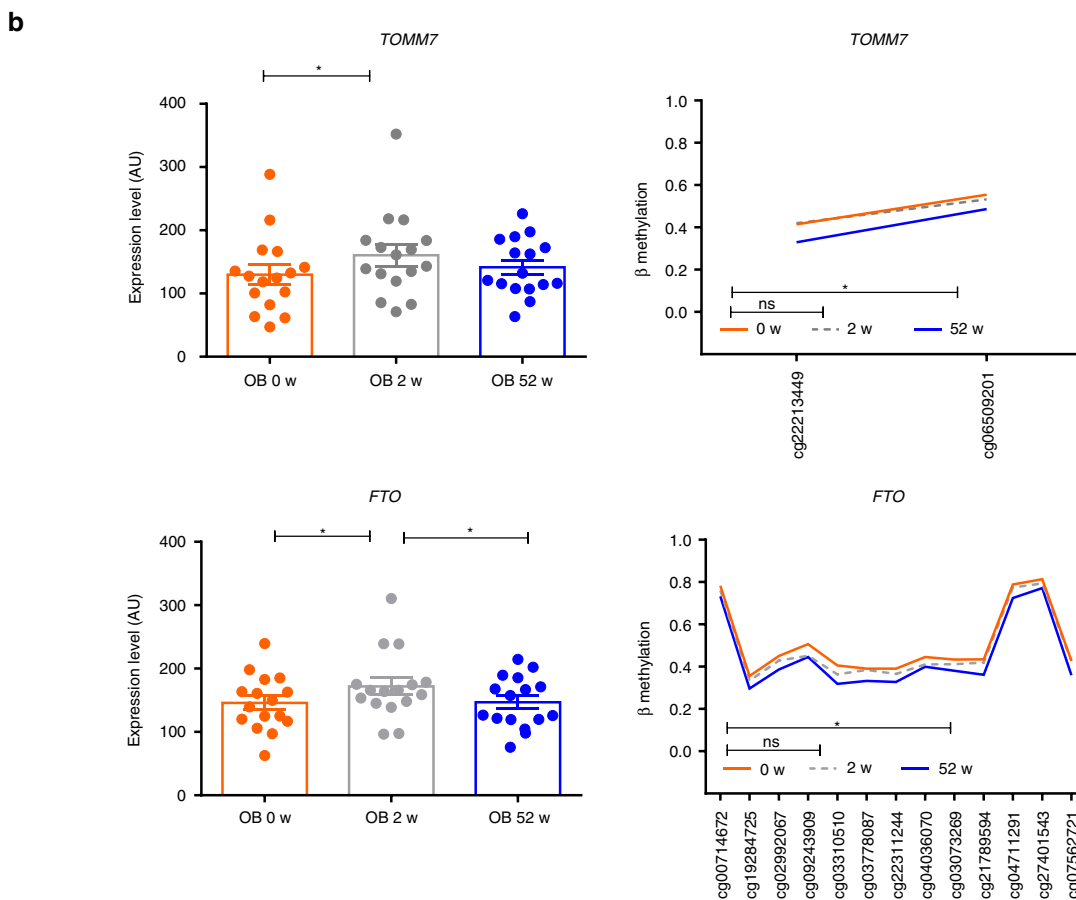
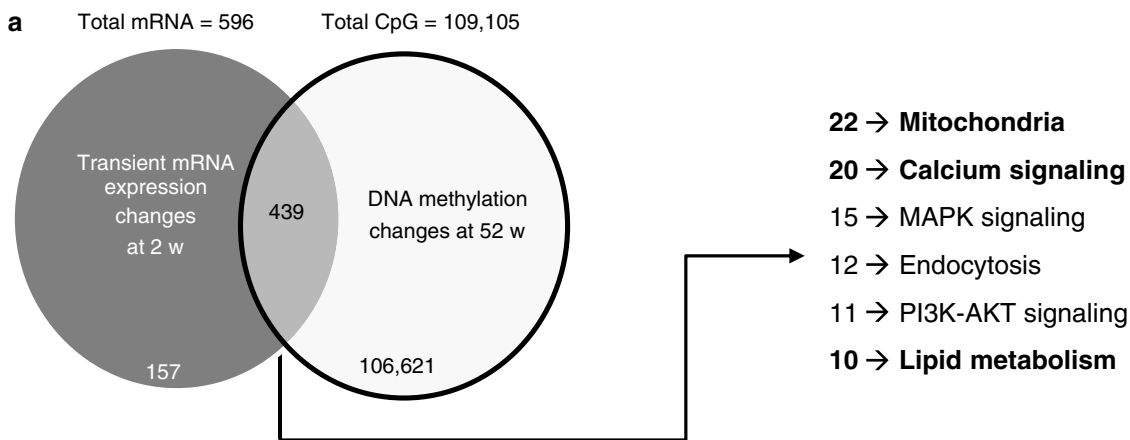
The previous version of Figure 5 was:



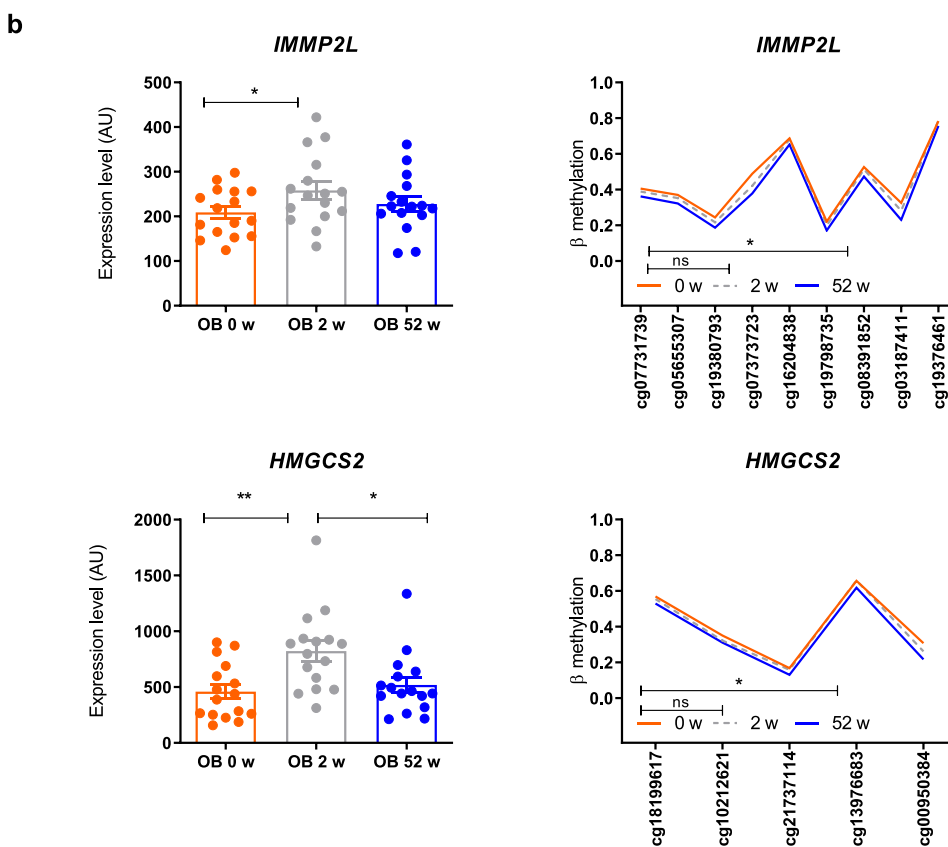
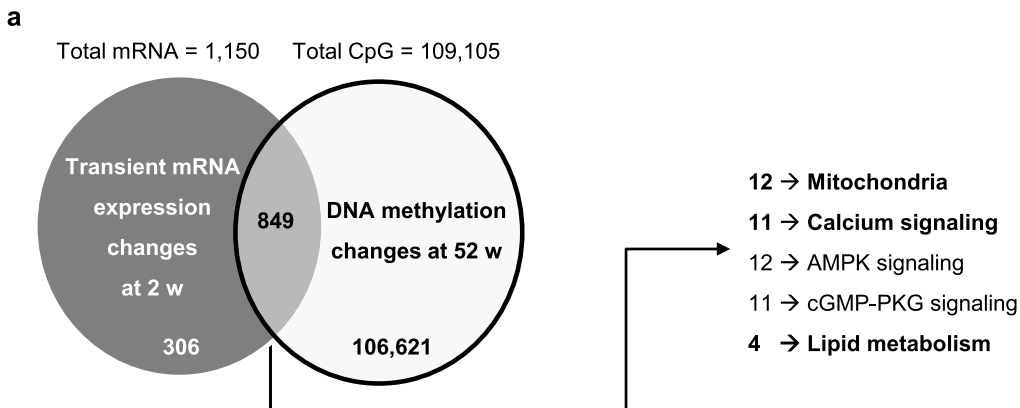
The correct version appears as:



The previous version of Figure 6 was:



The correct version appears as:



These errors have been corrected in the HTML and PDF versions of the article. The HTML has been updated to include a corrected version of the Supplementary information.

Published online: 10 June 2022

**Open Access** This article is licensed under a Creative Commons Attribution 4.0 International License, which permits use, sharing, adaptation, distribution and reproduction in any medium or format, as long as you give appropriate credit to the original author(s) and the source, provide a link to the Creative Commons license, and indicate if changes were made. The images or other third party material in this article are included in the article's Creative Commons license, unless indicated otherwise in a credit line to the material. If material is not included in the article's Creative Commons license and your intended use is not permitted by statutory regulation or exceeds the permitted use, you will need to obtain permission directly from the copyright holder. To view a copy of this license, visit <http://creativecommons.org/licenses/by/4.0/>.

© The Author(s) 2022

## ARTICLE OPEN



## Bariatric Surgery

# Metabolic surgery-induced changes of the growth hormone system relate to improved adipose tissue function

Sofiya Gancheva<sup>1,2,3</sup>, Sabine Kahl<sup>2,3</sup>, Christian Herder<sup>1,2,3</sup>, Klaus Strassburger<sup>3,4</sup>, Theresia Sarabhai<sup>1,2,3</sup>, Kalliopi Pafili<sup>1,2,3</sup>, Julia Szendroedi<sup>1,2,3,5</sup>, Matthias Schlensak<sup>6</sup> and Michael Roden<sup>1,2,3</sup>✉

© The Author(s) 2023

**AIMS:** Body weight loss improves insulin resistance and growth hormone secretion in obesity, which may be regulated by leptin according to preclinical studies. How changes in leptin, lipids and insulin sensitivity after bariatric (metabolic) surgery affect the human growth hormone system is yet unclear.

**PARTICIPANTS AND METHODS:** People with obesity (OBE,  $n = 79$ , BMI  $50.8 \pm 6.3$  kg/m<sup>2</sup>) were studied before, 2, 12, 24 and 52 weeks after metabolic surgery and compared to lean healthy humans (control; CON,  $n = 24$ , BMI  $24.3 \pm 3.1$  kg/m<sup>2</sup>). Tissue-specific insulin sensitivity was assessed by hyperinsulinemic-euglycemic clamps with D-[6,6-<sup>2</sup>H<sub>2</sub>]glucose. Fasting leptin, growth hormone (GH), insulin-like growth factor 1 (IGF-1) and IGF-binding proteins (IGFBP1, IGFBP3) were measured using ELISA.

**RESULTS:** At baseline, OBE exhibited higher glycemia and leptinemia as well as pronounced peripheral, adipose tissue and hepatic insulin resistance compared to CON. GH and IGFBP1 were lower, while IGF1 was comparable between groups. At 52 weeks, OBE had lost 33% body weight and doubled their peripheral insulin sensitivity, which was paralleled by continuous increases in GH, IGF-1 and IGFBP1 as well as decrease in leptin. The rise in GH correlated with reductions in free fatty acids, adipose tissue insulin resistance and insulinemia, but not with changes in body weight, peripheral insulin sensitivity, glycemia or leptinemia. The rise in IGF-1 correlated with reduction in high-sensitive C-reactive protein.

**CONCLUSION:** Reversal of alterations of the GH-IGF-1 axis after surgically-induced weight loss is unlikely related to improved leptin secretion and/or insulin sensitivity, but is rather associated with restored adipose tissue function and reduced low-grade inflammation.

*International Journal of Obesity*; <https://doi.org/10.1038/s41366-023-01292-7>

## INTRODUCTION

The rising prevalence of obesity and its associated complications such as type 2 diabetes (T2D), cardiovascular disease or cancers is becoming an increasing burden to healthcare systems globally [1]. In addition, endocrine disorders such as thyroid dysfunction [2] and particularly impaired growth hormone (GH) secretion [3] have been linked to the obesity epidemic.

Body weight loss improves insulin sensitivity even leading to remission of T2D, but may also normalise GH secretion by yet unclear mechanisms [4]. Effective weight loss upon bariatric (metabolic) surgery has been shown to profoundly alter gastrointestinal hormones controlling glucose and energy homeostasis [5] but also to increase circulating GH concentrations. In contrast, cross-sectional studies on its impact on circulating insulin-like growth factor 1 (IGF-1) revealed conflicting results, by showing unchanged [6–8], decreased [9, 10] or even increased concentrations [11, 12] in lean humans compared with people with obesity.

IGF-1 is involved in the regulation of both GH and insulin secretion to promote physiological carbohydrate and lipid metabolism [13], but its contribution to the improvement in tissue-specific insulin sensitivity after bariatric surgery also remains unclear.

The complex regulation of the GH-IGF-1 axis includes hypothalamic neuropeptides, ghrelin, insulin, free fatty acids (FFA), nutritional factors and IGF1-binding proteins (IGFBPs) [14]. Leptin, a key signal of long-term energy availability and an indicator of fat mass, inhibits GH secretion [15] and has been implicated in the regulation of IGF-1 secretion [16]. Indeed, recent studies showed that leptin substitution in children increases IGF-1 levels [17]. Furthermore, improvement of insulin sensitivity after metabolic surgery determines the restoration of leptin sensitivity through a molecular mechanism involving fatty acid-control of muscle malonyl-Co-A synthesis [15], indicating a direct link between leptin levels and lipid availability. Furthermore, increased muscle lipid oxidation pathways and regulation of muscle differentiation

<sup>1</sup>Department of Endocrinology and Diabetology, Medical Faculty and University Hospital, Heinrich-Heine University, Düsseldorf, Germany. <sup>2</sup>Institute for Clinical Diabetology, German Diabetes Center, Leibniz Center for Diabetes Research at Heinrich Heine University, Düsseldorf, Germany. <sup>3</sup>German Center for Diabetes Research (DZD e.V.), Partner Düsseldorf, Munich-Neuherberg, Düsseldorf, Germany. <sup>4</sup>Institute for Biometrics and Epidemiology, German Diabetes Center, Leibniz Center for Diabetes Research at Heinrich Heine University, Düsseldorf, Germany. <sup>5</sup>Department of Internal Medicine I and Clinical Chemistry, Heidelberg University Hospital, Heidelberg, Germany. <sup>6</sup>Obesity and Reflux Center, Neuwerk Hospital, Mönchengladbach, Germany. ✉email: michael.roden@ddz.de

Received: 4 December 2022 Revised: 26 February 2023 Accepted: 1 March 2023

Published online: 23 March 2023

**Table 1.** Participants' characteristics.

Parameter	CON	OBE				
		Baseline	2 w	12 w	24 w	52 w
N (male)	24 (10)	79 (16)	66 (14)	76 (15)	73 (16)	68 (15)
Age (years)	43.7 ± 11.8	40.3 ± 9.2				
BMI (kg/m <sup>2</sup> )	24.3 ± 3.1	50.8 ± 6.3 <sup>a</sup>	47.0 ± 5.9 <sup>b</sup>	41.7 ± 5.8 <sup>b</sup>	37.7 ± 5.7 <sup>b</sup>	33.8 ± 5.5 <sup>b</sup>
Glucose (mg/dl)	84 ± 8	98 ± 26 <sup>a</sup>	92 ± 23 <sup>b</sup>	85 ± 16 <sup>b</sup>	82 ± 12 <sup>b</sup>	80 ± 10 <sup>b</sup>
Insulin (μU/ml)	6(3;8)	21(17;31) <sup>a</sup>	19(14;23) <sup>b</sup>	12(8;17) <sup>b</sup>	9(7;13) <sup>b</sup>	8(5;11) <sup>b</sup>
HbA1c (%)	5.2 ± 0.4	5.9 ± 0.9 <sup>a</sup>	5.5 ± 0.8 <sup>b</sup>	5.3 ± 0.5 <sup>b</sup>	5.2 ± 0.5 <sup>b</sup>	5.1 ± 0.4 <sup>b</sup>
FFA (μmol/l)	388 (316; 630)	679 (509; 822) <sup>a</sup>	1003 (864; 1169) <sup>b</sup>	658 (566; 833)	592 (460; 779)	466 (357; 618) <sup>b</sup>
Triglycerides (mg/dl)	105 ± 91	131 ± 63	129 ± 46	115 ± 35	101 ± 31 <sup>b</sup>	88 ± 30 <sup>b</sup>
hsCRP (mg/dl)	0.2 ± 0.1	1.0 ± 0.8 <sup>a</sup>	1.1 ± 1.8	0.6 ± 0.4 <sup>b</sup>	0.4 ± 0.4 <sup>b</sup>	0.3 ± 0.5 <sup>b</sup>
CCL18 (pg/ml)	37682 ± 14453	74662 ± 25808 <sup>a</sup>	74502 ± 23446	73024 ± 26199	67003 ± 22096 <sup>b</sup>	49535 ± 16623 <sup>b</sup>
Adipo-IR (AU)	2538 ± 1651	17064 ± 10720 <sup>a</sup>	21764 ± 14247 <sup>b</sup>	8876 ± 5492 <sup>b</sup>	7732 ± 10000 <sup>b</sup>	4443 ± 37097 <sup>b</sup>
FFA suppression (%)	90.3 ± 5.3	85.4 ± 12.7	59.3 ± 21.7 <sup>b</sup>	90.5 ± 7.2 <sup>b</sup>	94.3 ± 3.5 <sup>b</sup>	94.6 ± 3.5 <sup>b</sup>

Mean ± SD or median (Q1;Q3).

*Adipo-IR* adipose tissue insulin resistance index, *BMI* body mass index, *CCL18* CC chemokine ligand 18, *FFA suppression* (FFA<sub>fasting</sub>-FFA<sub>clamp 360 min</sub>)\*100/FFA<sub>fasting</sub>, *CON* lean healthy controls, *FFA* plasma free fatty acids, *hsCRP* high-sensitive C-reactive protein, *HIS* hepatic insulin sensitivity index (100/(fasting endogenous glucose production\*fasting insulin)), *OBE* people with obesity at baseline.

<sup>a</sup>*p* < 0.05 vs CON.

<sup>b</sup>*p* < 0.05 vs OBE at baseline.

in people with obesity at 52 weeks after metabolic surgery [18] could relate to improved leptin and GH secretion. However, a direct association and possible mediators have not been demonstrated so far.

Previous studies were performed on rather small cohorts without detailed metabolic characterisation or without a lean control group and longer-term recording of the GH-IGF-1 axis after metabolic surgery [9, 15, 19–22]. The present study closely monitored the post-surgical time course of changes in the GH-IGF1 axis in comprehensively phenotyped individuals with class 3 obesity to elucidate factors associated with the reversal of altered GH-IGF-1 secretion. We hypothesised that post-surgical GH-IGF-1 axis improvements relate to the restoration of adipose tissue dysfunction and insulin sensitivity via changes in the secretion patterns of adipokines and pro-inflammatory cytokines.

## METHODS

### Study population

We studied people with obesity of Caucasian origin (OBE, *n* = 79) before and 2, 12, 24 and 52 weeks after sleeve gastrectomy (*n* = 30) or gastric bypass surgery (*n* = 49). Healthy Caucasians without obesity were examined once as controls (CON, *n* = 24). T2D was present in 19 of the participants with obesity. All participants were non-smokers, engaged only in light physical activity and neither had previous pituitary disease (including known GH deficiency) or surgery nor received GH replacement. Data of some participants were part of previous reports of the BARIA\_DDZ cohort [18, 23]. They provided informed written consent to this registered clinical cohort study (NCT01477957), which was approved by the ethics board of Heinrich-Heine University and University Hospital Düsseldorf and the ethics board of the North Rhine regional physicians' association.

### Clamp test

Each participant underwent 3 h hyperinsulinemic-euglycemic clamps employing the isotopic dilution technique using D-[6,6-<sup>2</sup>H<sub>2</sub>]glucose for measuring whole-body (mainly skeletal muscle) insulin sensitivity from insulin-stimulated rate of glucose disposal (clamp-Rd) [18, 23]. Fasting hepatic insulin sensitivity (HIS) was calculated by the formula: 100/(fasting endogenous glucose production (EGP)\*fasting insulin) [23]. Adipose tissue insulin resistance was assessed in the fasted state from Adipo-IR, calculated as FFA<sub>fasting</sub>\*insulin<sub>fasting</sub> [24, 25] and during the hyperinsulinemic-

euglycemic clamp from the percent suppression of FFA concentrations, calculated as [(FFA<sub>fasting</sub> - FFA<sub>clamp360 min</sub>)\*100/FFA<sub>fasting</sub>] [26, 27]. Steady-state rates of glucose appearance (Ra) were calculated as [tracer infusion rate]\*[tracer enrichment]/[percent tracer enrichment in plasma]-[tracer infusion rate] [28]. While in the fasted state, EGP equals Ra, clamp-Ra and -Rd were calculated using Steele's steady state equations.

### Blood analyses

Blood samples were collected before and during clamps for measuring hormones and metabolites. Metabolites, insulin, C-peptide, hsCRP, transforming growth factor β1 (TGFβ1), interleukin 1 receptor antagonist (IL-1ra), CC chemokine ligand 18 (CCL18), total adiponectin and leptin were quantified as described [29–31]. In vitro lipolysis was prevented by collecting blood into orlistat-containing vials [32] for microfluorimetric FFA quantification (Wako Chem USA Inc. Osaka, Japan). Serum concentrations of GH, IGF-1, IGFBP1 and IGFBP3 were measured by ELISA (Quantikine® ELISA immunoassay, R&D Systems, Inc., MN, USA) in samples obtained in the morning after overnight fasting. The intraassay coefficients of variations (CVs) for GH, IGF-1, IGFBP1 and IGFBP3 were 3.6%, 2.3%, 2.7% and 1.4%, respectively, and interassay CVs for GH, IGF-1, IGFBP1 and IGFBP3 were 6.5%, 3.5%, 6.8% and 9.6%, respectively.

### Statistical evaluation

Normally distributed parameters are presented as means ± SD or means ± SEM, otherwise as median (Q1;Q3). Not-normally distributed data were log<sub>e</sub>-transformed to achieve near-normal distribution. Statistical analyses using covariance pattern model for repeated measures analysis were performed. Analysis of covariance (ANCOVA) models of the cohort of participants with obesity as well as regression models were adjusted for age and sex and performed using SAS (version 9.4; SAS Institute, Cary, NC, USA).

## RESULTS

### OBE exhibit lower circulating GH, but not IGF-1 levels than CON

Before surgery (baseline), OBE had similar age, but higher fasting glycemia and Adipo-IR as well as lower clamp-Rd and HIS when compared to CON (Table 1, Fig. 1a, b). They also had higher plasma FFA but comparable triglycerides (Table 1). Serum insulin, leptin and IGFBP3 were higher, IGF-1 similar, while GH and IGFBP1 were lower

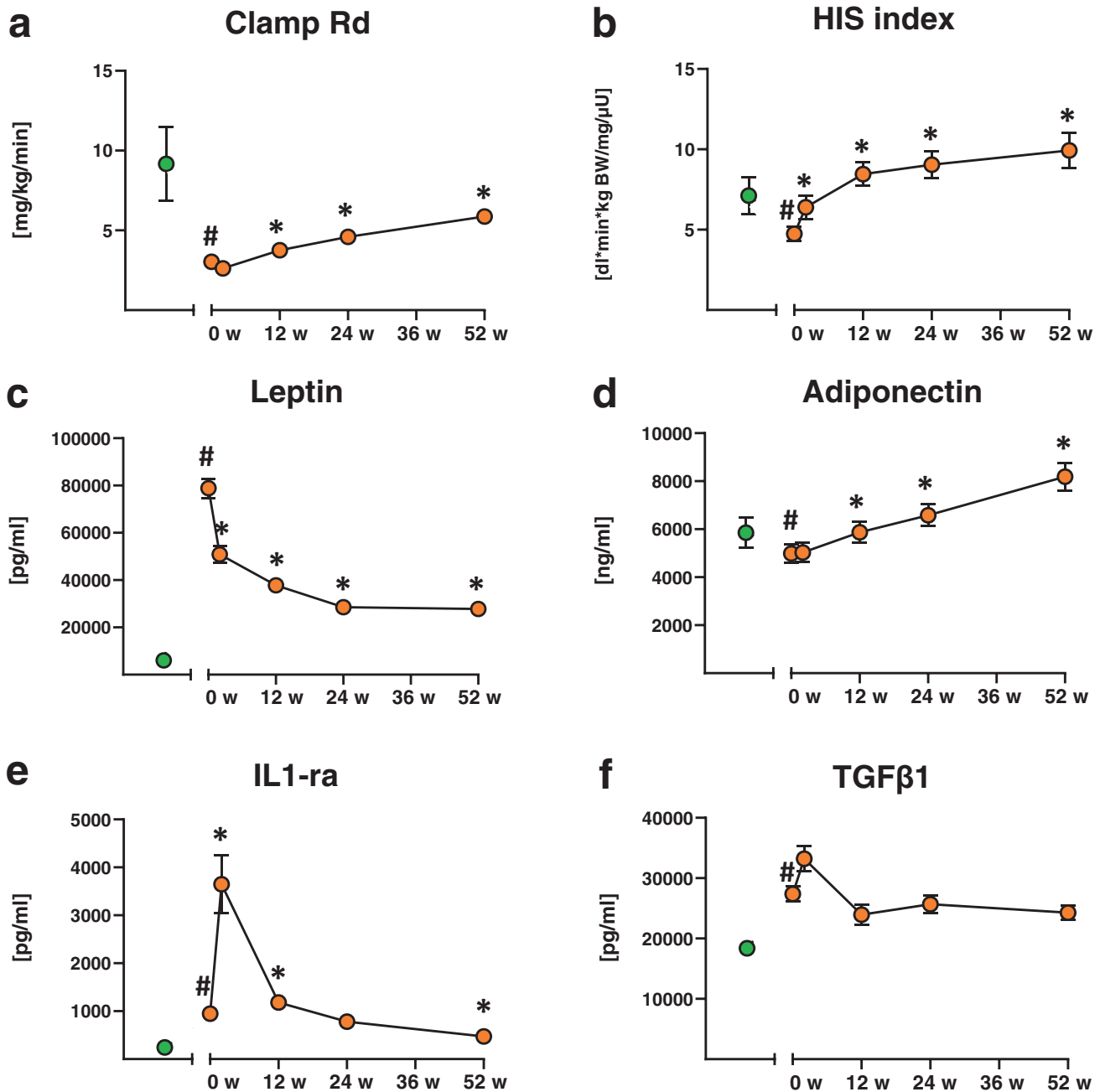


**Fig. 1 Time course of changes in insulin sensitivity, adipokines and cytokines.** Changes in rate of glucose disposal during the hyperinsulinemic-euglycemic clamp (clamp-Rd) (a), hepatic insulin sensitivity index (HIS) (b), leptin (c), total adiponectin (d), interleukin 1 receptor antagonist (IL-1ra) (e) and transforming growth factor  $\beta$ 1 (TGF $\beta$ 1) (f). Control humans depicted by green circles, people with obesity before (0 w) and 2, 12, 24 and 52 weeks after surgery depicted by orange circles. Data are mean  $\pm$  SEM, # $p$  < 0.05 vs controls, \* $p$  < 0.05 vs obese at baseline (0 w).

in OBE (Table 1, Fig. 2a–d). BMI was higher in individuals with T2D compared to those without T2D, but levels of leptin, GH, IGF-1, IGFBP1 and IGFBP3 were comparable (Suppl. Fig. 1).

#### GH rapidly and continuously rises, while IGF-1 levels transiently decrease upon metabolic surgery

At 2 weeks after surgery, body weight loss of  $10 \pm 3$  kg was paralleled by a transient increase in FFA, Adipo-IR and HIS, but no change in whole-body insulin sensitivity (Table 1, Fig. 1a, b). Serum insulin, insulin-mediated percent FFA suppression and leptin decreased in OBE early after surgery (Table 1, Fig. 1c). In parallel,

the pro-inflammatory biomarkers, IL-1ra and TGF $\beta$ 1, were transiently higher ( $p$  < 0.01) or tended to be higher ( $p$  = 0.11), respectively, compared to baseline (Fig. 1e, f).

Until 52 weeks after surgery, OBE exhibited an average weight loss of 33% and continuous improvements in whole-body, adipose tissue and HIS (Fig. 1a, b, Table 1). Similarly, glycemia, Adipo-IR, FFA, hsCRP and IL-1ra were normalised at 52 weeks (Table 1, Fig. 1e). Serum insulin, CCL18 and leptin levels were decreased by 63%, 34% and 65% at 52 weeks, respectively (Table 1, Fig. 1c), while total adiponectin markedly increased (Fig. 1d). Time courses of changes in BMI, insulin, glucose, HbA1c, triglycerides, FFA,

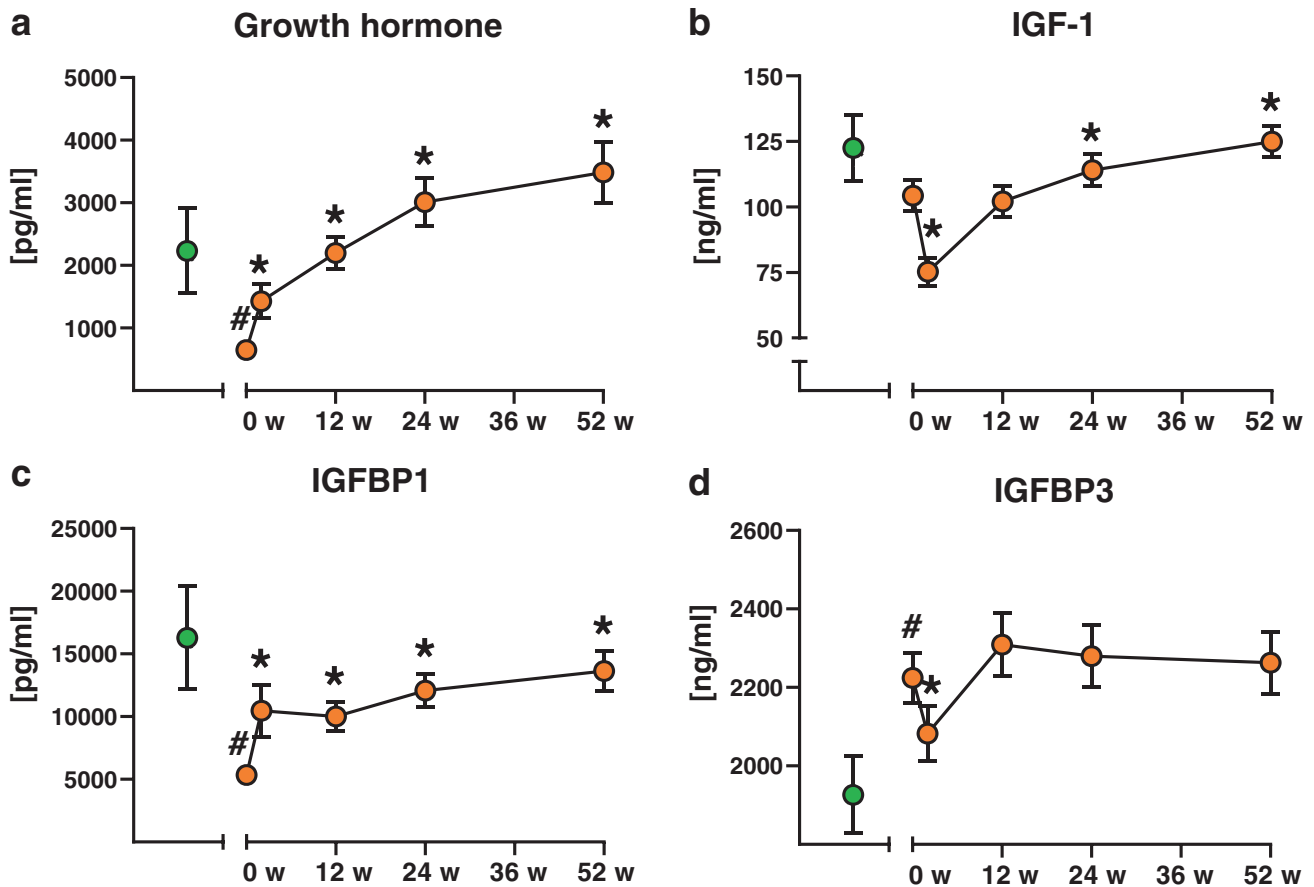


**Fig. 2 Time course of changes in growth hormone and its mediators.** Changes in growth hormone (GH) (a), insulin-like growth factor-1 (IGF-1) (b), IGF-1 binding protein 1 (IGFBP1) (c) and IGFBP3 (d). Control humans depicted by green circles, people with obesity before (0 w) and 2, 12, 24 and 52 weeks after surgery depicted by orange circles. Data are mean  $\pm$  SEM, # $p < 0.05$  vs controls, \* $p < 0.05$  vs obese at baseline (0 w).

hsCRP, Adipo-IR and IL-6 have been reported in a previous analysis of the BARIA\_DDZ cohort [18].

At 2 weeks, serum GH and IGFBP1 were already increased, but IGF-1 and IGFBP3 levels dropped by 28% and 6% from baseline, respectively (Fig. 2b, d). During the follow-up, GH and IGFBP1 levels continuously rose and were higher or equal to that of CON, respectively, at 52 weeks (Fig. 2a, c). IGF-1 rose only later, at 24 and 52 weeks after surgery (Fig. 2b).

In participants with T2D, body weight loss was lower, but improvement of adipose tissue insulin sensitivity was higher at 24 and 52 weeks after surgery compared to participants without T2D (Suppl. Fig. 1). Increases in IGFBP1 at 12 weeks and IGFBP3 at 52 weeks were higher in individuals without T2D compared to participants with T2D (Suppl. Fig. 1). Despite lower peripheral insulin sensitivity at baseline ( $p < 0.0001$ , data not shown), participants with T2D had greater improvements in insulin-stimulated Rd at 2, 12, and 52 weeks compared to participants without T2D ( $p = 0.007$ ,  $p = 0.0006$  and  $p = 0.02$ , respectively, data not shown).

Of note, there were no differences in the time courses of changes of BMI, hepatic and adipose tissue insulin sensitivity as well as GH, IGF-1, IGFBP1, IGFBP3 and leptin concentrations between participants undergoing sleeve gastrectomy and gastric bypass surgery (Suppl. Fig. 2).

#### Reversal of the GH/IGF1 system relates to improved FFA and adipose tissue insulin sensitivity, but not whole-body insulin sensitivity

Multiple regression analysis adjusted for age and sex revealed no association between the long-term improvement in GH

concentrations and changes in body weight, peripheral or HIS, glycemia or leptin levels, but a negative association with the reduction in insulinemia, FFA, and Adipo-IR (Table 2). The 52-week increase in IGF-1 related positively to the changes in leptin and insulin and negatively to the changes in hsCRP (Table 2). Of note, the transient lowering of IGF-1 at 2 weeks related to the increase in hsCRP, while the decrease in IGFBP3 related to the increase in Adipo-IR and hsCRP ( $p = 0.04$ ,  $p = 0.04$  and  $p = 0.03$ , respectively, data not shown). The 2-week increase of IGFBP1 related positively to the higher FFA concentrations ( $p = 0.008$ , data not shown).

#### DISCUSSION

This study demonstrates that the reversal of alterations of the GH-IGF-1 axis after bariatric surgery relates to improvements in adipose tissue function, but not whole-body and HIS. In particular, normalisation of the obesity-related so-called “functional hyposomatotropism” by surgical weight loss is associated with the reduction in lipid availability, adipose tissue insulin resistance and low-grade inflammation, underlining an important role of adipose tissue also for the regulation of GH-IGF-1 axis in metabolic diseases.

First, this study found lower GH concentrations in humans with obesity than in lean humans in the setting of similar IGF-1 concentrations, indicating a preserved IGF-1 feedback mechanism. Alterations of the GH-IGF-1 axis in obesity have been demonstrated previously by reduced fasting or stimulated GH [8, 33] and controversial data has been reported for IGF-1 concentrations [3, 34]. The latter is likely due to the complex regulation of IGF-1,

**Table 2.** Multiple regression analysis (adjusted for age and sex) for changes in serum GH and IGF-1 levels over 52 weeks after surgery.

Dependent	Parameter	Estimate	P value
Change in lnGH from baseline to 52 weeks ( $\Delta$ lnGH)	$\Delta$ body weight	-0.017	0.395
	$\Delta$ fasting blood glucose	-0.015	0.384
	$\Delta$ HbA1c	-0.585	0.219
	$\Delta$ lnFFA	-0.941	<b>0.027</b>
	$\Delta$ lnInsulin	-1.410	<b>0.027</b>
	$\Delta$ lnClamp-Rd	1.725	0.117
	$\Delta$ lnLeptin	-0.098	0.757
	$\Delta$ lnhsCRP	-0.325	0.066
	$\Delta$ lnAdipo-IR	-1.479	<b>0.002</b>
	$\Delta$ FFAsuppr	0.111	<b>0.012</b>
Change in lnIGF-1 from baseline to 52 weeks ( $\Delta$ lnIGF-1)	$\Delta$ body weight	0.002	0.666
	$\Delta$ fasting blood glucose	-0.002	0.428
	$\Delta$ HbA1c	0.011	0.912
	$\Delta$ lnFFA	0.144	0.108
	$\Delta$ lnInsulin	0.243	<b>0.042</b>
	$\Delta$ lnClamp-Rd	-0.044	0.832
	$\Delta$ lnLeptin	0.209	<b>0.007</b>
	$\Delta$ lnhsCRP	-0.093	<b>0.018</b>
	$\Delta$ lnAdipo-IR	0.204	0.091
	$\Delta$ FFAsuppr	0.007	0.471

FFA free fatty acids, GH growth hormone, IGF-1 insulin-like growth factor 1, hsCRP high-sensitive C-reactive protein,  $\Delta$  refer to the difference between values at baseline and 52 weeks, ln natural logarithm, clamp-Rd insulin-stimulated rate of glucose disposal.

Bold values identify statistical significance ( $P < 0.05$ ).

which in addition to GH involves several other factors, e. g. hypothalamic neuropeptides, ghrelin, insulin, FFA, macronutrients and IGFbPs [14, 35].

The observed increase in GH and IGF-1 levels confirms data at 6- and 12-m follow-up from other prospective bariatric surgery cohorts [9, 19, 22, 36], while the novel data for the 2-w timepoint allows further insights into short-term changes. These revealed a transient reduction in IGF-1 and IGFbP3 levels, which associated with increased hsCRP, suggesting a tight link between inflammatory processes and IGF-1 signaling. This is supported by data showing that interleukin 1 (IL-1), tumour necrosis factor  $\alpha$  and the mitogen activated protein kinase pathway regulate IGF-1 and IGFbPs in cross-sectional human [37] and mechanistic rodent studies [38]. The present study also showed a negative association between circulating GH and insulin levels in line with the observation of fasting insulin as a predictor of integrated 24-h GH release [39]. Indeed, insulin infusion lowers the GH response to GH-releasing hormone via the pituitary [40], suggesting an IGF-1-like effect [41]. In addition, the postoperative GH response in persons with obesity undergoing bariatric surgery seems to be mainly modulated by insulin [21]. GH is also a determinant of lean (muscle) mass after metabolic surgery [42] and exercise training [43]. In this context, the improved insulin and GH levels could be responsible for the increase in muscle lipid oxidation pathways and epigenetic regulation of muscle differentiation, as assessed from Gene Ontology analyses in people with obesity at 52 weeks after bariatric surgery [18]. Despite lack of lean body mass measurements in the present study, the improved muscle differentiation and GH levels after bariatric surgery possibly

contribute to preservation of lean mass after surgery as seen with GH treatment during hypocaloric diet [44].

Of note, this study uncovers a direct link between the surgically-induced improvement in GH levels and adipose tissue insulin sensitivity as well as lipid availability. Adipose tissue dysfunction has developed as the key mechanism underlying the pathophysiology of whole-body insulin resistance mediated by lipotoxicity and low-grade inflammation [27, 45, 46]. GH action also targets lipolysis, lipogenesis as well as adipocyte proliferation, differentiation and function, including adipose tissue inflammation and adipokine secretion [47]. A possible mechanism underlying this link may be upregulation of the GH-dependent signal transducer and activator of transcription-5 phosphorylation as shown in skeletal muscle during acute FFA-suppression by acipimox [48], which is mediated by adipocyte JAK2 signaling [49]. Notably, presence of T2D does not seem to play a relevant role for the reversal of the alterations of the GH-IGF-1 axis, as most observed changes were not dependent on T2D status and no association was found between glycemia and GH-IGF-1 changes. This suggests that early metabolic alterations in insulin sensitivity and adipose tissue function rather than overt diabetes and hyperglycemia are linked to changes in the GH system [50].

Furthermore, the adipokine leptin, which signals adipose tissue mass and energy balance to the brain, also inhibits GH secretion [15, 51] and contributes to IGF-1 regulation [16] and could therefore account for the changes in the GH-IGF axis induced by surgical weight loss. While this study confirms the substantial and continuous improvement of hyperleptinemia following metabolic surgery, no relationship was found between the decrease in circulating leptin and the improvement of GH levels. Of note, leptin secretion may be inhibited under conditions of greater insulin sensitivity [52, 53], so that the present results suggest a dissociation between adipose tissue and skeletal muscle insulin sensitivity with regard to leptin control of the GH-IGF-1 axis. Of note, leptin levels remained elevated at 52 weeks after surgery when compared to lean healthy controls, while the circulating GH concentrations at 52 weeks reached those of the nonobese control group. In line with previous reports, the type of metabolic surgery did neither affect change in GH and leptin [22] nor in body weight loss as well as in improvements of hepatic and adipose tissue insulin sensitivity [18].

Finally, IGFbP1 is negatively associated with impaired glucose tolerance [54] and obesity [55] and serves as a marker of HIS [56], while IGFbP3 correlates directly with hepatic insulin resistance and diabetes incidence [57, 58]. Thus, the long-term changes in IGFbP1 and IGFbP3 after metabolic surgery, as seen in the present study, reflect the glucometabolic improvement in line with previous reports [20]. The transient changes in IGFbP1 and IGFbP3 at 2 weeks after surgery and their relationship to changes in FFA and hsCRP point to a previously unknown link between IGFbPs and adipose tissue function and low-grade inflammation in obesity. This may be due to IGF-1-independent effects of IGFbP3 and IGFbP1 on adipose tissue, such as action via type V TGF $\beta$  receptors [59, 60].

In conclusion, the present findings provide detailed insights into dynamic endocrine changes in persons with obesity following metabolic surgery by linking reversal of the dysregulation of the GH-IGF-1 axis to adipose tissue metabolism and function. Specifically, these results point to a future role of modulating GH and its mediators in the treatment of obesity and obesity-related disorders.

#### DATA AVAILABILITY

The datasets used and analysed during the current study are available from the corresponding author on reasonable request.

#### REFERENCES

- Blüher M. Obesity: global epidemiology and pathogenesis. *Nat Rev Endocrinol.* 2019;15:288–98.

2. Biondi B. Thyroid and obesity: an intriguing relationship. *J Clin Endocrinol Metab.* 2010;95:3614–7.
3. Scacchi M, Pincelli AL, Cavagnini F. Growth hormone in obesity. *Int J Obesity Related Metab Disord: J Int Assoc Study Obesity.* 1999;23:260–71.
4. Rasmussen MH, Hvidberg A, Juul A, Main KM, Gotfredsen A, Skakkebaek NE, et al. Massive weight loss restores 24-hour growth hormone release profiles and serum insulin-like growth factor-I levels in obese subjects. *J Clin Endocrinol Metab.* 1995;80:1407–15.
5. Perakakis N, Kokkinos A, Peradze N, Tentolouris N, Ghaly W, Pilitsi E, et al. Circulating levels of gastrointestinal hormones in response to the most common types of bariatric surgery and predictive value for weight loss over one year: Evidence from two independent trials. *Metab: Clin Exp.* 2019;101:153997.
6. Yu AP, Ugwu FN, Tam BT, Lee PH, Ma V, Pang S, et al. Obestatin and growth hormone reveal the interaction of central obesity and other cardiometabolic risk factors of metabolic syndrome. *Sci Rep.* 2020;10:5495.
7. Cordido F, Casanueva FF, Vidal JI, Dieguez C. Study of insulin-like growth factor I in human obesity. *Hormone Res.* 1991;36:187–91.
8. Utz AL, Yamamoto A, Sluss P, Breu J, Miller KK. Androgens May Mediate a Relative Preservation of IGF-I Levels in Overweight and Obese Women Despite Reduced Growth Hormone Secretion. *J Clin Endocrinol Metab.* 2008;93:4033–40.
9. Juiz-Valiña P, Pena-Bello L, Cordido M, Outeiriño-Blanco E, Pértega S, Varela-Rodríguez B, et al. Altered GH-IGF-1 Axis in Severe Obese Subjects is Reversed after Bariatric Surgery-Induced Weight Loss and Related with Low-Grade Chronic Inflammation. *J Clin Med.* 2020;9:2614.
10. Edén Engström B, Burman P, Holdstock C, Ohrvall M, Sundbom M, Karlsson FA. Effects of gastric bypass on the GH/IGF-I axis in severe obesity—and a comparison with GH deficiency. *Eur J Endocrinol.* 2006;154:53–9.
11. Ricco RC, Ricco RG, Queluz MC, de Paula MTS, Atique PV, Custódio RJ, et al. IGF-1R mRNA expression is increased in obese children. *Growth Hormone IGF Res: Off J Growth Hormone Res Soc Int IGF Res Soc.* 2018;39:1–5.
12. l'Allemand D, Schmidt S, Rousson V, Brabant G, Gasser T, Grüters A. Associations between body mass, leptin, IGF-1 and circulating adrenal androgens in children with obesity and premature adrenarche. *Eur J Endocrinol.* 2002;146:537–43.
13. Yakar S, Setser J, Zhao H, Stannard B, Haluzik M, Glatt V, et al. Inhibition of growth hormone action improves insulin sensitivity in liver IGF-1-deficient mice. *J Clin Invest.* 2004;113:96–105.
14. Haywood NJ, Slater TA, Matthews CJ, Wheatcroft SB. The insulin like growth factor and binding protein family: Novel therapeutic targets in obesity & diabetes. *Mol Metab.* 2019;19:86–96.
15. Mingrone G, Manco M, Granato L, Calvani M, Scarfone A, Mora EV, et al. Leptin pulsatility in formerly obese women. *FASEB J: Off Publ Feder Am Soc Exp Biol.* 2005;19:1380–2.
16. Chan JL, Williams CJ, Raciti P, Blakeman J, Kelesidis T, Kelesidis I, et al. Leptin does not mediate short-term fasting-induced changes in growth hormone pulsatility but increases IGF-I in leptin deficiency states. *J Clin Endocrinol Metab.* 2008;93:2819–27.
17. Beghini M, Brandt S, Körber I, Kohlsdorf K, Vollbach H, Lennerz B, et al. Serum IGF1 and linear growth in children with congenital leptin deficiency before and after leptin substitution. *Int J Obesity (2005).* 2021;45:1448–56.
18. Gancheva S, Ouni M, Jelenik T, Koliaki C, Szendroedi J, Toledo FGS, et al. Dynamic changes of muscle insulin sensitivity after metabolic surgery. *Nat Commun.* 2019;10:4179.
19. Valera Mora ME, Manco M, Capristo E, Guidone C, Iaconelli A, Gnuli D, et al. Growth hormone and ghrelin secretion in severely obese women before and after bariatric surgery. *Obesity (Silver Spring, Md.).* 2007;15:2012–8.
20. Brynskov T, Laugesen CS, Floyd AK, Frystyk J, Sørensen TL. The IGF-Axis and Diabetic Retinopathy Before and After Gastric Bypass Surgery. *Obesity Surg.* 2017;27:408–15.
21. De Marinis L, Bianchi A, Mancini A, Gentilella R, Perrelli M, Giampietro A, et al. Growth hormone secretion and leptin in morbid obesity before and after biliopancreatic diversion: relationships with insulin and body composition. *J Clin Endocrinol Metab.* 2004;89:174–80.
22. Kruljac I, Mirošević G, Kirigin LS, Nikolić M, Ljubičić N, Budimir I, et al. Changes in metabolic hormones after bariatric surgery and their predictive impact on weight loss. *Clin Endocrinol.* 2016;85:852–60.
23. Koliaki C, Szendroedi J, Kaul K, Jelenik T, Nowotny P, Jankowiak F, et al. Adaptation of hepatic mitochondrial function in humans with non-alcoholic fatty liver is lost in steatohepatitis. *Cell Metab.* 2015;21:739–46.
24. Faramia J, Hao Z, Mumphy MB, Townsend RL, Miard S, Carreau AM, et al. IGFBP-2 partly mediates the early metabolic improvements caused by bariatric surgery. *Cell Rep Med.* 2021;2:100248.
25. Kwok KHM, Andersson DP, Rydén M, Arner P. A longitudinal study of the antilipolytic effect of insulin in women following bariatric surgery. *Int J Obesity.* 2021;45:2675–8.
26. Gastaldelli A, Gaggini M, DeFronzo RA. Role of Adipose Tissue Insulin Resistance in the Natural History of Type 2 Diabetes: Results From the San Antonio Metabolism Study. *Diabetes.* 2017;66:815–22.
27. Klein S, Gastaldelli A, Yki-Järvinen H, Scherer PE. Why does obesity cause diabetes? *Cell Metab.* 2022;34:11–20.
28. Matsuda M, DeFronzo RA. Insulin sensitivity indices obtained from oral glucose tolerance testing: comparison with the euglycemic insulin clamp. *Diabetes Care.* 1999;22:1462–70.
29. Fritsch M, Koliaki C, Livingstone R, Phielix E, Bierwagen A, Meisinger M, et al. Time course of postprandial hepatic phosphorus metabolites in lean, obese, and type 2 diabetes patients. *Am J Clin Nutr.* 2015;102:1051–8.
30. Wolf K, Popp A, Schneider A, Breitner S, Hampel R, Rathmann W, et al. Association Between Long-term Exposure to Air Pollution and Biomarkers Related to Insulin Resistance, Subclinical Inflammation, and Adipokines. *Diabetes.* 2016;65:3314–26.
31. Herder C, Baumert J, Zierer A, Roden M, Meisinger C, Karakas M, et al. Immunological and cardiometabolic risk factors in the prediction of type 2 diabetes and coronary events: MONICA/KORA Augsburg case-cohort study. *PLoS ONE.* 2011;6:e19852.
32. Nowotny B, Zahiragic L, Krog D, Nowotny PJ, Herder C, Carstensen M, et al. Mechanisms underlying the onset of oral lipid-induced skeletal muscle insulin resistance in humans. *Diabetes.* 2013;62:2240–8.
33. Glad CAM, Svensson PA, Nystrom FH, Jacobson P, Carlsson LMS, Johannsson G, et al. Expression of GHR and Downstream Signaling Genes in Human Adipose Tissue-Relation to Obesity and Weight Change. *J Clin Endocrinol Metab.* 2019;104:1459–70.
34. Carlzon D, Svensson J, Petzold M, Karlsson MK, Ljunggren Ö, Tivesten Å, et al. Both low and high serum IGF-1 levels associate with increased risk of cardiovascular events in elderly men. *J Clin Endocrinol Metab.* 2014;99:E2308–16.
35. Vottero A, Guzzetti C, Loche S. New aspects of the physiology of the GH-IGF-1 axis. *Endocr Dev.* 2013;24:96–105.
36. Al-Regaiey K, Alshubrami S, Al-Beeshi I, Alnasser T, Alwabel A, Al-Beladi H, et al. Effects of gastric sleeve surgery on the serum levels of GH, IGF-1 and IGF-binding protein 2 in healthy obese patients. *BMC Gastroenterol.* 2020;20:199.
37. Rajpathak SN, McGinn AP, Strickler HD, Rohan TE, Pollak M, Cappola AR, et al. Insulin-like growth factor-(IGF)-axis, inflammation, and glucose intolerance among older adults. *Growth Hormone IGF Res: Off J Growth Hormone Res Soc Int IGF Res Soc.* 2008;18:166–73.
38. Fukushima M, Okamoto Y, Katsumata H, Ishikawa M, Ishii S, Okamoto M, et al. Growth hormone ameliorates adipose dysfunction during oxidative stress and inflammation and improves glucose tolerance in obese mice. *Hormone Metab Res = Hormon- und Stoffwechselforschung = Hormones et métabolisme.* 2014;46:656–62.
39. Clasey JL, Weltman A, Patrie J, Weltman JY, Pezzoli S, Bouchard C, et al. Abdominal visceral fat and fasting insulin are important predictors of 24-hour GH release independent of age, gender, and other physiological factors. *J Clin Endocrinol Metab.* 2001;86:3845–52.
40. Lanzi R, Manzoni MF, Andreotti AC, Malighetti ME, Bianchi E, Sereni LP, et al. Evidence for an inhibitory effect of physiological levels of insulin on the growth hormone (GH) response to GH-releasing hormone in healthy subjects. *J Clin Endocrinol Metab.* 1997;82:2239–43.
41. Melmed S. Insulin suppresses growth hormone secretion by rat pituitary cells. *J Clin Invest.* 1984;73:1425–33.
42. Savastano S, Di Somma C, Angrisani L, Orio F, Longobardi S, Lombardi G, et al. Growth hormone treatment prevents loss of lean mass after bariatric surgery in morbidly obese patients: results of a pilot, open, prospective, randomized, controlled study. *J Clin Endocrinol Metab.* 2009;94:817–26.
43. Kraemer WJ, Ratamess NA, Hymer WC, Nindl BC, Fragala MS. Growth Hormone(s), Testosterone, Insulin-Like Growth Factors, and Cortisol: Roles and Integration for Cellular Development and Growth With Exercise. *Front Endocrinol.* 2020;11:33.
44. Nørrelund H, Børglum J, Jørgensen JO, Richelsen B, Møller N, Nair KS, et al. Effects of growth hormone administration on protein dynamics and substrate metabolism during 4 weeks of dietary restriction in obese women. *Clin Endocrinol.* 2000;52:305–12.
45. Roden M, Shulman GI. The integrative biology of type 2 diabetes. *Nature.* 2019;576:51–60.
46. Blüher M. Adipose tissue inflammation: a cause or consequence of obesity-related insulin resistance? *Clin Sci (London, England: 1979).* 2016;130:1603–14.
47. Berryman DE, Henry B, Hjortebjerg R, List EO, Kopchick JJ. Developments in our understanding of the effects of growth hormone on white adipose tissue from mice: implications to the clinic. *Expert Rev Endocrinol Metab.* 2016;11:197–207.
48. Møller N, Gormsen LC, Schmitz O, Lund S, Jørgensen JOL, Jessen N. Free Fatty Acids Inhibit Growth Hormone/Signal Transducer and Activator of Transcription-5 Signaling in Human Muscle: A Potential Feedback Mechanism. *Journal Clin Endocrinol Metab.* 2009;94:2204–7.

49. Corbit KC, Camporez JPG, Tran JL, Wilson CG, Lowe DA, Nordstrom SM, et al. Adipocyte JAK2 mediates growth hormone-induced hepatic insulin resistance. *JCI Insight*. 2017;2:e91001.
50. Salgin B, Marcovecchio ML, Williams RM, Jackson SJ, Bluck LJ, Humphreys SM, et al. Effects of growth hormone and free fatty acids on insulin sensitivity in patients with type 1 diabetes. *J Clin Endocrinol Metab*. 2009;94:3297–305.
51. Casanueva FF, Dieguez C. Neuroendocrine regulation and actions of leptin. *Front Neuroendocrinol*. 1999;20:317–63.
52. Wellhoener P, Fruehwald-Schultes B, Kern W, Dantz D, Kerner W, Born J, et al. Glucose metabolism rather than insulin is a main determinant of leptin secretion in humans. *J Clin Endocrinol Metab*. 2000;85:1267–71.
53. Mueller WM, Gregoire FM, Stanhope KL, Mobbs CV, Mizuno TM, Warden CH, et al. Evidence that glucose metabolism regulates leptin secretion from cultured rat adipocytes. *Endocrinology*. 1998;139:551–8.
54. Sandhu MS, Heald AH, Gibson JM, Cruickshank JK, Dunger DB, Wareham NJ. Circulating concentrations of insulin-like growth factor-I and development of glucose intolerance: a prospective observational study. *Lancet (London, England)*. 2002;359:1740–5.
55. Frystyk J, Brick DJ, Gerweck AV, Utz AL, Miller KK. Bioactive insulin-like growth factor-I in obesity. *J Clin Endocrinol Metab*. 2009;94:3093–7.
56. Kotronen A, Lewitt M, Hall K, Brismar K, Yki-Järvinen H. Insulin-like growth factor binding protein 1 as a novel specific marker of hepatic insulin sensitivity. *J Clin Endocrinol Metab*. 2008;93:4867–72.
57. Rajpathak SN, He M, Sun Q, Kaplan RC, Muzumdar R, Rohan TE, et al. Insulin-like growth factor axis and risk of type 2 diabetes in women. *Diabetes*. 2012;61:2248–54.
58. Frystyk J, Skjaerbaek C, Vestbo E, Fisker S, Orskov H. Circulating levels of free insulin-like growth factors in obese subjects: the impact of type 2 diabetes. *Diabetes/metabolism Res Rev*. 1999;15:314–22.
59. Jogie-Brahim S, Feldman D, Oh Y. Unraveling insulin-like growth factor binding protein-3 actions in human disease. *Endocr Rev*. 2009;30:417–37.
60. Wheatcroft SB, Kearney MT. IGF-dependent and IGF-independent actions of IGF-binding protein-1 and -2: implications for metabolic homeostasis. *Trends Endocrinol Metab*. 2009;20:153–62.

## ACKNOWLEDGEMENTS

We would like to thank all volunteers for their participation in this study and Drs Tomas Jelenik, Chrysi Koliaki, Daniel Markgraf for their important contributions to the clinical examination and/or laboratory assessments as well as Kai Tinnes, Myrko Esser, David Höhn, Andrea Sparla, Kerstin Förster, Fariba Zivehe, Jan-Marc Leonhard, Michelle Reina Do Fundo, Karin Röhrig and Ulrike Partke for their excellent technical assistance.

## AUTHOR CONTRIBUTIONS

SG performed clinical experiments, collected and analysed data and wrote, edited, and reviewed the paper. SK, KP, TS and JS performed clinical experiments and edited and reviewed the paper. CH performed laboratory analyses and edited and reviewed the paper. KS performed statistical analyses, edited and reviewed the paper. MS performed bariatric surgery procedures and edited and reviewed the paper. MR initiated the investigation, designed and led the clinical experiments and wrote, reviewed and edited the paper. All authors gave final approval of the version to be published. MR is the guarantor of this work and, as such, had full access to all the data in the study and takes responsibility for the integrity of the data and the accuracy of the data analysis.

## FUNDING

This study was supported in part by the German Diabetes Center (DDZ), which is funded by the Ministry of Culture and Science of the State of Northrhine Westphalia and the German Federal Ministry of Health (BMG), by grants of the Federal Ministry for Research (BMBF) to the German Center for Diabetes Research (DZD e. V., DZD Grant 2016). Parts of the study were also supported by grants from the European Funds for Regional Development (EFRE-0400191), the German Research Foundation (DFG, SFB 1116/2, GRK 2576), the German Diabetes Association (DDG), the Schmutzler-Stiftung, the European Community (HORIZON-HLTH-2022-STAYHLTH-02-01: Panel A) to the INTERCEPT-T2D consortium and is receiving funding from the programme “Profilbildung 2020”, an initiative of the Ministry of Culture and Science of the State of Northrhine Westphalia. The sole responsibility for the content of this publication lies with the authors. The funding sources had no role in study design, data collection, data analysis, data interpretation or writing of the report. Open Access funding enabled and organized by Projekt DEAL.

## COMPETING INTERESTS

SG, SK, KP, TS, JS, CH, KS and MS declare no competing interests. MR is on scientific advisory boards of Allergan, Astra-Zeneca, Bristol-Myers Squibb, Eli Lilly, Gilead Sciences, Inventiva, Intercept Pharma, Novartis, Novo Nordisk, Servier Laboratories, Target RWE and Terra Firma and has received support for investigator-initiated studies from Boehringer Ingelheim, Nutricia/Danone and Sanofi-Aventis.

## ADDITIONAL INFORMATION

**Supplementary information** The online version contains supplementary material available at <https://doi.org/10.1038/s41366-023-01292-7>.

**Correspondence** and requests for materials should be addressed to Michael Roden.

**Reprints and permission information** is available at <http://www.nature.com/reprints>

**Publisher's note** Springer Nature remains neutral with regard to jurisdictional claims in published maps and institutional affiliations.



**Open Access** This article is licensed under a Creative Commons Attribution 4.0 International License, which permits use, sharing, adaptation, distribution and reproduction in any medium or format, as long as you give appropriate credit to the original author(s) and the source, provide a link to the Creative Commons license, and indicate if changes were made. The images or other third party material in this article are included in the article's Creative Commons license, unless indicated otherwise in a credit line to the material. If material is not included in the article's Creative Commons license and your intended use is not permitted by statutory regulation or exceeds the permitted use, you will need to obtain permission directly from the copyright holder. To view a copy of this license, visit <http://creativecommons.org/licenses/by/4.0/>.

© The Author(s) 2023